UNICAMP

UNIVERSIDADE ESTADUAL DE CAMPINAS

Instituto de Matemática, Estatística e Computação Científica

JEAN RENEL FRANÇOIS

A multidimensional semi-discrete Lagrangian-Eulerian scheme for scalar and systems of hyperbolic conservation laws with a positivity principle

Um esquema Lagrangiano-Euleriano semi-discreto multidimensional para leis de conservação hiperbólicas escalares e sistemas com um princípio de positividade

Campinas

2021

Jean Renel François

A multidimensional semi-discrete Lagrangian-Eulerian scheme for scalar and systems of hyperbolic conservation laws with a positivity principle

Um esquema Lagrangiano-Euleriano semi-discreto multidimensional para leis de conservação hiperbólicas escalares e sistemas com um princípio de positividade

Tese apresentada ao Instituto de Matemática, Estatística e Computação Científica da Universidade Estadual de Campinas como parte dos requisitos exigidos para a obtenção do título de Doutor em Matemática Aplicada.

Thesis presented to the Institute of Mathematics, Statistics and Scientific Computing of the University of Campinas in partial fulfillment of the requirements for the degree of Doctor in Applied Mathematics.

Orientador: Eduardo Cardoso de Abreu

Coorientador: Wanderson José Lambert

Este trabalho corresponde à versão final da Tese defendida pelo aluno Jean Renel François e orientado pelo Prof. Dr. Eduardo Cardoso de Abreu.

Campinas

2021

Ficha catalográfica
Universidade Estadual de Campinas
Biblioteca do Instituto de Matemática, Estatística e Computação Científica
Ana Regina Machado - CRB 8/5467

F848m François, Jean Renel, 1985-
A multidimensional semi-discrete Lagrangian-Eulerian scheme for scalar and systems of hyperbolic conservation laws with a positivity principle / Jean Renel François. – Campinas, SP : [s.n.], 2021.

Orientador: Eduardo Cardoso de Abreu.
Coorientador: Wanderson José Lambert.
Tese (doutorado) – Universidade Estadual de Campinas, Instituto de Matemática, Estatística e Computação Científica.

1. Leis de conservação hiperbólicas. 2. Método lagrangiano-euleriano. 3. Esquema semi-discreto (Equações diferenciais). 4. Análise assintótica fraca. 5. Princípio de positividade. I. Abreu, Eduardo Cardoso de, 1974-. II. Lambert, Wanderson José. III. Universidade Estadual de Campinas. Instituto de Matemática, Estatística e Computação Científica. IV. Título.

Informações para Biblioteca Digital

Título em outro idioma: Um esquema lagrangiano-euleriano semi-discreto multidimensional para leis de conservação hiperbólicas escalares e sistemas com um princípio de positividade
Palavras-chave em inglês:
Hyperbolic conservation laws
Lagrangian-Eulerian method
Semi-discrete scheme (Differential equations)
Weak asymptotic analysis
Positivity principle
Área de concentração: Matemática Aplicada
Titulação: Doutor em Matemática Aplicada
Banca examinadora:
Eduardo Cardoso de Abreu
John Alexander Pérez Sepúlveda
Aparecido Jesuino de Souza
Cassio Machiaveli Oishi
Giuseppe Romanazzi
Data de defesa: 23-07-2021
Programa de Pós-Graduação: Matemática Aplicada

Identificação e informações acadêmicas do(a) aluno(a)
- ORCID do autor: https://orcid.org/0000-0002-0767-4847
- Currículo Lattes do autor: http://lattes.cnpq.br/0633028636115259

Tese de Doutorado defendida em 23 de julho de 2021 e aprovada

pela banca examinadora composta pelos Profs. Drs.

Prof(a). Dr(a). EDUARDO CARDOSO DE ABREU

Prof(a). Dr(a). JOHN ALEXANDER PÉREZ SEPÚLVEDA

Prof(a). Dr(a). APARECIDO JESUINO DE SOUZA

Prof(a). Dr(a). CASSIO MACHIAVELI OISHI

Prof(a). Dr(a). GIUSEPPE ROMANAZZI

A Ata da Defesa, assinada pelos membros da Comissão Examinadora, consta no SIGA/Sistema de Fluxo de Dissertação/Tese e na Secretaria de Pós-Graduação do Instituto de Matemática, Estatística e Computação Científica.

I dedicate this work to my mother Lonie Dorlus and my aunt Manette Pierre.

Acknowledgements

First of all, I thank God. I would like to thank my advisor, Prof. Dr. Eduardo Abreu and my co-advisor Prof. Dr. Wanderson Lambert, because they drove me with enthusiasm, wisdom, assistance, dedication and so much understanding in this journey. Thanks to the Institute of Mathematics, Statistics, and Scientific Computing (IMECC)-Graduate Program in Applied Mathematics - for providing me the opportunity to be a student of this prestigious institution.

I show my gratitude to my family, even far away, they find a meaningful way to support me every day. I am grateful to all my colleagues, Jardel, Arthur, Paola, Luis, John Alexander and Felipe, who in one way or another found the time and willingness to help me get on the right path. And finally, I wish to give my heartfelt thanks to my partner, Aurora, whose unconditional love, patience, and continual support of my academic endeavors enabled me to complete this thesis.

This study was financed in part by the Coordenação de Aperfeiçoamento de Pessoal de Nível Superior - Brasil (CAPES) - Finance Code 001.

I would like to dedicate this work to my mother, Lonie Dorlus, a warrior with unconditional strength who taught me that there are no obstacles to pursuing a dream.

The completeness of intelligence is strength and determination.
Jean Renel François

Resumo

Nesta tese, uma nova classe de esquemas semi-discretos Lagrangianos-Eulerianos (SDLE) com a propriedade *positivity preserving* foi projetada e rigorosamente analisada para a resolução de problemas de valor inicial multidimensionais para modelos escalares e sistemas de leis de conservação. A construção desta classe de esquemas é baseada na região espaço-temporal *no-flow surface*, que fora apresentada anteriormente para esquemas totalmente discretos. A implementação do esquema no caso de sistemas é uma aplicação direta de componentes do caso escalar multidimensional, mas, mais importante, a nova abordagem semi-discreta não requer estratégias de divisão dimensional (i.e., dimensional splitting). A prova de convergência para solução entrópica para o caso escalar multidimensional é fornecida por meio de uma análise assintótica fraca. Também foi provado que o novo esquema bidimensional Lagrangiano-Euleriano satisfaz o princípio do máximo (caso escalar) junto com estimativas relevantes, o que também implica a unicidade da solução fraca satisfazendo a condição de entropia de Kruzhkov. Vale ressaltar que também destacamos a possibilidade do uso das *no-flow curves* como uma nova técnica de análise de dessingularização para construção de fluxos numéricos, localmente conservativos, e computacionalmente estáveis, para a resolução de problemas hiperbólicos não lineares, nos casos escalares e de sistemas. Além disso, foi provada também que o novo esquema semi-discreto Lagrangiano-Euleriano, no contexto mais geral de sistemas hiperbólicos multidimensionais de leis de conservação, satisfaz o princípio de positividade introduzido por P. Lax e X.-D. Liu (1996, 2003). De fato, usando as propriedades das *no-flow curves*, não é necessário obter os autovalores associados ao fluxo hiperbólico para garantir a positividade fraca do novo esquema numérico semi-discreto proposto. Também usamos estimativas adequadas das *no-flow curves* para cálculos numericamente estáveis - para resolver equações escalares e sistemas multidimensionais - de uma forma semelhante à da conhecida condição de estabilidade de Courant - Friedrichs - Lewy (CFL), mas sem a necessidade de empregar os autovalores (valores exatos ou aproximados) do Jacobiano relevante das funções de fluxo hiperbólico. Outra característica interessante da construção semi-discreta *no-flow curves* Lagrangiana-Euleriana é que as matrizes são simétricas por construção (na verdade, são diagonais), o que é independente e aplicavel para uma classe geral de fluxo hiperbólico para problemas escalares e sistemas. Também demonstramos a aplicação do esquema semi-discreto para problemas hiperbólicos escalares e sistemas bidimensionais não triviais que exibem intrincadas interações de ondas. O esquema SDLE multidimensional mantém a simplicidade, com uma resolução muito boa, é eficiente em termos de custo computacional e de memória, e também é simples de implementar, pois nenhum problema de Riemann (local) é resolvido; portanto, os cálculos de tipo *field-by-field type decompositions* no caso de sistemas hiperbólicos são totalmente evitados. Todas essas propriedades são significativas e garantem a simplicidade e o poder dessa classe de esquemas semi-discretos positivos.

Palavras-chave: Leis de conservação hiperbólicas, Método Lagrangiano-Euleriano, Análise de dessingularização (Blow–up analysis), Esquema semi–discreto, Variação total não crescente (Total variation nonincreasing–TVNI), Análise assintótica fraca, Solução de entropia de Kruzhkov, Princípio de positividade.

Abstract

In this thesis, we design and analyze a new class of positive Semi-Discrete Lagrangian-Eulerian (SDLE) schemes for solving multidimensional initial value problems for scalar models and systems of conservation laws. The construction of the schemes is based on the space-time no-flow surface region, previously presented and analyzed for fully discrete schemes. The implementation of the scheme in the case of systems is a straightforward componentwise application of the multidimensional scalar case, but, importantly, the new semi-discrete approach does not require dimensional splitting strategies. Entropy-convergence proof for the multidimensional scalar case is provided via weak asymptotic analysis. We also prove that the new two-dimensional Lagrangian-Eulerian scheme satisfies the scalar maximum principle along with relevant estimates, which also implies the uniqueness of the weak solution satisfying Kruzhkov entropy condition. It is worth pointing out that we also highlight the possibility of the use of the no-flow curves as a novel desingularization analysis technique for construction of computationally stable numerical flux, in locally conservative form, for numerically solving nonlinear hyperbolic problems. Moreover, we show that the new semi-discrete Lagrangian-Eulerian scheme, in the more general context of multidimensional hyperbolic systems of conservation laws, also satisfies the positivity principle introduced by P. Lax and X.-D. Liu (1996, 2003). Indeed, by using the properties of the *no-flow curves*, it is not necessary to obtain the eigenvalues associated with the hyperbolic flux to guarantee the positivity in a weak sense of the new proposed semi-discrete numerical scheme. We also use suitable estimates on the *no-flow curves* for numerically stable computations – for solving scalar equations and multidimensional systems – in a fashion similar to that of the well-known stability condition by Courant–Friedrichs–Lewy (CFL), but without the need to employ the eigenvalues (exact or approximate values) of the relevant Jacobian of the hyperbolic flux functions. Another interesting feature of the semi-discrete no-flow Lagrangian-Eulerian construction is that the matrices are symmetric for free (actually, they are diagonal), which is independent for a general class of hyperbolic flux for scalar problems and systems as well. We also demonstrate the application of our semi-discrete scheme to nontrivial two-dimensional scalar problems and systems that display intricate wave interactions. The multidimensional SDLE scheme retains simplicity, with a very good resolution, is efficient in terms of computational and memory cost, and is simple to implement as well since no (local) Riemann problems are solved; hence, time-consuming field-by-field type decompositions are avoided in the case of systems. These features are significant and ensure the simplicity and power of this class of positive semi-discrete schemes.

Keywords: Hyperbolic conservation laws, Lagrangian–Eulerian method, Blow–up analysis, Semi–discrete scheme, Total variation nonincreasing (TVNI), Weak asymptotic analysis, Kruzhkov entropy solution, Positivity principle.

List of Figures

List of Tables

Contents

1 Introduction

In this work, we present a new class of semi-discrete Lagrangian-Eulerian schemes for solving multidimensional initial value problems for models of scalar and systems of conservation laws. The construction of the scheme is based on the novel concept of no-flow curves recently introduced in the literature [13], which has been presented and analyzed successfully for fully-discrete schemes in a solid mathematical foundation. The space-time *no-flow* construction as in [13], *per time step*, is the key ingredient for our two-dimensional semi-discrete formulation and to produce an accurate approximation of the local speeds of wave propagation in control volumes. By the use of weak asymptotic theory, the scheme shows good properties such as maximum principle along with relevant estimates, which also implies the uniqueness of the weak solution satisfying Kruzhkov entropy condition and property of being Total Variation Non-Increasing (TVNI, for scalar case) and satisfying a positive principle.

To illustrate the viability of our method, we present a set of significant computational aspects with numerical experiments related to linear and nonlinear hyperbolic conservation laws, subject to convex and non-convex flux functions (scalar and systems in one-space dimension and two-space dimensions).

1.1 Motivation and significance of the thesis

A large variety of efficient numerical methods like finite volume methods, finite difference methods, as well as Eulerian-Lagrangian methods, Discontinuous Galerkin method, and central schemes type, have been of great importance to approximate hyperbolic system of conservation law problems in recent past years. First, in the context of the accurate approximation transport equations, J. Douglas Jr and T. Russell introduced in 1982 the "*Modified Method of Characteristics*" (MMOC) [44], which is based on an Eulerian-Lagrangian framework for temporal discretization of convection-dominated diffusion equations. This method provides computational efficiency with no spurious effects on numerical solutions, and allows to use long time steps without loss of accuracy for linear and non-linear transport problems [36, 44], but fails to preserve the local mass of fluids. The local conservation of the mass is of great importance for many important physical problems in the literature. This lack of conservation gives rise to several well-known methods written in an Eulerian-Lagrangian framework, such as, the "*Eulerian-Lagrangian Localized Adjoint Methods*" (ELLAM) [27, 28], the "*Modified Method of Characteristic with Adjusted Advection*" (MMOCAA) [42] and the "*Locally Conservative Eulerian-Lagrangian methods*" (LCELM) [43].

The ELLAM scheme developed by Micheal Celia, Thomas Russell, Ismael Herrera and Richard Ewing in 1990 [27, 28] has the fluid mass locally conservative, but with high computational cost. In 1998, J. Douglas Jr, F. Furtado, and F. Pereira proposed the MMOCAA method [42] based on the MMOC framework. This method conserves globally the mass of fluids (in space) at all time levels and keeps the computational efficiency of the original MMOC procedure. The MMOC and MMOCCA procedures consist of writing the partial differential system (or, at least, the parabolic-type equations in the system) in a non-divergence form and make use of the characteristics associated with the first-order transport part of the system in a fractional step procedure that splits the transport from the diffusive part of the system.

In the LCELM paper [43] 2000, the authors applied an innovative and distinct procedure from the one used by MMOC and MMOCCA (writing the transport equation in a divergent form), which results in a fast, stable, accurate, and locally conservative scheme for the problem of two-phase flow, immiscible, incompressible flow in porous media. This scheme is very competitive from a computational point of view, but suffers from some numerical diffusion. To be precise in the description, here we quote the work (LCELM) [43] "*In contrast [to the previous works MMOC, MMOCAA and ELLAM techniques], the LCELM method will relate to the divergence form of the equations and then will split the transport from the diffusion. It is the use of the divergence form that allows the localization of the transport so that the desired conservation property can also be localized.*" To the best of our knowledge, the LCELM [43] procedure was the first work in the literature to introduce such *local conservation relation*, in a space-time divergence form, but only for scalar parabolic convection-diffusion models in porous media transport problems, which was coined at that time as *integral curves*, (see Eqs. (5.4a)-(5.4b) in the LCELM paper [43]). Moreover, as described the work (LCELM) [43], the so-called *integral curves* used in the discrete LCELM procedure were associated with points on the boundary (usually vertices) of the finite elements in that framework of locally conservative Eulerian-Lagrangian numerical methods.

To eliminate numerical diffusion and also to be able to use long time steps, the authors J. Aquino, A. S. Francisco, F. Pereira, and H. P. Amaral Souto present in 2008 a geometric construction of a distinct Eulerian-Lagrangian formulation linked to the *integral tube* concept, named *the Forward Integral-Tube Tracking* (FIT) scheme. This scheme inherits the local conservation property of the LCELM with no numerical diffusion and aiming at minimizing spurious effects in the numerical solutions [21]. This scheme has been presented for multi-dimensional advection-dominated radionuclide transport problems, different from the schemes mentioned above, which are for multi-dimensional scalar non-linear convection-diffusion equations. This Lagrangian approach provides a very accurate solution to pure advection problems with no rigorous mathematical proofs of convergence [20, 21].

In the same line of the FIT scheme, the authors E. Abreu, W. Lambert, J. Pérez, and A. Santo have put in evidence a locally conservative and divergence space-time finite control volume in a fully-discrete Lagrangian-Eulerian framework from 2015 to 2019, but for scalar and system of hyperbolic conservation laws linked to a *no-flow curves* concept, then extended to balance problems and two-dimensional problems (see [13, 15, 74, 75]). The relevance of this formulation has been put in evidence with success in several non-trivial problems and also developed theoretically linked to several transport models such as the Burgers' equation with Greenberg-LeRoux's [51] and Riccati's source terms [48], the shallow-water system [52], Broadwell's rarefied gas dynamics [73], Baer-Nunziato's system [35], linear, non-linear convex and non-linear non-convex 2D scalar conservation laws [13], and the 2D Buckley-Leverett equation with gravity [10, 13].

The first key idea behind the construction of the fully-discrete Lagrangian-Eulerian scheme for two-dimensional nonlinear hyperbolic conservation laws is to transform the hyperbolic problem into a convenient form of balance laws [74]; see also [13]. Following the works [13, 74], the authors in [6] developed the first genuinely multidimensional fully-discrete Lagrangian-Eulerian scheme in the sense that the scheme does not require the use of dimensional splitting strategies. It is worth mentioning that the work [6] (see also [11]) also gives additional theoretical foundations to the Lagrangian-Eulerian framework as well as provides a key building block for the design of the multidimensional semi-discrete Lagrangian-Eulerian scheme introduced in this thesis. Another feature of the Lagrangian-Eulerian method is the *flux separation strategy* and its impact on being well-balanced. For instance, the numerical tests in [13] show that the discretizations resulting from the flux separation strategy seem to be of good quality when applied to two-by-two shallow-water and five-by-five Baer–Nunziato's systems. Moreover, such strategy appears to be very appropriate to deal with convex and nonlinear non-convex two-dimensional (2D) scalar conservation laws.

On other hand, over the past decades original and extremely innovative studies into advances in semi-discrete schemes have been developed to numerically solve problems associated with systems of hyperbolic conservation laws and related convection-dominated problems. Some of these schemes include the Runge-Kutta Discontinuous Galerkin method [33], the semi-discrete central scheme [57, 59] and the Godunov-type semi-discrete central scheme [58], spectral methods for hyperbolic problems [50], semi-Lagrangian methods [71], and Arbitrary Lagrangian-Eulerian methods [67], just to name a few. The integration of semi-discrete approximations in time-dependent problems is encountered in a variety of applications. In addition, it can be regarded as a way to reduce excessive diffusion effects. Such formulations, in general, lead to Ordinary Differential Equation (ODE) systems called methods of lines, which can then be numerically solved in time through different strategies, such as the first-order Euler method and the Runge-Kutta-type schemes [63]. Separating the time and space discretization processes in the semi-discrete approach allows

enormous flexibility and is a well-suited strategy to derive very high-order schemes, such as the families of Uniformly Non-Oscillatory (UNO) and Essentially Non-Oscillatory (ENO) schemes (see [54]). One of the advantages of the semi-discrete formulation is that we can separately increase the order of spatial and temporal accuracy and, thus, it can be efficiently used time steps as small as required [59].

Moreover, for our particular purposes, it is worth mentioning the study of Tadmor and Kurganov (2000) [59] (see also [57]), who came up with an ingenious and effective idea to develop an interesting landmark in the field of semi-discrete schemes. Their proposed scheme retains the simplicity of being independent of the eigenstructure of the problem, yet enjoys a much smaller numerical viscosity (of the corresponding order $O(\Delta x)^{2r-1}$, where r is the formal order of the scheme, which is also related to the reconstruction of a piecewise polynomial interpolant of degree $r-1$ [58]). The main idea behind the construction of semi-discrete central schemes is the use of more precise information on the local propagation speeds in such a way that these methods maintain their high-resolution independent of $O(1/\Delta t)$, and letting $\Delta t \downarrow 0$, they provide a particularly simple semi-discrete formulation (see, e.g. [57, 58, 59] for more details).

In this thesis, the semi-discrete formulation is based on the new concept *no-flow curve* [13]. This new concept allows us to replace a quantity of numerical dissipation of the type $O([\Delta x]/[\Delta t])$ appearing in the numerical flux function of the fully-discrete Lagrangian-Eulerian scheme with stability estimates of the type $O(H(u)/u)$ where u and $H(u)$ are as defined in model problem (2.1). This simple and interesting technique is the key (and natural) ingredient of the Lagrangian-Eulerian framework that provides information about the local (and global) wave propagation speed. Thus, the use of the no-flow curve reveals to be a desingularization analysis tool for the construction of computationally stable numerical flux in conservative form when the limit $\Delta t \to 0$ is taken. In other words, in our semi-discrete scheme, the so-called *integral curves* as in [43], or the *no-flow curves*, with a reinterpretation of an anti-diffusion coefficient into the viscosity coefficient as in [13] for fully-discrete Lagrangian-Eulerian schemes, are defined by the quantity $H(u)/u$. In addition, a key hallmark of such method is the dynamic tracking forward of no-flow curves, per time step. This is a considerable improvement compared to the classical backward tracking over time of the characteristic curves over each time step interval, which is based on the strong form of the problem. Indeed, in the case of systems and multi-D problems, we can say that backward tracking is not understood (see [55]). Here, we are interesting in designing a novel semi-discrete scheme based on the new concept of no-flow curves subject to $[O(H(u)/u)] \propto \left[\dfrac{\Delta x}{\Delta t}\right] \to 0$, which is substantially different in theory foundations from the previous and seminal LCELM paper [43].

An advantage of our proposed Lagrangian-Eulerian scheme is its simple implementation: no (local) Riemann problems are solved and, hence, time-consuming field-by-

field decomposition to trace the direction of the wind (particularly in the case of systems) is avoided. An important hallmark of our Lagrangian-Eulerian method is the dynamic forward tracking of the no-flow region (per time step). This represents a considerable improvement compared to the classical backward tracking in time of the characteristic curves over each time step interval, which is based on the strong form of the problem. In fact, since our approach avoids the need of using Riemann solvers, we develop the proposed Semi-Discrete Lagrangian-Eulerian (SDLE) scheme for multidimensional (multi-D) problems (scalar equations and systems) by implementing the scalar framework presented in this work (currently under investigation [7]) in a simple fashion but without any dimensional splitting and whose approximate solution is the Kruzhkov entropy solution (in the scalar multi-D problem). The 2D semi-discrete scheme is a straightforward, but non-trivial extension of the one-dimensional case, that is, a dimension-by-dimension approach. The no-flow space-time construction [13], *per time step*, is also a key ingredient for the semi-discrete formulation and to produce an accurate approximation of the local speeds of wave propagation in the control volumes. In the case of systems, the latter approach is a straightforward componentwise application of the multidimensional scalar space-time no-flow recipe. This formulation is also valid for higher dimensions. We also use suitable estimates on the no-flow curves for numerically stable computations – for solving scalar equations and multidimensional systems – in a fashion similar to that of the well-known stability condition by Courant–Friedrich–Lewy (CFL), but without the need to employ the eigenvalues (exact and approximate values) of the relevant Jacobian of the hyperbolic flux functions.

In addition, we use the weak asymptotic theory [2, 3] to prove the convergence of the semi-discrete Lagrangian-Eulerian scheme introduced in this thesis to the weak (Kruzhkov) entropic solution. Various weak asymptotic methods have been introduced by V. Danilov and collaborators: D. Mitrovic, G.A. Omel'yanov and V.M. Shelkovich [38, 39, 40, 41] (see also [2, 3] and the references cited therein) within the framework of the Maslov–Whitham asymptotic analysis [37]. These methods have proven to be an efficient mathematical tool to study the creation and superposition of singular solutions to various nonlinear PDEs, such as σ-waves and the more general $\sigma^{(n)}$-waves. In particular, the authors in [3] used the weak asymptotic method for scalar equations and systems in multi-D problems (see also [2]) to deal with entropy solutions of degenerate parabolic and hyperbolic equations in several space variables under rather weak regularity hypothesis on the flux and diffusion functions (see [19, 68] for other methods to approximate this class of hyperbolic and parabolic equations). In [2, 3], the authors employed the construction based on weak asymptotic methods to prove the compactness of the approximate solutions and their convergence to an entropy solution, which is, moreover, unique. The weak asymptotic solution consists in reducing the PDEs to a family of ODEs for variable t by substituting the differences in space variable using a parameter ϵ. From the theory of ODEs, the

existence and stability of the solution can be proven, and taking $\epsilon \to 0$ results in the weak solution of the original PDE. Therefore, the proposed weak asymptotic solution analysis when applied to the SDLE framework fits suitably within the classical theory, as it improves the mathematical formulation for the construction of new accurate numerical schemes. A weak asymptotic method for hyperbolic problems was recently developed in [8, 9]. The authors of such studies made some contributions to prove the convergence of the scalar fully-discrete Lagrangian-Eulerian scheme linking the theoretical development to the computational approach within solid ODE theories. Using the weak asymptotic analysis, together with the SDLE scheme, constitutes a useful tool to conduct numerical studies into hyperbolic-transport problems.

The SDLE approach allows us to combine the no-flow curves with a piecewise linear approximation to deal with variable u and the (numerical) flux terms in a robust fashion. Also, by means of a suitable semi-discrete formulation, we are capable of giving sufficient and robust conditions for Total Variation Non-Increasing (TVNI), or Total Variation Diminishing (TVD) (see [53]). In addition, we can obtain the maximum principle and the entropy (Kruzhkov) solution for the hyperbolic model thanks to a proper and suitable interpretation of the (numerical) approximate solutions resulting from the weak asymptotic analysis. Although such piecewise linear approximation poses several technical challenges, it also opens up new possibilities to apply the weak asymptotic theory in a large range of new methods. Moreover, we present in this study a general way to deal with reconstructed variables in the numerical method.

An entropy-convergence proof for the multidimensional scalar case is given via weak asymptotic analysis [2, 3, 8]. We also prove that the new two-dimensional Lagrangian-Eulerian scheme satisfies the scalar maximum principle along with pertinent estimates, which also imply uniqueness of weak solution satisfying Kruzhkov's entropy condition. Moreover, we show that the new semi-discrete Lagrangian-Eulerian scheme, in the more general context of multidimensional hyperbolic systems of conservation laws, also satisfies the positivity principle in the sense of the papers [X.-D. Liu and P. D. Lax, positive schemes for solving multi-dimensional hyperbolic systems of conservation laws, CFD Journal, 5 (1996) 1-24] [66] and [X.-D. Liu and P. D. Lax, Positive schemes for solving multi-dimensional hyperbolic systems of conservation laws II, Journal of Computational Physics 187 (2003) 428-440] [65], but the class of positive semi-discrete Lagrangian-Eulerian method presented and analyzed in this work does not use field by field decompositions.

1.2 Aims and main features

The main objective of this thesis is to obtain a semi-discrete formulation for scalar and systems of hyperbolic conservation law problems in one space dimension and

two space dimensions. Below, we summarize the main aspects of our work:

- The SDLE scheme is based on the novel concept of *no-flow curves* recently introduced in the literature [13]. This new concept allows us to replace a numerical coefficient dissipation of the type $O([\Delta x]/[\Delta t])$ appearing in the numerical Lagrangian flux function of the fully-discrete Lagrangian-Eulerian scheme with stability estimates of the type $O(H(u)/u)$ where u and $H(u)$ are linked to the differential equation $u_t + H(u)_x = 0$.

- We also highlight the possibility of the use of the no-flow curves as a new blow-up numerical analysis technique. For concreteness, we show how to use the no-flow curve as a new desingularization analysis tool for the construction of computationally stable numerical flux in conservative form.

- The two-dimensional semi-discrete scheme is a natural, but non-trivial extension of the one-dimensional case with technical challenges when it comes up to prove convergence of approximate solutions generated by the scheme to the unique entropy solution.

- The extension to system is naturally a straightforward componentwise application of the multidimensional scalar case (1D and 2D). No (local) Riemann problems are solved and, hence, time-consuming field-by-field decompositions are avoided. Our approach does not require dimensional splitting strategies, but only the available easy information of the quantities u and the flux functions. Therefore, the foundations for the construction of the parametric *no-flow* equations and their corresponding numerical flux for the class of Lagrangian-Eulerian schemes in several dimensions (scalar and systems) preserve the same simple approximation features as in the 1D and 2D cases.

- Weak numerical asymptotic analysis is used to prove that solutions obtained by the novel semi-discrete scheme satisfy maximum principle property and a Kruzhkov entropy solution, as well as robust conditions for TVNI (scalar case), and positivity principle for multidimensional system of hyperbolic conservation laws [8, 9]. The latter is a suitable designing principle for solving multidimensional hyperbolic systems of conservation laws.

- Thanks to the *no-flow concept*, we have no need of the eigenvalues associated with the hyperbolic flux to guarantee the weak positivity of our numerical scheme. This concept (*weak positivity*) is introduced in this thesis to prove that the solution conserved the L^1 norm, even for systems.

- The extension of the general result of the stability conditions in L^1-bound, in two space dimensions, is made dimension-by-dimension. For concreteness, such extension

results in that the stability condition by Courant–Friedrichs–Lewy (CFL) becomes more restraint.

- The main difference in the extension of the one-dimensional scheme to the multi-dimensional formulation lies in the fact that the approach used for total variation non-increasing is completely different from the one used in one-dimensional case. The proof of total variation non-increasing in one-dimensional case is made using Harten's lemma, which works with the linearized form of the scheme. When it comes to a higher dimension, the proof of the TVNI condition is made in a non-linear conservative form. The line of this proof is different in relation to Harten's lemma, it is not an extension or a reformulation of that lemma.
- We discuss and detail convincing robust numerical results in order to verify that this new positive scheme is easy to implement and capable of capturing accurate solutions for hyperbolic problems.

1.3 Highlights of this thesis

Here, we highlight some interesting points from the sequel of novel results obtained through the development of this thesis, as well as the new semi-discrete method.

- No-flow curves and novel semi-discrete TVNI Lagrangian-Eulerian scheme (SDLE).
- A blow-up numerical weak asymptotic analysis; Kruzhkov entropy solution.
- SDLE is Riemann-solver free and does not require field-by-field type decompositions.
- No dimensional splitting strategy is required.
- The 2D SDLE scheme satisfies a positivity principle for systems.
- No need for eigenvalues to guarantee the weak positivity of the numerical method.
- Non-trivial 1D and 2D hyperbolic-transport models - scalar and systems.
- Entropy glitch effect is well resolved.

1.4 Scientific contribution

During the course of this thesis, the following scientific developments have been achieved

Submitted manuscripts under review:

- E. Abreu, J. François, W. Lambert, J. Pérez, "*A Lagrangian-Eulerian semi-discrete scheme for hyperbolic-transport models.*"

- E. Abreu, J. François, W. Lambert, J. Pérez, "*A class of positive semi-discrete Lagrangian-Eulerian schemes for multidimensional systems of hyperbolic conservation laws.*"

Presentations in conferences:

- Workshop on Numerical Analysis and Applications. "*A semi-discrete Lagrangian-Eulerian approach for hyperbolic conservation laws*". IMECC-UNICAMP, March 2019

- Virtual congress, E. Abreu, J. François, W. Lambert, J. Pérez, "*A class of semi-discrete Lagrangian–Eulerian schemes for hyperbolic-transport models in porous media*", WCCM-ECCOMAS CONGRESS, January 2021.

- Minisymposium, E. Abreu, J. François, W. Lambert, J. Pérez, P. Ferraz "*A Lagrangian-Eulerian Scheme for Numerical Modeling and Simulation of coupled Transport Subsurface Flow Systems with Discontinuous Coefficients*", GS21 SIAM, June 2021.

- 8° Congreso Metropolitano de Modelado y Simulación Numérica 2021, Virtual Congress, 5-7 de mayo, 2021, Schedule in México by Universidad Nacional Autónoma de México, Joint work with: E. Abreu, J. François, W. Lambert, J. Pérez.

1.5 Organization of the thesis

All that remains in the thesis is organized as follows: In Chapter 2, we present the constructed new class Semi-Discrete Lagrangian-Eulerian (SDLE) schemes linked to the concept of *no-flow curve*. We rigorously test the convergence (via the weak asymptotic solution theory) of the approximations provided by the proposed semi-discrete scheme towards the unique entropy solution to a general initial value problem for a conservation law with convex and non-convex flux. Additionally, we prove that the scheme satisfies some kind of Kruzhkov entropy solution, as well as some robust conditions for TVNI properties including the precompactness of the sequence of solutions constructed with the semi-discrete scheme. Then we present and discuss robust numerical examples for scalar linear and non-linear hyperbolic problems to verify the theory and application of the method in one-dimensional hyperbolic models, including a short review of the Wasserstein distance. In Chapter 3, we introduce the SDLE scheme for scalar two-dimensional hyperbolic conservation laws and via the weak asymptotic solution theory we provide rigorous proof of the entropy-convergence of the approximations produced by the semi-discrete

scheme to the unique solution for a general scalar multidimensional initial value problem of a conservation law with convex and non-convex flux including conditions for Total Variation Non-increasing $TVNI$. Further, we prove that the scheme satisfies a maximum principle property and a Kruzhkov entropy solution well as. We also prove the precompactness of the sequence of solutions constructed with the semi-discrete scheme. Finally, we present significant application aspects with numerical experiments for non-trivial nonlinear hyperbolic problems arising in physics of fluids, engineering, and applied sciences. In Chapter 4, we detail the extension of the scalar semi-discrete scheme (1D, 2D) to (1D, 2D)-systems of hyperbolic conservation laws. Next, we show that in the more general context of multidimensional hyperbolic systems of conservation laws, the scheme satisfies the positivity principle. We implement a set of robust numerical examples to verify the theory and illustrate the capabilities of the SDLE method. Lastly, our conclusion and perspectives for the future are presented in Chapter 5.

2 Semi-Discrete Lagrangian-Eulerian scheme for scalar hyperbolic conservation laws in one space dimension

In this chapter, we introduce a new class of Semi-Discrete Lagrangian-Eulerian (SDLE) schemes based on the same framework of the fully-discrete Lagrangian-Eulerian scheme presented in [74], to solve initial value problems that involve hyperbolic conservation laws of the form,

$$\frac{\partial u}{\partial t} + \frac{\partial H(u)}{\partial x} = 0, \quad x \in \mathbb{R}, \quad t > 0, \qquad u(x,0) = u_0(x). \tag{2.1}$$

Here, $H \in C^2(\Omega)$, $H : \Omega \to \mathbb{R}$, $u_0(x) \in L^\infty(\mathbb{R})$, and $u = u(x,t) : \mathbb{R} \times \mathbb{R}^+ \longrightarrow \Omega \subset \mathbb{R}$. The proposed semi-discrete method is based on the novel concept of Lagrangian-Eulerian no-flow curves (*per time step*), which has been previously implemented for fully-discrete Lagrangian-Eulerian schemes [8, 9, 10, 11, 13, 14, 15, 74, 75]. Hyperbolic conservation laws such as model (2.1) appear in applications arising in several areas of study such as physics of fluids, engineering, and applied sciences (see e.g., [6, 10, 13, 32] and references cited therein). The analysis tool presented in this chapter (also presented in the next chapter for two-dimensional problems) is based on a recent weak asymptotic analysis introduced in [2, 3], in which we have improved our understanding of the mathematical analysis for its application to numerical approximation of differential equations. We also present significant application aspects with numerical experiments for non-trivial nonlinear hyperbolic problems arising in physics of fluids, engineering and applied sciences, aiming to support general assumptions about the scheme related to real examples.

2.1 Construction of the new class of semi-discrete Lagrangian-Eulerian schemes in one space dimension

To construct the semi-discrete scheme, we first consider the scalar one-dimensional Cauchy problem (2.1). As in [9, 10, 13, 14], let's $D_j^{n,n+1} = \{(x,t) \,/\, \sigma_j^n(t) \leqslant x \leqslant \sigma_{j+1}^n(t),\ t^n \leqslant t \leqslant t^{n+1}\}$ be the cell-centered finite volume within a Lagrangian framework, where $\sigma_j^n(t)$ and $\sigma_{j+1}^n(t)$, $t \in [t^n, t^{n+1}]$ are two *no-flow curves* such that $\sigma_j^n(t^n) = x_j^n$ and $\sigma_{j+1}^n(t^n) = x_{j+1}^n$, i.e., the space-time local control volume, $D_j^{n,n+1}$, (see Figure 1) is the set contained between $[x_j^n, x_{j+1}^n]$ (bottom) and $[\overline{x}_j^{n+1}, \overline{x}_{j+1}^{n+1}]$ (top). At the next time level ($t = t^{n+1}$), we define $\sigma_j^n(t^{n+1}) = \overline{x}_j^{n+1}$ and $\sigma_{j+1}^n(t^{n+1}) = \overline{x}_{j+1}^{n+1}$ as the endpoints of the *no-flow curves*.

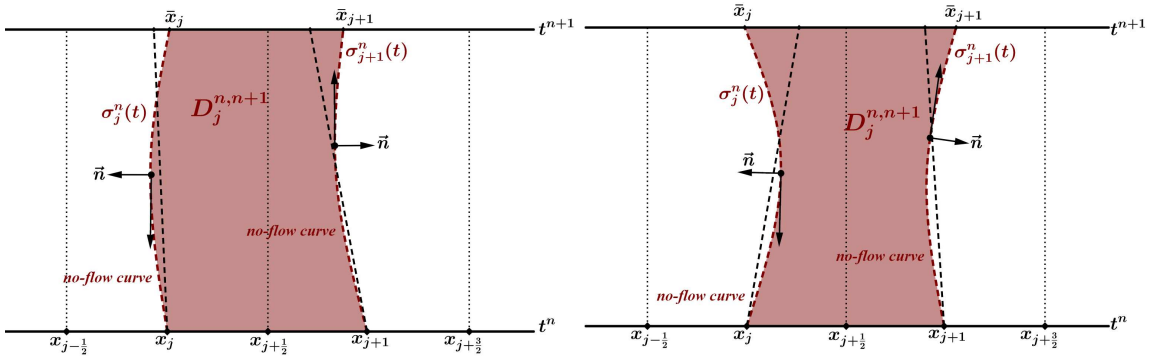

Figure 1 – Possible geometric representations of the Lagrangian-Eulerian space-time control volume $D_j^{n,n+1}$ (*and no-flow curves* $\sigma_j^n(t)$ *and* $\sigma_{j+1}^n(t)$) and its first-order approximation (straight lines) from time level t^n to time level t^{n+1}. On the uniform grid we denote $\Delta x = x_{j+\frac{1}{2}} - x_{j-\frac{1}{2}}$ and $x_{j+\frac{1}{2}} = (j+1/2)\Delta x$, for $j \in \mathbb{Z}$. $\vec{n}$ denotes the outward normal vector.

Let us first write (2.1) in its divergent form (along with $u(x,0) = u_0(x)$ for $x \in \mathbb{R}$),

$$\nabla \cdot \begin{bmatrix} H(u) \\ u \end{bmatrix} = 0, \quad t > 0, \quad x \in \mathbb{R}, \qquad u(x,0) = u_0(x), \quad x \in \mathbb{R}. \tag{2.2}$$

Applying the divergence theorem in (2.2) over $D_j^{n,n+1}$ results in ($s = \partial D_j^{n,n+1}$)

$$\iint\limits_{D_j^{n,n+1}} \nabla \cdot \begin{bmatrix} H(u) \\ u \end{bmatrix} dV = \oint\limits_{\partial D_j^{n,n+1}} \begin{bmatrix} H(u) \\ u \end{bmatrix} \cdot \vec{n} ds \quad \text{and} \quad \oint\limits_{\partial D_j^{n,n+1}} \begin{bmatrix} H(u) \\ u \end{bmatrix} \cdot \vec{n} ds = 0. \tag{2.3}$$

Given the importance of *local conservation* in many nonlinear hyperbolic problems arising in physics of fluids, engineering and fundamental applied sciences, to name but a few fields with increasing research activity and their solutions, the numerical scheme is thus naturally expected to satisfy some kind of local conservation property in the space-time local control volumes $D_j^{n,n+1}$ from time t^n in the space domain $[x_j^n,\, x_{j+1}^n]$ to future time t^{n+1} in the space domain $[\overline{x}_j^{n+1},\, \overline{x}_{j+1}^{n+1}]$. Let us suppose that there is no-flow through curves $\sigma_j^n(t)$ and $\sigma_{j+1}^n(t)$ over the control volumes $D_j^{n,n+1}$. This means that the space-time local control volumes $D_j^{n,n+1}$ will be satisfied in different meshes given by

$$\int_{\overline{x}_j^{n+1}}^{\overline{x}_{j+1}^{n+1}} u(x, t^{n+1}) dx = \int_{x_j^n}^{x_{j+1}^n} u(x, t^n) dx. \tag{2.4}$$

Now, the *impervious zero-flux* (no-flow curves) family of curves $\sigma_p^n(t)$ governing the (local) *no-flow regions* $D_j^{n,n+1}$, with $p = j,\, j+1$, must be defined. Thus, let $\tau_p(t) = [\sigma_p^n(t), t]^T$ be a parameterized curve with respect to Figure 1 and its tangent vector $\dfrac{d\tau_p(t)}{dt} = [\dfrac{d\sigma_p^n(t)}{dt}, 1]^T$. For $t^n \leqslant t \leqslant t^{n+1}$, we obtain $\dfrac{d\tau_p(t)}{dt} \perp \vec{n}$ if slope $\dfrac{d\tau_p(t)}{dt}$ matches the slope of vector

$[H(u),u]^T$ over curves $\sigma_p^n(t)$ for $p \in \mathbb{Z}$, where, as a result of Eq. (2.3), the normal vector $\vec{n}$ is orthogonal to vector $[H(u),u]^T$. Therefore, there exists a $\varpi \neq 0$ such that $[H(u),u]^T = \varpi \left[\frac{d\sigma_p^n(t)}{dt}, 1\right]^T$, which results in an equivalent set of initial value problems *in the weak (distributional) sense for the underlying conservation law* to deal with the dynamic forward tracking of (2.2),

$$\begin{cases} \dfrac{d\sigma_p^n(t)}{dt} = \dfrac{H(u(\sigma_p^n(t),t))}{u(\sigma_p^n(t),t)}, \qquad t^n \leqslant t \leqslant t^{n+1}, \quad p = j, j+1, \\ \sigma_p^n(t^n) = x_p^n, \quad \text{where } \sigma_p^0(t^0) = x_p^0, \text{ along with } u(\sigma_p^0(t^0),t^0) = u_0(x), \end{cases} \tag{2.5}$$

for all the indexes p in the mesh grid. $u(\sigma_p^0(t^0),t^0) = u_0(x)$ is the initial data at the initial time. It should be noted that the system of ODEs (2.5) applying to each level of time is the mathematical formula of what we call the *no-flow curves*.

We are going to discuss an explicit scalar semi-discrete Lagrangian-Eulerian method in one-dimensional space, which will be extended in two-dimensional spaces in the next chapter. Thus, assuming that we have already computed an approximation of the solution at time level $t = t^n$ and at each time level (for $t = 0$ we have the initial datum), we reconstruct a piecewise linear approximation of the form,

$$L_j(x,t) = u_j(t) + (u_x)_j(t)(x - x_j), \quad x_{j-\frac{1}{2}} \leqslant x \leqslant x_{j-\frac{1}{2}}, \tag{2.6}$$

where $(u_x)_j(t)$ is an approximation to the exact derivative, $u_x(x_j,t)$; and u_j^n is the average of the solution over the uniform grid (see Figure 2). For example, we obtain a scalar TVD reconstruction via the slope limiter,

$$(u_x)_j^n = \text{MM1}\left(\frac{u_j^n - u_{j-1}^n}{\Delta x}, \frac{u_{j+1}^n - u_j^n}{\Delta x}\right), \tag{2.7}$$

where MM1 is the usual minmod limiter defined by

$$\text{MM1}(\Phi_1,\Phi_2) = \frac{1}{2}\left[sign(\Phi_1) + sign(\Phi_2)\right] min\left(|\Phi_1|, |\Phi_2|\right);$$

and $sign(\Phi_1)$, the signal of variable Φ_1. In the numerical experiments (see Section 2.3), we will use the following slope limiter to approximate the numerical derivatives:

$$(u_x)_j^n = \text{MM2}\left(\alpha\theta\frac{u_j^n - u_{j-1}^n}{\Delta x}, \alpha\frac{u_{j+1}^n - u_{j-1}^n}{2\Delta x}, \alpha\theta\frac{u_{j+1}^n - u_j^n}{\Delta x}\right), \qquad 1 \leqslant \theta \leqslant 2, \tag{2.8}$$

where α is an adjusted parameter in the numerical experiments and the minmod limiter $\text{MM2}(\Phi_1,\Phi_2,\Phi_3)$ is given by

$$\text{MM2}(\Phi_1,\Phi_2,\Phi_3) = \text{MM1}\left(\text{MM1}(\Phi_1,\Phi_2),\Phi_3\right).$$

Thus, considering the local conservation relation given by (2.4), and the piecewise linear

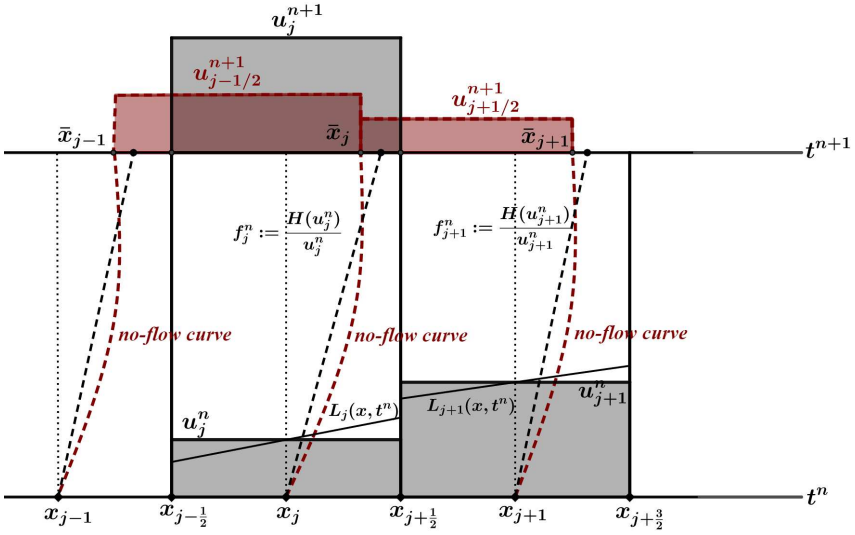

Figure 2 – For illustration purposes, we present the approximation of the quantities involved in the control volume $D_j^{n,n+1}(x,t)$, from time step t^n to t^{n+1}; the no-flow curves $f_j^n := \dfrac{H(u_j^n)}{u_j^n}$ and $f_{j+1}^n := \dfrac{H(u_{j+1}^n)}{u_{j+1}^n}$; the inflow and outflow balance, namely u_j^n and u_{j+1}^n, as well as its corresponding derivatives $(u_x)_j^n$ and $(u_x)_{j+1}^n$; and, finally, the final values u_j^{n+1} and u_{j+1}^{n+1} at time t^{n+1}.

approximations (2.6), we are able to determine the cell average on the nonuniform grid as

$$u_{j+\frac{1}{2}}^{n+1} = \frac{1}{\bar{\Delta}x_j}\int_{\bar{x}_j}^{\bar{x}_{j+1}} u(\xi,t^{n+1})d\xi, \qquad u_{j+\frac{1}{2}}^{n+1} = \frac{1}{\bar{\Delta}x_j}\left[\int_{x_j}^{x_{j+\frac{1}{2}}} L_j(\xi,t^n)d\xi + \int_{x_{j+\frac{1}{2}}}^{x_{j+1}} L_{j+1}(\xi,t^n)d\xi\right].$$

Thus, by a straightforward calculation, we obtain

$$u_{j+\frac{1}{2}}^{n+1} = \frac{1}{\bar{\Delta}x_j}\left[\frac{\Delta x}{2}\left(u_j^n + u_{j+1}^n\right) + \frac{\Delta x^2}{8}\left((u_x)_j^n - (u_x)_{j+1}^n\right)\right]. \tag{2.9}$$

Here, $\bar{\Delta}x_j = \overline{x}_{j+1}^{n+1} - \overline{x}_j^{n+1}$ defines a new mesh width in the x variable at the next time level $t = t^{n+1}$ on interval $[\overline{x}_j^{n+1}, \overline{x}_{j+1}^{n+1}]$ and is given by

$$\bar{\Delta}x_j = (x_{j+1}^n + f_{j+1}^n\Delta t) - (x_j^n + f_j^n\Delta t) = \Delta x + (f_{j+1}^n - f_j^n)\Delta t, \quad \overline{x}_j^{n+1} = x_j^n + f_j^n\Delta t, \tag{2.10}$$

where f_j^n is a local approximation of the no-flow curves in (2.5) defined by

$$f_j^n = \frac{H(u_j^n)}{u_j^n} \approx \frac{H(u)}{u} \text{ for each } j \in \mathbb{Z}. \tag{2.11}$$

In this work, we will focus on this simplest approximation, which leads to a very good and robust scheme. The same is done over the *no-flow region*, $D_{j-1}^{n,n+1} = \{(x,t) \,/\, \sigma_{j-1}^n(t) \leqslant x \leqslant \sigma_j^n(t),\ t^n \leqslant t \leqslant t^{n+1}\}$, to obtain the cell average on the nonuniform grid over the interval $[\overline{x}_{j-1}^{n+1}, \overline{x}_j^{n+1}]$, as follows:

$$u_{j-\frac{1}{2}}^{n+1} = \frac{1}{\bar{\Delta}x_{j-1}}\left[\frac{\Delta x}{2}\left(u_{j-1}^n + u_j^n\right) + \frac{\Delta x^2}{8}\left((u_x)_{j-1}^n - (u_x)_j^n\right)\right], \quad \bar{\Delta}x_{j-1} = \Delta x + (f_j^n - f_{j-1}^n)\Delta t.$$

Finally, through a projection over the original uniform grid, the local approximation solution, u_j^{n+1}, for all $j \in \mathbb{Z}$ is given by (notice that the control volumes $D_j^{n,n+1}$ are naturally self-adaptive with zero cost of implementation in the design of the scheme, yielding a better local approximation),

$$u_j^{n+1} = \frac{1}{\Delta x}\left[m_{1,j}u_{j-\frac{1}{2}}^{n+1} + m_{2,j}u_{j+\frac{1}{2}}^{n+1}\right], \tag{2.12}$$

where $m_{1,j} = \dfrac{\Delta x}{2} + \Delta t f_j^n$ and $m_{2,j} = \dfrac{\Delta x}{2} - \Delta t f_j^n$ are the projection coefficients [10, 13]. These coefficients can be rewritten according to the nonuniform grid as $m_{1,j} = \bar{\Delta}x_{j-1} - m_{2,j-1}$ and $m_{2,j} = \bar{\Delta}x_j - m_{1,j+1}$ to obtain

$$m_{1,j} = \frac{1}{2}\left(\bar{\Delta}x_{j-1} + \Delta t f_j^n + \Delta t f_{j-1}^n\right) \quad \text{and} \quad m_{2,j} = \frac{1}{2}\left(\bar{\Delta}x_j - \Delta t f_j^n - \Delta t f_{j+1}^n\right). \tag{2.13}$$

Then, substituting (2.13) in (2.12) results in the *fully-discrete Lagrangian-Eulerian scheme* with reconstruction in its conservative form ([6, 10, 13]),

$$u_j^{n+1} = u_j^n - \frac{\Delta t}{\Delta x}\left[F\left(u_j^n, u_{j+1}^n\right) - F\left(u_{j-1}^n, u_j^n\right)\right], \tag{2.14}$$

linked to the related numerical flux,

$$\begin{aligned} F\left(u_j^n, u_{j+1}^n\right) = \frac{1}{4}\Bigg[&\frac{\Delta x}{\Delta t}\left(u_j^n - u_{j+1}^n\right) + \Delta x\frac{f_j^n + f_{j+1}^n}{\bar{\Delta}x_j}\left(u_j^n + u_{j+1}^n\right) \\ &+ \frac{\Delta x^2}{4}\frac{f_j^n + f_{j+1}^n}{\bar{\Delta}x_j}\left((u_x)_j^n - (u_x)_{j+1}^n\right) + \frac{\Delta x^2}{4\Delta t}\left((u_x)_j^n + (u_x)_{j+1}^n\right)\Bigg]. \end{aligned} \tag{2.15}$$

It should be noted that (2.14) and (2.15) do not admit a semi-discrete form because the *numerical flux function* blows up when $\Delta t \to 0$. Therefore, in the next subsection, we will show that the *no-flow curves* (2.5) might actually be an effective solution and a new tool, to circumvent the *nature of the blow-up singularity*, thus yielding a new class of explicit semi-discrete Lagrangian-Eulerian schemes.

2.1.1 Properties of the no-flow curves and the new semi-discrete scheme

A dimensionless analysis (see also [13]) of the system of ODEs (2.5) which models the no-flow curves reveal us that $\left[\dfrac{d\sigma_p^n(t)}{dt}\right]$ is in agreement with $\left[\dfrac{\Delta x}{\Delta t}\right]$, and therefore we obtain

$$\left[\frac{d\sigma_p^n(t)}{dt}\right] \propto [O(H(u)/u)], \tag{2.16}$$

where u and $H(u)$ are as in (2.1). From (2.16) we remove the blow-up singularity of the numerical flux (2.15) by replacing $\dfrac{\Delta x}{\Delta t}$ with a stability condition that depends on $O(H(u)/u)$ (this result will be proved in Section 2.2 below).

Formally, the explicit SDLE scheme is constructed as follows. First, we replace $\dfrac{\Delta x}{\Delta t}$ as some approximation function to the *local speeds* in the control volumes $D_j^{n,n+1}$,

$b_{j+\frac{1}{2}} = b_{j+\frac{1}{2}}(f_j, f_{j+1})$, into the scheme (2.14)-(2.15), where, by (2.11) $f_j \equiv \dfrac{H(u_j)}{u_j} \approx \dfrac{H(u)}{u}$ for each $j \in \mathbb{Z}$ *per time step*. This can be simply evaluated at each time interval $[t^n, t^{n+1}]$. For concreteness, we will replace $\dfrac{\Delta x}{\Delta t}$ with some suitable function $b_{j+\frac{1}{2}} = b_{j+\frac{1}{2}}\left(\dfrac{H(u_j^n)}{u_j^n}, \dfrac{H(u_{j+1}^n)}{u_{j+1}^n}\right)$ thanks to the "*no-flow trick*" provided by (2.16). Thus, the explicit semi-discrete approximation for (2.1) can be written as

$$\frac{d}{dt}u_j(t) = \lim_{\Delta t \longrightarrow 0} \frac{u_j^{n+1} - u_j^n}{\Delta t},$$

which leads to the new class of numerical semi-discrete schemes given by

$$\frac{d}{dt}u_j(t) = -\frac{1}{\Delta x}\left[\mathcal{F}(u_j, u_{j+1}) - \mathcal{F}(u_{j-1}, u_j)\right], \tag{2.17}$$

where

$$\mathcal{F}(u_j, u_{j+1}) = \frac{1}{4}\left[b_{j+\frac{1}{2}}\left(u^-_{j+\frac{1}{2}} - u^+_{j+\frac{1}{2}}\right) + (f_j + f_{j+1})\left(u^-_{j+\frac{1}{2}} + u^+_{j+\frac{1}{2}}\right)\right] \tag{2.18}$$

is the associated new Lagrangian numerical flux function, with

$$u^-_{j+\frac{1}{2}} = u_j + \frac{\Delta x}{4}(u_x)_j \quad \text{and} \quad u^+_{j+\frac{1}{2}} = u_{j+1} - \frac{\Delta x}{4}(u_x)_{j+1}. \tag{2.19}$$

The proof of the entropy-convergence of the proposed explicit semi-discrete scheme (2.17)-(2.19) via the weak asymptotic analysis will be presented and discussed in details in the next section.

2.2 Convergence proof of the proposed SDLE via weak asymptotic analysis

We consider the 1D problem (2.1) and $x \in \mathbb{S}^1 = \mathbb{R}/\mathbb{Z}$. We also consider variable $t \in \mathbb{R}^+$, thus $u = u(x,t) : \mathbb{S}^1 \times \mathbb{R}^+ \to \Omega \subset \mathbb{R}$, and the flux function $H = H(u) : \Omega \to \mathbb{R}$.

We assume that function $H(u)$ is locally Lipschitzian function in u in that,

Assumption 1 - For all $c > 0$, $\exists L > 0$ such that

$$|t| \leqslant c, |u_1| \leqslant c, |u_2| \leqslant c \longrightarrow |H(u_1) - H(u_2)| \leqslant L|u_1 - u_2|. \tag{2.20}$$

The weak asymptotic solution is a sequence of solutions $(u_\epsilon)_\epsilon = (u(x,t,\epsilon))_\epsilon$ of class $\mathcal{C}^1$ in t and class L^∞ and is piecewise continuous in x such that, for all $\psi = \psi(x) \in \mathcal{C}_c^\infty(\mathbb{R})$ (smooth with compact support) and for all t,

$$\lim_{\epsilon \to 0} \int_{\mathbb{R}} ((u_\epsilon)_t \psi - H(u_\epsilon)\psi_x)dx = 0 \quad \text{and} \quad u_\epsilon(x,0) = u_0(x). \tag{2.21}$$

The weak asymptotic method consists of first proposing a PDE with a special flux (using parameter ϵ). Then, for each fixed ϵ, we obtain an ODE for variable t. From the theory of ODEs, we prove the existence and stability of the solution. Finally, we demonstrate that, when taking $\epsilon \to 0$, the limit satisfies (2.21).

In our approach, we use an auxiliary function, $f(u) = H(u)/u$ (i.e., *the no-flow curve*). To simplify the following exposition (and without loss of generality), we assume that there exists a $a > 0$ such that $u > a > 0$.

Remark 2.1. *If initial data $u_0(x) \in L^\infty(\mathbb{R})$ in Eq. (2.1) can assume negative, positive, and null values, we consider $N = \sup_{x\in\mathbb{R}} |u_0(x)| + \beta$ for β a positive constant. Then, we consider the following auxiliary problem:*

$$\frac{\partial u}{\partial t} + \frac{\partial H(u-N)}{\partial x} = 0, \quad x \in \mathbb{R}, \quad t > 0, \qquad u(x,0) = u_0(x) + N. \tag{2.22}$$

Note that the new initial data for (2.22) assume only positive values. Under a suitable hypothesis (see Proposition 2.3), we demonstrate that the numerical method satisfies the maximum principle, i.e., solution $u(x,t)$ takes its values between the maximum and minimum values of the initial data. Then, since the solution to (2.22) assumes only positive values, the $u > a > 0$ assumption is valid. In 2.2.5, we prove that if $u(x,t)$ is the (weak and entropy) solution to (2.22), then $u(x,t) - N$ is the solution to (2.1).

Remark 2.2. *From Remark 2.1, given any Cauchy problem for (2.1), we can define auxiliary problem (2.22), which assumes only positive values. This auxiliary problem satisfies the $u > a > 0$ hypothesis, and the convergence proof is valid for the solution to (2.22), which is $u(x,t)$, and for that to (2.1), which is $u(x,t) - N$. The $u > a > 0$ assumption helps us to avoid several technical details in such proofs. In addition, through Remark 2.1, we guarantee the convergence of the numerical method for (2.1) without using any technical details. This is a more elegant strategy to deal with problems of the Lagrangian-Eulerian type via the no-flow curve, which requires $H(u)/u$ to be defined.*

In summary, for the sake of concreteness and simplicity, and without loss of generality, the proof of convergence of the SDLE scheme via the weak asymptotic analysis covers all initial data $u_0(x) \in L^\infty(\mathbb{R})$ in Eq. (2.1) for negative, positive, and null values, which is necessary for industrial and real world problems.

Notice that, in this case, $f(u)$ is a locally Lipschitz function in u in that, for all $c > 0$, $\exists \bar{K} > 0$ such that

$$|t| \leqslant c, |u_1| \leqslant c, |u_2| \leqslant c \longrightarrow |f(u_1) - f(u_2)| \leqslant \bar{K}|u_1 - u_2| \quad \forall\, x \in \mathbb{S}^1. \tag{2.23}$$

Indeed we have

$$\begin{aligned}|f(u_1)-f(u_2)| &= \left|\frac{H(u_1)}{u_1}-\frac{H(u_2)}{u_2}\right| \\ &\leqslant \left|\frac{H(u_1)-H(u_2)}{u_1}\right| + \left|\frac{H(u_2)}{u_2u_1}\right| |u_1-u_2|,\end{aligned}$$

which results

$$\begin{aligned}|f(u_1)-f(u_2)| &\leqslant \frac{L}{|u_1|}|u_1-u_2| + \frac{M}{|u_2u_1|}|u_1-u_2| \\ &\leqslant \bar{K}\,|u_1-u_2|\end{aligned}$$

where $\bar{K}=\left(\frac{L}{c}+\frac{M_c}{c^2}\right)$, $M_c=\max\limits_{|u|\leqslant c} H(u)$ and L Lipschitz constant of H.

2.2.1 Stability conditions and weak asymptotic solution

From numerical method (2.17)-(2.19), we obtain the following PDE:

$$\partial_t(u_\epsilon) = -\frac{1}{\epsilon}\left[\mathcal{F}(u_\epsilon, u_{\epsilon+1}) - \mathcal{F}(u_{\epsilon-1}, u_\epsilon)\right], \tag{2.24}$$

where function $\mathcal{F}(u_\epsilon, u_{\epsilon+1})$ is defined by

$$\begin{aligned}\mathcal{F}(u_\epsilon, u_{\epsilon+1}) = &\frac{1}{4}\left[b_{\epsilon+1/2}\left(u_\epsilon + \frac{\epsilon}{4}(u_x)_\epsilon - \left(u_{\epsilon+1} - \frac{\epsilon}{4}(u_x)_{\epsilon+1}\right)\right)\right] + \\ &+\frac{1}{4}\left[(f(u_\epsilon)+f(u_{\epsilon+1}))\left(u_\epsilon + \frac{\epsilon}{4}(u_x)_\epsilon + \left(u_{\epsilon+1} - \frac{\epsilon}{4}(u_x)_{\epsilon+1}\right)\right)\right],\end{aligned} \tag{2.25}$$

with initial condition $u_\epsilon(x,0)=u_0(x,0)$.

Remark 2.3. *We are interested in studying the ODE in variable t obtained from Eq. (2.24) by fixing ϵ and considering x to be a parameter. We define $u_{\epsilon+i}$ and $(u_x)_{\epsilon+i}$ as*

$$u_{\epsilon+i} = u(x+i\epsilon, t, \epsilon) \quad \textit{and} \quad (u_x)_{\epsilon+i} = (u_x)(x+i\epsilon, t, \epsilon). \tag{2.26}$$

Here, we are using that $u_x=(u_x)(x,t,\epsilon)$ is the approximation to the partial derivative of function $u(x,t,\epsilon)$ with respect to x. Generally, we use a minmod function. Thus, there is a bounded function $\mathcal{M}$ such that

$$u_x = \frac{\mathcal{M}(u(x-p\epsilon,t,\epsilon), u(x-(p-1)\epsilon,t,\epsilon), \cdots, u(x+(p-1)\epsilon,t,\epsilon), u(x+p\epsilon,t,\epsilon))}{\epsilon}, \tag{2.27}$$

where p is an integer that depends on the particular function used to approximate u_x. We notice that applying approximation (2.26) in Eq. (2.24) we will obtain an ODE in time and a discrete parameter in space x.

In what follows, for any approximation of $u_x=(u_x)(x,t,\epsilon)$, we assume that there exist $a>0$ and $a_i\geqslant 0$ for $i=-p,\cdots,p$, for which $(u_x)(x,t,\epsilon)$ satisfies

$$|(u_x)(x,t,\epsilon)| \leqslant \frac{a}{\epsilon}\sum_{i=-p}^{p} a_i |u(x-i\epsilon,t,\epsilon)|. \tag{2.28}$$

We mention the variable $b_{\epsilon+1/2}$ that depends on the *no-flow curves* is important because it comes naturally from the original problem (2.1). Thus, we will obtain rigorous estimates over $b_{\epsilon+1/2}$ for the stability of the semi-discrete scheme (2.17)-(2.19). The quantity $b_{\epsilon+1/2}$ generally depends on function $f(u)$ which is evaluated with some suitable values. Since we use estimates for $b_{_{\epsilon+1/2}}$, we assume that there exists a $\varrho > 0$ such that

$$|b_{_{\epsilon+1/2}}| \leqslant \varrho M, \quad \text{where} \quad M = \sup_{u\in\Omega, t\in[0,T], x\in\mathbb{S}^1} |f(u)| < \infty. \tag{2.29}$$

Based on these conditions and definitions, we state our first result concerning the existence and stability of the solution provided by the numerical method:

Proposition 2.1. *There exists a solution to (2.24), a family of functions $(x,t) \to u(x,t,\epsilon) : \mathbb{S}^1 \times \mathbb{R}^+ \to \mathbb{R}$ for a small enough ϵ, which, for a fixed ϵ, are of class $\mathcal{C}^1$ and class L^∞ for $x \in \mathbb{S}^1$ and satisfy (2.21). Moreover, if*

$$b_{_{\epsilon+1/2}} \geqslant |(f(u_{_\epsilon}) + f(u_{_{\epsilon+1}}))|, \tag{2.30}$$

$$\frac{dt}{\epsilon}(b_{_{\epsilon+1/2}} + |(f(u_{_\epsilon}) + f(u_{_{\epsilon+1}}))|) \leqslant 2, \text{and} \tag{2.31}$$

$$|u_{_\epsilon}| \geqslant \frac{\epsilon}{4}(u_x)_\epsilon, \tag{2.32}$$

then the family $\{u(\cdot,t,\epsilon)\}_\epsilon$ is bounded in $L^1(\mathbb{S}^1)$ uniformly in ϵ. In fact, $||u(.,t,\epsilon)||_{L^1(\mathbb{S}^1)} \leqslant ||u_0||_{L^1(\mathbb{S}^1)}$ for all t. Furthermore, if initial condition $u_0(x)$ and $H(u)$ are continuous, then $u(x,t,\epsilon)$ is also continuous in x.

Proof. First, we fix ϵ and obtain an ODE from (2.24) for variable t and for a parameter x as follows:

$$u'(x,t,\epsilon) = F_\epsilon(u(x,t,\epsilon)), \quad u(0,x) = u_0(x). \tag{2.33}$$

Notice that x is also a parameter in Eq. (2.33). By using notation $u(x) = u(x,t,\epsilon)$, we define $F_\epsilon : L^\infty(\mathbb{S}^1) \longrightarrow L^\infty(\mathbb{S}^1)$ as

$$F_\epsilon(u(x)) = -\frac{1}{\epsilon}\left[\mathcal{F}(u(x), u(x+\epsilon)) - \mathcal{F}(u(x-\epsilon), u(x))\right]. \tag{2.34}$$

From Eq. (2.25), we write $\mathcal{F}(u(x), u(x+\epsilon)) =$

$$\begin{aligned}\frac{1}{4}\Bigg[& b_{_{\epsilon+1/2}}\left(u(x) + \frac{\epsilon}{4}(u_x)(x,t,\epsilon) - \left(u(x+\epsilon) - \frac{\epsilon}{4}(u_x)(x+\epsilon,t,\epsilon)\right)\right) + \\ & \Big\{(f(u(x),x,t) + f(u(x+\epsilon),x,t))\Big[u(x) + \frac{\epsilon}{4}(u_x)(x,t,\epsilon) + \\ & + \left(u(x+\epsilon) - \frac{\epsilon}{4}(u_x)(x+\epsilon,t,\epsilon)\right)\Big]\Big\}\Bigg].\end{aligned} \tag{2.35}$$

The flux function F_ϵ, defined in Eq. (2.34), is a Lipschitz function in variable u because $f(\cdot)$ and $(u_x)(x,t,\epsilon)$ are Lipschitz functions, and F_ϵ is a combination of these two functions (in a very simple way). Based on the classical theory of ODEs in Banach spaces, in the Lipschitzian case, there is a local solution for $t \in [0, \delta(\epsilon)]$ for some $\delta(\epsilon)$ that depends on ϵ. For the global solution, since f is bounded (because H is assumed to be bounded), we can extend the solution to $\delta(\epsilon) \to \infty$. From Assumption 1 in Eq. (2.20), the Lipschitz constants of each F_ϵ can be chosen uniformly on bounded sets $L^\infty(\mathbb{S}^1)$. To demonstrate the existence of solution (2.33) globally (in time), it suffices to prove that, for fixed ϵ, there exists a $c_\epsilon(t) < \infty$ such that $||u(\cdot,t,\epsilon)||_\infty \leqslant c_\epsilon(t) < \infty$. Here, c_ϵ is a continuous function on $[0,\infty)$, with no uniformity in ϵ. We also have that $H(u)$ is a bounded function; thus, if $u \geqslant a > 0$, then f is also bounded. Using the estimates for $|(u_x)(x,t,\epsilon)|$ and $|b_{\epsilon+1/2}|$ from Eqs. (2.28) and (2.29), the ODE, given by (2.24), satisfies

$$|\partial_t(u(x,t,\epsilon))| \leqslant \frac{1}{\epsilon}||u(\cdot,t,\epsilon)||_\infty \theta M, \tag{2.36}$$

where M is given by (2.29),

$$\theta = \left(1 + \frac{a}{4}\sum_{i=-p}^{p}|a_i|\right)(\varrho+2), \qquad \text{and} \qquad ||u(\cdot,t,\epsilon)||_\infty = \operatorname*{ess\,sup}_{x\in\mathbb{S}^1}|u(x,t,\epsilon)|.$$

Solving (2.36), we obtain

$$||u(\cdot,t,\epsilon)||_\infty \leqslant ||u_0(\cdot)||_\infty + \frac{\theta M}{\epsilon}\int_0^t ||u(\cdot,\tau,\epsilon)||_\infty d\tau.$$

From Gronwall formula, we obtain that

$$||u(\cdot,t,\epsilon)||_\infty \leqslant c_\epsilon(t), \qquad \text{where} \qquad c_\epsilon(t) = ||u_0(\cdot)||_\infty \exp\left(\frac{\theta M t}{\epsilon}\right). \tag{2.37}$$

Bound (2.37) indicates the existence of a global solution to ODE (2.24) for each fixed ϵ. However, note that there is no uniformity in ϵ. To demonstrate that the solutions to the ODEs provide a weak asymptotic solution to (2.1), we will prove that the solution is L^1 bounded uniformly with respect to ϵ. To that end, let $T > 0$ for $t + dt \leqslant T$ and $dt > 0$, where dt satisfies some Courant–Friedrichs–Lewy (CFL) condition. From the mean value theorem, we write (2.24) as

$$\begin{aligned}
u(x,t+dt,\epsilon) = u_\epsilon &- \frac{dt}{4\epsilon}\left(b_{\epsilon+1/2}\left(u_\epsilon + \frac{\epsilon}{4}(u_x)_\epsilon - \left(u_{\epsilon+1} - \frac{\epsilon}{4}(u_x)_{\epsilon+1}\right)\right)\right) \\
&- \frac{dt}{4\epsilon}\left((f(u_\epsilon)+f(u_{\epsilon+1}))\left(u_\epsilon + \frac{\epsilon}{4}(u_x)_\epsilon + \left(u_{\epsilon+1} - \frac{\epsilon}{4}(u_x)_{\epsilon+1}\right)\right)\right) \\
&+ \frac{dt}{4\epsilon}\left(b_{\epsilon-1/2}\left(u_{\epsilon-1} + \frac{\epsilon}{4}(u_x)_{\epsilon-1} - \left(u_\epsilon - \frac{\epsilon}{4}(u_x)_\epsilon\right)\right)\right) \\
&+ \frac{dt}{4\epsilon}\left((f(u_{\epsilon-1})+f(u_\epsilon))\left(u_{\epsilon-1} + \frac{\epsilon}{4}(u_x)_{\epsilon-1} + \left(u_\epsilon - \frac{\epsilon}{4}(u_x)_\epsilon\right)\right)\right) + r(x,t,\epsilon,dt),
\end{aligned} \tag{2.38}$$

where $||r(\cdot,t,\epsilon,dt)||_1 \to 0$ (or $||r(\cdot,t,\epsilon,dt)||_\infty \to 0$), uniformly in $t \in [0,T]$ and fixed ϵ (with no uniformity in ϵ) when $dt \to 0$. This behavior results from the continuous differentiability of map $t \longrightarrow u(\cdot,t,\epsilon)$, $[0,\infty) \longrightarrow L^\infty(\mathbb{S}^1)$ for fixed ϵ. After some algebraic steps, we rearrange (2.38) as

$$\begin{aligned} u(x,t+dt,\epsilon) &= \left(u_\epsilon + \frac{\epsilon}{4}(u_x)_\epsilon\right)\left(\frac{1}{2} - \frac{A_\epsilon dt}{4\epsilon}\right) + \left(u_\epsilon - \frac{\epsilon}{4}(u_x)_\epsilon\right)\left(\frac{1}{2} - \frac{B_\epsilon dt}{4\epsilon}\right) \\ &+ \left(u_{\epsilon-1} + \frac{\epsilon}{4}(u_x)_{\epsilon-1}\right)\left(\frac{A_{\epsilon-1} dt}{4\epsilon}\right) + \left(u_{\epsilon+1} - \frac{\epsilon}{4}(u_x)_{\epsilon+1}\right)\left(\frac{B_{\epsilon+1} dt}{4\epsilon}\right), \end{aligned} \tag{2.39}$$

for which, for all $\epsilon > 0$, we define

$$A_\epsilon = b_{\epsilon+1/2} + (f(u_\epsilon) + f(u_{\epsilon+1})) \text{ and } B_{\epsilon+1} = b_{\epsilon+1/2} - (f(u_\epsilon) + f(u_{\epsilon+1})). \tag{2.40}$$

Since we are interested in obtaining the L^1 bound, we take the absolute value,

$$\begin{aligned} |u(x,t+dt,\epsilon)| &\leqslant \left|u_\epsilon + \frac{\epsilon}{4}(u_x)_\epsilon\right|\left|\frac{1}{2} - \frac{A_\epsilon dt}{4\epsilon}\right| + \left|u_\epsilon - \frac{\epsilon}{4}(u_x)_\epsilon\right|\left|\frac{1}{2} - \frac{B_\epsilon dt}{4\epsilon}\right| \\ &+ \left|u_{\epsilon-1} + \frac{\epsilon}{4}(u_x)_{\epsilon-1}\right|\left|\frac{A_{\epsilon-1} dt}{4\epsilon}\right| + \left|u_{\epsilon+1} - \frac{\epsilon}{4}(u_x)_{\epsilon+1}\right|\left|\frac{B_{\epsilon+1} dt}{4\epsilon}\right|. \end{aligned} \tag{2.41}$$

Since (2.30) and (2.31) are satisfied, we have that, for all ϵ,

$$\left|\frac{1}{2} - \frac{A_\epsilon dt}{4\epsilon}\right| = \frac{1}{2} - \frac{A_\epsilon dt}{4\epsilon}, \qquad \left|\frac{1}{2} - \frac{B_\epsilon dt}{4\epsilon}\right| = \frac{1}{2} - \frac{B_\epsilon dt}{4\epsilon},$$

and A_ϵ and B_ϵ are non-negative values. From (2.32), we obtain that

$$\left|u_\epsilon + \frac{\epsilon}{4}(u_x)_\epsilon\right| = |u_\epsilon| + sign(u_\epsilon)\frac{\epsilon}{4}(u_x)_\epsilon \quad \text{and} \quad \left|u_\epsilon - \frac{\epsilon}{4}(u_x)_\epsilon\right| = |u_\epsilon| - sign(u_\epsilon)\frac{\epsilon}{4}(u_x)_\epsilon,$$

where $sign(a)$ is the sign of value a. Thus, (2.41) reduces to

$$\begin{aligned} |u(x,t+dt,\epsilon)| &\leqslant \left(|u_\epsilon| + sign(u_\epsilon)\frac{\epsilon}{4}(u_x)_\epsilon\right)\left(\frac{1}{2} - \frac{A_\epsilon dt}{4\epsilon}\right) + \\ &+ \left(|u_\epsilon| - sign(u_\epsilon)\frac{\epsilon}{4}(u_x)_\epsilon\right)\left(\frac{1}{2} - \frac{B_\epsilon dt}{4\epsilon}\right) \\ &+ \left(|u_{\epsilon-1}| + sign(u_{\epsilon-1})\frac{\epsilon}{4}(u_x)_{\epsilon-1}\right)\left(\frac{A_{\epsilon-1} dt}{4\epsilon}\right) + \left(|u_{\epsilon+1}| - sign(u_{\epsilon+1})\frac{\epsilon}{4}(u_x)_{\epsilon+1}\right)\left(\frac{B_{\epsilon+1} dt}{4\epsilon}\right). \end{aligned} \tag{2.42}$$

This proves that conditions (2.30)-(2.32) provide stability to the method because, by integrating (2.42) and the appropriate translations of $\pm\epsilon$, we obtain

$$||u(\cdot,t+dt,\epsilon)||_1 = \int_{\mathbb{S}^1} |u(x,t+dt,\epsilon)|dx \leqslant \int_{\mathbb{S}^1} |u(x,t,\epsilon)|dx + dt\ r_1(t,\epsilon,dt). \tag{2.43}$$

Here, remainder value $r_1(t,\epsilon,dt) = ||r(\cdot,t,\epsilon,dt)||_1$ is bounded, and $r_1(t,\epsilon,dt) \to 0$ when $dt \to 0$, uniformly in $t \in [0,T]$ for each fixed ϵ. Notice that, for each $T > 0$ given,

we can divide interval $[0,T]$ into n sub-intervals $[jdt_n,(j+1)dt_n]$, where $dt_n=\dfrac{T}{n}$ and $0\leqslant j\leqslant n-1$. Applying this in (2.43), we get

$$\int_{\mathbb{S}^1}|u(x,T,\epsilon)|dx\leqslant\int_{\mathbb{S}^1}|u(x,T-dt_n,\epsilon)|dx+dt_n\ r_1(T-dt,\epsilon,dt). \tag{2.44}$$

Applying recursively for all intervals, we obtain

$$\int_{\mathbb{S}^1}|u(x,T,\epsilon)|dx\leqslant\int_{\mathbb{S}^1}|u_0(x)|dx+dt_n\ \sum_{i=1}^{n}r_1(T-idt,\epsilon,dt). \tag{2.45}$$

Note that

$$dt_n\ |\sum_{i=1}^{n}r_1(T-idt,\epsilon,dt)|\leqslant\frac{T}{n}n\max_i|r_1(T-idt,\epsilon,dt)|=T\max_i|r_1(T-idt,\epsilon,dt)|.$$

Thus, taking the limit $dt\longrightarrow 0$ and using that $r_1(t,\epsilon,dt)\longrightarrow 0$, when $dt\longrightarrow 0$ we obtain

$$||u(\cdot,T,\epsilon)||_1=\int_{\mathbb{S}^1}|u(x,T,\epsilon)|dx\leqslant\int_{\mathbb{S}^1}|u_0(x)|dx=||u_0(\cdot)||_1, \tag{2.46}$$

which gives us the L^1 bounds uniform in ϵ.

To complete the proof of the proposition, we must demonstrate that the solution to (2.24) satisfies the definition of weak solution (2.21). To prove this, we define integral as

$$\begin{aligned}I:=\int_{\mathbb{S}^1}\Bigg\{-\frac{1}{4\epsilon}\Bigg[&\left(b_{\epsilon+1/2}\left(u_\epsilon+\frac{\epsilon}{4}(u_x)_\epsilon+\left(u_{\epsilon+1}-\frac{\epsilon}{4}(u_x)_{\epsilon+1}\right)\right)\right)\\&+\left((f(u_\epsilon)+f(u_{\epsilon+1}))\left(u_\epsilon+\frac{\epsilon}{4}(u_x)_\epsilon+\left(u_{\epsilon+1}-\frac{\epsilon}{4}(u_x)_{\epsilon+1}\right)\right)\right)\\&-\left(b_{\epsilon-1/2}\left(u_{\epsilon-1}+\frac{\epsilon}{4}(u_x)_{\epsilon-1}-\left(u_\epsilon-\frac{\epsilon}{4}(u_x)_\epsilon\right)\right)\right)\\&-\left((f(u_{\epsilon-1})+f(u_\epsilon))\left(u_{\epsilon-1}+\frac{\epsilon}{4}(u_x)_{\epsilon-1}+\left(u_\epsilon-\frac{\epsilon}{4}(u_x)_\epsilon\right)\right)\right)\Bigg]\psi(x)-H(u_\epsilon)\psi_x(x)\Bigg\}dx.\end{aligned} \tag{2.47}$$

Changing the order in the integration variable, we get

$$\begin{aligned}\int_{\mathbb{S}^1}\Bigg\{\frac{1}{4}\Bigg[&\left(b_{\epsilon+1/2}\left(u_\epsilon+\frac{\epsilon}{4}(u_x)_\epsilon-\left(u_{\epsilon+1}-\frac{\epsilon}{4}(u_x)_{\epsilon+1}\right)\right)\right)+\\&+\left((f(u_\epsilon)+f(u_{\epsilon+1}))\left(u_\epsilon+\frac{\epsilon}{4}(u_x)_\epsilon+\left(u_{\epsilon+1}-\frac{\epsilon}{4}(u_x)_{\epsilon+1}\right)\right)\right)\Bigg]\frac{\psi(x+\epsilon)-\psi(x)}{\epsilon}\\&-H(u_\epsilon)\psi_x(x)\Bigg\}dx.\end{aligned} \tag{2.48}$$

Using that $(\psi(x+\epsilon)-\psi(x))/\epsilon=\psi_x(x)+\mathbb{O}(\epsilon)$, that u_ϵ and $(u_x)_\epsilon$ are bounded, and that function $u(x,t,\epsilon)$ is continuous minus a set of null measure (their discontinuities are in a set of null measure), we have that

$$\begin{aligned}&\lim_{\epsilon\longrightarrow 0}\left|\int_{\mathbb{S}^1}\left[\frac{1}{4}\left(b_{\epsilon+1/2}\left(u_\epsilon-u_{\epsilon+1}+\frac{\epsilon}{4}((u_x)_\epsilon+(u_x)_{\epsilon+1})\right)\right)\right]\left(\frac{\psi(x+\epsilon)-\psi(x)}{\epsilon}\right)dx\right|\\&\leqslant\lim_{\epsilon\longrightarrow 0}\left(\int_{\mathbb{S}^1}\frac{1}{4}b_{\epsilon+1/2}|u_\epsilon-u_{\epsilon+1}|\psi_x(x)dx+\mathbb{O}(\epsilon)\right)=0,\end{aligned} \tag{2.49}$$

and using that $H(u) = uf(u)$,

$$\lim_{\epsilon\to 0}\int_{\mathbb{S}^1}\frac{1}{4}\left[\left(\left(f(u_\epsilon)+f(u_{\epsilon+1})\right)\left(u_\epsilon+\frac{\epsilon}{4}(u_x)_\epsilon+\left(u_{\epsilon+1}-\frac{\epsilon}{4}(u_x)_{\epsilon+1}\right)\right)\right)\right]\frac{\psi(x+\epsilon)-\psi(x)}{\epsilon} \tag{2.50}$$

$$\begin{aligned}-H(u_\epsilon)\psi_x(x)dx &= \lim_{\epsilon\to 0}\int_{\mathbb{S}^1}\left(\frac{1}{4}\left[\left(f(u_\epsilon)+f(u_{\epsilon+1})\right)\left(u_\epsilon+u_{\epsilon+1}\right)\right]-u_\epsilon f(u_\epsilon)\right)\psi_x(x)dx+\mathbb{O}(\epsilon)\\ &= \lim_{\epsilon\to 0}\int_{\mathbb{S}^1}\frac{1}{4}\left(u_\epsilon(f(u_{\epsilon+1})-f(u_\epsilon))+f(u_\epsilon)(u_{\epsilon+1}-u_\epsilon)+u_{\epsilon+1}f(u_{\epsilon+1})-u_\epsilon f(u_\epsilon)\right)\psi_x(x)dx\\ &+\mathbb{O}(\epsilon).\end{aligned} \tag{2.51}$$

Defining J as the integral in (2.51) and using that f is a Lipschitz function with constant $\bar{K}$ [Eq. (2.23)],

$$|J| \leqslant \lim_{\epsilon\to 0}\int_{\mathbb{S}^1}\frac{1}{4}\left((\bar{K}|u_\epsilon|+M+L)|u_{\epsilon+1}-u_\epsilon|\right)\psi_x(x)dx, \tag{2.52}$$

where M is given by (2.29) and L Lipschitz constant of H. Using that u_ϵ is continuous (up to a set of null measure), i.e., $\lim_{\epsilon\to 0}|u_{\epsilon+1}-u_\epsilon| = 0$, thus $\lim_{\epsilon\to 0} J = 0$. Finally, from Eqs. (2.51) and (2.52), we prove that $I \to 0$ when $\epsilon \to 0$, i.e., u_ϵ satisfies (2.21), and the proof is completed. ▫.

Remark 2.4. *Eqs.* (2.30) *and* (2.31) *represent the conditions for the stability of the method. However, we can obtain some particular (and useful) estimates for* (2.31)*. If, in condition* (2.30)*, we use that*

$$b_{\epsilon+1/2} = |(f(u_\epsilon)+f(u_{\epsilon+1}))|,$$

then condition (2.31) *reduces to*

$$\frac{dt}{\epsilon}|(f(u_\epsilon)+f(u_{\epsilon+1}))| \leqslant 1. \tag{2.53}$$

Moreover, we can obtain a global estimate for (2.53) *if we consider $b_{\epsilon+1/2}$ is two times the maximum of f from* (2.29)*. In this case, the global CFL condition for* (2.53)*, which is linked to the proposed SDLE scheme (2.17)-(2.19), becomes*

$$b_{\epsilon+1/2} = 2M \quad \longrightarrow \quad \frac{dt}{\epsilon}M \leqslant \frac{1}{2}. \tag{2.54}$$

2.2.2 Conditions for Total Variation Non-increasing ($TVNI_\epsilon$)

We can now prove some further results regarding the scheme described by ODEs of type (2.24). The scheme has a total variation non-increasing property that depends on ϵ. This enables us to define a kind of total variation useful for this study.

We say that a numerical scheme is ϵ total variation non-increasing, denoted as $TVNI_\epsilon$, if

$$TV_\epsilon(u(\cdot,t+dt,\epsilon)) \leqslant TV_\epsilon(u(\cdot,t,\epsilon), \tag{2.55}$$

where

$$TV_\epsilon(u(\cdot,t,\epsilon)) = \int_{\mathbb{S}^1} |u(x+\epsilon,t,\epsilon) - u(x,t,\epsilon)|dx. \tag{2.56}$$

Notice that the total variation for fixed ϵ can be obtained by $TV_\epsilon(u(\cdot,t+dt,\epsilon))/\epsilon$.

Using a similar idea from Harten (see [53]), we can prove the following result:

Lemma 2.1. *If the numerical scheme can be written in the semi-discrete form,*

$$(u(x,t,\epsilon))_t = \frac{C_{x+\frac{\epsilon}{2}}\Delta_{\frac{\epsilon}{2}}u(x,t,\epsilon) - D_{x-\frac{\epsilon}{2}}\Delta_{-\frac{\epsilon}{2}}u(x,t,\epsilon)}{\epsilon}, \tag{2.57}$$

with $C_{x+\frac{\epsilon}{2}}$ and $D_{x-\frac{\epsilon}{2}}$ as the arbitrary values satisfying

$$C_{x+\frac{\epsilon}{2}} \geqslant 0, \quad D_{x-\frac{\epsilon}{2}} \geqslant 0 \text{ and } \quad \frac{dt}{\epsilon}\left(C_{x+\frac{\epsilon}{2}} + D_{x+\frac{\epsilon}{2}}\right) \leqslant 1, \tag{2.58}$$

then the system is $TVNI_\epsilon$ and satisfies

$$TV_\epsilon(u(\cdot,t,\epsilon)) \leqslant TV_\epsilon(u_0(\cdot)), \quad \forall t \in [0,T] \text{ and } u_0(x) \text{ is the initial condition.} \tag{2.59}$$

In Eq. (2.57), we define

$$\Delta_{i\frac{\epsilon}{2}}u(x,t,\epsilon) = u\left(x+(i+1)\frac{\epsilon}{2},t,\epsilon\right) - u\left(x+(i-1)\frac{\epsilon}{2},t,\epsilon\right) \quad \text{for } i \in \mathbb{Z}. \tag{2.60}$$

Note that by using (2.60), we can define $TV_\epsilon(u(\cdot,t,\epsilon))$ as

$$TV_\epsilon(u(\cdot,t,\epsilon)) = \int_{\mathbb{S}^1} |\Delta_{\frac{\epsilon}{2}}u(x,t,\epsilon)|dx. \tag{2.61}$$

Proof of Lemma 2.1**.** From the mean value theorem (for fixed ϵ), we can write (2.57) as

$$u(x,t+dt,\epsilon) = u_\epsilon + \frac{dt}{\epsilon}\left(C_{x+\frac{\epsilon}{2}}\Delta_{\frac{\epsilon}{2}}u(x,t,\epsilon) - D_{x-\frac{\epsilon}{2}}\Delta_{-\frac{\epsilon}{2}}u(x,t,\epsilon)\right) + dtr(x,t,\epsilon,dt) \tag{2.62}$$

for $||r(\cdot,t,\epsilon,dt)||_1 \longrightarrow 0$ (or $||r(\cdot,t,\epsilon,dt)||_\infty \longrightarrow 0$), uniformly in $t \in [0,T]$, and fixed ϵ when $dt \longrightarrow 0$.

Subtracting $u(x,t+dt,\epsilon)$ from $u(x+\epsilon,t+dt,\epsilon)$, both given by (2.62), we obtain

$$\begin{aligned}\Delta_{\frac{\epsilon}{2}}u(x,t+dt,\epsilon) &= \Delta_{\frac{\epsilon}{2}}u(x,t,\epsilon)\left(1 - \frac{dt}{\epsilon}\left(D_{x+\frac{\epsilon}{2}} + C_{x+\frac{\epsilon}{2}}\right)\right)\\ &+ \frac{dt}{\epsilon}D_{x-\frac{\epsilon}{2}}\Delta_{\epsilon-\frac{1}{2}}u(x,t,\epsilon) + \frac{dt}{\epsilon}C_{x+\frac{3\epsilon}{2}}\Delta_{\epsilon+\frac{3}{2}}u(x,t,\epsilon) + dt\Delta_{\frac{\epsilon}{2}}r(x,t,\epsilon,dt),\end{aligned} \tag{2.63}$$

where $\Delta_{\frac{\epsilon}{2}}r(x,t,\epsilon,dt) = r(x,t+\epsilon,\epsilon,dt) - r(x,t,\epsilon,dt)$. Due to (2.58), all coefficients of (2.63) are non-negative; therefore, we have that

$$\begin{aligned}|\Delta_{\frac{\epsilon}{2}}u(x,t+dt,\epsilon)| &\leqslant |\Delta_{\frac{\epsilon}{2}}u(x,t,\epsilon)|\left(1 - \frac{dt}{\epsilon}\left(D_{x+\frac{\epsilon}{2}} + C_{x+\frac{\epsilon}{2}}\right)\right)\\ &+ \frac{dt}{\epsilon}D_{x-\frac{\epsilon}{2}}|\Delta_{\epsilon-\frac{1}{2}}u(x,t,\epsilon)| + \frac{dt}{\epsilon}C_{x+\frac{3\epsilon}{2}}|\Delta_{\frac{3\epsilon}{2}}u(x,t,\epsilon)| + dt|\Delta_{\frac{\epsilon}{2}}r(x,t,\epsilon,dt)|.\end{aligned} \tag{2.64}$$

Integrating (2.64) in $x \in \mathbb{S}^1$, we notice that, due to translations of $\pm\epsilon$, there is a two-by-two simplification of the terms of (2.64) as in Eq. (2.43). Thus, we get

$$\begin{aligned} TV_\epsilon(u(x,t+dt,\epsilon)) &= \int_{\mathbb{S}^1} |\Delta_{\frac{\epsilon}{2}} u(x,t+dt,\epsilon)|dx \\ &\leqslant \int_{\mathbb{S}^1} |\Delta_{\frac{\epsilon}{2}} u(x,t,\epsilon)|dx + dt \int_{\mathbb{S}^1} |\Delta_{\frac{\epsilon}{2}} r(x,t,\epsilon,dt)|dx \\ &= TV_\epsilon(u(x,t,\epsilon)) + dt \int_{\mathbb{S}^1} |\Delta_{\frac{\epsilon}{2}} r(x,t,\epsilon,dt)|dx. \end{aligned} \tag{2.65}$$

Since $\int_{\mathbb{S}^1} |\Delta_{\frac{\epsilon}{2}} r(x,t,\epsilon,dt)dx| \leqslant 2\int_{\mathbb{S}^1} |r(x,t,\epsilon,dt)|dx = ||r(\cdot,t,\epsilon,dt)||_1 \longrightarrow 0$ when $dt \longrightarrow 0$ and using an argument similar to that we used to prove (2.46), we obtain (2.59). ▫.

To demonstrate that our scheme satisfies the $TVNI_\epsilon$ property, we must prove that our method satisfies the hypothesis of Lemma 2.1. We assume some conditions on function (u_x) and that there exists $(\alpha)_\epsilon$ and $(\gamma)_\epsilon$, which depend on x, such that

$$(u_x)_{\epsilon+1} + (u_x)_\epsilon = (\alpha)_\epsilon (u_{\epsilon+1} - u_\epsilon) \quad \text{and} \tag{2.66}$$

$$(u_x)_{\epsilon+1} - (u_x)_\epsilon = (\gamma)_\epsilon (u_{\epsilon+1} - u_\epsilon). \tag{2.67}$$

Thus, we can prove the following proposition on the $TVNI_\epsilon$ condition of our method:

Proposition 2.2. *Let us assume that the approximation to the derivatives satisfies* (2.66) *and* (2.67)*, and that* $b_{\epsilon+1/2}$ *and* $b_{\epsilon-1/2}$ *are chosen to satisfy*

$$b_{\epsilon+1/2}\left(1 - \frac{\epsilon}{4}(\alpha)_\epsilon\right) - (f(u_\epsilon) + f(u_{\epsilon+1}))\left(1 - \frac{\epsilon}{4}(\gamma)_\epsilon\right) - 2u_\epsilon f'((\theta_x)_{\epsilon+1}) \geqslant 0 \tag{2.68}$$

$$b_{\epsilon-1/2}\left(1 - \frac{\epsilon}{4}(\alpha)_{\epsilon-1}\right) + (f(u_{\epsilon-1}) + f(u_\epsilon))\left(1 + \frac{\epsilon}{4}(\gamma)_{\epsilon-1}\right) + 2u_\epsilon f'((\theta_x)_\epsilon) \geqslant 0 \tag{2.69}$$

$$\frac{dt}{\epsilon}\left(b_{\epsilon+1/2}\left(1 - \frac{\epsilon}{4}(\alpha)_\epsilon\right) + \frac{\epsilon}{4}(\gamma)_\epsilon\left(f(u_\epsilon) + f(u_{\epsilon+1})\right) + (u_{\epsilon+1} - u_\epsilon) f'((\theta_x)_{\epsilon+1})\right) \leqslant \frac{1}{2}. \tag{2.70}$$

Then, numerical scheme (2.24) *is* $TVNI_\epsilon$*. Here,* $(\theta_x)_{\epsilon+1}$ *is a value between* u_ϵ *and* $u_{\epsilon+1}$*.*

Proof. We must write our numerical scheme in the form of (2.57). We can write the Right Hand Side (RHS) of Eq. (2.24) (disregarding $1/4\epsilon$) as

$$\begin{aligned} RHS = &- b_{\epsilon+1/2}\left(u_\epsilon + \frac{\epsilon}{4}(u_x)_\epsilon - \left(u_{\epsilon+1} - \frac{\epsilon}{4}(u_x)_{\epsilon+1}\right)\right) \\ &- (f(u_\epsilon) + f(u_{\epsilon+1}))\left(u_\epsilon + \frac{\epsilon}{4}(u_x)_\epsilon + \left(u_{\epsilon+1} - \frac{\epsilon}{4}(u_x)_{\epsilon+1}\right)\right) \\ &+ b_{\epsilon-1/2}\left(u_{\epsilon-1} + \frac{\epsilon}{4}(u_x)_{\epsilon-1} - \left(u_\epsilon - \frac{\epsilon}{4}(u_x)_\epsilon\right)\right) \\ &+ (f(u_{\epsilon-1}) + f(u_\epsilon))\left(u_{\epsilon-1} + \frac{\epsilon}{4}(u_x)_{\epsilon-1} + \left(u_\epsilon - \frac{\epsilon}{4}(u_x)_\epsilon\right)\right). \end{aligned} \tag{2.71}$$

Using that

$$\begin{aligned} &(f(u_\epsilon) + f(u_{\epsilon+1}))(u_\epsilon + u_{\epsilon+1}) - (f(u_{\epsilon-1}) + f(u_\epsilon))(u_{\epsilon-1} + u_\epsilon) = \\ &(f(u_\epsilon) + f(u_{\epsilon+1}))\Delta_{\frac{\epsilon}{2}} u + (f(u_{\epsilon-1}) + f(u_\epsilon))\Delta_{-\frac{\epsilon}{2}} u + 2u_\epsilon(f(u_{\epsilon+1}) - f(u_{\epsilon-1})), \end{aligned}$$

we can rearrange (2.71) as

$$\begin{aligned} RHS =& b_{\epsilon+1/2}\left(\Delta_{\frac{\epsilon}{2}}u-\frac{\epsilon}{4}((u_x)_{\epsilon}+(u_x)_{\epsilon+1})\right)-b_{\epsilon-1/2}\left(\Delta_{-\frac{\epsilon}{2}}u-\frac{\epsilon}{4}((u_x)_{\epsilon-1}+(u_x)_{\epsilon})\right)\\ &-(f(u_{\epsilon})+f(u_{\epsilon+1}))\left(\Delta_{\frac{\epsilon}{2}}u-\frac{\epsilon}{4}((u_x)_{\epsilon+1}-(u_x)_{\epsilon})\right)\\ &-(f(u_{\epsilon-1})+f(u_{\epsilon}))\left(\Delta_{-\frac{\epsilon}{2}}u+\frac{\epsilon}{4}((u_x)_{\epsilon}-(u_x)_{\epsilon-1})\right)-2u_{\epsilon}(f(u_{\epsilon+1})-f(u_{\epsilon-1})). \end{aligned} \tag{2.72}$$

Using the mean value theorem, we can write

$$\begin{aligned} f(u_{\epsilon+1})-f(u_{\epsilon-1}) &= f(u_{\epsilon+1})-f(u_{\epsilon})+f(u_{\epsilon})-f(u_{\epsilon-1})\\ &= f'((\theta_x)_{\epsilon+1})\Delta_{\frac{\epsilon}{2}}u+f'((\theta_x)_{\epsilon})\Delta_{-\frac{\epsilon}{2}}u, \end{aligned} \tag{2.73}$$

where $(\theta_x)_{\epsilon+1}$ is a value between u_{ϵ} and $u_{\epsilon+1}$. Using (2.73), (2.66), and (2.67), we obtain

$$\begin{aligned} RHS =& b_{\epsilon+1/2}\Delta_{\frac{\epsilon}{2}}u\left(1-\frac{\epsilon}{4}(\alpha)_{\epsilon}\right)-b_{\epsilon-1/2}\Delta_{-\frac{\epsilon}{2}}u\left(1-\frac{\epsilon}{4}(\alpha)_{\epsilon-1}\right)\\ &-(f(u_{\epsilon})+f(u_{\epsilon+1}))\Delta_{\frac{\epsilon}{2}}u\left(1-\frac{\epsilon}{4}(\gamma)_{\epsilon}\right)-(f(u_{\epsilon-1})+f(u_{\epsilon}))\Delta_{-\frac{\epsilon}{2}}u\left(1+\frac{\epsilon}{4}(\gamma)_{\epsilon-1}\right)\\ &-2u_{\epsilon}\left(f'((\theta_x)_{\epsilon+1})\Delta_{\frac{\epsilon}{2}}u+f'((\theta_x)_{\epsilon})\Delta_{-\frac{\epsilon}{2}}u\right). \end{aligned} \tag{2.74}$$

Rearranging (2.74) in the form of (2.57), we get

$$\begin{aligned} RHS =& \left(b_{\epsilon+1/2}\left(1-\frac{\epsilon}{4}(\alpha)_{\epsilon}\right)-(f(u_{\epsilon})+f(u_{\epsilon+1}))\left(1-\frac{\epsilon}{4}(\gamma)_{\epsilon}\right)-2u_{\epsilon}f'((\theta_x)_{\epsilon+1})\right)\Delta_{\frac{\epsilon}{2}}u\\ &-\left(b_{\epsilon-1/2}\left(1-\frac{\epsilon}{4}(\alpha)_{\epsilon-1}\right)+(f(u_{\epsilon-1})+f(u_{\epsilon}))\left(1+\frac{\epsilon}{4}(\gamma)_{\epsilon-1}\right)+2u_{\epsilon}f'((\theta_x)_{\epsilon})\right)\Delta_{-\frac{\epsilon}{2}}u. \end{aligned} \tag{2.75}$$

Comparing (2.75) with (2.57), we have that

$$C_{x+\frac{\epsilon}{2}}=b_{\epsilon+1/2}\left(1-\frac{\epsilon}{4}(\alpha)_{\epsilon}\right)-(f(u_{\epsilon})+f(u_{\epsilon+1}))\left(1-\frac{\epsilon}{4}(\gamma)_{\epsilon}\right)-2u_{\epsilon}f'((\theta_x)_{\epsilon+1}),$$

$$D_{x-\frac{\epsilon}{2}}=b_{\epsilon-1/2}\left(1-\frac{\epsilon}{4}(\alpha)_{\epsilon-1}\right)+(f(u_{\epsilon-1})+f(u_{\epsilon}))\left(1+\frac{\epsilon}{4}(\gamma)_{\epsilon-1}\right)+2u_{\epsilon}f'((\theta_x)_{\epsilon}).$$

Thus, if conditions (2.68)-(2.70) are satisfied, then the numerical scheme is $TVNI_{\epsilon}$. □

Example 2.1. *Here, we give an example of approximations* (2.66) *and* (2.67)*. For function* $u_{\epsilon}=u(x,t,\epsilon)$*, approximation (2.8) can be written as*

$$(u_x)_{\epsilon}=minmod\left(2\alpha\frac{u_{\epsilon}-u_{\epsilon-1}}{\epsilon},\alpha\frac{u_{\epsilon+1}-u_{\epsilon-1}}{2\epsilon},2\alpha\frac{u_{\epsilon+1}-u_{\epsilon}}{\epsilon}\right) \tag{2.76}$$

for $(u_x)_{\epsilon}=(u_x)(x,t,\epsilon)$ *and* θ*=2. From* (2.76)*, notice that* $(u_x)_{\epsilon}$ *is smaller (or equal to) any expression inside the minmod function. Thus, we have, for instance, that*

$$(u_x)_{\epsilon}=\left(\frac{2(\xi_1)\alpha}{\epsilon}\right)(u_{\epsilon+1}-u_{\epsilon}) \quad with \ -1\leqslant\xi_1\leqslant 1. \tag{2.77}$$

Using a similar argument, we have that

$$(u_x)_{\epsilon+1} = \left(\frac{2(\xi_2)\alpha}{\epsilon}\right)(u_{\epsilon+1} - u_\epsilon) \quad \text{with } -1 \leqslant \xi_2 \leqslant 1. \tag{2.78}$$

From Eqs. (2.77) and (2.78), we obtain (2.66)

$$(u_x)_\epsilon + (u_x)_{\epsilon+1} = \left(\frac{2(\xi_1+\xi_2)\alpha}{\epsilon}\right)(u_{\epsilon+1} - u_\epsilon) = (\alpha)_\epsilon(u_{\epsilon+1} - u_\epsilon).$$

Since $-1 \leqslant \xi_1 \leqslant 1$ and $-1 \leqslant \xi_2 \leqslant 1$, then $-2 \leqslant \xi_1 + \xi_2 \leqslant 2$, which leads to

$$-\frac{4\alpha}{\epsilon} \leqslant (\alpha)_\epsilon \leqslant \frac{4\alpha}{\epsilon}.$$

Using a similar argument, we prove that

$$(u_x)_{\epsilon+1} - (u_x)_\epsilon = (\gamma)_\epsilon(u_{\epsilon+1} - u_\epsilon), \quad \text{with } -\frac{4\alpha}{\epsilon} \leqslant (\gamma)_\epsilon \leqslant \frac{4\alpha}{\epsilon}.$$

Based on this estimate, it is necessary that $\alpha = 1$ to achieve global stability. However, for some numerical experiments, we are able to consider larger values for α in (2.8).

The idea in Example 2.1 could also be used for different approximations to the derivative of u_x, and Proposition 2.2 would still be valid.

In the next subsection, we prove two very important results: the maximum principle property and the Kruzhkov entropy solution.

2.2.3 The maximum principle and the entropy solution

Here, we obtain an abstract proposition that can be used for any numerical method satisfying the hypothesis of Lemma 2.1. In this case, we show that our numerical scheme satisfies the maximum principle.

In the next proposition, we use $u_0(x,\epsilon)$ as a continuous approximation of $u_0(x)$, the initial data for (2.1).

In the following proposition, we use this approximation and state our result as follows:

Proposition 2.3. *Let us assume that numerical method (2.24) can be written in the form of (2.57) and satisfies the hypothesis of Lemma 2.1. Then, any local solution on $[0,T)$, for $T > 0$ of (2.1) using scheme (2.24) takes its values between range $[\min_{x\in\mathbb{S}^1} u_0(x), \max_{x\in\mathbb{S}^1} u_0(x)]$.*

Proof. We consider $x \in \mathbb{S}^1$. First, we take values ϵ (for example ϵ can be rational values) so that $\{n\epsilon\}_{n\in\mathbb{Z}}$ forms a dense set in $\mathbb{S}^1$. By contradiction, we assume that there exists a $\epsilon_0 > 0$ satisfying, for $T > 0$,

$$\sup_{x\in\mathbb{S}^1} u(x,t,\epsilon_0) > \sup_{x\in\mathbb{S}^1} u_0(x,\epsilon_0) \quad \text{for some } t \in [0,T]. \tag{2.79}$$

Since $u_0(x,\epsilon)$ is continuous, we can choose a small enough ϵ_0 and $\eta > 0$ so that for all (x,t), $\{u(x,t,\epsilon_0)\} \subset [\min_{x\in\mathbb{S}^1} u_0(x,\epsilon) - \eta, \max_{x\in\mathbb{S}^1} u_0(x,\epsilon) + \eta]$. Given that $u_0(x,\epsilon_0)$ is smooth, then solution $u(x,t,\epsilon_0)$ from Eq. (2.24) is also smooth because this space can be considered the Banach space $\mathcal{C}(\mathbb{S})$ in the L^∞ norm. Thus, there exists t_0, x_0 such that $\sup_{x\in\mathbb{S}^1} u(x,t,\epsilon_0) = u(x_0,t_0,\epsilon_0)$. Since (x_0,t_0) is a maximum, solution $u(x,t,\epsilon_0)$ satisfies

$$\partial_t u(x_0,t_0,\epsilon_0) \geqslant 0. \tag{2.80}$$

Remark 2.5. *Note that if the point (x_0,t_0) is (internal) critical we have $\partial_t u(x_0,t_0,\epsilon_0) = 0$. On the other hand, if the point (x_0,t_0) lies on the boundary, the function is increasing until it reaches this extremum point, then $\partial_t u(x_0,t_0,\epsilon_0) > 0$ follows. In any case (2.80) is true.*

Moreover, if scheme (2.24) can be written in the form of (2.57) satisfying the hypothesis of Lemma 2.1, we obtain

$$\partial_t u(x_0,t_0,\epsilon_0) = \frac{1}{\epsilon_0}\left(C_{x_0+\frac{\epsilon_0}{2}} \Delta_{\frac{\epsilon_0}{2}} u - D_{x_0-\frac{\epsilon_0}{2}} \Delta_{-\frac{\epsilon_0}{2}} u\right), \tag{2.81}$$

where $C_{x_0+\frac{\epsilon_0}{2}} \geqslant 0$ and $D_{x_0-\frac{\epsilon_0}{2}} \geqslant 0$. We also have that $\Delta_{\frac{\epsilon_0}{2}} u = u(x_0+\epsilon_0,t,\epsilon_0) - u(x_0,t,\epsilon_0)$ and $\Delta_{-\frac{\epsilon_0}{2}} u = u(x_0,t,\epsilon_0) - u(x_0-\epsilon_0,t,\epsilon_0)$. Using the previous notation, we have that

$$u(x_0-\epsilon_0,t_0,\epsilon_0) \leqslant u(x_0,t_0,\epsilon_0) \longrightarrow \Delta_{-\frac{\epsilon_0}{2}} u \geqslant 0$$

and

$$u(x_0+\epsilon_0,t_0,\epsilon_0) \leqslant u(x_0,t_0,\epsilon_0) \longrightarrow \Delta_{\frac{\epsilon_0}{2}} u \leqslant 0.$$

Therefore, from Eq. (2.81), we have that

$$\partial_t u(x_0,t_0,\epsilon_0) \leqslant 0. \tag{2.82}$$

From inequalities (2.80) and (2.82), we obtain that $\partial_t u(x_0,t_0,\epsilon_0) = 0$. Thus, the second member of (2.81) is null. This means that $u(x_0-\epsilon_0,t_0,\epsilon_0) = u(x_0+\epsilon_0,t_0,\epsilon_0) = u(x_0,t_0,\epsilon_0)$, which, by recursion, results in $u(x_0+n\epsilon_0,t_0,\epsilon_0) = u(x_0,t_0,\epsilon_0)$ for all n. In other words, u is constant because u is (at least) continuous and $\mathbb{N}\epsilon_0$ is dense in $\mathbb{S}^1$ module 1 (because ϵ_0 is taken as irrational). From ODE (2.24), u is constant, and the solution is trivial, leading to a contradiction by the assumption. The same argument can be used by substituting sup by inf in Eq. (2.79), and the proof is completed. □

Proposition 2.3 yields the following Corollary:

Corollary 2.1. *Let us assume that numerical method (2.24) satisfies the conditions of Proposition 2.2. Then, it also satisfies the maximum principle, i.e., the solution satisfies $u \in [\min_{x\in\mathbb{S}^1} u_0(x), \max_{x\in\mathbb{S}^1} u_0(x)]$.*

The next step of our construction is to prove that the proposed scheme satisfies a kind of entropy condition. In this thesis, we use the Kruzhkov entropy solution.

We say that a solution $u(x,t) \in L^{\infty}(\mathbb{S}^1 \times [0,T))$ satisfies the Kruzhkov entropy solution if

$$\int_0^T \int_{\mathbb{S}^1} \Big(|u(x,t)-K|\, g_t(x,t) + sign(u(x,t)-K)[u(x,t)f(u(x,t)) - Kf(K)]g_x(x,t)\Big)dxdt + \int_{\mathbb{S}^1} |u_0(x)-K|\, g(x,0)dx \geqslant 0 \tag{2.83}$$

for all $g(x,t) \in \mathcal{C}_0^{\infty}(\mathbb{S}^1 \times [0,T))$.

For this proof, we assume that the sequence generated by scheme (2.24) is pre-compact. Here, we assume that

$$\mu = ||u_0(x)||_{\infty}.$$

Proposition 2.4. *(Kruzhkov entropy solution) Let us assume that the conditions of Proposition 2.2 are satisfied. Then, $u(x,t,\epsilon) \longrightarrow u(x,t)$ when $\epsilon \longrightarrow 0$ in $L^1_{loc}(\mathbb{S}^1 \times [0,\infty))$, when $u(x,t)$ is the only entropy solution to (2.1).*

Proof. We consider a (fixed but generic) constant $K \in [-\mu,\mu]$ and $b_{\epsilon+1/2} = \hat{M}$ for all ϵ. For almost $(x,t) \in \mathbb{S}^1 \times (0,\infty)$ and fixed x and then using (2.24), we get

$$\begin{aligned}
\frac{d}{dt}|u(x,t,\epsilon)-K| &= sign(u_{\epsilon}-K)\frac{d}{dt}u(x,t,\epsilon) \\
&= -\frac{1}{4\epsilon}sign(u_{\epsilon}-K)\Big[\hat{M}\Big(u_{\epsilon} + \frac{\epsilon}{4}(u_x)_{\epsilon} - \Big(u_{\epsilon+1} - \frac{\epsilon}{4}(u_x)_{\epsilon+1}\Big)\Big) \\
&+ \Big((f(u_{\epsilon}) + f(u_{\epsilon+1}))\Big(u_{\epsilon} + \frac{\epsilon}{4}(u_x)_{\epsilon} + \Big(u_{\epsilon+1} - \frac{\epsilon}{4}(u_x)_{\epsilon+1}\Big)\Big)\Big) \\
&- \Big(\hat{M}\Big(u_{\epsilon-1} + \frac{\epsilon}{4}(u_x)_{\epsilon-1} - \Big(u_{\epsilon} - \frac{\epsilon}{4}(u_x)_{\epsilon}\Big)\Big)\Big) + \\
&- \Big((f(u_{\epsilon-1}) + f(u_{\epsilon}))\Big(u_{\epsilon-1} + \frac{\epsilon}{4}(u_x)_{\epsilon-1} + \Big(u_{\epsilon} - \frac{\epsilon}{4}(u_x)_{\epsilon}\Big)\Big)\Big)\Big].
\end{aligned} \tag{2.84}$$

Rearranging the terms, we obtain

$$\begin{aligned}
\frac{d}{dt}|u(x,t,\epsilon)-K| &= sign(u_{\epsilon}-K)\frac{d}{dt}u(x,t,\epsilon) \\
&= \frac{1}{4\epsilon}sign(u_{\epsilon}-K)\Big[u_{\epsilon+1}\hat{B}_{\epsilon+1} + u_{\epsilon-1}\hat{A}_{\epsilon-1} - u_{\epsilon}(\hat{B}_{\epsilon}+\hat{A}_{\epsilon})\Big] + \\
&- \frac{1}{16}sign(u_{\epsilon}-K)\Big[(u_x)_{\epsilon+1}\hat{B}_{\epsilon+1} - (u_x)_{\epsilon-1}\hat{A}_{\epsilon-1} - (u_x)_{\epsilon}(\hat{B}_{\epsilon}-\hat{A}_{\epsilon})\Big],
\end{aligned} \tag{2.85}$$

where

$$\hat{A}_{\epsilon} = \hat{M} + f(u_{\epsilon}) + f(u_{\epsilon+1}) \text{ and } \hat{B}_{\epsilon+1} = \hat{M} - (f(u_{\epsilon}) + f(u_{\epsilon+1})). \tag{2.86}$$

To prove that our method satisfies the Kruzhkov entropy solution, we rewrite (2.85) as

$$\begin{aligned}\frac{d}{dt}|u(x,t,\epsilon)-K| &= sign(u_\epsilon-K)\frac{d}{dt}u(x,t,\epsilon)\\ &= \frac{1}{4\epsilon}sign(u_\epsilon-K)\left[u_{\epsilon+1}\hat{B}_{\epsilon+1}+u_{\epsilon-1}\hat{A}_{\epsilon-1}-K(\hat{M}-2f(K)+\hat{M}+2f(K))\right]\\ &- \frac{1}{4\epsilon}sign(u_\epsilon-K)\left(u_\epsilon(\hat{B}_\epsilon+\hat{A}_\epsilon)-K(\hat{M}-2f(K)+\hat{M}+2f(K))\right)\\ &- \frac{1}{16}sign(u_\epsilon-K)\left[(u_x)_{\epsilon+1}\hat{B}_{\epsilon+1}-(u_x)_{\epsilon-1}\hat{A}_{\epsilon-1}-(u_x)_\epsilon(\hat{B}_\epsilon-\hat{A}_\epsilon)\right]. \qquad (2.87)\end{aligned}$$

Now, we analyze

$$\begin{aligned}&sign(u_\epsilon-K)\left(u_\epsilon(\hat{B}_\epsilon-K(\hat{M}-2f(K))\right)=\\ &=sign(u_\epsilon-K)((u_\epsilon-K)\hat{M}+(Kf(K)-u_\epsilon f(u_{\epsilon-1})+(Kf(K)-u_\epsilon f(u_\epsilon)))). \qquad (2.88)\end{aligned}$$

We are interested in studying (2.88). We have the following possibilities between K and u_ϵ:

1. $K = u_\epsilon$. In this case, since the numerical method is $TVNI_\epsilon$ according to the hypothesis of the numerical scheme, the set for which $K = u_\epsilon \neq u_{\epsilon-1}$ has null measure in $\mathbb{S}^1 \times \mathbb{R}^+$. Thus, if $K = u_\epsilon$, then

   $$((u_\epsilon-K)\hat{M}+(Kf(K)-u_\epsilon f(u_{\epsilon-1})+(Kf(K)-u_\epsilon f(u_\epsilon))=(Kf(K)-u_\epsilon f(u_{\epsilon-1})\neq 0$$

   only in a null measure set.

2. $K \neq u_\epsilon$. Since f is a Lipschitz function, we have that

   $$\begin{aligned}&|Kf(K)-u_\epsilon f(u_{\epsilon-1})+Kf(K)-u_\epsilon f(u_\epsilon)|\\ &\leqslant |Kf(K)-u_\epsilon f(u_{\epsilon-1})|+|Kf(K)-u_\epsilon f(u_\epsilon)|\\ &\leqslant 2(M+Lu_\epsilon)|K-u_\epsilon|+u_\epsilon L|u_\epsilon-u_{\epsilon-1}|\leqslant 2(M+L\mu))|K-u_\epsilon|+\mu L|u_\epsilon-u_{\epsilon-1}|.\end{aligned} \qquad (2.89)$$

   Here, we use that $Kf(K)-u_\epsilon f(u_\epsilon)=(K-u_\epsilon)f(K)+u_\epsilon(f(K)-f(u_\epsilon)$ and $Kf(K)-u_\epsilon f(u_{\epsilon-1})=(K-u_\epsilon)f(K)+u_\epsilon(f(K)-f(u_\epsilon))+u_\epsilon(f(u_\epsilon)-f(u_{\epsilon-1}))$ and L is the Lipschitz constant of f. The states for which $u(x,t,\epsilon)$ is discontinuous is a set of null measure. In the case of the states for which $u(x,t,\epsilon)$ is continuous, we can choose a small enough ϵ such that $|u_\epsilon-u_{\epsilon-1}|\leqslant|K-u_\epsilon|$.

Thus, up to a null measure set, and for a small enough ϵ and $\hat{M}>2M+3L\mu$, we have

$$sign(u_\epsilon-K)(\hat{M}(u_\epsilon-K))=\hat{M}|u_\epsilon-K|\geqslant 2Kf(K)-u_\epsilon(f(u_{\epsilon-1})+f(u_\epsilon)).$$

This leads to

$$\begin{aligned} &sign(u_\epsilon - K)\left(u_\epsilon \hat{B}_\epsilon - K(\hat{M} - 2f(K))\right) = \\ &= sign(u_\epsilon - K)((u_\epsilon - K)\hat{M} + (2Kf(K) - u_\epsilon(f(u_{\epsilon-1}) + f(u_\epsilon))) \\ &= |(u_\epsilon - K)\hat{M} + (2Kf(K) - u_\epsilon(f(u_{\epsilon-1}) + f(u_\epsilon))| = |u_\epsilon \hat{B}_\epsilon - K(\hat{M} - 2f(K))|. \end{aligned} \tag{2.90}$$

The same argument can be used for

$$\begin{aligned} &sign(u_\epsilon - K)\left(u_\epsilon \hat{A}_\epsilon - K(\hat{M} + 2f(K))\right) = \\ &= sign(u_\epsilon - K)((u_\epsilon - K)\hat{M} - (2Kf(K) - u_\epsilon(f(u_{\epsilon-1}) + f(u_\epsilon))), \end{aligned} \tag{2.91}$$

and, for a small enough ϵ and up to a null measure set, we can write

$$\begin{aligned} &sign(u_\epsilon - K)\left(u_\epsilon \hat{A}_\epsilon - K(\hat{M} + 2f(K))\right) = \\ &= sign(u_\epsilon - K)((u_\epsilon - K)\hat{M} - (2Kf(K) - u_\epsilon(f(u_{\epsilon-1}) + f(u_\epsilon))) \\ &= |(u_\epsilon - K)\hat{M} - (2Kf(K) - u_\epsilon(f(u_{\epsilon-1}) + f(u_\epsilon))| = |u_\epsilon \hat{A}_\epsilon - K(\hat{M} + 2f(K))|. \end{aligned} \tag{2.92}$$

Using (2.90), (2.92) and applying the modulus in (2.87), we have that, for a small enough ϵ and up to a null measure set,

$$\begin{aligned} \frac{d}{dt}|u(x,t,\epsilon) - K| \leqslant &\frac{1}{4\epsilon}\left(|u_{\epsilon+1}\hat{B}_{\epsilon+1} - K(\hat{M} - 2f(K))| - |u_\epsilon \hat{B}_\epsilon - K(\hat{M} - 2f(K))|\right) \\ &- \frac{1}{4\epsilon}\left(|u_\epsilon \hat{A}_\epsilon - K(\hat{M} + 2f(K))| - |u_{\epsilon-1}\hat{A}_{\epsilon-1} - K(\hat{M} + 2f(K))|\right) \\ &- \frac{1}{16} sign(u_\epsilon - K)\left[(u_x)_{\epsilon+1}\hat{B}_{\epsilon+1} - (u_x)_{\epsilon-1}\hat{A}_{\epsilon-1} - (u_x)_\epsilon(\hat{B}_\epsilon - \hat{A}_\epsilon)\right]. \end{aligned} \tag{2.93}$$

Multiplying inequality (2.93) by the non-negative test function $g = g(x,t) \in C_0^\infty(\mathbb{S}^1 \times [0,T)), T > 0$, and integrating by parts, we obtain (notice that the null measure set does not modify the value of the integral)

$$\begin{aligned} &-\int_{\mathbb{S}^1} |u_0(x) - A|\, g(x,0)dx - \int_0^T \int_{\mathbb{S}^1} |u(x,t,\epsilon) - A|\, g_t(x,t)dxdt \\ &\leqslant \int_0^T \int_{\mathbb{S}^1} \Big\{ \frac{1}{4\epsilon}\left(|u_{\epsilon+1}\hat{B}_{\epsilon+1} - K(\hat{M} - 2f(K))| - |u_\epsilon \hat{B}_\epsilon - K(\hat{M} - 2f(K))|\right) \\ &- \frac{1}{4\epsilon}\left(|u_\epsilon \hat{A}_\epsilon - K(\hat{M} + 2f(K))| - |u_{\epsilon-1}\hat{A}_{\epsilon-1} - K(\hat{M} + 2f(K))|\right) \\ &- \frac{1}{16} sign(u_\epsilon - K)\left[(u_x)_{\epsilon+1}\hat{B}_{\epsilon+1} - (u_x)_{\epsilon-1}\hat{A}_{\epsilon-1} - (u_x)_\epsilon(\hat{B}_\epsilon - \hat{A}_\epsilon)\right] \Big\}\, g\, dx\, dt. \end{aligned} \tag{2.94}$$

Note that if we take $\epsilon \longrightarrow \epsilon - 1$ in the index, we have that $|u_{\epsilon+1}\hat{B}_{\epsilon+1} - K(\hat{M} - 2f(K))|\ g(x,t) \longrightarrow |u_\epsilon \hat{B}_\epsilon - K(\hat{M} - 2f(K))|\ g(x-\epsilon,t)$; and if we take $\epsilon \longrightarrow \epsilon + 1$ in the index, we have that $|u_{\epsilon-1}\hat{A}_{\epsilon-1} - K(\hat{M} + 2f(K))|\ g(x,t) \longrightarrow |u_\epsilon \hat{A}_\epsilon - K(\hat{M} + 2f(K))|\ g(x+\epsilon,t)$.

Inequality (2.94) is written as

$$
\begin{aligned}
&-\int_{\mathbb{S}^1}|u_0(x)-A|\,g(x,0)dx-\int_0^T\int_{\mathbb{S}^1}|u(x,t,\epsilon)-A|\,g_t(x,t)dxdt\\
&\leqslant\int_0^T\int_{\mathbb{S}^1}\Big\{\frac{1}{4}\Big(-|u_\epsilon\hat{B}_\epsilon-K(\hat{M}-2f(K))|\Big)\left(\frac{g(x,t)-g(x-\epsilon,t)}{\epsilon}\right)dxdt\\
&+\int_0^T\int_{\mathbb{S}^1}\frac{1}{4}\Big(|u_\epsilon\hat{A}_\epsilon-K(\hat{M}+2f(K))|\Big)\left(\frac{g(x+\epsilon,t)-g(x,t)}{\epsilon}\right)dxdt\\
&-\frac{1}{16}\int_0^T\int_{\mathbb{S}^1}\Big\{sign(u_\epsilon-K)\Big[(u_x)_{\epsilon+1}\hat{B}_{\epsilon+1}-(u_x)_{\epsilon-1}\hat{A}_{\epsilon-1}-(u_x)_\epsilon(\hat{B}_\epsilon-\hat{A}_\epsilon)\Big]\Big\}gdxdt.
\end{aligned}
\tag{2.95}
$$

Since $g\in C_0^\infty(\mathbb{S}^1\times[0,T))$, Eq. (2.95) becomes

$$
\begin{aligned}
&-\int_{\mathbb{S}^1}|u_0(x)-A|\,g(x,0)dx-\int_0^T\int_{\mathbb{S}^1}|u(x,t,\epsilon)-A|\,g_t(x,t)dxdt\\
&\leqslant\int_0^T\int_{\mathbb{S}^1}\Big\{\frac{1}{4}\Big(|u_\epsilon\hat{A}_\epsilon-K(\hat{M}+2f(K))|-|u_\epsilon\hat{B}_\epsilon-K(\hat{M}-2f(K))|\Big)g_x(x,t)\Big)dxdt\\
&-\frac{1}{16}\int_0^T\int_{\mathbb{S}^1}\Big\{sign(u_\epsilon-K)\Big[(u_x)_{\epsilon+1}\hat{B}_{\epsilon+1}-(u_x)_{\epsilon-1}\hat{A}_{\epsilon-1}-(u_x)_\epsilon(\hat{B}_\epsilon-\hat{A}_\epsilon)\Big]\Big\}gdxdt\\
&+I(\epsilon).
\end{aligned}
\tag{2.96}
$$

Here, $I(\epsilon)\longrightarrow 0$ when $\epsilon\longrightarrow 0$. Considering that (2.90) and (2.92) are valid, we obtain

$$
\begin{aligned}
&|u_\epsilon\hat{A}_\epsilon-K(\hat{M}+2f(K))|-|u_\epsilon\hat{B}_\epsilon-K(\hat{M}-2f(K))|=\\
&sign(u_\epsilon-K)\Big[u_\epsilon\hat{A}_\epsilon-K(\hat{M}+2f(K))-(u_\epsilon\hat{B}_\epsilon-K(\hat{M}-2f(K)))\Big]=\\
&sign(u_\epsilon-K)\Big[u_\epsilon(2f(u_\epsilon)+f(u_{\epsilon+1})+f(u_{\epsilon-1})-4Kf(K)\Big].
\end{aligned}
\tag{2.97}
$$

By substituting (2.97) in (2.96), we get

$$
\begin{aligned}
&-\int_{\mathbb{S}^1}|u_0(x)-A|\,g(x,0)dx-\int_0^T\int_{\mathbb{S}^1}|u(x,t,\epsilon)-A|\,g_t(x,t)dxdt\\
&\leqslant\int_0^T\int_{\mathbb{S}^1}\Big\{\frac{1}{4}\Big(sign(u_\epsilon-K)\Big[u_\epsilon(2f(u_\epsilon)+f(u_{\epsilon+1})+f(u_{\epsilon-1})-4Kf(K)\Big]\Big)g_x(x,t)\Big)dxdt\\
&+I(\epsilon)-\frac{1}{16}\int_0^T\int_{\mathbb{S}^1}\Big\{sign(u_\epsilon-K)\Big[(u_x)_{\epsilon+1}\hat{B}_{\epsilon+1}-(u_x)_{\epsilon-1}\hat{A}_{\epsilon-1}-(u_x)_\epsilon(\hat{B}_\epsilon-\hat{A}_\epsilon)\Big]\Big\}gdxdt.
\end{aligned}
\tag{2.98}
$$

To complete this proof, we must analyze

$$
\frac{1}{16}\int_0^T\int_{\mathbb{S}^1}\Big\{sign(u_\epsilon-K)\Big[(u_x)_{\epsilon+1}\hat{B}_{\epsilon+1}-(u_x)_{\epsilon-1}\hat{A}_{\epsilon-1}-(u_x)_\epsilon(\hat{B}_\epsilon-\hat{A}_\epsilon)\Big]\Big\}g(x,t)dxdt.
\tag{2.99}
$$

Considering previous arguments, we know that, since the scheme is $TVNI_\epsilon$, for each fixed t, there exists only a finite number of x such that $u_\epsilon(x,t,\epsilon)-K$ changes the signal. Then,

we split $\mathbb{S}^1 = \mathbb{S}_1 \cup \mathbb{S}_2 \cup \mathbb{S}_3$ such that

$$x \in \mathbb{S}_1 \longrightarrow sign(u_\epsilon(x,t,\epsilon) - K) < 0, \tag{2.100}$$

$$x \in \mathbb{S}_2 \longrightarrow sign(u_\epsilon(x,t,\epsilon) - K) > 0, \tag{2.101}$$

and $\mathbb{S}_3$ has null measure. Here, $\mathbb{S}_1$ and $\mathbb{S}_2$ consist (each) of a finite number of sub-intervals. We rewrite the spatial integral on $\mathbb{S}^1$ in (2.99) as

$$\begin{aligned} &-\int_{\mathbb{S}_1} \Big\{ \Big[(u_x)_{\epsilon+1}\hat{B}_{\epsilon+1} - (u_x)_{\epsilon-1}\hat{A}_{\epsilon-1} - (u_x)_\epsilon(\hat{B}_\epsilon - \hat{A}_\epsilon) \Big] \Big\} g(x,t)dxdt \\ &+\int_{\mathbb{S}_2} \Big\{ \Big[(u_x)_{\epsilon+1}\hat{B}_{\epsilon+1} - (u_x)_{\epsilon-1}\hat{A}_{\epsilon-1} - (u_x)_\epsilon(\hat{B}_\epsilon - \hat{A}_\epsilon) \Big] \Big\} g(x,t)dxdt. \end{aligned} \tag{2.102}$$

Now, notice that due to translations of $\pm\epsilon$, we have that

$$\int_{\mathbb{S}_1} \Big\{ \Big[(u_x)_{\epsilon+1}\hat{B}_{\epsilon+1} - (u_x)_{\epsilon-1}\hat{A}_{\epsilon-1} - (u_x)_\epsilon(\hat{B}_\epsilon - \hat{A}_\epsilon) \Big] \Big\} g(x,t)dxdt = 0$$

because the terms inside the integral cancel out (actually, they do not only cancel out at the extremes of the sub-intervals of $\mathbb{S}_1$). The same argument is valid for the integral on $\mathbb{S}_2$. Since the argument is valid for any $t \in [0,T]$, we have that (2.99) is equal to zero.

Then, Eq. (2.98) is written as

$$\begin{aligned} &\int_{\mathbb{S}^1} |u_0(x) - A|\, g(x,0)dx + \int_0^T \int_{\mathbb{S}^1} |u(x,t,\epsilon) - A|\, g_t(x,t)dxdt + \\ &\int_0^T \int_{\mathbb{S}^1} \Big\{ \frac{1}{4} \Big(sign(u_\epsilon - K) \left[u_\epsilon(2f(u_\epsilon) + f(u_{\epsilon+1}) + f(u_{\epsilon-1})) - 4Kf(K) \right] \Big) g_x(x,t) \Big) dxdt \\ &\geqslant -I(\epsilon). \end{aligned} \tag{2.103}$$

Here, $u_\epsilon = u(x,t,\epsilon)$. In Subsection 2.2.4, we show that family $u(x,t,\epsilon)$ for $\epsilon > 0$ is a pre-compact sequence in $L^1(\mathbb{S}^1 \times [0,T])$. Let $u(x,t)$ be an accumulation point of family $u(x,t,\epsilon)$. Thus, for a sub-sequence ϵ_r, we have that $u(x,t,\epsilon_r) \longrightarrow u(x,t)$ when $r \longrightarrow \infty$ in $L^1(\mathbb{S}^1 \times [0,T])$. In other words, notice we have $u(x,t,\epsilon_r + 1) \longrightarrow u(x,t)$ and $u(x,t,\epsilon_r - 1) \longrightarrow u(x,t)$ except in a set of null measure. Now, by taking the limit as $\epsilon = \epsilon_r \longrightarrow 0$ in (2.103), we obtain the entropy relation. Remember that $I(\epsilon) \longrightarrow 0$ and notice that $f(u_\epsilon) \longrightarrow f(u)$ and $f(u_{\epsilon\pm1}) \longrightarrow f(u)$, we get

$$\begin{aligned} &\int_0^T \int_{\mathbb{S}^1} \Big(|u(x,t) - K|\, g_t(x,t) + sign(u(x,t) - K)[u(x,t)f(u(x,t) - Kf(K))]g_x(x,t) \Big) dxdt \\ &\quad + \int_{\mathbb{S}^1} |u_0(x) - K|\, g(x,0)dx \geqslant 0. \end{aligned} \tag{2.104}$$

In Eq. (2.104), $K \in [-\mu, \mu]$. However, for $|K| \geqslant \mu$, notice that the inequality that is Eq. (2.104) reduces to the equality (weak solution),

$$\int_0^T \int_{\mathbb{S}^1} \Big(u(x,t)g_t(x,t) + u(x,t)f(u(x,t)g_x(x,t) \Big) dxdt + \int_{\mathbb{S}^1} u_0(x)g(x,0)dx = 0.$$

From these results, we obtain that (2.104) holds for all $K \in \mathbb{R}$. Since $T > 0$ and $g = g(x,t) \in C_0^\infty(\mathbb{S}^1 \times [0,T))$ are arbitrary, inequality (2.104) leads to solution $u(x,t)$, which is the (unique) entropy solution to (2.1). In particular, an accumulation point $u(x,t)$ of $u(x,t,\epsilon)$ using (2.24) is what is unique about it. This implies that $u(x,t,\epsilon)$ converges to $u(x,t)$ as $\epsilon \to 0$ in $L^1_{loc}(\mathbb{S}^1 \times [0,\infty))$ because T is arbitrary, which completes the proof. ▫

The previous results prove that the proposed method (2.24)-(2.25) obtained from the SDLE scheme (2.17)-(2.19) converges to the entropy solution to (2.1).

2.2.4 The pre-compactness of sequence $u(x,t,\epsilon)$

To prove that sequence $u(x,t,\epsilon)$ is pre-compact, we used some of the results reported in [2]. The first result we need is Lemma 1 in [2].

Lemma 1. *Suppose that* $u(x) \in L^1(\mathbb{T}^n)$, $h > 0$. *Then*

$$\int_{\mathbb{T}^n} |u(x)(signu)^h(x) - |u(x)||dx \leqslant 2\omega^x(h),$$

where

$$\omega^x(h) = \sup_{|\Delta x| \leqslant h} \int_{\mathbb{T}^n} |u(x+\Delta x) - u(x)|dx$$

is the continuity modulus of $u(x)$ in $L^1(\mathbb{T}^n)$.

Here, $\mathbb{T}^n$ is the n-dimensional torus. In this study, we are interested in a one-dimensional problem. For $n = 1$, $\mathbb{T}^n$ reduces to $\mathbb{S}^1$. Since the proof of the previous Lemma does not depend on the scheme, we refer to [2].

Notice that $\omega^x(h)$ is a measure of $TVNI_\epsilon$, as described in Eq. (2.56). Thus, under the same hypothesis of Proposition 2.2, we can prove the following Corollary:

Corollary 2.2. *Let us assume that* $u(x,t,\epsilon)$ *is given by scheme* (2.24) *and satisfies the hypothesis of Proposition* 2.2, *then, for all* $t > 0$, $\Delta x \in \mathbb{R}$, *we have that*

$$\int_{\mathbb{S}^1} |u(x+\Delta x,t,\epsilon) - u(x,t,\epsilon)|dx \leqslant \int_{\mathbb{S}^1} |u_0(x+\Delta x,t,\epsilon) - u_0(x,t,\epsilon)|dx \leqslant \omega^x(|\Delta x|),$$

where

$$\omega^x(|\Delta x|) \leqslant \sup_{|\Delta x| \leqslant h} \int_{\mathbb{S}^1} |u_0(x+\Delta x,t,\epsilon) - u_0(x,t,\epsilon)|dx$$

is the continuity modulus of initial data $u_0(x)$ *in* $\mathbb{S}^1$.

The proof of Corollary 2.2 follows from Proposition 2.2 and the supremum properties of a function. Now, we prove the result to obtain the pre-compactness of sequence $u(x,t,\epsilon)$. The first useful result, similar to that obtained in [2], is:

Lemma 2.2. *Let us assume that* $\phi(x) \in C^1(\mathbb{S}^1)$. *Then* $\forall \Delta t > 0$,

$$\int_{\mathbb{S}^1} (u(c, t+\Delta t, \epsilon) - u(x,t,\epsilon))\phi(x)dx \leqslant N||\nabla\phi||_\infty \mu(\mathbb{S}^1)\Delta t. \tag{2.105}$$

Here, $\mu(\mathbb{S}^1)$ is the measure of $\mathbb{S}^1$ and

$$N = \left(\frac{\hat{M}}{2} + M\right)\left(\mu + \frac{\epsilon}{8}\upsilon\right) \quad \text{and} \quad \mu = ||u_0||_\infty.$$

Proof. Let us denote $I(t) = \int_{\mathbb{S}^1} u(x,t,\epsilon)\phi(x)dx$. Differentiating $I(t)$ from t and using (2.24), we have that

$$\begin{aligned} I'(t) = \int_{\mathbb{S}^1} -\frac{1}{4\epsilon}\Big[&\left(b_{\epsilon+1/2}\left(u_\epsilon + \frac{\epsilon}{4}(u_x)_\epsilon - \left(u_{\epsilon+1} - \frac{\epsilon}{4}(u_x)_{\epsilon+1}\right)\right)\right) + \\ &+ \left((f(u_\epsilon) + f(u_{\epsilon+1}))\left(u_\epsilon + \frac{\epsilon}{4}(u_x)_\epsilon + \left(u_{\epsilon+1} - \frac{\epsilon}{4}(u_x)_{\epsilon+1}\right)\right)\right) \\ &- \left(b_{\epsilon-1/2}\left(u_{\epsilon-1} + \frac{\epsilon}{4}(u_x)_{\epsilon-1} - \left(u_\epsilon - \frac{\epsilon}{4}(u_x)_\epsilon\right)\right)\right) + \\ &- \left((f(u_{\epsilon-1}) + f(u_\epsilon))\left(u_{\epsilon-1} + \frac{\epsilon}{4}(u_x)_{\epsilon-1} + \left(u_\epsilon - \frac{\epsilon}{4}(u_x)_\epsilon\right)\right)\right)\Big]\phi(x)dx. \end{aligned} \tag{2.106}$$

Changing the order in the integration variable, we obtain

$$\begin{aligned} I'(t) = \int_{\mathbb{S}^1} \Big\{\frac{1}{4}\Big[&\left(b_{\epsilon+1/2}\left(u_\epsilon + \frac{\epsilon}{4}(u_x)_\epsilon - \left(u_{\epsilon+1} - \frac{\epsilon}{4}(u_x)_{\epsilon+1}\right)\right)\right) + \\ &+ \left((f(u_\epsilon) + f(u_{\epsilon+1}))\left(u_\epsilon + \frac{\epsilon}{4}(u_x)_\epsilon + \left(u_{\epsilon+1} - \frac{\epsilon}{4}(u_x)_{\epsilon+1}\right)\right)\right)\Big] \frac{\phi(x+\epsilon) - \phi(x)}{\epsilon}dx. \end{aligned} \tag{2.107}$$

Since $I'(t) = G(t)$ implies that $|I(t+\Delta t) - I(t)| \leqslant \max G(t)\Delta t$, we can estimate the RHS of Eq. (2.107) as

$$\begin{aligned} |RHS| \leqslant \Big\{\frac{1}{4}\Big[&\left(\left|b_{\epsilon+1/2}\right|\left(|u_\epsilon| + \frac{\epsilon}{4}\left|(u_x)_\epsilon\right| + \left|u_{\epsilon+1}\right| + \frac{\epsilon}{4}\left|(u_x)_{\epsilon+1}\right|\right)\right) + \\ &+ \left((|f(u_\epsilon)| + \left|f(u_{\epsilon+1})\right|)\left(|u_\epsilon| + \frac{\epsilon}{4}\left|(u_x)_\epsilon\right| + \left(\left|u_{\epsilon+1}\right| - \frac{\epsilon}{4}\left|(u_x)_{\epsilon+1}\right|\right)\right)\right)\Big] \left|\frac{\phi(x+\epsilon) - \phi(x)}{\epsilon}\right| dx. \end{aligned} \tag{2.108}$$

Using that

$$\left|\frac{\phi(x \pm \epsilon) - \phi(x)}{\epsilon}\right| dx \leqslant ||\nabla\phi||_\infty,$$

$b_{\epsilon+1/2} = \hat{M}$, $||(u_x)||_\infty = \upsilon$, $||u(x,t,\epsilon)||_\infty = \mu$, and M given by (2.29), condition (2.105) is satisfied. □

Since we obtained similar estimates in [2], we used Lemma 3 reported in [2].

Lemma 3. *For every* $t \geqslant 0$, $\Delta t > 0$

$$\int_{\mathbb{S}^1} |u(x, t+\Delta t, \epsilon) - u(x,t,\epsilon)|dx \leqslant \omega^t(\Delta t),$$

where $\omega^t(\Delta t) = \inf_{h>0}(4\omega^x(h) + cN\Delta t/h)$, *and* c *is a universal constant.*

Note that, in $\omega^t(\Delta t)$, since this parameter is the infimun, $\omega^t(\Delta t)$, for fixed Δt, reduces to $\inf_{h>0}(4\omega^x(h))$.

Moreover, since $\omega^x(h) \longrightarrow 0$ as $h \longrightarrow 0$ and does not depend on ϵ (based on previous results), family $u(x,t,\epsilon)$ is uniformly bounded and equicontinuous in $L^1(\mathbb{S}^1 \times [0,T])$ for every $T > 0$. Thus, $u(x,t,\epsilon)$ is a pre-compact sequence in $L^1(\mathbb{S}^1 \times [0,T])$, which implies that we can extract a sequence $\epsilon_k \longrightarrow 0$ such that $u_k(x,t) = u(x,t,\epsilon_k) \longrightarrow u(x,t)$ as $k \longrightarrow \infty$ in $L^1_{loc}(\mathbb{S}^1 \times [0,\infty])$.

2.2.5 Weak solution of an auxiliary problem

Here, we give the proof considering the classical weak solution defined in $\mathbb{R} \times \mathbb{R}^+$. The proof is similar for different domains. First, we consider the weak solution to (2.22) to be

$$\int_{\mathbb{R}^+}\int_{\mathbb{R}} (u\varphi_t + H(u-N)\varphi_x)\,dxdt + \int_{\mathbb{R}} (u_0(x)+N)\varphi(x,0)dx = 0, \tag{2.109}$$

where $\varphi = \varphi(x,t)$ is a test function. By substituting $u - N = U$ in (2.109), we obtain

$$\begin{aligned}&\int_{\mathbb{R}^+}\int_{\mathbb{R}} ((U+N)\varphi_t + H(U)\varphi_x)\,dxdt + \int_{\mathbb{R}} (u_0(x)+N)\varphi(x,0)dx = \\ &\int_{\mathbb{R}^+}\int_{\mathbb{R}} (U\varphi_t + H(U)\varphi_x)\,dxdt + \int_{\mathbb{R}} (u_0(x)+N)\varphi(x,0)dx + \int_{\mathbb{R}^+}\int_{\mathbb{R}} N\varphi_t dxdt = 0.\end{aligned} \tag{2.110}$$

Using Fubini's theorem for the integral and assuming that $\varphi(x,t)$ has compact support, then

$$\int_{\mathbb{R}^+}\int_{\mathbb{R}} N\varphi_t dxdt = -\int_{\mathbb{R}} N\varphi(x,0)dx. \tag{2.111}$$

By substituting (2.111) in (2.110), we get

$$\int_{\mathbb{R}^+}\int_{\mathbb{R}} (U\varphi_t + H(U)\varphi_x)\,dxdt + \int_{\mathbb{R}} u_0(x)\varphi(x,0)dx = 0, \tag{2.112}$$

which is the solution to (2.1). The previous calculations are reversible, i.e., (2.112) to (2.109). Thus, if $u(x,t)$ is the solution to (2.1), then $u(x,t) - N$ is the solution to (2.22), and the reciprocal is true.

A similar calculation can be performed to prove that the entropy solutions are the same.

2.3 Numerical experiments

We start with a simple linear advection problem, but with an important accuracy test to prove that the proposed SDLE scheme (2.17)-(2.19) does not deteriorate

as time step Δt decreases when used with several time steps. Next, we consider an inviscid Burgers' model associated with the Wasserstein distance. It should be noted that, by means of stability conditions (2.30) and (2.31) in Proposition 2.1, we can use the no-flow stability estimate $b_{j+\frac{1}{2}}$ in the new Lagrangian numerical flux function (2.18) as follows:

$$b_{j+\frac{1}{2}} = \zeta \max_{j} \{|f_j + f_{j+1}|\}, \qquad 1 \leqslant \zeta \leqslant 2 \tag{2.113}$$

subject to CFL-type stability condition (2.54).

Example 2.2. ***Accuracy test - Linear advection-transport problem***

The new SDLE approach is designed to avoid excessive *numerical diffusion* when several time steps are used in computational studies (e.g., see such spurious effect in the experiments produced by the classical Lax-Friedrichs scheme in the right column in Figure 3). This situation also occurs in real-life and industrial problems such as those related to the spreading of contaminants (or tracers) in subsurface formations, which is modeled using the linear advection model.

Let us consider the initial value problem associated with Eq. (2.1), where $H(u) = u$ and periodic initial data $u(x, 0) = \text{sen}x$. This problem admits a global smooth solution computed using our semi-discrete scheme at time $T = 1$ in a mesh refinement study, as shown in Figure 3. The frames on the left (from top to bottom) present a computational analysis conducted with the novel SDLE scheme when several time steps are used in a reduced manner to mimic a concrete situation that allows us to test if the computed solution is affected by excessive numerical diffusion. The resulting numerical solutions are convincing in verifying the theory and illustrating the capabilities of the approach presented here because of their excellent resemblance with the exact solution. We notice that a high-resolution and second-order ($L^1 - norm$) rate of convergence is achieved in the smooth linear case, as reported in the table of Figure 3.

Example 2.3. ***Inviscid Burgers' equation with Wasserstein distance***

In [45], a class of monotone schemes (Lax-Friedrichs, Enquist-Osher, and Godunov schemes) for scalar conservation laws was proven to be W_1-contractive and converge at a rate of order $O(\Delta x^2)$ in the Wasserstein distance. The Wasserstein distance between two probability measures (μ and ν) on $\mathbb{R}$ can equivalently be defined as

$$W_1(\mu, \nu) := \sup_{||\varphi||_{Lip} \leqslant 1} \int_{\mathbb{R}} \varphi(x) d(\mu - \nu)(x). \tag{2.114}$$

Here, the supremum is taken over all functions $\varphi : \mathbb{R} \longrightarrow \mathbb{R}$ with Lipschitz semi-norm $||\varphi||_{Lip} := \sup_{x \neq y} \left| \dfrac{\varphi(y) - \varphi(x)}{y - x} \right|$ at most 1. Given Borel measurable functions $u, v : \mathbb{R} \longrightarrow \mathbb{R}$ satisfying the analogous properties, we have (see [45])

$$\int_{\mathbb{R}} (u - v)(x) dx = 0, \qquad \int_{\mathbb{R}} |x||u - v|(x) dx \leqslant \infty. \tag{2.115}$$

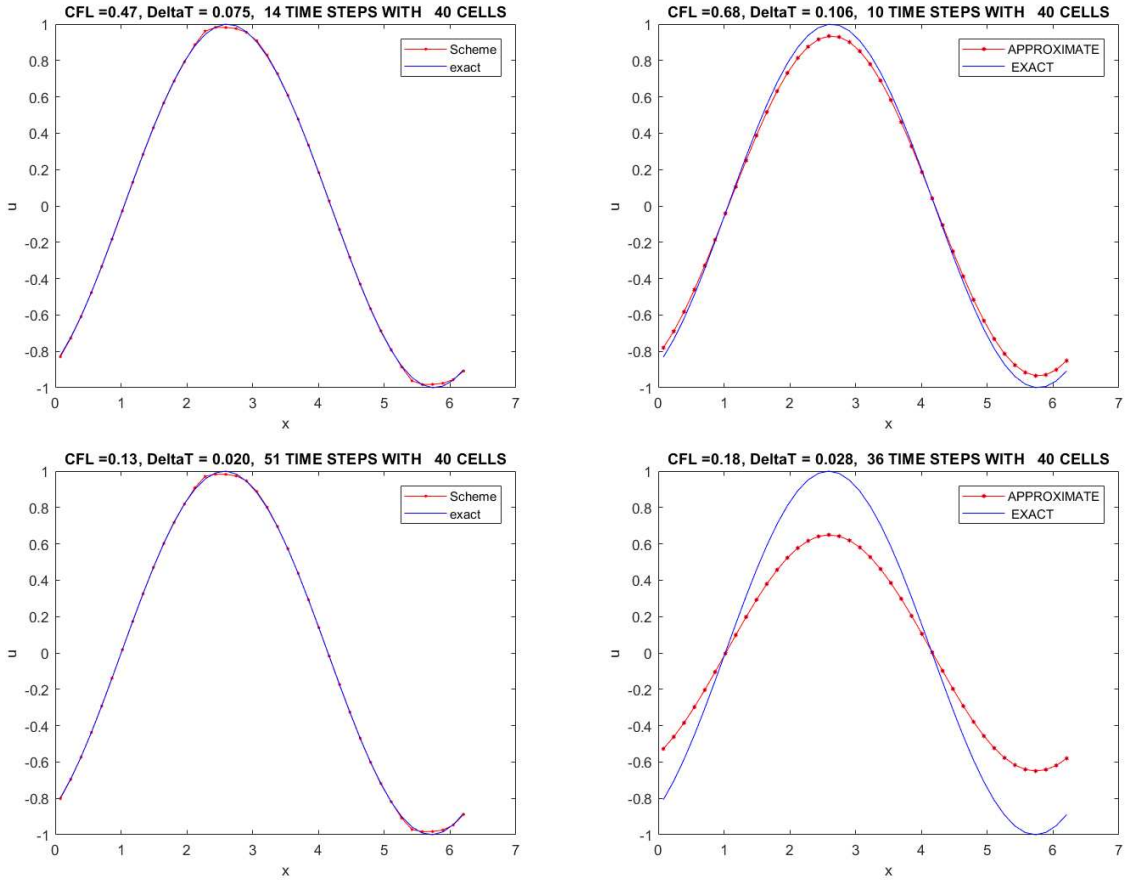

N	$\|\|U-u\|\|_{L^1}$	**Rate**	$\|\|U-u\|\|_{L^\infty}$	**Rate**	$\|\|U-u\|\|_{L^2}$	**Rate**
40	2.6234e-02	-	1.1898e-02	-	1.3313e-02	-
80	6.5036e-03	2.0121e+00	5.1802e-03	1.1997e+00	3.8495e-03	1.7901e+00
160	1.5472e-03	2.0716e+00	1.9706e-03	1.3944e+00	1.1327e-03	1.7648e+00
320	3.8130e-04	2.0207e+00	8.5002e-04	1.2131e+00	3.4145e-04	1.7301e+00
640	9.5181e-05	2.0022e+00	3.6783e-04	1.2085e+00	1.0386e-04	1.7171e+00
1280	2.3618e-05	2.0108e+00	1.4220e-04	1.3711e+00	3.1954e-05	1.7005e+00

Figure 3 – Numerical solution computed using the semi-discrete Lagrangian-Eulerian scheme (left), with $\alpha = 2$, $\zeta = 1$ and $\theta = 2$, and numerical solution computed using the Lax-Friedrichs scheme (right) at time $T = 1$. L^1, L^∞, and L^2-norms of the errors estimated with SDLE ($\alpha = 2$, $\zeta = 1$, and $\theta = 2$) using second-order Runge-Kutta method.

The Wasserstein distance (also known as the $Lip^{'}-norm$) is defined as (in its discrete form)

$$W_1(u,v) := \sup_{||\varphi||_{Lip}\leqslant 1} \int_{\mathbb{R}} \varphi(x) d(u-v)(x),\ W_1(u_{\Delta x}, v_{\Delta x}) := \sum_{i\in\mathbb{N}} \left| \sum_{j<i} (u_j - v_j) \right| \Delta x^2.$$

The Wasserstein error (W_1) must be well-defined and finite by measuring the amount of work that goes into moving the surplus of mass to behind the shock, where there is a shortage of mass. We will reproduce numerical experiments reported in [45] using the following monotone schemes: Lax-Friedrichs, Godunov, Rusanov and the fully-discrete

Lagrangian-Eulerian Finite Volume (LEFV) scheme [11, 13] and the Lagrangian-Eulerian Nonstaggered scheme (LENS) [10] and compare with our SDLE scheme. Although our scheme is not monotone, we see from the results presented in Figure 4 a very good evidence that our scheme also exhibits the desire result to be $O(\Delta x^2)$ in the $Lip^{'}$-norm (in the Wasserstein distance).

Let us consider initial value problem (2.1) with flux function $H(u) = \dfrac{u^2}{2}$ on interval $[0, 1]$, with initial data containing two jumps defined as follows:

$$u_0(x) = \begin{cases} 2, & x < 0.25, \\ 1, & 0.25 \leqslant x < 0.5, \\ 0, & x \geqslant 0.5. \end{cases} \tag{2.116}$$

The exact solution to this problem is divided into two parts as follows, when $t < 0.25$ (left) and $t \geqslant 0.25$ (right):

$$u(x,t) = \begin{cases} 2, & x < 0.25 + 1.5t, \\ 1, & 0.25 + 1.5t \leqslant x < 0.5 + 0.5t, \\ 0, & x \geqslant 0.5 + 0.5t. \end{cases} \qquad u(x,t) = \begin{cases} 2, & x < 3/8 + t, \\ 0, & x \geqslant 3/8 + t. \end{cases}$$

According to Figure 4, the SDLE scheme (*even though is not monotone*) is able to numerically solve the shock interaction ($t < 0.25$ on the left frame) in the $Lip^{'}$-error with $O(\Delta x^2)$ and in the $L^1 - error$ with $O(\Delta x)$, as stated in [45]. The situation is similar after the two shocks interact at $t \geqslant 0.25$ (right frame).

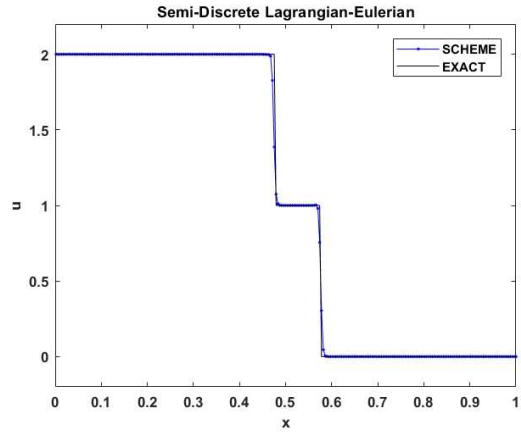

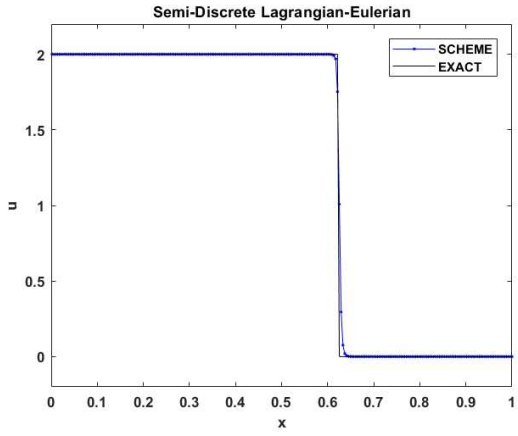

N	$\|\|U-u\|\|_{L^1}$	**Rate**	$Lip^{'}$	**Rate**
32	4.524e-02	-	4.844e-03	-
64	2.415e-02	9.054e-01	1.175e-03	2.042e+00
128	1.182e-02	1.030e+00	2.342e-04	2.327e+00
256	5.978e-03	9.838e-01	5.803e-05	2.013e+00
512	2.614e-03	1.192e+00	1.692e-05	1.777e+00
1024	1.493e-03	8.085e-01	4.299e-06	1.976e+00
2048	7.144e-04	1.063e+00	8.749e-07	2.296e+00
4096	3.377e-04	1.080e+00	2.170e-07	2.011e+00

N	$\|\|U-u\|\|_{L^1}$	**Rate**	$Lip^{'}$	**Rate**
32	5.534e-02	-	4.197e-03	-
64	2.500e-02	1.145e+00	9.517e-04	2.141e+00
128	1.265e-02	9.822e-01	2.331e-04	2.029e+00
256	6.699e-03	9.179e-01	5.882e-05	1.986e+00
512	3.044e-03	1.137e+00	1.404e-05	2.066e+00
1024	1.560e-03	9.640e-01	3.538e-06	1.988e+00
2048	8.317e-04	9.079e-01	9.059e-07	1.965e+00
4096	3.792e-04	1.132e+00	2.178e-07	2.056e+00

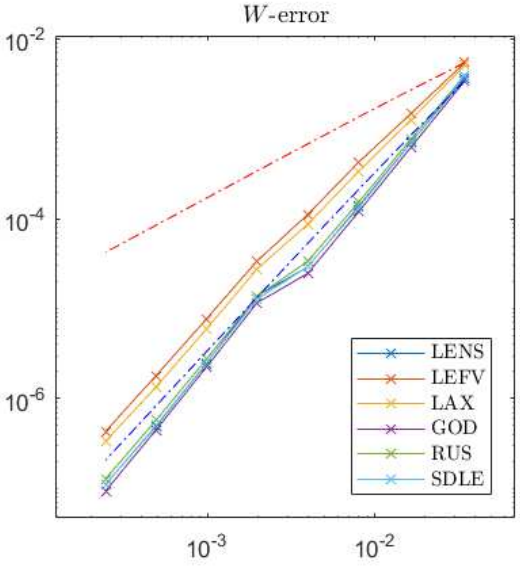

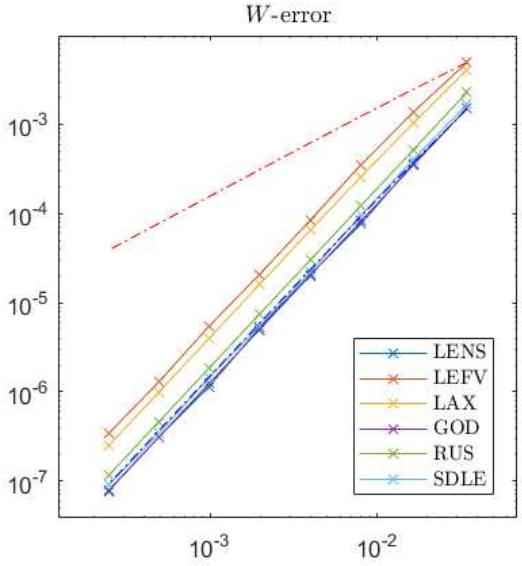

Figure 4 – **TOP**: Approximate solutions computed with the Semi-Discrete Lagrangian-Eulerian (SDLE) scheme at times $T = 0.15$ (left) and $T = 0.25$ (right), with 256 grid cells, $\alpha = 2$, $\zeta = 2$ and $\theta = 1.5$. **MIDDLE**: The corresponding L^1, $Lip^{'}-$ norms of the errors between numerical approximations u and exact solution U computed with the SDLE scheme using the second-order Runge–Kutta method. **BOTTOM**: The corresponding Log-Log plots for the $Lip^{'}-norm$ of the error versus cell sizes at times $T = 0.15$ (left) and $T = 0.25$ (right), with $\alpha = 2$, $\zeta = 2$ and $\theta = 1.5$. The error obtained with the SDLE scheme for these cases is similar to that obtained with the high-resolution Godunov scheme and better than those obtained with the classical Rusanov and Lax-Friedrichs schemes. The SDLE scheme is also designed to produce better results when compared to first-order L^1 or second-order $Lip^{'}-$ (former fully-discrete Lagrangian-Eulerian schemes). The red dotted line indicates the first order and the blue dotted line the second order.

3 Semi-Discrete Lagrangian-Eulerian scheme for scalar hyperbolic conservation laws in two-space dimensions

In the previous chapter, the scalar semi-discrete Lagrangian-Eulerian scheme has been analyzed and presented to approximate solutions of hyperbolic conservation laws connected to a convergence proof via weak asymptotic theory in one space dimension. Now on, we shall describe and analyze the two-dimensional scalar semi-discrete scheme, which is a natural (non-trivial) extension of the one-dimensional case in the sense that is obtained using a dimension-by-dimension approach and in all coordinate directions the numerical flux function in one-dimensional case is straightforwardly applied, but with significant differences in relation to the one-dimensional case when it comes to the weak asymptotic theory. This approach is completely determined once the intercell numerical fluxes are specified and a choice of mesh has been made. The 2D semi-discrete Lagrangian-Eulerian scheme is genuinely multidimensional in the sense that the scheme does not require the use of dimensional splitting strategies, but only the available information of the quantities u and fluxes $H(u)$ and $G(u)$ in Eq. (3.1).

3.1 2D semi-discrete Lagrangian-Eulerian scheme for scalar hyperbolic conservation laws

Considering the previous discussions, we now construct the new 2D semi-discrete Lagrangian-Eulerian scheme to solve Cauchy problem for the following scalar conservation law,

$$\frac{\partial u}{\partial t} + \frac{\partial H(u)}{\partial x} + \frac{\partial G(u)}{\partial y} = 0, \quad u(x, y, 0) = u_0(x, y), \tag{3.1}$$

where H, $G \in C^2$, $u_0(x, y) \in L^\infty_{loc}(\mathbb{R}^2)$.

Prior to evolving the computed approximate solution, $u(x_j, y_k, t^n)$, in time from t^n to t^{n+1}, we first reconstruct a piecewise-linear approximation of u as follows for all cells in the computational mesh grid (in the same fashion as in the 1D case),

$$L_{j,k}(x, y, t^n) = u^n_{j,k} + (u_x)^n_{j,k}\,(x - x_j) + (u_y)^n_{j,k}\,(y - y_k)\,, \tag{3.2}$$

with $x \in [x_{j-\frac{1}{2}}, x_{j+\frac{1}{2}}]$ and $y \in [y_{k-\frac{1}{2}}, y_{k+\frac{1}{2}}]$, where $(u_x)^n_{j,k}$ and $(u_y)^n_{j,k}$ denote an (at least first-order) approximation to the x-and y-derivatives of u at the cell centers (x_j, y_k). In

other words, $u(x_j, y_k, t^n) := L_{j,k}(x_j, y_k, t^n)$ in the mesh grid point values (x_j, y_k) such that $u(x_j, y_k, t^n) := u^n_{j,k}$ when $(u_x)^n_{j,k} = 0$ and $(u_y)^n_{j,k} = 0$.

The formal 2D extension of the semi-discrete scheme is straightforward (notice that it does not require dimensional splitting strategies) and given by

$$\frac{d}{dt}u_{j,k}(t) = -\frac{\mathcal{F}_{j+1/2,k} - \mathcal{F}_{j-1/2,k}}{\Delta x} - \frac{\mathcal{G}_{j,k+1/2} - \mathcal{G}_{j,k-1/2}}{\Delta y}, \tag{3.3}$$

where following the "*no-flow*" property (2.16), the constructed corresponding (coupled) multidimensional numerical fluxes in the $x-$ and $y-$directions are, respectively, given by

$$\begin{aligned}
\mathcal{F}_{j+\frac{1}{2},k} =& \frac{1}{4}\left[b^x_{j+\frac{1}{2},k}\left(u^-_{j+\frac{1}{2},k} - u^+_{j+\frac{1}{2},k}\right) + (f_{j,k} + f_{j+1,k})\left(u^-_{j+\frac{1}{2},k} + u^+_{j+\frac{1}{2},k}\right)\right] \quad \text{and} \\
\mathcal{G}_{j,k+\frac{1}{2}} =& \frac{1}{4}\left[b^y_{j,k+\frac{1}{2}}\left(u^-_{j,k+\frac{1}{2}} - u^+_{j,k+\frac{1}{2}}\right) + (g_{j,k} + g_{j,k+1})\left(u^-_{j,k+\frac{1}{2}} + u^+_{j,k+\frac{1}{2}}\right)\right],
\end{aligned} \tag{3.4}$$

along with the discretized multidimensional (2D) no-flow curves,

$$f_{j,k} = \frac{H(u_{jk})}{u_{jk}} \quad \text{and} \quad g_{j,k} = \frac{G(u_{jk})}{u_{jk}}, \tag{3.5}$$

in a straightforward manner. The Lagrangian-Eulerian framework for semi-discrete schemes can be extended to several dimensions following the same simplicity.

We analyze the convergence of the SDLE scheme for scalar 2D hyperbolic conservation laws through a discretization on a uniform Cartesian grid in Section 3.2, this analysis (entropy-convergence proof, scalar maximum principle, and a kind of Kruzhkov entropy solution) confirms that the blow-up singularity of the numerical fluxes in 2D is also removed by the *two-dimensional no flow equations* in (3.5). The intermediate values are given by

$$\begin{aligned}
u^+_{j+1/2,k} :=& u_{j+1,k}(t) - \frac{\Delta x}{4}(u_x)_{j+1,k}(t), \qquad \text{and} \qquad u^-_{j+1/2,k} := u_{j,k}(t) + \frac{\Delta x}{4}(u_x)_{j,k}(t), \\
u^+_{j,k+1/2} :=& u_{j,k+1}(t) - \frac{\Delta y}{4}(u_y)_{j,k+1}(t), \qquad \text{and} \qquad u^-_{j,k+1/2} := u_{j,k}(t) + \frac{\Delta y}{4}(u_y)_{j,k}(t),
\end{aligned} \tag{3.6}$$

where numerical derivatives $(u_x)_{j,k}(t)$ and $(u_y)_{j,k}(t)$ were computed using the slope limiter approximations,

$$\begin{aligned}
(u_x)_{j,k}(t) =& \text{minmod}\left(\alpha\theta\frac{u_{j,k}(t) - u_{j-1,k}(t)}{\Delta x}, \alpha\frac{u_{j+1,k}(t) - u_{j-1,k}(t)}{2\Delta x}, \alpha\theta\frac{u_{j+1,k}(t) - u_{j,k}(t)}{\Delta x}\right) \\
(u_y)_{j,k}(t) =& \text{minmod}\left(\alpha\theta\frac{u_{j,k}(t) - u_{j,k-1}(t)}{\Delta y}, \alpha\frac{u_{j,k+1}(t) - u_{j,k-1}(t)}{2\Delta y}, \alpha\theta\frac{u_{j,k+1}(t) - u_{j,k}(t)}{\Delta y}\right),
\end{aligned} \tag{3.7}$$

with $\alpha = 1, 2$ and $1 \leqslant \theta \leqslant 2$. The slope limiter approximations (3.7) will be used in numerical experiments (see Section 3.3).

The *no-flow parameters*, $b^x_{j+\frac{1}{2},k}$ and $b^y_{j,k+\frac{1}{2}}$, linked to the no-flow curves, are powerful key ingredients for this class of semi-discrete schemes given in general form by (3.3) and (3.4), along with (3.5)-(3.7), and subject to the following CFL stability condition (to be discussed and proved in details in what follows; see Eqs. (3.20), (3.21) and (3.50)):

$$\max_{j,k}\left(\frac{\Delta t}{\Delta x}\max_{j,k}|f_{j,k}|,\frac{\Delta t}{\Delta y}\max_{j,k}|g_{j,k}|\right)\leqslant\frac{1}{4}. \tag{3.8}$$

Notice that the *no-flow parameters* $b^x_{j+\frac{1}{2},k}$ and $b^y_{j,k+\frac{1}{2}}$ can be viewed in the same fashion of slope limiters in the sense of a novel powerful tool to suppress numerical spurious oscillations as well as to achieve very good resolution for efficient computations. In computing practice (Section 3.3), we have observed stable solutions when only using the control volume over the no-flow equations (3.5), which is consistent with the results of our rigorous analysis (Sections 3.2, 3.2.2, and 3.2.3).

3.2 Convergence proof of the semi-discrete Lagrangian-Eulerian scheme via weak asymptotic analysis

Here, we consider a 2D problem. However, the n-multidimensional case is similar, and the proof can be adapted for any $n\in\mathbb{N}$. We consider $(x,y)\in\mathbb{T}=\mathbb{R}^2/\mathbb{Z}^2$. Here, we choose in $(x,y)\in\mathbb{T}$ to avoid technical problems with the boundary conditions, since the implementation of numerical schemes are given in finite domains, however the proofs given in this work are very similar if we consider $(x,y)\in\mathbb{R}^2$ and they are easily adapted; the variable $t\in\mathbb{R}^+$, thus $u=u(x,y,t):\mathbb{T}\times\mathbb{R}^+\to\Omega\subset\mathbb{R}$; and flux functions $H=H(u):\Omega\to\mathbb{R}$ and $G=G(u):\Omega\to\mathbb{R}$.

We assume that functions $H(u)$ and $G(u)$ are locally Lipschitzian functions in u in that,

Assumption 1 - for all $c>0$, $\exists\ L_1>0$ and $L_2>0$ such that $|u_1|\leqslant c$, $|u_2|\leqslant c$, we have that

$$|H(u_1)-H(u_2)|\leqslant L_1|u_1-u_2|\quad\text{ and }\quad|G(u_1)-G(u_2)|\leqslant L_2|u_1-u_2|. \tag{3.9}$$

The weak asymptotic solution is a sequence of solutions $(u_\epsilon)_\epsilon=(u(x,y,t,\epsilon))_\epsilon$ of class $\mathcal{C}^1$ in t and class L^∞ and is piecewise continuous in (x,y) such that, for all $\psi=\psi(x,y)\in\mathcal{C}^\infty_c(\mathbb{R}^2)$ (smooth with compact support) and for all t,

$$\lim_{\epsilon\to0}\int_{\mathbb{R}}\int_{\mathbb{R}}((u_\epsilon)_t\psi-H(u_\epsilon)\partial_x\psi-G(u_\epsilon)\partial_y\psi)dxdy=0\quad\text{ and }\quad u_\epsilon(x,y,0)=u_0(x,y). \tag{3.10}$$

The weak asymptotic method, as in the one dimensional case (Section 2.2), consists in first proposing a Partial Differential Equation (PDE) with a special flux (using parameter ϵ). Then, for each fixed ϵ, we obtain an Ordinary Differential Equation (ODE) for variable

t. From the theory of ODEs, we prove the existence and stability of the solution. Finally, we demonstrate that, when taking $\epsilon \to 0$, the limit satisfies (3.10).

In our approach, we use two auxiliary functions, $f(u) = H(u)/u$ and $g(u) = G(u)/u$ (i.e., the no-flow curves). To simplify the following exposition (and without loss of generality), we will assume that there exists a $a > 0$ such that $u > a > 0$. In Remark 3.4, we discuss the general case.

Notice that, in this case, $f(u)$ is a locally Lipschitzian function in u in that, for all $c > 0$, $\exists \bar{K}_1 > 0$, such that

$$|u_1| \leqslant c, |u_2| \leqslant c \longrightarrow |f(u_1) - f(u_2)| \leqslant \bar{K}_1 |u_1 - u_2|, \tag{3.11}$$

where $\bar{K}_1 = \left(\frac{L_1}{c} + \frac{M_{c1}}{c^2}\right)$, $M_{c1} = \max_{|u| \leqslant c} H(u)$ and L_1 Lipschitz constant of H.

Function $g(u)$ is a locally Lipschitzian function in u in that, for all $c > 0$, $\exists \bar{K}_2 > 0$, such that

$$|u_1| \leqslant c, |u_2| \leqslant c \longrightarrow |g(u_1) - g(u_2)| \leqslant \bar{K}_2 |u_1 - u_2|, \tag{3.12}$$

where $\bar{K}_2 = \left(\frac{L_2}{c} + \frac{M_{c2}}{c^2}\right)$, $M_{c2} = \max_{|u| \leqslant c} G(u)$ and L_2 Lipschitz constant of G.

3.2.1 Stability conditions and weak asymptotic solution

To obtain the scheme used in weak asymptotic theory, we use the numerical method (3.3)-(3.7). From this numerical method, we derive the following PDE in the weak asymptotic framework:

$$\partial_t(u_\epsilon) = -\frac{1}{\epsilon_1}\left[\mathcal{F}(u_{\epsilon_1;\epsilon_2}, u_{\epsilon_1+1;\epsilon_2}) - \mathcal{F}(u_{\epsilon_1-1;\epsilon_2}, u_{\epsilon_1;\epsilon_2})\right] - \frac{1}{\epsilon_2}\left[\mathcal{G}(u_{\epsilon_1;\epsilon_2}, u_{\epsilon_1;\epsilon_2+1}) - \mathcal{G}(u_{\epsilon_1;\epsilon_2-1}, u_{\epsilon_1;\epsilon_2})\right], \tag{3.13}$$

where function $\mathcal{F}(u_{\epsilon_1;\epsilon_2}, u_{\epsilon_1+1;\epsilon_2})$ is defined by

$$\begin{aligned}\mathcal{F}(u_{\epsilon_1;\epsilon_2}, u_{\epsilon_1+1;\epsilon_2}) &= \frac{1}{4}\left[b^x_{\epsilon_1+1/2;\epsilon_2}\left(u_{\epsilon_1;\epsilon_2} + \frac{\epsilon_1}{4}(u_x)_{\epsilon_1;\epsilon_2} - \left(u_{\epsilon_1+1;\epsilon_2} - \frac{\epsilon_1}{4}(u_x)_{\epsilon_1+1;\epsilon_2}\right)\right)\right] \\ &+ \frac{1}{4}\left[(f(u_{\epsilon_1;\epsilon_2}) + f(u_{\epsilon_1+1;\epsilon_2}))\left(u_{\epsilon_1;\epsilon_2} + \frac{\epsilon_1}{4}(u_x)_{\epsilon_1;\epsilon_2} + \left(u_{\epsilon_1+1;\epsilon_2} - \frac{\epsilon_1}{4}(u_x)_{\epsilon_1+1;\epsilon_2}\right)\right)\right],\end{aligned} \tag{3.14}$$

and function $\mathcal{G}(u_{\epsilon_1;\epsilon_2}, u_{\epsilon_1;\epsilon_2+1})$ is

$$\begin{aligned}\mathcal{G}(u_{\epsilon_1;\epsilon_2}, u_{\epsilon_1;\epsilon_2+1}) &= \frac{1}{4}\left[b^y_{\epsilon_1;\epsilon_2+1/2}\left(u_{\epsilon_1;\epsilon_2} + \frac{\epsilon_2}{4}(u_y)_{\epsilon_1;\epsilon_2} - \left(u_{\epsilon_1;\epsilon_2+1} - \frac{\epsilon_2}{4}(u_y)_{\epsilon_1;\epsilon_2+1}\right)\right)\right] \\ &+ \frac{1}{4}\left[(f(u_{\epsilon_1;\epsilon_2}) + f(u_{\epsilon_1;\epsilon_2+1}))\left(u_{\epsilon_1;\epsilon_2} + \frac{\epsilon_2}{4}(u_y)_{\epsilon_1;\epsilon_2} + \left(u_{\epsilon_1;\epsilon_2+1} - \frac{\epsilon_2}{4}(u_y)_{\epsilon_1;\epsilon_2+1}\right)\right)\right],\end{aligned} \tag{3.15}$$

with initial condition $u_\epsilon(x, y, 0) = u_0(x, y, 0)$. We would like to stress that $b^x_{\epsilon_1+1/2;\epsilon_2}$ and $b^y_{\epsilon_1;\epsilon_2+1/2}$ depend on x and y.

Remark 3.1. *We are interested in studying the ODE in variable t obtained from Eq. (3.13) by fixing ϵ_1 and ϵ_2 and considering x and y to be parameters. We define $u_{\epsilon_1+i;\epsilon_2+j}$ and $(u_x)_{\epsilon_1+i;\epsilon_2+j}$ as*

$$u_{\epsilon_1+i;\epsilon_2+j} = u(x+i\epsilon_1, y+j\epsilon_2, t, \epsilon), \quad (u_x)_{\epsilon_1+i;\epsilon_2+j} = (u_x)(x+i\epsilon_1, y+j\epsilon_2, t, \epsilon). \tag{3.16}$$

Here, we are using that $u_x = (u_x)(x,y,t,\epsilon)$ and $u_y = (u_y)(x,y,t,\epsilon)$ are the approximations to the partial derivative of $u(x,t,\epsilon)$ with respect to variables x and y, respectively. Generally, we use minmod type functions. Thus, we have bounded functions $\mathcal{M}_1$ and $\mathcal{M}_2$ such

$$u_x = \frac{\mathcal{M}_1(u(x-p\epsilon_1, y, t, \epsilon), \cdots, u(x+(p-1)\epsilon_1, y, t, \epsilon), u(x+p\epsilon_1, y, t, \epsilon))}{\epsilon_1} \quad \text{and} \tag{3.17}$$

$$u_y = \frac{\mathcal{M}_2(u(x, y-q\epsilon_2, t, \epsilon), \cdots, u(x, y+(q-1)\epsilon_1, t, \epsilon), u(x, y+q\epsilon_2, t, \epsilon))}{\epsilon_2}, \tag{3.18}$$

where p and q are integers that depend on the particular functions used to approximate u_x and u_y. Hence, along of text, after applying approximation (3.16) in Eq. (3.13), we will obtain an ODE in time, as well as the discrete parameter in spaces x and y.

In what follows, for any approximations of $u_x = (u_x)(x,y,t,\epsilon)$ and $u_y = (u_y)(x,y,t,\epsilon)$, we assume that there exist $d > 0$ and $d_i \geqslant 0$ for $i = -\vartheta \cdots \vartheta$, where $\vartheta = \max(p,q)$, for which $(u_x)(x,y,t,\epsilon)$ and $(u_y)(x,y,t,\epsilon)$ satisfy,

$$|u_x| \leqslant \frac{d}{\epsilon_1} \sum_{i=-\vartheta}^{\vartheta} d_i |u(x-i\epsilon_1, y, t, \epsilon)| \quad \text{and} \quad |u_y| \leqslant \frac{d}{\epsilon_2} \sum_{i=-\vartheta}^{\vartheta} d_i |u(x, y-i\epsilon_2, t, \epsilon)|. \tag{3.19}$$

In Eq. (3.19), since u_x and u_y are bounded, we obtain a global estimate for $|u_x|$ and $|u_y|$.

No-flow variables $b^x_{\epsilon_1+1/2;\epsilon_2}$ and $b^y_{\epsilon_1;\epsilon_2+1/2}$ are important because they are naturally chosen from original problem (3.1) so that we can obtain the stability for the resulting semi-discrete numerical method (3.3)-(3.7).

This quantity generally depends on functions $f(u)$ and $g(u)$, which are evaluated in some suitable values. Since we use estimates for $b^x_{\epsilon_1+1/2;\epsilon_2}$ and $b^y_{\epsilon_1;\epsilon_2+1/2}$, we obtain a global bounded estimate for these two quantities. To that end, we assume that there exists a $\varrho > 0$ such that

$$|b^x_{\epsilon_1+1/2;\epsilon_2}| \leqslant \varrho M_1 \quad \text{and} \quad |b^y_{\epsilon_1;\epsilon_2+1/2}| \leqslant \varrho M_2, \quad \text{where} \tag{3.20}$$

$$M_1 = \sup_{u\in\Omega, t\in[0,T], (x,y)\in\mathbb{T}} |f(u)| < \infty \quad \text{and} \quad M_2 = \sup_{u\in\Omega, t\in[0,T], (x,y)\in\mathbb{T}} |g(u)| < \infty. \tag{3.21}$$

Based on these conditions and definitions, we state our first result concerning the existence and stability of the solution obtained from the numerical method:

Proposition 3.1. *There exists a solution to (3.13), a family of functions $(x,y,t) \to u(x,y,t,\epsilon) : \mathbb{T}\times\mathbb{R}^+ \to \mathbb{R}$ for a small enough ϵ, which, for a fixed ϵ, are of class $\mathcal{C}^1$ and class L^∞ for $(x,y) \in \mathbb{T}$ and satisfy (3.10). Moreover, if*

$$b^x_{\epsilon_1+1/2;\epsilon_2} \geqslant |(f(u_{\epsilon_1;\epsilon_2}) + f(u_{\epsilon_1+1;\epsilon_2}))|, \quad b^y_{\epsilon_1;\epsilon_2+1/2} \geqslant |(g(u_{\epsilon_1;\epsilon_2}) + g(u_{\epsilon_1;\epsilon_2+1}))|, \tag{3.22}$$

$$\frac{dt}{\epsilon_1}(b^x_{\epsilon_1+1/2;\epsilon_2} + |(f(u_{\epsilon_1;\epsilon_2}) + f(u_{\epsilon_1+1;\epsilon_2}))|) \leqslant 1, \ \frac{dt}{\epsilon_2}(b^y_{\epsilon_1;\epsilon_2+1/2} + |(g(u_{\epsilon_1;\epsilon_2}) + g(u_{\epsilon_1;\epsilon_2+1}))|) \leqslant 1 \tag{3.23}$$

$$|u_{\epsilon_1;\epsilon_2}| \geqslant \frac{\epsilon_1}{4}(u_x)_{\epsilon_1;\epsilon_2} \quad \text{and} \quad |u_{\epsilon_1;\epsilon_2}| \geqslant \frac{\epsilon_2}{4}(u_y)_{\epsilon_1;\epsilon_2}, \tag{3.24}$$

then family $\{u(\cdot,t,\epsilon)\}_\epsilon$ is bounded in $L^1(\mathbb{T})$ uniformly in ϵ. In fact, $||u(.,t,\epsilon)||_{L^1(\mathbb{T})} \leqslant ||u_0||_{L^1(\mathbb{T})}$ for all t. Furthermore, if initial condition $u_0(x,y)$, $H(u)$ and $G(u)$ are continuous, then $u(x,y,t,\epsilon)$ is also continuous in (x,y).

Proof. First, we fix $\epsilon = (\epsilon_1,\epsilon_2)$ and obtain an ODE from (3.13) for variable t and for parameters x and y as follows:

$$u'(x,y,t,\epsilon) = F_\epsilon(u(x,y,t,\epsilon),x,y,t), \quad u(x,y,0) = u_0(x,y). \tag{3.25}$$

Notice that (x,y) are also a parameters in Eq. (3.25). By using notation $u(x,y) = u(x,y,t,\epsilon)$, we define $F_\epsilon : L^\infty(\mathbb{T})\times\mathbb{T}\times[0,\infty) \longrightarrow L^\infty(\mathbb{T})$ as

$$\begin{aligned} F_\epsilon(u(x,y),x,y,t) = &-\frac{1}{\epsilon_1}\left[\mathcal{F}(u(x,y),u(x+\epsilon_1,y),x,y,t) - \mathcal{F}(u(x-\epsilon_1,y),u(x,y),x,y,t)\right] \\ &-\frac{1}{\epsilon_2}\left[\mathcal{G}(u(x,y),u(x,y+\epsilon_2),x,y,t) - \mathcal{G}(u(x,y-\epsilon_2),u(x,y),x,y,t)\right]. \end{aligned} \tag{3.26}$$

From Eqs. (3.14) and (3.15), we write
$\mathcal{F}(u(x,y),u(x+\epsilon_1,y),x,y,t) =:$

$$\begin{aligned} &\frac{1}{4}\Bigg[b^x_{\epsilon_1+1/2;\epsilon_2}\left(u(x,y) + \frac{\epsilon_1}{4}(u_x)(x,y,t,\epsilon) - \left(u(x+\epsilon_1,y) - \frac{\epsilon_1}{4}(u_x)(x+\epsilon_1,y,t,\epsilon)\right)\right) + \\ &\Big\{(f(u(x,y),x,y,t) + f(u(x+\epsilon_1,y),x,y,t))\Big[u(x,y) + \frac{\epsilon_1}{4}(u_x)(x,y,t,\epsilon) \\ &+ \left(u(x+\epsilon_1,y) - \frac{\epsilon_1}{4}(u_x)(x+\epsilon_1,y,t,\epsilon)\right)\Big]\Big\}\Bigg], \end{aligned} \tag{3.27}$$

and $\mathcal{G}(u(x,y),u(x,y+\epsilon_2),x,y,t) =:$

$$\begin{aligned} &\frac{1}{4}\Bigg[b^y_{\epsilon_1;\epsilon_2+1/2}\left(u(x,y) + \frac{\epsilon_2}{4}(u_y)(x,y,t,\epsilon) - \left(u(x,y+\epsilon_2,y) - \frac{\epsilon_2}{4}(u_y)(x,y+\epsilon_2,t,\epsilon)\right)\right) + \\ &\Big\{(g(u(x,y),x,y,t) + g(u(x,y+\epsilon_2),x,y,t))\Big[u(x,y) + \frac{\epsilon_2}{4}(u_y)(x,y,t,\epsilon) \\ &+ \left(u(x,y+\epsilon_2) - \frac{\epsilon_2}{4}(u_y)(x,y+\epsilon_2,t,\epsilon)\right)\Big]\Big\}\Bigg]. \end{aligned} \tag{3.28}$$

Flux F_ϵ, defined in Eq. (3.26), is a Lipschitzian function in variable u because $f(\cdot)$, $g(\cdot)$, $(u_x)(x,y,t,\epsilon)$, and $(u_y)(x,y,t,\epsilon)$ are Lipschitzian functions, and flux F_ϵ is a combination of these Lipschitzian functions (in a very simple fashion). Based on the classical theory for ODEs in Banach spaces, in the Lipschitzian case, there is a local solution for $t \in [0, \delta(\epsilon)]$ for some $\delta(\epsilon)$ that depends on ϵ. For the global solution, since f and g are bounded (because H and G are assumed to be bounded), we can extend the solution to $\delta(\epsilon) \to \infty$. From Assumption 1 in Eq. (3.9), the Lipschitz constants of each F_ϵ can be chosen uniformly on the bounded sets $L^\infty(\mathbb{T}) \times \mathbb{T} \times [0, \infty)$. To demonstrate the existence of solution (3.25) globally (in time), it suffices to prove that, for fixed $\epsilon = (\epsilon_1, \epsilon_2)$, there exists a $c_\epsilon(t) < \infty$ such that $||u(\cdot,t,\epsilon)||_\infty \leqslant c_\epsilon(t) < \infty$. Here, c_ϵ is a continuous function on $[0,\infty)$, with no uniformity in ϵ. We also have that $H(u)$ and $G(u)$ are bounded functions; thus, if $u \geqslant a > 0$, then f and g are also bounded. Let M_1 and M_2 satisfying (3.21). Using the estimates for $|(u_x)(x,y,t,\epsilon)|$, $|(u_y)(x,y,t,\epsilon)|$, $\left|b^x_{\epsilon_1+1/2;\epsilon_2}\right|$ and $\left|b^y_{\epsilon_1;\epsilon_2+1/2}\right|$ from Eqs. (3.19) and (3.20), the ODE, given by (3.13), satisfies

$$|\partial_t(u(x,y,t,\epsilon))| \leqslant \frac{1}{\tilde{\epsilon}} ||u(\cdot,t,\epsilon)||_\infty \, \theta \, M, \tag{3.29}$$

where $\tilde{\epsilon} = \min(\epsilon_1, \epsilon_2)$ and $M = \max(M_1, M_2)$,

$$\theta = \left(2 + \frac{d}{2} \sum_{i=-\vartheta}^{\vartheta} |d_i|\right)(\varrho + 2) \quad \text{and} \quad ||u(\cdot,t,\epsilon)||_\infty = \operatorname{ess\,sup}_{(x,y)\in\mathbb{T}} |u(x,y,t,\epsilon)|. \tag{3.30}$$

Solving (3.29), we get

$$||u(\cdot,t,\epsilon)||_\infty \leqslant ||u_{0,\epsilon}||_\infty + \frac{\theta M}{\tilde{\epsilon}} \int_0^t ||u(\cdot,\tau,\epsilon)||_\infty d\tau.$$

From Gronwall formula, we obtain that

$$||u(\cdot,t,\epsilon)||_\infty \leqslant c(t), \quad \text{where} \quad c(t) = ||u_{0,\epsilon}|| \exp\left(\frac{\theta M t}{\tilde{\epsilon}}\right). \tag{3.31}$$

Bound (3.31) indicates the existence of a global solution to ODE (3.13) for each fixed ϵ. However, notice that there is no uniformity in ϵ. To demonstrate that the solutions to the ODEs provide a weak asymptotic solution to (3.1), we will prove that the solution is L^1 bounded uniformly with respect to ϵ. To do so, let $T > 0$ for $t + dt \leqslant T$ and $dt > 0$, where

dt satisfies some CFL condition. From the mean value theorem, we write (3.13) as

$$
\begin{aligned}
&u(x,y,t+dt,\epsilon) = \\
&u_{\epsilon_1,\epsilon_2} - \frac{dt}{4\epsilon_1}\left(b^x_{\epsilon_1+1/2;\epsilon_2}\left(u_{\epsilon_1,\epsilon_2} + \frac{\epsilon_1}{4}(u_x)_{\epsilon_1,\epsilon_2} - \left(u_{\epsilon_1+1,\epsilon_2} - \frac{\epsilon_1}{4}(u_x)_{\epsilon_1+1,\epsilon_2}\right)\right)\right) \\
&- \frac{dt}{4\epsilon_1}\left((f(u_{\epsilon_1,\epsilon_2}) + f(u_{\epsilon_1+1,\epsilon_2}))\left(u_{\epsilon_1,\epsilon_2} + \frac{\epsilon_1}{4}(u_x)_{\epsilon_1,\epsilon_2} + \left(u_{\epsilon_1+1,\epsilon_2} - \frac{\epsilon_1}{4}(u_x)_{\epsilon_1+1,\epsilon_2}\right)\right)\right) \\
&+ \frac{dt}{4\epsilon_1}\left(b^x_{\epsilon_1-1/2;\epsilon_2}\left(u_{\epsilon_1-1,\epsilon_2} + \frac{\epsilon_1}{4}(u_x)_{\epsilon_1-1,\epsilon_2} - \left(u_{\epsilon_1,\epsilon_2} - \frac{\epsilon_1}{4}(u_x)_{\epsilon_1,\epsilon_2}\right)\right)\right) \\
&+ \frac{dt}{4\epsilon_1}\left((f(u_{\epsilon_1-1,\epsilon_2}) + f(u_{\epsilon_1,\epsilon_2}))\left(u_{\epsilon_1-1,\epsilon_2} + \frac{\epsilon_1}{4}(u_x)_{\epsilon_1-1,\epsilon_2} + \left(u_{\epsilon_1,\epsilon_2} - \frac{\epsilon_1}{4}(u_x)_{\epsilon_1,\epsilon_2}\right)\right)\right) \\
&- \frac{dt}{4\epsilon_2}\left(b^y_{\epsilon_1;\epsilon_2+1/2}\left(u_{\epsilon_1,\epsilon_2} + \frac{\epsilon_2}{4}(u_y)_{\epsilon_1,\epsilon_2} - \left(u_{\epsilon_1,\epsilon_2+1} - \frac{\epsilon_2}{4}(u_y)_{\epsilon_1,\epsilon_2+1}\right)\right)\right) \\
&- \frac{dt}{4\epsilon_2}\left((g(u_{\epsilon_1,\epsilon_2}) + g(u_{\epsilon_1,\epsilon_2+1}))\left(u_{\epsilon_1,\epsilon_2} + \frac{\epsilon_2}{4}(u_y)_{\epsilon_1,\epsilon_2} + \left(u_{\epsilon_1,\epsilon_2+1} - \frac{\epsilon_2}{4}(u_y)_{\epsilon_1,\epsilon_2+1}\right)\right)\right) \\
&+ \frac{dt}{4\epsilon_2}\left(b^y_{\epsilon_1;\epsilon_2-1/2}\left(u_{\epsilon_1,\epsilon_2-1} + \frac{\epsilon_2}{4}(u_y)_{\epsilon_1,\epsilon_2-1} - \left(u_{\epsilon_1,\epsilon_2} - \frac{\epsilon_2}{4}(u_y)_{\epsilon_1,\epsilon_2}\right)\right)\right) + \\
&+ \frac{dt}{4\epsilon_2}\left((g(u_{\epsilon_1,\epsilon_2-1}) + g(u_{\epsilon_1,\epsilon_2}))\left(u_{\epsilon_1,\epsilon_2-1} + \frac{\epsilon_2}{4}(u_y)_{\epsilon_1,\epsilon_2-1} + \left(u_{\epsilon_1,\epsilon_2} - \frac{\epsilon_2}{4}(u_y)_{\epsilon_1,\epsilon_2}\right)\right)\right) \\
&+ r(x,y,t,\epsilon,dt),
\end{aligned}
\tag{3.32}
$$

where $||r(\cdot,t,\epsilon,dt)||_\infty \to 0$, uniformly in $t \in [0,T]$ and fixed ϵ (with no uniformity in ϵ) when $dt \to 0$. This behavior results from the continuous differentiability of map $t \longrightarrow u(\cdot,t,\epsilon)$, $[0,\infty) \longrightarrow L^\infty(\mathbb{T})$ for fixed ϵ. After some algebraic manipulation, we rearrange (3.32) as

$$
\begin{aligned}
&u(x,y,t+dt,\epsilon) = \\
&\left(u_{\epsilon_1,\epsilon_2} + \frac{\epsilon_1}{4}(u_x)_{\epsilon_1,\epsilon_2}\right)\left(\frac{1}{4} - \frac{A_{\epsilon_1,\epsilon_2}dt}{4\epsilon_1}\right) + \left(u_{\epsilon_1,\epsilon_2} - \frac{\epsilon_1}{4}(u_x)_{\epsilon_1,\epsilon_2}\right)\left(\frac{1}{4} - \frac{B_{\epsilon_1,\epsilon_2}dt}{4\epsilon_1}\right) \\
&+ \left(u_{\epsilon_1-1,\epsilon_2} + \frac{\epsilon_1}{4}(u_x)_{\epsilon_1-1,\epsilon_2}\right)\left(\frac{A_{\epsilon_1-1,\epsilon_2}dt}{4\epsilon_1}\right) + \left(u_{\epsilon_1+1,\epsilon_2} - \frac{\epsilon_1}{4}(u_x)_{\epsilon_1+1,\epsilon_2}\right)\left(\frac{B_{\epsilon_1+1,\epsilon_2}dt}{4\epsilon_1}\right) \\
&+ \left(u_{\epsilon_1,\epsilon_2} + \frac{\epsilon_2}{4}(u_y)_{\epsilon_1,\epsilon_2}\right)\left(\frac{1}{4} - \frac{C_{\epsilon_1,\epsilon_2}dt}{4\epsilon_2}\right) + \left(u_{\epsilon_1,\epsilon_2} - \frac{\epsilon_2}{4}(u_y)_{\epsilon_1,\epsilon_2}\right)\left(\frac{1}{4} - \frac{D_{\epsilon_1,\epsilon_2}dt}{4\epsilon_2}\right) \\
&+ \left(u_{\epsilon_1,\epsilon_2-1} + \frac{\epsilon_2}{4}(u_y)_{\epsilon_1,\epsilon_2-1}\right)\left(\frac{C_{\epsilon_1,\epsilon_2-1}dt}{4\epsilon_2}\right) + \left(u_{\epsilon_1,\epsilon_2+1} - \frac{\epsilon_2}{4}(u_y)_{\epsilon_1,\epsilon_2+1}\right)\left(\frac{D_{\epsilon_1,\epsilon_2+1}dt}{4\epsilon_2}\right) \\
&+ r(x,y,t,\epsilon,dt),
\end{aligned}
\tag{3.33}
$$

for which

$$
A_{\epsilon_1;\epsilon_2} = b^x_{\epsilon_1+1/2;\epsilon_2} + (f(u_{\epsilon_1;\epsilon_2}) + f(u_{\epsilon_1+1;\epsilon_2})), \quad B_{\epsilon_1+1;\epsilon_2} = b^x_{\epsilon_1+1/2;\epsilon_2} - (f(u_{\epsilon_1;\epsilon_2}) + f(u_{\epsilon_1+1;\epsilon_2})).
\tag{3.34}
$$

$$
C_{\epsilon_1;\epsilon_2} = b^y_{\epsilon_1;\epsilon_2+1/2} + (g(u_{\epsilon_1;\epsilon_2}) + g(u_{\epsilon_1;\epsilon_2+1})), \quad D_{\epsilon_1;\epsilon_2+1} = b^y_{\epsilon_1;\epsilon_2+1/2} - (g(u_{\epsilon_1;\epsilon_2}) + g(u_{\epsilon_1;\epsilon_2+1})).
\tag{3.35}
$$

Since we are interested in obtaining the L^1 bound, we take the absolute value,

$$
\begin{aligned}
&|u(x,y,t+dt,\epsilon)| \leqslant \\
&\left|u_{\epsilon_1,\epsilon_2}+\frac{\epsilon_1}{4}(u_x)_{\epsilon_1,\epsilon_2}\right|\left|\frac{1}{4}-\frac{A_{\epsilon_1,\epsilon_2}dt}{4\epsilon_1}\right|+\left|u_{\epsilon_1,\epsilon_2}-\frac{\epsilon_1}{4}(u_x)_{\epsilon_1,\epsilon_2}\right|\left|\frac{1}{4}-\frac{B_{\epsilon_1,\epsilon_2}dt}{4\epsilon_1}\right| \\
&+\left|u_{\epsilon_1-1,\epsilon_2}+\frac{\epsilon_1}{4}(u_x)_{\epsilon_1-1,\epsilon_2}\right|\left|\frac{A_{\epsilon_1-1,\epsilon_2}dt}{4\epsilon_1}\right|+\left|u_{\epsilon_1+1,\epsilon_2}-\frac{\epsilon_1}{4}(u_x)_{\epsilon_1+1,\epsilon_2}\right|\left|\frac{B_{\epsilon_1+1,\epsilon_2}dt}{4\epsilon_1}\right| \\
&+\left|u_{\epsilon_1,\epsilon_2}+\frac{\epsilon_2}{4}(u_y)_{\epsilon_1,\epsilon_2}\right|\left|\frac{1}{4}-\frac{C_{\epsilon_1,\epsilon_2}dt}{4\epsilon_2}\right|+\left|u_{\epsilon_1,\epsilon_2}-\frac{\epsilon_2}{4}(u_y)_{\epsilon_1,\epsilon_2}\right|\left|\frac{1}{4}-\frac{D_{\epsilon_1,\epsilon_2}dt}{4\epsilon_2}\right| \\
&+\left|u_{\epsilon_1,\epsilon_2-1}+\frac{\epsilon_2}{4}(u_y)_{\epsilon_1,\epsilon_2-1}\right|\left|\frac{C_{\epsilon_1,\epsilon_2-1}dt}{4\epsilon_2}\right|+\left|u_{\epsilon_1,\epsilon_2+1}-\frac{\epsilon_2}{4}(u_y)_{\epsilon_1,\epsilon_2+1}\right|\left|\frac{D_{\epsilon_1,\epsilon_2+1}dt}{4\epsilon_2}\right| \\
&+|r(x,y,t,\epsilon,dt)|. \qquad (3.36)
\end{aligned}
$$

Since (3.22) and (3.23) are satisfied, we have that, for all $\epsilon=(\epsilon_1,\epsilon_2)$,

$$
\begin{aligned}
&\left|\frac{1}{4}-\frac{A_{\epsilon_1,\epsilon_2}dt}{4\epsilon_1}\right|=\frac{1}{4}-\frac{A_{\epsilon_1,\epsilon_2}dt}{4\epsilon_1}, \quad \left|\frac{1}{4}-\frac{B_{\epsilon_1,\epsilon_2}dt}{4\epsilon_1}\right|=\frac{1}{4}-\frac{B_{\epsilon_1,\epsilon_2}dt}{4\epsilon_1}, \\
&\left|\frac{1}{4}-\frac{C_{\epsilon_1,\epsilon_2}dt}{4\epsilon_2}\right|=\frac{1}{4}-\frac{C_{\epsilon_1,\epsilon_2}dt}{4\epsilon_2}, \quad \left|\frac{1}{4}-\frac{D_{\epsilon_1,\epsilon_2}dt}{4\epsilon_2}\right|=\frac{1}{4}-\frac{D_{\epsilon_1,\epsilon_2}dt}{4\epsilon_2}
\end{aligned}
$$

and $A_{\epsilon_1;\epsilon_2}$, $B_{\epsilon_1;\epsilon_2}$ and $C_{\epsilon_1;\epsilon_2}$ and $D_{\epsilon_1;\epsilon_2}$ are non-negative values. From (3.24), we obtain that

$$
\begin{aligned}
\left|u_{\epsilon_1;\epsilon_2}\pm\frac{\epsilon_1}{4}(u_x)_{\epsilon_1;\epsilon_2}\right| &= \left|u_{\epsilon_1;\epsilon_2}\right|\pm sign(u_{\epsilon_1;\epsilon_2})\frac{\epsilon_1}{4}(u_x)_{\epsilon_1;\epsilon_2}, \\
\left|u_{\epsilon_1;\epsilon_2}\pm\frac{\epsilon_2}{4}(u_y)_{\epsilon_1;\epsilon_2}\right| &= \left|u_{\epsilon_1;\epsilon_2}\right|\pm sign(u_{\epsilon_1;\epsilon_2})\frac{\epsilon_2}{4}(u_y)_{\epsilon_1;\epsilon_2},
\end{aligned}
$$

where $sign(a)$ is the signal of value a. Thus, (3.36) reduces to

$$
\begin{aligned}
&|u(x,y,t+dt,\epsilon)| \leqslant \left(\left|u_{\epsilon_1;\epsilon_2}\right|+sign(u_{\epsilon_1;\epsilon_2})\frac{\epsilon_1}{4}(u_x)_{\epsilon_1;\epsilon_2}\right)\left(\frac{1}{4}-\frac{A_{\epsilon_1,\epsilon_2}dt}{4\epsilon_1}\right) \\
&+\left(\left|u_{\epsilon_1;\epsilon_2}\right|-sign(u_{\epsilon_1;\epsilon_2})\frac{\epsilon_1}{4}(u_x)_{\epsilon_1;\epsilon_2}\right)\left(\frac{1}{4}-\frac{B_{\epsilon_1,\epsilon_2}dt}{4\epsilon_1}\right) \\
&+\left(\left|u_{\epsilon_1-1;\epsilon_2}\right|+sign(u_{\epsilon_1-1;\epsilon_2})\frac{\epsilon_1}{4}(u_x)_{\epsilon_1-1;\epsilon_2}\right)\left(\frac{A_{\epsilon_1-1,\epsilon_2}dt}{4\epsilon_1}\right) \\
&+\left(\left|u_{\epsilon_1+1;\epsilon_2}\right|-sign(u_{\epsilon_1+1;\epsilon_2})\frac{\epsilon_1}{4}(u_x)_{\epsilon_1+1;\epsilon_2}\right)\left(\frac{B_{\epsilon_1+1,\epsilon_2}dt}{4\epsilon_1}\right) \\
&+\left(\left|u_{\epsilon_1;\epsilon_2}\right|+sign(u_{\epsilon_1;\epsilon_2})\frac{\epsilon_2}{4}(u_y)_{\epsilon_1;\epsilon_2}\right)\left(\frac{1}{4}-\frac{C_{\epsilon_1,\epsilon_2}dt}{4\epsilon_2}\right) \\
&+\left(\left|u_{\epsilon_1;\epsilon_2}\right|-sign(u_{\epsilon_1;\epsilon_2})\frac{\epsilon_2}{4}(u_y)_{\epsilon_1;\epsilon_2}\right|\left(\frac{1}{4}-\frac{D_{\epsilon_1,\epsilon_2}dt}{4\epsilon_2}\right) \\
&+\left(\left|u_{\epsilon_1;\epsilon_2-1}\right|+sign(u_{\epsilon_1;\epsilon_2-1})\frac{\epsilon_2}{4}(u_y)_{\epsilon_1;\epsilon_2-1}\right)\left(\frac{C_{\epsilon_1,\epsilon_2-1}dt}{4\epsilon_2}\right) \\
&+\left(\left|u_{\epsilon_1;\epsilon_2+1}\right|-sign(u_{\epsilon_1;\epsilon_2+1})\frac{\epsilon_1}{4}(u_y)_{\epsilon_1;\epsilon_2+1}\right)\left(\frac{D_{\epsilon_1,\epsilon_2+1}dt}{4\epsilon_2}\right)+|r(x,y,t,\epsilon,dt)|. \qquad (3.37)
\end{aligned}
$$

Due to translations of $\pm\epsilon$, after integrating (3.37) we obtain

$$||u(\cdot,t+dt,\epsilon)||_1 = \int_{\mathbb{T}} |u(x,y,t+dt,\epsilon)|dxdy \leqslant \int_{\mathbb{T}} |u(x,y,t,\epsilon)|dxdy + dt\ r_1(t,\epsilon,dt) \quad (3.38)$$

$$\leqslant ||u(\cdot,t,\epsilon)||_1 + dt\ r_1(t,\epsilon,dt), \quad (3.39)$$

with $r_1(t,\epsilon,dt) = \int_{\mathbb{T}} |r(x,y,t,\epsilon,dt)|dxdy$ and the integral over $\mathbb{T}$ is a double integral. Here, remainder that the value $r_1(t,\epsilon,dt)$ is bounded, and $r_1(t,\epsilon,dt) \to 0$ when $dt \to 0$, uniformly in $t \in [0,T]$ for each fixed ϵ. Notice that, for each $T > 0$ given, we can divide interval $[0,T]$ into n subintervals $[jdt_n,(j+1)dt_n]$, where $dt_n = \dfrac{T}{n}$ and $0 \leqslant j \leqslant n-1$. Applying this in (3.39), we get

$$\int_{\mathbb{T}} |u(x,y,T,\epsilon)|dxdy \leqslant \int_{\mathbb{T}} |u(x,y,T-dt_n,\epsilon)|dxdy + dt_n\ r_1(T-dt,\epsilon,dt). \quad (3.40)$$

Applying recursively for all intervals, we obtain

$$\int_{\mathbb{T}} |u(x,y,T,\epsilon)|dxdy \leqslant \int_{\mathbb{T}} |u_0(x,y)|dxdy + dt_n \sum_{i=1}^{n} r_1(T-idt,\epsilon,dt). \quad (3.41)$$

Note that

$$dt_n\ |\sum_{i=1}^{n} r_1(T-idt,\epsilon,dt)| \leqslant \frac{T}{n} n \max_i |r_1(T-idt,\epsilon,dt)| = T \max_i |r_1(T-idt,\epsilon,dt)|.$$

Thus, taking the limit $dt \longrightarrow 0$ and using that $r_1(t,\epsilon,dt) \longrightarrow 0$ when $dt \longrightarrow 0$, we obtain

$$||u(\cdot,T,\epsilon)||_1 = \int_{\mathbb{T}} |u(x,y,T,\epsilon)|dxdy \leqslant \int_{\mathbb{T}} |u_0(x,y)|dxdy = ||u_0(\cdot)||_1, \quad (3.42)$$

which gives us the L^1 bounds uniform in ϵ. This proves that conditions (3.22)-(3.24) provide stability to the method.

To complete the proof of the proposition, we must demonstrate that the solution to (3.13) satisfies the definition of weak solution (3.10). To prove this, we define the integral as $I := I_x + I_y$, where

$$\begin{aligned} I_x = \int_{\mathbb{T}} \Bigg\{ \Bigg[& -\frac{1}{4\epsilon_1} \left(b^x_{\epsilon_1+1/2;\epsilon_2} \left(u_{\epsilon_1,\epsilon_2} + \frac{\epsilon_1}{4}(u_x)_{\epsilon_1,\epsilon_2} - \left(u_{\epsilon_1+1,\epsilon_2} - \frac{\epsilon_1}{4}(u_x)_{\epsilon_1+1,\epsilon_2} \right) \right) \right) \\ & - \frac{1}{4\epsilon_1} \left((f(u_{\epsilon_1,\epsilon_2}) + f(u_{\epsilon_1+1,\epsilon_2})) \left(u_{\epsilon_1,\epsilon_2} + \frac{\epsilon_1}{4}(u_x)_{\epsilon_1,\epsilon_2} + \left(u_{\epsilon_1+1,\epsilon_2} - \frac{\epsilon_1}{4}(u_x)_{\epsilon_1+1,\epsilon_2} \right) \right) \right) \\ & + \frac{1}{4\epsilon_1} \left(b^x_{\epsilon_1-1/2;\epsilon_2} \left(u_{\epsilon_1-1,\epsilon_2} + \frac{\epsilon_1}{4}(u_x)_{\epsilon_1-1,\epsilon_2} - \left(u_{\epsilon_1,\epsilon_2} - \frac{\epsilon_1}{4}(u_x)_{\epsilon_1,\epsilon_2} \right) \right) \right) \\ & + \frac{1}{4\epsilon_1} \left((f(u_{\epsilon_1-1,\epsilon_2}) + f(u_{\epsilon_1,\epsilon_2})) \left(u_{\epsilon_1-1,\epsilon_2} + \frac{\epsilon_1}{4}(u_x)_{\epsilon_1-1,\epsilon_2} + \left(u_{\epsilon_1,\epsilon_2} - \frac{\epsilon_1}{4}(u_x)_{\epsilon_1,\epsilon_2} \right) \right) \right) \Bigg] \\ & (\psi(x,y) - H(u_\epsilon)\partial_x(\psi)(x,y)) \Bigg\} dxdy \end{aligned} \quad (3.43)$$

and

$$
\begin{aligned}
I_y = \int_{\mathbb{T}} \Bigg\{ \Bigg[& -\frac{1}{4\epsilon_2} \left(b^y_{\epsilon_1;\epsilon_2+1/2} \left(u_{\epsilon_1,\epsilon_2} + \frac{\epsilon_2}{4}(u_y)_{\epsilon_1,\epsilon_2} - \left(u_{\epsilon_1,\epsilon_2+1} - \frac{\epsilon_2}{4}(u_y)_{\epsilon_1,\epsilon_2+1} \right) \right) \right) \\
& - \frac{1}{4\epsilon_2} \left((g(u_{\epsilon_1,\epsilon_2}) + g(u_{\epsilon_1,\epsilon_2+1})) \left(u_{\epsilon_1,\epsilon_2} + \frac{\epsilon_2}{4}(u_y)_{\epsilon_1,\epsilon_2} + \left(u_{\epsilon_1,\epsilon_2+1} - \frac{\epsilon_2}{4}(u_y)_{\epsilon_1,\epsilon_2+1} \right) \right) \right) \\
& + \frac{1}{4\epsilon_2} \left(b^y_{\epsilon_1;\epsilon_2-1/2} \left(u_{\epsilon_1,\epsilon_2-1} + \frac{\epsilon_2}{4}(u_y)_{\epsilon_1,\epsilon_2-1} - \left(u_{\epsilon_1,\epsilon_2} - \frac{\epsilon_2}{4}(u_y)_{\epsilon_1,\epsilon_2} \right) \right) \right) \\
& + \frac{1}{4\epsilon_2} \left((g(u_{\epsilon_1,\epsilon_2-1}) + g(u_{\epsilon_1,\epsilon_2})) \left(u_{\epsilon_1,\epsilon_2-1} + \frac{\epsilon_2}{4}(u_y)_{\epsilon_1,\epsilon_2-1} + \left(u_{\epsilon_1,\epsilon_2} - \frac{\epsilon_2}{4}(u_y)_{\epsilon_1,\epsilon_2} \right) \right) \right) \Bigg] \\
& (\psi(x,y) - G(u_\epsilon)\partial_y(\psi)(x,y)) \Big\}\, dxdy. \qquad (3.44)
\end{aligned}
$$

We analyze integral I_x. The analysis of integral I_y is very similar. Changing the order in the integration variable of I_x, we obtain

$$
\begin{aligned}
& \int_{\mathbb{T}} \Bigg\{ \frac{1}{4} \Bigg[\left(b^x_{\epsilon_1+1/2;\epsilon_2} \left(u_{\epsilon_1;\epsilon_2} + \frac{\epsilon_1}{4}(u_x)_{\epsilon_1;\epsilon_2} - \left(u_{\epsilon_1+1;\epsilon_2} - \frac{\epsilon_1}{4}(u_x)_{\epsilon_1+1;\epsilon_2} \right) \right) \right) \\
& + \left((f(u_{\epsilon_1;\epsilon_2}) + f(u_{\epsilon_1+1;\epsilon_2})) \left(u_{\epsilon_1;\epsilon_2} + \frac{\epsilon_1}{4}(u_x)_{\epsilon_1;\epsilon_2} + \left(u_{\epsilon_1+1;\epsilon_2} - \frac{\epsilon_1}{4}(u_x)_{\epsilon_1+1;\epsilon_2} \right) \right) \right) \Bigg] \\
& \left(\frac{\psi(x+\epsilon_1,y) - \psi(x,y)}{\epsilon_1} - H(u_{\epsilon_1;\epsilon_2})\partial_x(\psi)(x,y) \right) \Bigg\}\, dxdy. \qquad (3.45)
\end{aligned}
$$

Using that $(\psi(x+\epsilon_1,y)-\psi(x,y))/\epsilon_1 = \psi_x(x,y)+\mathbb{O}(\epsilon_1)$ and $u_{\epsilon_1;\epsilon_2}$ and $(u_x)_{\epsilon_1;\epsilon_2}$ are bounded, and that function $u_{\epsilon_1;\epsilon_2}$ is continuous minus a set of null measure, we obtain

$$
\begin{aligned}
& \lim_{\epsilon_1 \longrightarrow 0} \Bigg| \int_{\mathbb{T}} \left[\frac{1}{4} \left(b^x_{\epsilon_1+1/2;\epsilon_2} \left(u_{\epsilon_1;\epsilon_2} - u_{\epsilon_1+1;\epsilon_2} + \frac{\epsilon_1}{4}((u_x)_{\epsilon_1;\epsilon_2} + (u_x)_{\epsilon_1+1;\epsilon_2}) \right) \right) \right] \\
& \left(\left(\frac{\psi(x+\epsilon_1,y) - \psi(x,y)}{\epsilon_1} \right) dxdy \right) \Bigg| \leqslant \\
& \leqslant \lim_{\epsilon_1 \longrightarrow 0} \left(\int_{\mathbb{T}} \frac{1}{4} b_{\epsilon_1+1/2;\epsilon_2} |u_{\epsilon_1;\epsilon_2} - u_{\epsilon_1+1;\epsilon_2}| \partial_x(\psi)(x,y) dxdy + \mathbb{O}(\epsilon_1) \right) = 0, \qquad (3.46)
\end{aligned}
$$

and using that $H(u) = uf(u)$,

$$
\begin{aligned}
& \lim_{\epsilon_1 \to 0} \int_{\mathbb{T}} \frac{1}{4} \left[(f(u_{\epsilon_1;\epsilon_2}) + f(u_{\epsilon_1+1;\epsilon_2})) \left(u_{\epsilon_1;\epsilon_2} + \frac{\epsilon_1}{4}(u_x)_{\epsilon_1;\epsilon_2} + \left(u_{\epsilon_1+1;\epsilon_2} - \frac{\epsilon_1}{4}(u_x)_{\epsilon_1+1;\epsilon_2} \right) \right) \right] \\
& \left(\frac{\psi(x+\epsilon,y) - \psi(x,y)}{\epsilon_1} - H(u_{\epsilon_1;\epsilon_2})\partial_x(\psi)(x,y) \right) dxdy = \\
& = \lim_{\epsilon_1 \to 0} \int_{\mathbb{T}} \left(\frac{1}{4} \left[(f(u_{\epsilon_1;\epsilon_2}) + f(u_{\epsilon_1+1;\epsilon_2}) \left(u_{\epsilon_1;\epsilon_2} + u_{\epsilon_1+1;\epsilon_2} \right) \right] - u_{\epsilon_1;\epsilon_2} f(u_{\epsilon_1;\epsilon_2}) \right) \partial_x(\psi)(x,y) dxdy \\
& + \mathbb{O}(\epsilon_1) \\
& = \lim_{\epsilon_1 \to 0} \int_{\mathbb{T}} \frac{1}{4} \left(u_{\epsilon_1;\epsilon_2}(f(u_{\epsilon_1+1;\epsilon_2}) - f(u_{\epsilon_1;\epsilon_2})) + f(u_{\epsilon_1;\epsilon_2})(u_{\epsilon_1+1;\epsilon_2} - u_{\epsilon_1;\epsilon_2}) \right. \\
& \left. + u_{\epsilon_1+1;\epsilon_2} f(u_{\epsilon_1+1;\epsilon_2}) - u_{\epsilon_1;\epsilon_2} f(u_{\epsilon_1;\epsilon_2}) \right) \partial_x(\psi)(x,y) dxdy + \mathbb{O}(\epsilon_1). \qquad (3.47)
\end{aligned}
$$

Defining J as the integral in (3.47) and using that f is a Lipschitzian function with constant $\bar{K}_1$ [Eq. (3.11)],

$$
|J| \leqslant \lim_{\epsilon \to 0} \int_{\mathbb{T}} \frac{1}{4} \left((\bar{K}_1 |u_{\epsilon_1;\epsilon_2}| + M_1 + L_1) |u_{\epsilon_1+1;\epsilon_2} - u_{\epsilon_1;\epsilon_2}| \right) \psi_x(x,y) dxdy, \qquad (3.48)
$$

where M_1 is given by (3.21) and L_1 is given by (3.9). Using that $u_{\epsilon_1;\epsilon_2}$ is continuous (minus a set of null measure), i.e., $\lim_{\epsilon_1\to 0}|u_{\epsilon_1+1;\epsilon_2}-u_{\epsilon_1;\epsilon_2}|=0$, thus $\lim_{\epsilon\to 0}J=0$. Finally, from Eqs. (3.47) and (3.46), we prove that $I_x\to 0$ when $\epsilon_1\to 0$. From a similar calculation, we demonstrate that $I_y\to 0$ when $\epsilon_2\to 0$. Since $I=I_x+I_y$, we have that $I\to 0$ when $\epsilon=(\epsilon_1,\epsilon_2)\to(0,0)$ i.e., $u_{\epsilon_1;\epsilon_2}$ satisfies (3.10), and the proof is completed. ▫.

Remark 3.2. *Eqs.* (3.22) *and* (3.23) *represent the conditions for the stability of the method. However, we can obtain some particular (and useful) estimates for* (3.23)*. If in condition* (3.22)*, we consider*

$$b^x_{\epsilon_1+1/2;\epsilon_2}=|(f(u_{\epsilon_1;\epsilon_2})+f(u_{\epsilon_1+1;\epsilon_2}))| \quad \textit{and} \quad b^y_{\epsilon_1;\epsilon_2+1/2}=|(g(u_{\epsilon_1;\epsilon_2})+g(u_{\epsilon_1;\epsilon_2+1}))|,$$

then condition (3.23) *reduces to*

$$\frac{dt}{\epsilon_1}|(f(u_{\epsilon_1;\epsilon_2})+f(u_{\epsilon_1+1;\epsilon_2}))|\leqslant\frac{1}{2} \quad \textit{and} \quad \frac{dt}{\epsilon_2}|(g(u_{\epsilon_1;\epsilon_2})+g(u_{\epsilon_1;\epsilon_2+1}))|\leqslant\frac{1}{2}. \tag{3.49}$$

Moreover, we can obtain a global estimate for (3.49) *if we consider* $b^x_{\epsilon_1+1/2;\epsilon_2}$ *and* $b^y_{\epsilon_1;\epsilon_2+1/2}$ *to be two times the maximum of* f *and* g*. In this case, the global CFL conditions for* (3.49)*, which are linked to the proposed SDLE scheme (3.3)-(3.7), become*

$$b^x_{\epsilon_1+1/2;\epsilon_2}=2M_1\longrightarrow\frac{dt}{\epsilon_1}M_1\leqslant\frac{1}{4} \quad \textit{and} \quad b^y_{\epsilon_1;\epsilon_2+1/2}=2M_2\longrightarrow\frac{dt}{\epsilon_2}M_2\leqslant\frac{1}{4}. \tag{3.50}$$

3.2.2 Conditions for Total Variation Non-increasing ($TVNI_\epsilon$)

Now we will prove some further important results regarding to the scheme described by ODEs of type (3.13). The first property is that the scheme has a total variation non-increasing that depends on ϵ, as it was done in the scalar one dimension case, but here with a completely different approach.

We say that a numerical scheme is ϵ total variation non-increasing, denoted as $TVNI_\epsilon$, if

$$TV_\epsilon(u(\cdot,t+dt,\epsilon))\leqslant TV_\epsilon(u(\cdot,t,\epsilon), \tag{3.51}$$

where

$$TV_\epsilon(u(\cdot,t,\epsilon))=(TV_\epsilon(u(\cdot,t,\epsilon)))_x+(TV_\epsilon(u(\cdot,t,\epsilon)))_y, \tag{3.52}$$

with

$$(TV_\epsilon(u(\cdot,t,\epsilon)))_x=\int_{\mathbb{T}}|u(x+\epsilon_1,y,t,\epsilon)-u(x,y,t,\epsilon)|dxdy \quad \text{and} \tag{3.53}$$

$$(TV_\epsilon(u(\cdot,t,\epsilon)))_y=\int_{\mathbb{T}}|u(x,y+\epsilon_2,t,\epsilon)-u(x,y,t,\epsilon)|dxdy. \tag{3.54}$$

Notice that the total variation for fixed $\epsilon=(\epsilon_1,\epsilon_2)$ can be obtained as follows:

$$\frac{(TV_\epsilon(u(\cdot,t,\epsilon)))_x}{\epsilon_1}+\frac{(TV_\epsilon(u(\cdot,t,\epsilon)))_y}{\epsilon_2}.$$

Here, we extend the result obtained in Section 2.2 to a nonlinear form.

Using the following definitions:

$$\Delta_{i\frac{\epsilon_1}{2}} u(x,y,t,\epsilon) = u\left(x+(i+1)\frac{\epsilon_1}{2},y,t,\epsilon\right) - u\left(x+(i-1)\frac{\epsilon_1}{2},y,t,\epsilon\right) \quad \text{for } i\in\mathbb{Z} \tag{3.55}$$

and

$$\Delta_{i\frac{\epsilon_2}{2}} u(x,y,t,\epsilon) = u\left(x,y+(i+1)\frac{\epsilon_2}{2},t,\epsilon\right) - u\left(x,y+(i-1)\frac{\epsilon_2}{2},t,\epsilon\right) \quad \text{for } i\in\mathbb{Z}, \tag{3.56}$$

we can prove the following result:

Theorem 3.1. *Let us consider that the numerical scheme is written in the form of* (3.13)*, that is,*

$$\begin{aligned}\partial_t(u_\epsilon) = &-\frac{1}{\epsilon_1}\left[\mathcal{F}(u_{\epsilon_1;\epsilon_2},u_{\epsilon_1+1;\epsilon_2}) - \mathcal{F}(u_{\epsilon_1-1;\epsilon_2},u_{\epsilon_1;\epsilon_2})\right]\\ &-\frac{1}{\epsilon_2}\left[\mathcal{G}(u_{\epsilon_1;\epsilon_2},u_{\epsilon_1;\epsilon_2+1}) - \mathcal{G}(u_{\epsilon_1;\epsilon_2-1},u_{\epsilon_1;\epsilon_2})\right].\end{aligned}$$

If conditions

$$\frac{dt}{\epsilon_1}\left(\frac{\partial F}{\partial x}(\cdot,\cdot) - \frac{\partial F}{\partial y}(\cdot,\cdot)\right) + \frac{dt}{\epsilon_2}\left(\frac{\partial G}{\partial x}(\cdot,\cdot) - \frac{\partial G}{\partial y}(\cdot,\cdot)\right) \leqslant 1 \tag{3.57}$$

and

$$\frac{\partial F}{\partial x}(\cdot,\cdot)\geqslant 0, \quad \frac{\partial G}{\partial x}(\cdot,\cdot)\geqslant 0, \quad \frac{\partial F}{\partial y}(\cdot,\cdot)\leqslant 0, \quad \textit{and} \quad \frac{\partial G}{\partial y}(\cdot,\cdot)\leqslant 0 \tag{3.58}$$

are satisfied, then the numerical scheme is TVNI$_\epsilon$, i.e.,

$$TV_\epsilon(u(\cdot,t,\epsilon)) \leqslant TV_\epsilon(u_0(\cdot,\epsilon)), \textit{ and } u_0(x,y) \textit{ is the initial condition.} \tag{3.59}$$

In Theorem 3.1, $\frac{\partial F}{\partial x}$ and $\frac{\partial G}{\partial x}$ represent the derivatives with respect to the first argument of functions $\mathcal{F}$ and $\mathcal{G}$, while $\frac{\partial F}{\partial y}$ and $\frac{\partial G}{\partial y}$ represent the derivatives with respect to the second argument of functions $\mathcal{F}$ and $\mathcal{G}$.

Proof. First, we obtain the estimate for $(TV_\epsilon(u(\cdot,t,\epsilon))_x$. A similar calculation is performed for $(TV_\epsilon(u(\cdot,t,\epsilon))_y$. From the mean value theorem (for fixed $\epsilon=(\epsilon_1,\epsilon_2)$), we can write (3.13) as

$$\begin{aligned}u(x,y,t+dt,\epsilon) = u_{\epsilon_1,\epsilon_2} &-\frac{dt}{\epsilon_1}\left[\mathcal{F}(u_{\epsilon_1;\epsilon_2},u_{\epsilon_1+1;\epsilon_2}) - \mathcal{F}(u_{\epsilon_1-1;\epsilon_2},u_{\epsilon_1;\epsilon_2})\right]\\ &-\frac{dt}{\epsilon_2}\left[\mathcal{G}(u_{\epsilon_1;\epsilon_2},u_{\epsilon_1;\epsilon_2+1}) - \mathcal{G}(u_{\epsilon_1;\epsilon_2-1},u_{\epsilon_1;\epsilon_2})\right] + dtr(x,y,t,\epsilon,dt)\end{aligned} \tag{3.60}$$

for $||r(\cdot,t,\epsilon,dt)|| \longrightarrow 0$, uniformly in $t \in [0,T]$, and for fixed $\epsilon = (\epsilon_1,\epsilon_2)$ when $dt \longrightarrow 0$. Subtracting $u(x,y,t+dt,\epsilon)$ from $u(x+\epsilon,y,t+dt,\epsilon)$, both given by (3.60), we obtain

$$\begin{aligned}\Delta_{\frac{\epsilon_1}{2}} u(x,y,t+dt,\epsilon) = \Delta_{\frac{\epsilon_1}{2}} u(x,y,t,\epsilon) &- \frac{dt}{\epsilon_1}\left[\mathcal{F}(u_{\epsilon_1+1;\epsilon_2}, u_{\epsilon_1+2;\epsilon_2}) - \mathcal{F}(u_{\epsilon_1;\epsilon_2}, u_{\epsilon_1+1;\epsilon_2})\right] \\ &+ \frac{dt}{\epsilon_1}\left[\mathcal{F}(u_{\epsilon_1;\epsilon_2}, u_{\epsilon_1+1;\epsilon_2}) - \mathcal{F}(u_{\epsilon_1-1;\epsilon_2}, u_{\epsilon_1;\epsilon_2})\right] \\ &- \frac{dt}{\epsilon_2}\left[\mathcal{G}(u_{\epsilon_1+1;\epsilon_2}, u_{\epsilon_1+1;\epsilon_2+1}) - \mathcal{G}(u_{\epsilon_1+1;\epsilon_2-1}, u_{\epsilon_1+1;\epsilon_2})\right] \\ &+ \frac{dt}{\epsilon_2}\left[\mathcal{G}(u_{\epsilon_1;\epsilon_2}, u_{\epsilon_1;\epsilon_2+1}) - \mathcal{G}(u_{\epsilon_1;\epsilon_2-1}, u_{\epsilon_1;\epsilon_2})\right] \\ &+ dt\tilde{r}(x,y,t,\epsilon,dt), \end{aligned} \tag{3.61}$$

where $\tilde{r}(x,y,t,\epsilon,dt) = r(x+\epsilon_1,y,t,\epsilon,dt) - r(x,y,t,\epsilon,dt)$. Now, we analyze each term of the right hand side of (3.61). Term $\frac{dt}{\epsilon_1}\left[\mathcal{F}(u_{\epsilon_1+1;\epsilon_2}, u_{\epsilon_1+2;\epsilon_2}) - \mathcal{F}(u_{\epsilon_1;\epsilon_2}, u_{\epsilon_1+1;\epsilon_2})\right]$ is written as $\frac{dt}{\epsilon_1}\left[\mathcal{F}(u_{\epsilon_1+1;\epsilon_2}, u_{\epsilon_1+2;\epsilon_2}) - \mathcal{F}(u_{\epsilon_1;\epsilon_2}, u_{\epsilon_1+1;\epsilon_2})\right] =:$

$$\begin{aligned} &= \frac{dt}{\epsilon_1}\left[\mathcal{F}(u_{\epsilon_1+1;\epsilon_2}, u_{\epsilon_1+2;\epsilon_2}) - \mathcal{F}(u_{\epsilon_1+1;\epsilon_2}, u_{\epsilon_1+1;\epsilon_2}) + \mathcal{F}(u_{\epsilon_1+1;\epsilon_2}, u_{\epsilon_1+1;\epsilon_2}) - \mathcal{F}(u_{\epsilon_1;\epsilon_2}, u_{\epsilon_1+1;\epsilon_2})\right] \\ &= \frac{dt}{\epsilon_1}\left(\frac{\partial F}{\partial y}(u_{\epsilon_1+1;\epsilon_2}, \theta_{\epsilon_1+1;\epsilon_2})\Delta_{\frac{3\epsilon_1}{2}} u(x,y,t,\epsilon) + \frac{\partial F}{\partial x}(\theta_{\epsilon_1;\epsilon_2}, u_{\epsilon_1+1;\epsilon_2})\Delta_{\frac{\epsilon_1}{2}} u(x,y,t,\epsilon)\right), \end{aligned} \tag{3.62}$$

where $\theta_{\epsilon_1+i;\epsilon_2}$ are states between $u_{\epsilon_1+i;\epsilon_2}$ and $u_{\epsilon_1+1+i;\epsilon_2}$ for $i = 0,1$. Here, we are using the mean value theorem and assuming enough smoothness of function $\mathcal{F}$. Using similar calculations, we can write

$$\begin{aligned} &\frac{dt}{\epsilon_1}\left[\mathcal{F}(u_{\epsilon_1;\epsilon_2}, u_{\epsilon_1+1;\epsilon_2}) - \mathcal{F}(u_{\epsilon_1-1;\epsilon_2}, u_{\epsilon_1;\epsilon_2})\right] =: \\ &= \frac{dt}{\epsilon_1}\left(\frac{\partial F}{\partial y}(u_{\epsilon_1;\epsilon_2}, \tilde{\theta}_{\epsilon_1;\epsilon_2})\Delta_{\frac{\epsilon_1}{2}} u(x,y,t,\epsilon) + \frac{\partial F}{\partial x}(\tilde{\theta}_{\epsilon_1-1;\epsilon_2}, u_{\epsilon_1;\epsilon_2})\Delta_{\frac{-\epsilon_1}{2}} u(x,y,t,\epsilon)\right), \end{aligned} \tag{3.63}$$

where $\tilde{\theta}_{\epsilon_1+i;\epsilon_2}$ are states between $u_{\epsilon_1+i;\epsilon_2}$ and $u_{\epsilon_1+1+i;\epsilon_2}$ for $i = -1,0$. Now, the terms involving function $\mathcal{G}$ should be rewritten as

$$\begin{aligned} &-\frac{dt}{\epsilon_2}\left[\mathcal{G}(u_{\epsilon_1+1;\epsilon_2}, u_{\epsilon_1+1;\epsilon_2+1}) - \mathcal{G}(u_{\epsilon_1+1;\epsilon_2-1}, u_{\epsilon_1+1;\epsilon_2})\right] + \frac{dt}{\epsilon_2}\left[\mathcal{G}(u_{\epsilon_1;\epsilon_2}, u_{\epsilon_1;\epsilon_2+1}) - \mathcal{G}(u_{\epsilon_1;\epsilon_2-1}, u_{\epsilon_1;\epsilon_2})\right] \\ &= -\frac{dt}{\epsilon_2}\left[\mathcal{G}(u_{\epsilon_1+1;\epsilon_2}, u_{\epsilon_1+1;\epsilon_2+1}) - \mathcal{G}(u_{\epsilon_1;\epsilon_2}, u_{\epsilon_1;\epsilon_2+1})\right] \\ &+ \frac{dt}{\epsilon_2}\left[\mathcal{G}(u_{\epsilon_1+1;\epsilon_2-1}, u_{\epsilon_1+1;\epsilon_2}) - \mathcal{G}(u_{\epsilon_1;\epsilon_2-1}, u_{\epsilon_1;\epsilon_2})\right]. \end{aligned} \tag{3.64}$$

Now, we can write

$$\begin{aligned} &\frac{dt}{\epsilon_2}\left[\mathcal{G}(u_{\epsilon_1+1;\epsilon_2}, u_{\epsilon_1+1;\epsilon_2+1}) - \mathcal{G}(u_{\epsilon_1;\epsilon_2}, u_{\epsilon_1;\epsilon_2+1})\right] = \\ &\frac{dt}{\epsilon_2}\frac{\partial G}{\partial y}(u_{\epsilon_1+1;\epsilon_2}, \eta_{\epsilon_1+1;\epsilon_2+1})\Delta_{\frac{\epsilon_1}{2}} u(x,y+\epsilon_2,t,\epsilon) + \frac{dt}{\epsilon_2}\frac{\partial G}{\partial x}(\tilde{\eta}_{\epsilon_1;\epsilon_2}, u_{\epsilon_1;\epsilon_2+1})\Delta_{\frac{\epsilon_1}{2}} u(x,y,t,\epsilon) \end{aligned} \tag{3.65}$$

and

$$\frac{dt}{\epsilon_2}\left[\mathcal{G}(u_{\epsilon_1+1;\epsilon_2-1},u_{\epsilon_1+1;\epsilon_2})-\mathcal{G}(u_{\epsilon_1;\epsilon_2-1},u_{\epsilon_1;\epsilon_2})\right]=\frac{dt}{\epsilon_2}\frac{\partial G}{\partial y}(u_{\epsilon_1+1;\epsilon_2-1},\eta_{\epsilon_1+1;\epsilon_2})\Delta_{\frac{\epsilon_1}{2}}u(x,y,t,\epsilon)$$
$$+\frac{dt}{\epsilon_2}\frac{\partial G}{\partial x}(\tilde{\eta}_{\epsilon_1;\epsilon_2-1},u_{\epsilon_1;\epsilon_2})\Delta_{\frac{\epsilon_1}{2}}u(x,y-\epsilon_2,t,\epsilon), \tag{3.66}$$

where $\tilde{\eta}_{\epsilon_1;\epsilon_2+i}$ are states between $u_{\epsilon_1;\epsilon_2+i}$ and $u_{\epsilon_1;\epsilon_2+i+1}$ for $i=-1,0$; and $\eta_{\epsilon_1+1;\epsilon_2+i}$, states between $u_{\epsilon_1+1;\epsilon_2+i}$ and $u_{\epsilon_1+1;\epsilon_2+i+1}$ for $i=0,1$.

Using (3.63) to (3.66) in (3.61), we obtain

$$\begin{aligned}
\Delta_{\frac{\epsilon_1}{2}}u(x,y,t+dt,\epsilon)&=\Delta_{\frac{\epsilon_1}{2}}u(x,y,t,\epsilon)\left[1-\frac{dt}{\epsilon_1}\left(\frac{\partial F}{\partial x}(\theta_{\epsilon_1;\epsilon_2},u_{\epsilon_1+1;\epsilon_2})-\frac{\partial F}{\partial y}(u_{\epsilon_1;\epsilon_2},\tilde{\theta}_{\epsilon_1+1;\epsilon_2})\right)\right.\\
&\left.-\frac{dt}{\epsilon_2}\left(\frac{\partial G}{\partial x}(\tilde{\eta}_{\epsilon_1;\epsilon_2},u_{\epsilon_1;\epsilon_2+1})-\frac{\partial G}{\partial y}(u_{\epsilon_1+1;\epsilon_2-1},\eta_{\epsilon_1+1;\epsilon_2}\right)\right]\\
&-\frac{dt}{\epsilon_1}\frac{\partial F}{\partial y}(u_{\epsilon_1+1;\epsilon_2},\theta_{\epsilon_1+1;\epsilon_2})\Delta_{\frac{3\epsilon_1}{2}}u(x,y,t,\epsilon)\\
&+\frac{dt}{\epsilon_1}\frac{\partial F}{\partial x}(\tilde{\theta}_{\epsilon_1-1;\epsilon_2},u_{\epsilon_1;\epsilon_2})\Delta_{\frac{-\epsilon_1}{2}}u(x,y,t,\epsilon)-\frac{dt}{\epsilon_2}\frac{\partial G}{\partial y}(u_{\epsilon_1+1;\epsilon_2},\eta_{\epsilon_1+1;\epsilon_2+1})\Delta_{\frac{\epsilon_1}{2}}u(x,y+\epsilon_2,t,\epsilon)\\
&+\frac{dt}{\epsilon_2}\frac{\partial G}{\partial x}(\tilde{\eta}_{\epsilon_1;\epsilon_2-1},u_{\epsilon_1;\epsilon_2})\Delta_{\frac{\epsilon_1}{2}}u(x,y-\epsilon_2,t,\epsilon)+dt\tilde{r}(x,y,t,\epsilon,dt).
\end{aligned}\tag{3.67}$$

From conditions (3.57) and (3.58), all coefficients of (3.67) are non-negative; therefore, we have that

$$\begin{aligned}
|\Delta_{\frac{\epsilon_1}{2}}u(x,y,t+dt,\epsilon)|&=|\Delta_{\frac{\epsilon_1}{2}}u(x,y,t,\epsilon)|\left[1-\frac{dt}{\epsilon_1}\left(\frac{\partial F}{\partial x}(\theta_{\epsilon_1;\epsilon_2},u_{\epsilon_1+1;\epsilon_2})-\frac{\partial F}{\partial y}(u_{\epsilon_1;\epsilon_2},\tilde{\theta}_{\epsilon_1+1;\epsilon_2})\right)\right.\\
&\left.-\frac{dt}{\epsilon_2}\left(\frac{\partial G}{\partial x}(\tilde{\eta}_{\epsilon_1;\epsilon_2},u_{\epsilon_1;\epsilon_2+1})-\frac{\partial G}{\partial y}(u_{\epsilon_1+1;\epsilon_2-1},\eta_{\epsilon_1+1;\epsilon_2}\right)\right]\\
&-\frac{dt}{\epsilon_1}\frac{\partial F}{\partial y}(u_{\epsilon_1+1;\epsilon_2},\theta_{\epsilon_1+2;\epsilon_2})|\Delta_{\frac{3\epsilon_1}{2}}u(x,y,t,\epsilon)|\\
&+\frac{dt}{\epsilon_1}\frac{\partial F}{\partial x}(\tilde{\theta}_{\epsilon_1-1;\epsilon_2},u_{\epsilon_1;\epsilon_2})\Delta_{\frac{-\epsilon_1}{2}}u(x,y,t,\epsilon)-\frac{dt}{\epsilon_2}\frac{\partial G}{\partial y}(u_{\epsilon_1+1;\epsilon_2},\eta_{\epsilon_1+1;\epsilon_2+1})|\Delta_{\frac{\epsilon_1}{2}}u(x,y+\epsilon_2,t,\epsilon)|\\
&+\frac{dt}{\epsilon_2}\frac{\partial G}{\partial x}(\tilde{\eta}_{\epsilon_1;\epsilon_2-1},u_{\epsilon_1;\epsilon_2})|\Delta_{\frac{\epsilon_1}{2}}u(x,y-\epsilon_2,t,\epsilon)|+dt\tilde{r}(x,y,t,\epsilon,dt).
\end{aligned}\tag{3.68}$$

Integrating (3.68) in $(x,y)\in\mathbb{T}$, we notice that, due to translations of $\pm\epsilon=\pm(\epsilon_1,\epsilon_2)$, there is a two-by-two simplification of the terms of (3.68). Thus, we get

$$(TV_\epsilon(u(x,y,t+dt,\epsilon))_x=\int_{\mathbb{T}}|\Delta_{\frac{\epsilon}{2}}u(x,y,t+dt,\epsilon)|dxdy=(TV_\epsilon(u(x,y,\epsilon))))_x$$
$$+dt||\tilde{r}(x,y,t,\epsilon,dt)||_1. \tag{3.69}$$

A similar situation occurs for the variation of y, which leads to

$$\begin{aligned}
(TV_\epsilon(u(x,y,t+dt,\epsilon))_y&=\int_{\mathbb{T}}|\Delta_{\frac{\epsilon}{2}}u(x,y,t+dt,\epsilon)|dxdy\\
&=(TV_\epsilon(u(x,y,\epsilon))_y+dt||\hat{r}(x,y,t,\epsilon,dt)||_1,
\end{aligned}\tag{3.70}$$

where $||\hat{r}(x,y,t,\epsilon,dt)||_1 = \int_{\mathbb{T}} |r(x,y+\epsilon_2,t,dt,\epsilon) - r(x,y,t,dt,\epsilon)|dxdy \longrightarrow 0$ when $dt \longrightarrow 0$. Thus, from (3.69) and (3.70), we obtain that

$$TV_\epsilon(u(x,y,t+dt,\epsilon)) \leqslant TV_\epsilon(u(x,y,t,\epsilon)) + dt\left(||\tilde{r}(x,y,t,\epsilon,dt)||_1 + ||\hat{r}(x,y,t,\epsilon,dt)||_1\right). \tag{3.71}$$

Using the same argument employed to prove (3.42), condition (3.59) is true. □.

To demonstrate that our scheme satisfies the $TVNI_\epsilon$ property, we must prove that our method satisfies the hypothesis of Theorem 3.1. We assume some conditions on functions (u_x) and (u_y) and that there exists $(\alpha_1)_{\epsilon_1;\epsilon_2}$, $(\alpha_2)_{\epsilon_1;\epsilon_2}$, $(\gamma_1)_{\epsilon_1;\epsilon_2}$, and $(\gamma_2)_{\epsilon_1;\epsilon_2}$, which belong to a set of indices Λ, such that

$$\begin{aligned}(u_x)_{\epsilon_1+1;\epsilon_2} - (u_x)_{\epsilon_1;\epsilon_2} &= (\alpha_1)_{\epsilon_1;\epsilon_2}(u_{\epsilon_1+1;\epsilon_2} - u_{\epsilon_1;\epsilon_2})\\ (u_x)_{\epsilon_1+1;\epsilon_2} + (u_x)_{\epsilon_1;\epsilon_2} &= (\alpha_2)_{\epsilon_1;\epsilon_2}(u_{\epsilon_1+1;\epsilon_2} - u_{\epsilon_1;\epsilon_2}),\end{aligned} \tag{3.72}$$

and

$$\begin{aligned}(u_y)_{\epsilon_1;\epsilon_2+1} - (u_y)_{\epsilon_1;\epsilon_2} &= (\gamma_1)_{\epsilon_1;\epsilon_2}(u_{\epsilon_1;\epsilon_2+1} - u_{\epsilon_1;\epsilon_2})\\ (u_y)_{\epsilon_1;\epsilon_2+1} + (u_y)_{\epsilon_1;\epsilon_2} &= (\gamma_2)_{\epsilon_1;\epsilon_2}(u_{\epsilon_1;\epsilon_2+1} - u_{\epsilon_1;\epsilon_2}).\end{aligned} \tag{3.73}$$

Thus, we can prove the proposition below on the $TVNI_\epsilon$ condition of our method. In the next result, we give a global estimate for $b^x_{\epsilon_1+1/2;\epsilon_2}$ and $b^y_{\epsilon_1;\epsilon_2+1/2}$. However, less restrictive conditions could be obtained by locally analyzing the conditions for $TVNI_\epsilon$.

Proposition 3.2. *Let us assume that the approximation to the derivatives satisfies* (3.72) *and* (3.73) *and that* $b^x = b^x_{\epsilon_1+1/2;\epsilon_2}$ *is chosen to satisfy*

$$b^x\left(1-\frac{\epsilon_1}{4}\alpha_2\right) \geqslant -f'(x_1)\left(x_1+y_1+\frac{\epsilon_1}{4}\alpha_1(x_1-y_1)\right) - (f(x_1)+f(y_1)\left(1+\frac{\epsilon_1}{4}\alpha_1\right) \tag{3.74}$$

and

$$b^x\left(1-\frac{\epsilon_1}{4}\alpha_2\right) \geqslant f'(y_1)\left(x_1+y_1+\frac{\epsilon_1}{4}\alpha_1(x_1-y_1)\right) + (f(x_1)+f(y_1)\left(1-\frac{\epsilon_1}{4}\alpha_1\right); \tag{3.75}$$

and $b^y = b^y_{\epsilon_1;\epsilon_2+1/2}$ *is chosen to satisfy*

$$b^y\left(1-\frac{\epsilon_2}{4}\gamma_2\right) \geqslant -g'(x_2)\left(x_2+y_2+\frac{\epsilon_2}{4}\gamma_1(x_2-y_2)\right) - (g(x_2)+g(y_2)\left(1+\frac{\epsilon_2}{4}\gamma_1\right) \tag{3.76}$$

and

$$b^y\left(1-\frac{\epsilon_2}{4}\gamma_2\right) \geqslant g'(y_2)\left(x_2+y_2+\frac{\epsilon_2}{4}\gamma_1(x_2-y_2)\right) + (g(x_2)+g(y_2)\left(1-\frac{\epsilon_2}{4}\gamma_1\right), \tag{3.77}$$

with dt, ϵ_1, *and* ϵ_2 *satisfying*

$$\begin{aligned}&\frac{dt}{\epsilon_1}\Big[2b^x\left(1-\frac{\epsilon_1}{4}\alpha_2\right) + f'(x_1)(x_1+y_1+\frac{\epsilon_1}{4}\alpha_1(x_1-y_1)) - f'(x_3)\left(x_3+y_3+\frac{\epsilon_1}{4}\alpha_1(x_3-y_3)\right)\\ &+(f(x_1)+f(y_1))\left(1+\frac{\epsilon_1}{4}\alpha_1\right) - (f(x_3)+f(y_3))\left(1+\frac{\epsilon_1}{4}\alpha_1\right)\Big]\\ &+\frac{dt}{\epsilon_2}\Big[2b^y\left(1-\frac{\epsilon_2}{4}\gamma_2\right) + g'(x_2)(x_2+y_2+\frac{\epsilon_2}{4}\gamma_1(x_2-y_2)) - g'(x_4)\left(x_4+y_4+\frac{\epsilon_2}{4}\gamma_1(x_4-y_4)\right)\\ &+(g(x_2)+g(y_2))\left(1+\frac{\epsilon_2}{4}\gamma_1\right) - (g(x_4)+g(y_4))\left(1+\frac{\epsilon_2}{4}\gamma_1\right)\Big] \leqslant 4.\end{aligned} \tag{3.78}$$

Then, numerical scheme (3.13) *is* $TVNI_\epsilon$.

In Proposition 3.2, x_i and y_i represent any value of variable $u(x,y,t)$ in Ω for $i=1,2,3,4$. Similarly, α_1, α_2, γ_1, γ_2 are values in the set of indices Λ.

Proof. We first consider $\mathcal{F}(u_{\epsilon_1;\epsilon_2}, u_{\epsilon_1+1;\epsilon_2})$, which is given by (3.14), and using (3.72), for the sake of clarity, we denote $u_{\epsilon_1;\epsilon_2} = x_1$ and $u_{\epsilon_1+1;\epsilon_2} = y_1$. Thus, we get

$$\mathcal{F}(x_1,y_1) = \frac{1}{4}\left[b^x(x_1-y_1)\left(1-\frac{\epsilon_1}{4}\alpha_2\right) + (f(x_1)+f(y_1)\left(x_1+y_1+\frac{\epsilon_1}{4}\alpha_1(x_1-y_1)\right)\right]. \tag{3.79}$$

Differentiating $\mathcal{F}(x_1,y_1)$ from x_1 and y_1, we, respectively, obtain

$$\frac{\partial F}{\partial x_1} = \frac{1}{4}\left[b^x\left(1-\frac{\epsilon_1}{4}\alpha_2\right) + f'(x_1)\left(x_1+y_1+\frac{\epsilon_1}{4}\alpha_1(x_1-y_1)\right) + (f(x_1)+f(y_1)\left(1+\frac{\epsilon_1}{4}\alpha_1\right)\right] \tag{3.80}$$

and

$$\frac{\partial F}{\partial y_1} = \frac{1}{4}\left[-b^x\left(1-\frac{\epsilon_1}{4}\alpha_2\right) + f'(y_1)\left(x_1+y_1+\frac{\epsilon_1}{4}\alpha_1(x_1-y_1)\right) + (f(x_1)+f(y_1)\left(1-\frac{\epsilon_1}{4}\alpha_1\right)\right]. \tag{3.81}$$

To obtain a global condition for b^x, we consider (x_1,y_1) to be all values between $(\min u_0, \max u_0)$. From conditions (3.58), we choose b^x in Eqs. (3.80) and (3.81) such that $\frac{\partial F}{\partial x_1} \geqslant 0$ and $\frac{\partial F}{\partial y_1} \leqslant 0$, which leads to (3.74) and (3.75).

For $\mathcal{G}(u_{\epsilon_1;\epsilon_2}, u_{\epsilon_1;\epsilon_2+1})$, which is given by (3.15), and using (3.73), for the sake of clarity, we denote $u_{\epsilon_1;\epsilon_2} = x_2$ and $u_{\epsilon_1;\epsilon_2+1} = y_2$. Using similar calculations, we get

$$\mathcal{G}(x_2,y_2) = \frac{1}{4}\left[b^y(x_2-y_2)\left(1-\frac{\epsilon_2}{4}\gamma_2\right) + (g(x_2)+g(y_2)\left(x_2+y_2+\frac{\epsilon_2}{4}\gamma_1(x_2-y_2)\right)\right]. \tag{3.82}$$

Differentiating $\mathcal{G}(x_2,y_2)$ from x_2 and y_2, we, respectively, obtain

$$\frac{\partial G}{\partial x_2} = \frac{1}{4}\left[b^y\left(1-\frac{\epsilon_2}{4}\gamma_2\right) + g'(x_2)\left(x_2+y_2+\frac{\epsilon_2}{4}\gamma_1(x_2-y_2)\right) + (g(x_2)+g(y_2)\left(1+\frac{\epsilon_2}{4}\gamma_1\right)\right] \tag{3.83}$$

and

$$\frac{\partial G}{\partial y_2} = \frac{1}{4}\left[-b^y\left(1-\frac{\epsilon_1}{4}\gamma_2\right) + g'(y_2)\left(x_2+y_2+\frac{\epsilon_2}{4}\alpha_1(x_2-y_2)\right) + (g(x_2)+g(y_2)\left(1-\frac{\epsilon_2}{4}\gamma_1\right)\right]. \tag{3.84}$$

To obtain a global condition for b^y, we consider (x_2, y_2) to be all values between $(\min u_0, \max u_0)$. From conditions (3.23), we choose b^y in Eqs. (3.83) and (3.84) such that $\dfrac{\partial G}{\partial x_2} \geqslant 0$ and $\dfrac{\partial G}{\partial y_2} \leqslant 0$, which leads to (3.76)-(3.77).

Condition (3.57) is more restrictive and is obtained by choosing dt, ϵ_1, and ϵ_2 to satisfy (3.78). ▫.

Example 3.1. *Here, we give an example of approximations* (3.72) *and* (3.73). *For function* $u_\epsilon = u(x,t,\epsilon)$, *such approximation can be written as*

$$(u_x)_{\epsilon_1;\epsilon_2} = minmod\left(2\alpha\frac{u_{\epsilon_1;\epsilon_2} - u_{\epsilon_1-1;\epsilon_2}}{\epsilon_1}, \alpha\frac{u_{\epsilon_1+1;\epsilon_2} - u_{\epsilon_1-1;\epsilon_2}}{2\epsilon_1}, 2\alpha\frac{u_{\epsilon_1+1;\epsilon_2} - u_{\epsilon_1;\epsilon_2}}{\epsilon_1}\right) \tag{3.85}$$

for $(u_x)_{\epsilon_1;\epsilon_2} = (u_x)(x,y,t,\epsilon)$ *and* θ*=2. From* (3.85), *notice that* $(u_x)_\epsilon$ *is smaller (or equal to) any expression inside the minmod function. Thus, we have, for instance, that*

$$(u_x)_{\epsilon_1;\epsilon_2} = \left(\frac{2(\xi_1)\alpha}{\epsilon_1}\right)(u_{\epsilon_1+1;\epsilon_2} - u_{\epsilon_1;\epsilon_2}), \qquad with\ -1 \leqslant \xi_1 \leqslant 1. \tag{3.86}$$

Using a similar argument, we have that

$$(u_x)_{\epsilon_1+1;\epsilon_2} = \left(\frac{2(\xi_2)\alpha}{\epsilon_1}\right)(u_{\epsilon_1+1;\epsilon_2} - u_{\epsilon_1;\epsilon_2}), \qquad with\ -1 \leqslant \xi_2 \leqslant 1. \tag{3.87}$$

From Eqs. (3.86) *and* (3.87), *we obtain* (3.72.*b*)

$$(u_x)_{\epsilon_1;\epsilon_2} + (u_x)_{\epsilon_1+1;\epsilon_2} = \left(\frac{2(\xi_1+\xi_2)\alpha}{\epsilon_1}\right)(u_{\epsilon_1+1;\epsilon_2} - u_{\epsilon_1;\epsilon_2}) = (\alpha_2)_\epsilon(u_{\epsilon_1+1;\epsilon_2} - u_{\epsilon_1;\epsilon_2}). \tag{3.88}$$

Since $-1 \leqslant \xi_1 \leqslant 1$ *and* $-1 \leqslant \xi_2 \leqslant 1$, *then* $-2 \leqslant \xi_1 + \xi_2 \leqslant 2$, *which leads to*

$$-\frac{4\alpha}{\epsilon_1} \leqslant (\alpha_2)_{\epsilon_1;\epsilon_2} \leqslant \frac{4\alpha_1}{\epsilon_1}. \tag{3.89}$$

Using a similar argument, we prove that

$$(u_x)_{\epsilon_1+1;\epsilon_2} - (u_x)_{\epsilon_1;\epsilon_2} = (\alpha_1)_{\epsilon_1;\epsilon_2}(u_{\epsilon_1+1;\epsilon_2} - u_{\epsilon_1;\epsilon_2}), \qquad with\ -\frac{4\alpha}{\epsilon_1} \leqslant (\alpha_1)_{\epsilon_1;\epsilon_2} \leqslant \frac{4\alpha}{\epsilon_1}. \tag{3.90}$$

If for $(u_y)_{\epsilon_1;\epsilon_2} = (u_y)(x,y,t,\epsilon)$, *we consider*

$$(u_y)_{\epsilon_1;\epsilon_2} = minmod\left(2\beta\frac{u_{\epsilon_1;\epsilon_2} - u_{\epsilon_1;\epsilon_2-1}}{\epsilon_2}, \beta\frac{u_{\epsilon_1;\epsilon_2+1} - u_{\epsilon_1;\epsilon_2-1}}{2\epsilon_2}, 2\beta\frac{u_{\epsilon_1;\epsilon_2+1} - u_{\epsilon_1;\epsilon_2}}{\epsilon_2}\right), \tag{3.91}$$

we get

$$(u_y)_{\epsilon_1;\epsilon_2+1} - (u_y)_{\epsilon_1;\epsilon_2} = (\gamma_1)_{\epsilon_1;\epsilon_2}(u_{\epsilon_1;\epsilon_2+1} - u_{\epsilon_1;\epsilon_2}), \qquad with\ -\frac{4\beta}{\epsilon_2} \leqslant (\gamma_1)_{\epsilon_1;\epsilon_2} \leqslant \frac{4\beta}{\epsilon_2}, \qquad and \tag{3.92}$$

$$(u_y)_{\epsilon_1;\epsilon_2} + (u_y)_{\epsilon_1;\epsilon_2+1} = (\gamma_2)_{\epsilon_1;\epsilon_2}(u_{\epsilon_1;\epsilon_2+1} - u_{\epsilon_1;\epsilon_2}), \qquad with\ -\frac{4\beta}{\epsilon_2} \leqslant (\gamma_2)_{\epsilon_1;\epsilon_2} \leqslant \frac{4\beta}{\epsilon_2}. \tag{3.93}$$

From this estimate, it is necessary that $\alpha \leqslant 1$ *and* $\beta \leqslant 1$ *to achieve global stability. However, for some numerical experiments, we are able to consider larger values for* α *in* (3.85).

The idea in Example 3.1 can also be used for different approximations to the derivative of u_x, and Proposition 3.2 would still be valid.

In the next section, we prove two very important results: our numerical method satisfies the maximum principle and the Kruzhkov entropy solution.

3.2.3 The maximum principle and the entropy solution

Here, we obtain an abstract proposition that can be used for any numerical method satisfying the hypothesis of Theorem 3.1. In this case, we show that our numerical scheme satisfies the maximum principle. Since the initial data in (3.1) satisfies $u_0(x,y) \in L^\infty(\mathbb{T})$, we are able to obtain a smooth approximation to $u_0(x,y)$, denoted as $u_0(x,y,\epsilon) \in \mathcal{C}^\infty(\mathbb{T})$, such that $u_0(x,y,\epsilon)$ uniformly converges to $u_0(x,y)$. In the following proposition, we use this approximation and state our result as follows:

Proposition 3.3. *Let us assume that numerical method (3.13) satisfies the hypothesis of Theorem 3.1. Then, any local solution on $[0,T)$, for $T>0$, of (3.1), using scheme (3.13), takes its values between range $[\min_{x\in\mathbb{T}} u_0(x,y), \max_{x\in\mathbb{T}} u_0(x,y)]$.*

Proof. We consider $(x,y) \in \mathbb{T}$. First, we take values ϵ (not fixed, for example ϵ can be rational values) so that $\{n\epsilon\}_{n\in\mathbb{Z}}$ forms a dense set in $\mathbb{T}$. By contradiction, we assume that there exists a $\epsilon_0 > 0$ satisfying, for $T>0$,

$$\sup_{(x,y)\in\mathbb{T}} u(x,y,t,\epsilon_0) > \sup_{(x,y)\in\mathbb{T}} u_0(x,y,\epsilon_0) \quad \text{for some } t\in[0,T]. \tag{3.94}$$

Since $u_0(x,y,\epsilon)$ is continuous, we can choose a small enough ϵ_0 and $\eta > 0$ so that $\{u(x,y,t,\epsilon_0)\} \subset [\min_{(x,y)\in\mathbb{T}} u_0(x,y,\epsilon)-\eta, \max_{(x,y)\in\mathbb{T}} u_0(x,y,\epsilon)+\eta]$. Given that $u_0(x,y,\epsilon_0)$ is smooth, then solution $u(x,y,t,\epsilon_0)$ from Eq. (3.13) is also smooth because this space can be considered a Banach space using the L^∞ norm. Thus, there exists x_0, y_0, and t_0 such that $\sup_{(x,y)\in\mathbb{T}} u(x,y,t,\epsilon_0) = u(x_0,y_0,t_0,\epsilon_0)$. Since (x_0,y_0,t_0) is a maximum, solution $u(x,y,t,\epsilon_0)$ satisfies

$$\partial_t u(x_0,y_0,t_0,\epsilon_0) \geqslant 0. \tag{3.95}$$

Remark 3.3. *Note that, in the proof if the point (x_0,y_0,t_0) is (internal) critical we have $\partial_t u(x_0,y_0,t_0,\epsilon_0) = 0$. On the other hand, if the point (x_0,y_0,t_0) lies on the boundary, the function is increasing until it reaches this extremum point, then $\partial_t u(x_0,y_0,t_0,\epsilon_0) > 0$ follows. In any case (3.95) is true.*

Moreover, if scheme (3.13) satisfies the hypothesis of Theorem 3.1, we obtain

$$\begin{aligned}\partial_t(u(x_0,y_0,t_0,\epsilon_0)) =:& \\ &-\frac{1}{(\epsilon_1)_0}\left[\mathcal{F}(u(x_0,y_0,t_0,\epsilon_0),u(x_0+(\epsilon_1)_0,y_0,t_0,\epsilon_0)\right. \\ &\left.-\mathcal{F}(u(x_0-(\epsilon_1)_0,y_0,t_0,\epsilon_0),u(x_0,y_0,t_0,\epsilon_0))\right] \\ &-\frac{1}{(\epsilon_2)_0}\left[\mathcal{G}(u(x_0,y_0,t_0,\epsilon_0),u(x_0,y_0+(\epsilon_2)_0,t_0,\epsilon_0)\right. \\ &\left.-\mathcal{G}(u(x_0,y_0-(\epsilon_2)_0,t_0,\epsilon_0),u(x_0,y_0,t_0,\epsilon_0))\right].\end{aligned} \tag{3.96}$$

We can rewrite (3.96) as

$$\begin{aligned}&\partial_t(u(x_0,y_0,t_0,\epsilon_0)) =: \\ &-\frac{1}{(\epsilon_1)_0}\left[\mathcal{F}(u(x_0,y_0,t_0,\epsilon_0),u(x_0+(\epsilon_1)_0,y_0,t_0,\epsilon_0)-\mathcal{F}(u(x_0,y_0,t_0,\epsilon_0),u(x_0,y_0,t_0,\epsilon_0)\right] \\ &-\frac{1}{(\epsilon_1)_0}\left[\mathcal{F}(u(x_0,y_0,t_0,\epsilon_0),u(x_0,y_0,t_0,\epsilon_0)-\mathcal{F}(u(x_0-(\epsilon_1)_0,y_0,t_0,\epsilon_0),u(x_0,y_0,t_0,\epsilon_0))\right] \\ &-\frac{1}{(\epsilon_2)_0}\left[\mathcal{G}(u(x_0,y_0,t_0,\epsilon_0),u(x_0,y_0+(\epsilon_2)_0,t_0,\epsilon_0)-\mathcal{G}(u(x_0,y_0,t_0,\epsilon_0),u(x_0,y_0,t_0,\epsilon_0)\right] \\ &-\frac{1}{(\epsilon_2)_0}\left[\mathcal{G}(u(x_0,y_0,t_0,\epsilon_0),u(x_0,y_0,t_0,\epsilon_0)-\mathcal{G}(u(x_0,y_0-(\epsilon_2)_0,t_0,\epsilon_0),u(x_0,y_0,t_0,\epsilon_0))\right].\end{aligned} \tag{3.97}$$

From the mean value theorem, (3.97) becomes

$$\begin{aligned}&\partial_t(u(x_0,y_0,t_0,\epsilon_0) =: \\ &-\frac{1}{(\epsilon_1)_0}\left[\frac{\partial\mathcal{F}}{\partial y}(u(x_0,y_0,t_0,\epsilon_0),\theta_1)\right](u(x_0+(\epsilon_1)_0,y_0,t_0,\epsilon_0)-u(x_0,y_0,t_0,\epsilon_0)) \\ &-\frac{1}{(\epsilon_1)_0}\left[\frac{\partial\mathcal{F}}{\partial x}(\theta_2,u(x_0,y_0,t_0,\epsilon_0))\right](u(x_0,y_0,t_0,\epsilon_0)-u(x_0-(\epsilon_1)_0,y_0,t_0,\epsilon_0)) \\ &-\frac{1}{(\epsilon_2)_0}\left[\frac{\partial\mathcal{G}}{\partial y}(u(x_0,y_0,t_0,\epsilon_0),\eta_1))\right](u(x_0,y_0+(\epsilon_2)_0,t_0,\epsilon_0)-(u(x_0,y_0,t_0,\epsilon_0)) \\ &-\frac{1}{(\epsilon_2)_0}\left[\frac{\partial\mathcal{G}}{\partial x}(\eta_2,u(x_0,y_0,t_0,\epsilon_0))\right](u(x_0,y_0,t_0,\epsilon_0)-(u(x_0,y_0-(\epsilon_2)_0,t_0,\epsilon_0)),\end{aligned} \tag{3.98}$$

where θ_1 is a state between $u(x_0+(\epsilon_1)_0,y_0,t_0,\epsilon_0)$ and $u(x_0,y_0,t_0,\epsilon_0)$; θ_2, a state between $u(x_0,y_0-(\epsilon_1)_0,t_0,\epsilon_0)$ and $u(x_0,y_0,t_0,\epsilon_0)$; η_1, a state between $u(x_0,y_0,t_0,\epsilon_0)$ and $u(x_0,y_0+(\epsilon_2)_0,t_0,\epsilon_0)$; and η_2, a state between $u(x_0,y_0-(\epsilon_2)_0,t_0,\epsilon_0)$ and $u(x_0,y_0,t_0,\epsilon_0)$. Since $u(x_0,y_0,t_0,\epsilon_0)$ is a maximum and conditions (3.58) are valid, from Eq. (3.98), we have that

$$\partial_t u(x_0,y_0,t_0,\epsilon_0)\leqslant 0. \tag{3.99}$$

From inequalities (3.95) and (3.99), we obtain that $\partial_t u(x_0,y_0,t_0,\epsilon_0)=0$. Thus, the right hand side of (3.98) is null. This leads to $u(x_0-(\epsilon_1)_0,y_0,t_0,\epsilon_0)=u(x_0+(\epsilon_1)_0,y_0,t_0,\epsilon_0)=$

$u(x_0, y_0, t_0, \epsilon_0)$ and $u(x_0, y_0 - (\epsilon_2)_0, t_0, \epsilon_0) = u(x_0, y_0 + (\epsilon_2)_0, t_0, \epsilon_0) = u(x_0, y_0, t_0, \epsilon_0)$. By recursion, we obtain that $u(x_0 + n(\epsilon_1)_0, y_0, t_0, \epsilon_0) = u(x_0, y_0 + m(\epsilon_2)_0, t_0, \epsilon_0) = u(x_0, y_0, t_0, \epsilon_0)$ for all n and m, i.e., u is constant because u is (at least) continuous and $\mathbb{N}(\epsilon_1)_0 \times \mathbb{N}(\epsilon_2)_0$ is dense in $\mathbb{T}$ modulus 1 (because $(\epsilon_1)_0$ and $(\epsilon_2)_0$ are taken as irrational numbers). From ODE (3.13), u is constant, and the solution is trivial, which leads to a contradiction by the assumption. The same argument can be used by substituting sup by inf in Eq. (3.94), and the proof is completed. ▫.

Proposition 3.3 yields the following Corollary:

Corollary 3.1. *Let us assume that numerical method* (3.13) *satisfies the conditions of Proposition* 3.2. *Then, it also satisfies the maximum principle, i.e., the solution satisfies* $u \in [\min_{(x,y)\in\mathbb{T}} u_0(x,y), \max_{(x,y)\in\mathbb{T}} u_0(x,y)]$.

In Section 3.2, we make the hypothesis that there exists a $a > 0$ such that $u > a > 0$. From the Corollary (3.1) we can verify that this hypothesis is not restrictive to our method.

Remark 3.4. *If initial data* $u_0(x,y) \in L^\infty(\mathbb{T})$ *in Eq.* (3.1) *assumes negative, positive, and null values, we consider* $N = \sup_{(x,y)\in\mathbb{T}} |u_0(x,y)| + \beta$ *for* β *a positive constant. Then, we consider the following auxiliary problem:*

$$\frac{\partial u}{\partial t} + \frac{\partial H(u-N)}{\partial x} + \frac{\partial G(u-N)}{\partial y} = 0, \quad (x,y) \in \mathbb{T}, \quad t > 0, \qquad u(x,y,0) = u_0(x,y) + N, \tag{3.100}$$

Notice that the new initial data for (3.100) *assume only positive values. Under a suitable hypothesis (see Proposition 3.3), we demonstrate that the numerical method satisfies the maximum principle, that is, solution* $u(x,y,t)$ *takes its values between the maximum and minimum values of the initial data. Then, the solution to* (3.100) *assumes only positive values; hence, the* $u > a > 0$ *assumption is valid. In 3.2.5, we prove that if* $u(x,y,t)$ *is the (weak and entropic) solution to* (3.100), *then* $u(x,y,t) - N$ *is the solution to* (3.1).

Remark 3.5. *From Remark* 3.4, *given any Cauchy problem for* (3.1), *we can define auxiliary problem* (3.100), *which assumes only positive values. This auxiliary problem satisfies the* $u > a > 0$ *hypothesis, and the proof of convergence is valid for the solution to* (3.100), *which is* $u(x,y,t)$, *and for that to* (3.1), *which is* $u(x,y,t) - N$. *The* $u > a > 0$ *assumption helps to avoid several technical details in such proofs. In addition, by means of Remark* 3.4, *we guarantee the convergence of the numerical method for* (3.1), *without using any technical details. This is a more elegant strategy to deal with problems of the Lagrangian–Eulerian type using the no-flow curve, which requires* $H(u)/u$ *and* $G(u)/u$ *to be defined. In summary, for the sake of concreteness and simplicity, and without loss of*

generality, the proof of convergence of the SDLE scheme via the weak asymptotic analysis covers all initial data $u_0(x,y) \in L^\infty(\mathbb{R}\times\mathbb{R})$ in Eq. (3.1) for negative, positive, and null values, which is necessary for industrial and real world problems.

The next step of our construction is to prove that the proposed scheme satisfies some kind of entropy condition. In this work, we use the Kruzhkov entropy solution. We say that a solution $u(x,y,t) \in L^\infty(\mathbb{T}\times[0,T))$ satisfies the Kruzhkov entropy solution if

$$\begin{aligned}
&\int_0^T \int_{\mathbb{T}} \Big(|u(x,y,t)-K|\,\varphi_t + sign(u(x,y,t)-K)[u(x,y,t)f(u(x,y,t)) - Kf(K))]\varphi_x \\
&+ sign(u(x,y,t)-K)[u(x,y,t)g(u(x,y,t)) - Kg(K))]\varphi_y(x,y,t)\Big)dxdydt + \\
&+ \int_{\mathbb{T}} |u_0(x,y)-K|\,\varphi(x,y,0)dxdy \geqslant 0
\end{aligned} \tag{3.101}$$

for all $\varphi = \varphi(x,y,t) \in \mathcal{C}_0^\infty(\mathbb{T}\times[0,T))$. In Eq. (3.101), the subscripts in function φ represent the partial derivatives.

In this proof, we use that the sequence generated by scheme (3.13) is pre-compact. Here, we assume that

$$\mu = ||u_0(x,y)||_\infty. \tag{3.102}$$

Proposition 3.4. *(Kruzhkov entropy) Let us assume that the conditions of Proposition 3.2 are satisfied. Then, $u(x,y,t,\epsilon) \longrightarrow u(x,y,t)$ when $\epsilon \longrightarrow 0$ in $L^1_{loc}(\mathbb{T}\times[0,\infty))$, when $u(x,y,t)$ is the unique entropy solution to (3.1).*

Proof. We consider a (fixed but generic) constant $K \in [-\mu,\mu]$, $b^x_{\epsilon_1+1/2;\epsilon_2} = \hat{M}_1$, and $b^y_{\epsilon_1;\epsilon_2+1/2} = \hat{M}_2$ for all ϵ. For almost $(x,y,t) \in \mathbb{T}\times(0,\infty)$ and fixed x and y, and then using (3.13),

$$\begin{aligned}
&\frac{d}{dt}|u(x,y,t,\epsilon)-K| = sign(u_{\epsilon_1;\epsilon_2}-K)\frac{d}{dt}u(x,y,t,\epsilon) \\
&= -\frac{1}{4\epsilon_1}sign(u_{\epsilon_1;\epsilon_2}-K)\Big[\hat{M}_1\left(u_{\epsilon_1;\epsilon_2} + \frac{\epsilon_1}{4}(u_x)_{\epsilon_1;\epsilon_2} - \left(u_{\epsilon_1+1;\epsilon_2} - \frac{\epsilon_1}{4}(u_x)_{\epsilon_1+1;\epsilon_2}\right)\right) \\
&+ \left((f(u_{\epsilon_1;\epsilon_2}) + f(u_{\epsilon_1+1;\epsilon_2}))\left(u_{\epsilon_1;\epsilon_2} + \frac{\epsilon_1}{4}(u_x)_{\epsilon_1;\epsilon_2} + \left(u_{\epsilon_1+1;\epsilon_2} - \frac{\epsilon_1}{4}(u_x)_{\epsilon_1+1;\epsilon_2}\right)\right)\right) \\
&- \left(\hat{M}_1\left(u_{\epsilon_1-1;\epsilon_2} + \frac{\epsilon_1}{4}(u_x)_{\epsilon_1-1;\epsilon_2} - \left(u_{\epsilon_1;\epsilon_2} - \frac{\epsilon_1}{4}(u_x)_{\epsilon_1;\epsilon_2}\right)\right)\right) \\
&- \left((f(u_{\epsilon_1-1;\epsilon_2}) + f(u_{\epsilon_1;\epsilon_2}))\left(u_{\epsilon_1-1;\epsilon_2} + \frac{\epsilon_1}{4}(u_x)_{\epsilon_1-1;\epsilon_2} + \left(u_{\epsilon_1;\epsilon_2} - \frac{\epsilon_1}{4}(u_x)_{\epsilon_1;\epsilon_2}\right)\right)\right)\Big] \\
&- \frac{1}{4\epsilon_1}sign(u_{\epsilon_1;\epsilon_2}-K)\Big[\hat{M}_2\left(u_{\epsilon_1;\epsilon_2} + \frac{\epsilon_2}{4}(u_y)_{\epsilon_1;\epsilon_2} - \left(u_{\epsilon_1;\epsilon_2+1} - \frac{\epsilon_2}{4}(u_y)_{\epsilon_1;\epsilon_2+1}\right)\right) \\
&+ \left((g(u_{\epsilon_1;\epsilon_2}) + g(u_{\epsilon_1;\epsilon_2+1}))\left(u_{\epsilon_1;\epsilon_2} + \frac{\epsilon_2}{4}(u_y)_{\epsilon_1;\epsilon_2} + \left(u_{\epsilon_1;\epsilon_2+1} - \frac{\epsilon_2}{4}(u_y)_{\epsilon_1;\epsilon_2+1}\right)\right)\right) \\
&- \left(\hat{M}_2\left(u_{\epsilon_1;\epsilon_2-1} + \frac{\epsilon_2}{4}(u_y)_{\epsilon_1;\epsilon_2-1} - \left(u_{\epsilon_1;\epsilon_2} - \frac{\epsilon_2}{4}(u_y)_{\epsilon_1;\epsilon_2}\right)\right)\right) \\
&- \left((g(u_{\epsilon_1;\epsilon_2-1}) + g(u_{\epsilon_1;\epsilon_2}))\left(u_{\epsilon_1;\epsilon_2-1} + \frac{\epsilon_2}{4}(u_y)_{\epsilon_1;\epsilon_2-1} + \left(u_{\epsilon_1;\epsilon_2} - \frac{\epsilon_2}{4}(u_y)_{\epsilon_1;\epsilon_2}\right)\right)\right)\Big].
\end{aligned} \tag{3.103}$$

Rearranging the terms, we obtain

$$\begin{aligned}
&\frac{d}{dt}|u(x,y,t,\epsilon)-K| = sign(u_{\epsilon_1;\epsilon_2}-K)\frac{d}{dt}u(x,y,t,\epsilon)\\
&=\frac{1}{4\epsilon_1}sign(u_{\epsilon_1;\epsilon_2}-K)\left[u_{\epsilon_1+1;\epsilon_2}\hat{B}_{\epsilon_1+1;\epsilon_2}+u_{\epsilon_1-1;\epsilon_2}\hat{A}_{\epsilon_1-1;\epsilon_2}-u_{\epsilon_1;\epsilon_2}(\hat{B}_{\epsilon_1;\epsilon_2}+\hat{A}_{\epsilon_1;\epsilon_2})\right]\\
&-\frac{1}{16}sign(u_{\epsilon_1;\epsilon_2}-K)\left[(u_x)_{\epsilon_1+1;\epsilon_2}\hat{B}_{\epsilon_1+1;\epsilon_2}-(u_x)_{\epsilon_1-1;\epsilon_2}\hat{A}_{\epsilon_1-1;\epsilon_2}-(u_x)_{\epsilon_1;\epsilon_2}(\hat{B}_{\epsilon_1;\epsilon_2}-\hat{A}_{\epsilon_1;\epsilon_2})\right]\\
&+\frac{1}{4\epsilon_2}sign(u_{\epsilon_1;\epsilon_2}-K)\left[u_{\epsilon_1;\epsilon_2+1}\hat{D}_{\epsilon_1;\epsilon_2+1}+u_{\epsilon_1;\epsilon_2-1}\hat{C}_{\epsilon_1;\epsilon_2-1}-u_{\epsilon_1;\epsilon_2}(\hat{D}_{\epsilon_1;\epsilon_2}+\hat{C}_{\epsilon_1;\epsilon_2})\right]\\
&-\frac{1}{16}sign(u_{\epsilon_1;\epsilon_2}-K)\left[(u_y)_{\epsilon_1;\epsilon_2+1}\hat{D}_{\epsilon_1;\epsilon_2+1}-(u_y)_{\epsilon_1;\epsilon_2-1}\hat{C}_{\epsilon_1;\epsilon_2-1}-(u_y)_{\epsilon_1;\epsilon_2}(\hat{D}_{\epsilon_1;\epsilon_2}-\hat{C}_{\epsilon_1;\epsilon_2})\right],
\end{aligned} \tag{3.104}$$

where

$$\hat{A}_{\epsilon_1;\epsilon_2}=\hat{M}_1+f(u_{\epsilon_1;\epsilon_2})+f(u_{\epsilon_1+1;\epsilon_2}) \quad \text{and} \quad \hat{B}_{\epsilon_1+1;\epsilon_2}=\hat{M}_1-(f(u_{\epsilon_1;\epsilon_2})+f(u_{\epsilon_1+1;\epsilon_2})), \tag{3.105}$$

$$\hat{C}_{\epsilon_1;\epsilon_2}=\hat{M}_2+g(u_{\epsilon_1;\epsilon_2})+g(u_{\epsilon_1;\epsilon_2+1}) \quad \text{and} \quad \hat{D}_{\epsilon_1;\epsilon_2+1}=\hat{M}_2-(g(u_{\epsilon_1;\epsilon_2})+g(u_{\epsilon_1;\epsilon_2+1})). \tag{3.106}$$

To prove that the method satisfies the Kruzhkov entropy solution, we rewrite (3.104) as

$$\begin{aligned}
&\frac{d}{dt}|u(x,y,t,\epsilon)-K| = sign(u_{\epsilon_1;\epsilon_2}-K)\frac{d}{dt}u(x,y,t,\epsilon)\\
&=sign(u_{\epsilon_1;\epsilon_2}-K)\left\{\frac{1}{4\epsilon_1}\left[u_{\epsilon_1+1;\epsilon_2}\hat{B}_{\epsilon_1+1;\epsilon_2}+u_{\epsilon_1-1;\epsilon_2}\hat{A}_{\epsilon_1-1;\epsilon_2}\right.\right.\\
&-K(\hat{M}_1-2f(K)+\hat{M}_1+2f(K))\\
&\left.-\Big(u_{\epsilon_1;\epsilon_2}(\hat{B}_{\epsilon_1;\epsilon_2}+\hat{A}_{\epsilon_1;\epsilon_2})-K(\hat{M}_1-2f(K)+\hat{M}_1+2f(K))\Big)\right]\\
&\left.-\frac{1}{16}\left[(u_x)_{\epsilon_1+1;\epsilon_2}\hat{B}_{\epsilon_1+1;\epsilon_2}-(u_x)_{\epsilon_1-1;\epsilon_2}\hat{A}_{\epsilon_1-1;\epsilon_2}-(u_x)_{\epsilon_1;\epsilon_2}(\hat{B}_{\epsilon_1;\epsilon_2}-\hat{A}_{\epsilon_1;\epsilon_2})\right]\right\}\\
&+sign(u_{\epsilon_1;\epsilon_2}-K)\left\{\frac{1}{4\epsilon_2}\left[u_{\epsilon_1;\epsilon_2+1}\hat{D}_{\epsilon_1;\epsilon_2+1}+u_{\epsilon_1;\epsilon_2-1}\hat{C}_{\epsilon_1;\epsilon_2-1}\right.\right.\\
&-K(\hat{M}_2-2g(K)+\hat{M}_2+2g(K))\\
&\left.-\Big(u_{\epsilon_1;\epsilon_2}(\hat{D}_{\epsilon_1;\epsilon_2}+\hat{C}_{\epsilon_1;\epsilon_2})-K(\hat{M}_2-2g(K)+\hat{M}_2+2g(K))\Big)\right]\\
&\left.-\frac{1}{16}\left[(u_y)_{\epsilon_1;\epsilon_2+1}\hat{D}_{\epsilon_1;\epsilon_2+1}-(u_y)_{\epsilon_1;\epsilon_2-1}\hat{C}_{\epsilon_1;\epsilon_2-1}-(u_y)_{\epsilon_1;\epsilon_2}(\hat{D}_{\epsilon_1;\epsilon_2}-\hat{C}_{\epsilon_1;\epsilon_2})\right]\right\}.
\end{aligned} \tag{3.107}$$

Now, we analyze

$$\begin{aligned}
&sign(u_{\epsilon_1;\epsilon_2}-K)\left(u_{\epsilon_1;\epsilon_2}\hat{B}_{\epsilon_1;\epsilon_2}-K(\hat{M}_1-2f(K))\right)=\\
&=sign(u_{\epsilon_1;\epsilon_2}-K)((u_{\epsilon_1;\epsilon_2}-K)\hat{M}_1+(Kf(K)-u_{\epsilon_1;\epsilon_2}f(u_{\epsilon_1-1;\epsilon_2})\\
&+(Kf(K)-u_{\epsilon_1;\epsilon_2}f(u_{\epsilon_1;\epsilon_2}))).
\end{aligned} \tag{3.108}$$

We are interested in studying (3.108). We have the following possibilities between K and $u_{\epsilon_1;\epsilon_2}$:

1. $K = u_{\epsilon_1;\epsilon_2}$. In this case, since the numerical method is $TVNI_\epsilon$ according to the hypothesis of the numerical scheme, the set for which $K = u_{\epsilon_1;\epsilon_2} \neq u_{\epsilon_1-1;\epsilon_2}$ has null measure in $\mathbb{T} \times \mathbb{R}^+$. Thus, for $K = u_{\epsilon_1;\epsilon_2}$, we obtain

$$((u_{\epsilon_1;\epsilon_2} - K)\hat{M}_1 + (Kf(K) - u_{\epsilon_1;\epsilon_2} f(u_{\epsilon_1-1;\epsilon_2}) + (Kf(K) - u_{\epsilon_1;\epsilon_2} f(u_{\epsilon_1;\epsilon_2})) = \\ = Kf(K) - u_{\epsilon_1;\epsilon_2} f(u_{\epsilon_1-1;\epsilon_2}) \neq 0$$

only in a null measure set.

2. $K \neq u_{\epsilon_1;\epsilon_2}$. Since f is a Lipschitzian function, we have that

$$\begin{aligned} &|Kf(K) - u_{\epsilon_1;\epsilon_2} f(u_{\epsilon_1-1;\epsilon_2}) + Kf(K) - u_{\epsilon_1;\epsilon_2} f(u_{\epsilon_1;\epsilon_2})| \leqslant \\ &\leqslant |Kf(K) - u_{\epsilon_1;\epsilon_2} f(u_{\epsilon_1-1;\epsilon_2})| + |Kf(K) - u_{\epsilon_1;\epsilon_2} f(u_{\epsilon_1;\epsilon_2})| \\ &\leqslant (2(M_1 + L_1\mu)|K - u_{\epsilon_1;\epsilon_2}| + \mu L_1 |u_{\epsilon_1;\epsilon_2} - u_{\epsilon_1-1;\epsilon_2}|. \end{aligned}$$

Here, we use that

$$Kf(K) - u_{\epsilon_1;\epsilon_2} f(u_{\epsilon_1;\epsilon_2}) = (K - u_{\epsilon_1;\epsilon_2}) f(K) + u_{\epsilon_1;\epsilon_2}(f(K) - f(u_{\epsilon_1;\epsilon_2}));$$

$$\begin{aligned} Kf(K) - u_{\epsilon_1;\epsilon_2} f(u_{\epsilon_1-1;\epsilon_2}) =& (K - u_{\epsilon_1;\epsilon_2}) f(K) + u_{\epsilon_1;\epsilon_2}(f(K) - f(u_{\epsilon_1;\epsilon_2}) \\ &+ (f(u_{\epsilon_1;\epsilon_2}) - f(u_{\epsilon_1-1;\epsilon_2}))); \end{aligned}$$

L_1 is the Lipschitzian constant of f; and M_1 denotes the sup of the modulus of f given by Eq. (3.21) and of μ given by Eq. (3.102). Here, we also use that the solution satisfies the maximum principle. The states for which $u(x, y, t, \epsilon)$ is discontinuous is a set of null measure. In the case of the states for which $u(x, y, t, \epsilon)$ is continuous, we can choose a small enough ϵ such that $|u_{\epsilon_1;\epsilon_2} - u_{\epsilon_1-1;\epsilon_2}| \leqslant |K - u_{\epsilon_1;\epsilon_2}|$.

Thus, up to a null measure set, and for a small enough ϵ and taking $\hat{M}_1 > 2M_1 + 3L_1\mu$, we have

$$sign(u_{\epsilon_1;\epsilon_2} - K)(\hat{M}_1(u_{\epsilon_1;\epsilon_2} - K)) = \hat{M}_1|u_{\epsilon_1;\epsilon_2} - K| \geqslant 2Kf(K) - u_{\epsilon_1;\epsilon_2}(f(u_{\epsilon_1-1;\epsilon_2}) + f(u_{\epsilon_1;\epsilon_2})). \tag{3.109}$$

This leads to

$$\begin{aligned} &sign(u_{\epsilon_1;\epsilon_2} - K)\left(u_{\epsilon_1;\epsilon_2}\hat{B}_{\epsilon_1;\epsilon_2} - K(\hat{M}_1 - 2f(K))\right) =: \\ &= sign(u_{\epsilon_1;\epsilon_2} - K)((u_{\epsilon_1;\epsilon_2} - K)\hat{M}_1 + (2Kf(K) - u_{\epsilon 1;\epsilon 2}(f(u_{\epsilon_1-1;\epsilon_2}) + f(u_{\epsilon_1;\epsilon_2}))) \\ &= |(u_{\epsilon_1;\epsilon_2} - K)\hat{M}_1 + (2Kf(K) - u_{\epsilon_1;\epsilon_2}(f(u_{\epsilon_1-1;\epsilon_2}) + f(u_{\epsilon_1;\epsilon_2}))| \\ &= |u_{\epsilon_1;\epsilon_2}\hat{B}_{\epsilon_1;\epsilon_2} - K(\hat{M}_1 - 2f(K))|. \end{aligned} \tag{3.110}$$

The same argument can be used for

$$\begin{aligned} &sign(u_{\epsilon_1;\epsilon_2} - K)\left(u_{\epsilon_1;\epsilon_2}\hat{A}_{\epsilon_1;\epsilon_2} - K(\hat{M}_1 + 2f(K))\right) =: \\ &= sign(u_{\epsilon_1;\epsilon_2} - K)((u_{\epsilon_1;\epsilon_2} - K)\hat{M}_1 - (f(K) - u_{\epsilon_1;\epsilon_2} f(u_{\epsilon_1-1;\epsilon_2}) - (f(K) - u_{\epsilon_1;\epsilon_2} f(u_{\epsilon_1;\epsilon_2}))), \end{aligned} \tag{3.111}$$

and, for a small enough ϵ and up to a null measure set, we can write

$$sign(u_{\epsilon_1;\epsilon_2}-K)\left(u_{\epsilon_1;\epsilon_2}\hat{A}_{\epsilon_1;\epsilon_2}-K(\hat{M}_1+2f(K))\right)=|u_{\epsilon_1;\epsilon_2}\hat{A}_{\epsilon_1;\epsilon_2}-K(\hat{M}_1+2f(K))|. \tag{3.112}$$

Performing similar calculations and taking $\hat{M}_2>2M_2+3L_2\mu$, where M_2 is given by (3.21), for a small enough $\epsilon=(\epsilon_1,\epsilon_2)$, we also have

$$sign(u_{\epsilon_1;\epsilon_2}-K)\left(u_{\epsilon_1;\epsilon_2}\hat{C}_{\epsilon_1;\epsilon_2}-K(\hat{M}_2+2g(K))\right)=|u_{\epsilon_1;\epsilon_2}\hat{C}_{\epsilon_1;\epsilon_2}-K(\hat{M}_2+2g(K))| \tag{3.113}$$

and

$$sign(u_{\epsilon_1;\epsilon_2}-K)\left(u_{\epsilon_1;\epsilon_2}\hat{D}_{\epsilon_1;\epsilon_2}-K(\hat{M}_2+2g(K))\right)=|u_{\epsilon_1;\epsilon_2}\hat{D}_{\epsilon_1;\epsilon_2}-K(\hat{M}_2+2g(K))|. \tag{3.114}$$

Now, consider a small enough ϵ, and except on a null set. Thus, we use equations (3.110), (3.112), (3.113) and (3.114) in (3.107) to obtain

$$\frac{d}{dt}|u(x,y,t,\epsilon)-K|\leqslant\Psi_{\epsilon_1;\epsilon_2}+\Theta_{\epsilon_1;\epsilon_2}, \tag{3.115}$$

where

$$\begin{aligned}\Psi_{\epsilon_1;\epsilon_2}&=\frac{1}{4\epsilon_1}\left(\left|u_{\epsilon_1+1;\epsilon_2}\hat{B}_{\epsilon_1+1;\epsilon_2}-K(\hat{M}_1-2f(K))\right|-\left|u_{\epsilon_1;\epsilon_2}\hat{B}_{\epsilon_1;\epsilon_2}-K(\hat{M}_1-2f(K))\right|\right)\\&-\frac{1}{4\epsilon_1}\left(\left|u_{\epsilon_1;\epsilon_2}\hat{A}_{\epsilon_1;\epsilon_2}-K(\hat{M}_1+2f(K))\right|-\left|u_{\epsilon_1-1;\epsilon_2}\hat{A}_{\epsilon_1-1;\epsilon_2}-K(\hat{M}_1+2f(K))\right|\right)\\&-\frac{1}{16}sign(u_{\epsilon_1;\epsilon_2}-K)\left[(u_x)_{\epsilon_1+1;\epsilon_2}\hat{B}_{\epsilon_1+1;\epsilon_2}-(u_x)_{\epsilon_1-1;\epsilon_2}\hat{A}_{\epsilon_1-1;\epsilon_2}-(u_x)_{\epsilon_1;\epsilon_2}(\hat{B}_{\epsilon_1;\epsilon_2}-\hat{A}_{\epsilon_1;\epsilon_2})\right]\end{aligned} \tag{3.116}$$

and

$$\begin{aligned}\Theta_{\epsilon_1;\epsilon_2}&=\frac{1}{4\epsilon_2}\left(\left|u_{\epsilon_1;\epsilon_2+1}\hat{D}_{\epsilon_1;\epsilon_2+1}-K(\hat{M}_2-2g(K))\right|-\left|u_{\epsilon_1;\epsilon_2}\hat{D}_{\epsilon_1;\epsilon_2}-K(\hat{M}_2-2g(K))\right|\right)\\&-\frac{1}{4\epsilon_2}\left(\left|u_{\epsilon_1;\epsilon_2}\hat{C}_{\epsilon_1;\epsilon_2}-K(\hat{M}_2+2g(K))\right|-\left|u_{\epsilon_1;\epsilon_2-1}\hat{C}_{\epsilon_1;\epsilon_2-1}-K(\hat{M}_2+2g(K))\right|\right)\\&-\frac{1}{16}sign(u_{\epsilon_1;\epsilon_2}-K)\left[(u_y)_{\epsilon_1;\epsilon_2+1}\hat{D}_{\epsilon_1;\epsilon_2+1}-(u_y)_{\epsilon_1;\epsilon_2-1}\hat{C}_{\epsilon_1;\epsilon_2-1}-(u_y)_{\epsilon_1;\epsilon_2}(\hat{D}_{\epsilon_1;\epsilon_2}-\hat{C}_{\epsilon_1;\epsilon_2})\right].\end{aligned} \tag{3.117}$$

In other to simplify our calculations, we prove our next result for

$$\frac{d}{dt}|u(x,y,t,\epsilon)-K|\leqslant\Psi_{\epsilon_1;\epsilon_2}. \tag{3.118}$$

Multiplying inequality (3.118) by the non-negative test function $\varphi=\varphi(x,y,t)\in C_0^\infty(\mathbb{T}\times[0,T)),T>0$, and integrating by parts, we obtain (notice that the null measure

set does not modify the value of the integral)

$$
\begin{aligned}
&-\int_{\mathbb{T}} |u_0(x,y)-K|\,\varphi(x,y,0)dxdy-\int_0^T\int_{\mathbb{T}} |u(x,y,t,\epsilon)-K|\,\varphi_t(x,y,t)dxdydt\leqslant\\
&\int_0^T\int_{\mathbb{T}}\Big\{\frac{1}{4\epsilon_1}\Big(|u_{\epsilon_1;\epsilon_2}\hat{B}_{\epsilon_1+1;\epsilon_2}-K(\hat{M}_1-2f(K))|-|u_{\epsilon_1;\epsilon_2}\hat{B}_{\epsilon_1;\epsilon_2}-K(\hat{M}_1-2f(K))|\Big)\\
&-\frac{1}{4\epsilon_1}\Big(|u_{\epsilon_1;\epsilon_2}\hat{A}_{\epsilon_1;\epsilon_2}-K(\hat{M}_1+2f(K))|-|u_{\epsilon_1-1;\epsilon_2}\hat{A}_{\epsilon_1-1;\epsilon_2}-K(\hat{M}_1+2f(K))|\Big)\\
&-P(K)\Big[(u_x)_{\epsilon_1+1;\epsilon_2}\hat{B}_{\epsilon_1+1;\epsilon_2}-(u_x)_{\epsilon_1-1;\epsilon_2}\hat{A}_{\epsilon_1-1;\epsilon_2}-(u_x)_{\epsilon_1;\epsilon_2}(\hat{B}_{\epsilon_1;\epsilon_2}-\hat{A}_{\epsilon_1;\epsilon_2})\Big]\Big\}\,g\,dx\,dy\,dt,
\end{aligned}
\tag{3.119}
$$

where $P(K)=\frac{1}{16}sign(u_{\epsilon_1;\epsilon_2}-K)$. Note that if we take $\epsilon_1\longrightarrow\epsilon_1-1$ in the index, we have that

$$
\Big|u_{\epsilon_1+1;\epsilon_2}\hat{B}_{\epsilon_1+1;\epsilon_2}-K(\hat{M}_1-2f(K))\Big|\varphi\longrightarrow\Big|u_{\epsilon_1;\epsilon_2}\hat{B}_{\epsilon_1;\epsilon_2}-K(\hat{M}_1-2f(K))\Big|\varphi(x-\epsilon_1,y,t),
$$

and that if we take $\epsilon_1\longrightarrow\epsilon_1+1$ in the index, we have that

$$
\Big|u_{\epsilon_1-1;\epsilon_2}\hat{A}_{\epsilon_1-1;\epsilon_2}-K(\hat{M}_1+2f(K))\Big|\varphi\longrightarrow\Big|u_{\epsilon_1;\epsilon_2}\hat{A}_{\epsilon_1;\epsilon_2}-K(\hat{M}_1+2f(K))\Big|\varphi(x+\epsilon_1,y,t).
$$

Thus, inequality (3.119) is written as

$$
\begin{aligned}
&-\int_{\mathbb{T}} |u_0(x,y)-K|\,\varphi(x,y,0)dxdy-\int_0^T\int_{\mathbb{T}} |u(x,y,t,\epsilon)-K|\,\varphi_t(x,y,t)dxdydt\leqslant\\
&\int_0^T\int_{\mathbb{T}}\Big\{\frac{1}{4}\Big(-\Big|u_{\epsilon_1;\epsilon_2}\hat{B}_{\epsilon_1;\epsilon_2}-K(\hat{M}_1-2f(K))\Big|\Big)\left(\frac{\varphi(x,y,t)-\varphi(x-\epsilon_1,y,t)}{\epsilon_1}\right)dxdydt+\\
&+\int_0^T\int_{\mathbb{T}}\frac{1}{4}\Big(\Big|u_{\epsilon_1;\epsilon_2}\hat{A}_{\epsilon_1-1;\epsilon_2}-K(\hat{M}_1+2f(K))\Big|\Big)\left(\frac{\varphi(x+\epsilon_1,y,t)-\varphi(x,y,t)}{\epsilon_1}\right)dxdydt\\
&-\int_0^T\int_{\mathbb{T}}P(K)\Big[(u_x)_{\epsilon_1+1;\epsilon_2}\hat{B}_{\epsilon_1+1;\epsilon_2}-(u_x)_{\epsilon_1-1;\epsilon_2}\hat{A}_{\epsilon_1-1;\epsilon_2}-(u_x)_{\epsilon_1;\epsilon_2}(\hat{B}_{\epsilon_1;\epsilon_2}-\hat{A}_{\epsilon_1;\epsilon_2})\Big]\varphi dxdydt.
\end{aligned}
\tag{3.120}
$$

Since $\varphi\in C_0^\infty(\mathbb{T}\times[0,T))$, Eq. (3.120) becomes

$$
\begin{aligned}
&-\int_{\mathbb{T}} |u_0(x,y)-K|\,\varphi(x,y,0)dxdy-\int_0^T\int_{\mathbb{T}} |u(x,y,t,\epsilon)-K|\,\varphi_t(x,y,t)dxdydt\leqslant\\
&\int_0^T\int_{\mathbb{T}}\Big\{\frac{1}{4}\Big(\Big|u_{\epsilon_1;\epsilon_2}\hat{A}_{\epsilon_1;\epsilon_2}-K(\hat{M}_1+2f(K))\Big|-\Big|u_{\epsilon_1;\epsilon_2}\hat{B}_{\epsilon_1;\epsilon_2}-K(\hat{M}_1-2f(K))\Big|\Big)\varphi_x\Big)dxdydt\\
&+I(\epsilon_1)\\
&-\int_0^T\int_{\mathbb{T}}P(K)\Big[(u_x)_{\epsilon_1+1;\epsilon_2}\hat{B}_{\epsilon_1+1;\epsilon_2}-(u_x)_{\epsilon_1-1;\epsilon_2}\hat{A}_{\epsilon_1-1;\epsilon_2}-(u_x)_{\epsilon_1;\epsilon_2}(\hat{B}_{\epsilon_1;\epsilon_2}-\hat{A}_{\epsilon_1;\epsilon_2})\Big]\varphi dxdydt.
\end{aligned}
\tag{3.121}
$$

Here, $I(\epsilon)\longrightarrow 0$ when $\epsilon\longrightarrow 0$. Considering that (3.110) and (3.112) are valid, we obtain

$$
\begin{aligned}
&|u_{\epsilon_1;\epsilon_2}\hat{A}_{\epsilon_1;\epsilon_2}-K(\hat{M}_1+2f(K))|-|u_{\epsilon_1;\epsilon_2}\hat{B}_{\epsilon_1;\epsilon_2}-K(\hat{M}-2f(K))|=\\
&=16P(K)\Big[u_{\epsilon_1;\epsilon_2}\hat{A}_{\epsilon_1;\epsilon_2}-K(\hat{M}_1+2f(K))-(u_{\epsilon_1;\epsilon_2}\hat{B}_{\epsilon_1;\epsilon_2}-K(\hat{M}_1-2f(K)))\Big]\\
&=16P(K)\left[u_{\epsilon_1;\epsilon_2}(2f(u_{\epsilon_1;\epsilon_2})+f(u_{\epsilon_1+1;\epsilon_2})+f(u_{\epsilon_1-1;\epsilon_2})-4Kf(K)\right].
\end{aligned}
\tag{3.122}
$$

By substituting (3.122) in (3.121), we have that

$$
\begin{aligned}
&-\int_{\mathbb{T}} |u_0(x,y)-K|\,\varphi(x,y,0)dxdy-\int_0^T\int_{\mathbb{T}} |u(x,y,t,\epsilon)-K|\,\varphi_t dxdydt \leqslant \\
&\int_0^T\int_{\mathbb{T}} \Big\{\frac{1}{4}\Big(16P(K)\left[u_{\epsilon_1;\epsilon_2}(2f(u_{\epsilon_1;\epsilon_2})+f(u_{\epsilon_1+1;\epsilon_2})+f(u_{\epsilon_1-1;\epsilon_2})-4Kf(K)\right]\Big)\varphi_x\Big)dxdydt \\
&+I(\epsilon_1) \\
&-\int_0^T\int_{\mathbb{T}} P(K)\left[(u_x)_{\epsilon_1+1;\epsilon_2}\hat{B}_{\epsilon_1+1;\epsilon_2}-(u_x)_{\epsilon_1-1;\epsilon_2}\hat{A}_{\epsilon_1-1;\epsilon_2}-(u_x)_{\epsilon_1;\epsilon_2}(\hat{B}_{\epsilon_1;\epsilon_2}-\hat{A}_{\epsilon_1;\epsilon_2})\right]\varphi dxdydt.
\end{aligned}
\tag{3.123}
$$

To complete our proof, we must analyze

$$
\int_0^T\int_{\mathbb{T}} P(K)\left[(u_x)_{\epsilon_1+1;\epsilon_2}\hat{B}_{\epsilon_1+1;\epsilon_2}-(u_x)_{\epsilon_1-1;\epsilon_2}\hat{A}_{\epsilon_1-1;\epsilon_2}-(u_x)_{\epsilon_1;\epsilon_2}(\hat{B}_{\epsilon_1;\epsilon_2}-\hat{A}_{\epsilon_1;\epsilon_2})\right]\varphi dxdydt. \tag{3.124}
$$

Considering previous arguments, we know that, since the proposed scheme is $TVNI_\epsilon$, for each fixed t, there exists only a finite number of (x,y) such that $u_\epsilon(x,y,t,\epsilon)-K$ changes the signal. Then, we split $\mathbb{T}=\mathbb{S}_1\cup\mathbb{S}_2\cup\mathbb{S}_3$ such that

$$
(x,y)\in\mathbb{S}_1 \longrightarrow sign(u_\epsilon(x,y,t,\epsilon)-K)<0 \quad \text{and} \tag{3.125}
$$

$$
(x,y)\in\mathbb{S}_2 \longrightarrow sign(u_\epsilon(x,y,t,\epsilon)-K)>0, \tag{3.126}
$$

and $\mathbb{S}_3$ has null measure. Here, $\mathbb{S}_1$ and $\mathbb{S}_2$ consist (each) of a finite number of subintervals. We rewrite the spatial integral on $\mathbb{T}$ in (3.124) as

$$
\begin{aligned}
&-\int_{\mathbb{S}_1}\Big\{\left[(u_x)_{\epsilon_1+1;\epsilon_2}\hat{B}_{\epsilon_1+1;\epsilon_2}-(u_x)_{\epsilon_1-1;\epsilon_2}\hat{A}_{\epsilon_1-1;\epsilon_2}-(u_x)_{\epsilon_1;\epsilon_2}(\hat{B}_{\epsilon_1;\epsilon_2}-\hat{A}_{\epsilon_1;\epsilon_2})\right]\Big\}\varphi(x,y,t)dxdydt \\
&\quad+\int_{\mathbb{S}_2}\Big\{\left[(u_x)_{\epsilon_1+1;\epsilon_2}\hat{B}_{\epsilon_1+1;\epsilon_2}-(u_x)_{\epsilon_1-1;\epsilon_2}\hat{A}_{\epsilon_1-1;\epsilon_2}-(u_x)_{\epsilon_1;\epsilon_2}(\hat{B}_{\epsilon_1;\epsilon_2}-\hat{A}_{\epsilon_1;\epsilon_2})\right]\Big\}\varphi dxdydt.
\end{aligned}
$$

Now, notice that, due to translations of $\pm\epsilon$, we have that

$$
\int_{\mathbb{S}_1}\Big\{\left[(u_x)_{\epsilon_1+1;\epsilon_2}\hat{B}_{\epsilon_1+1;\epsilon_2}-(u_x)_{\epsilon_1-1;\epsilon_2}\hat{A}_{\epsilon_1-1;\epsilon_2}-(u_x)_{\epsilon_1;\epsilon_2}(\hat{B}_{\epsilon_1;\epsilon_2}-\hat{A}_{\epsilon_1;\epsilon_2})\right]\Big\}\varphi dxdydt=\mathbb{O}(\epsilon_1) \tag{3.127}
$$

because the terms inside the integral cancel out (actually, they do not cancel out only at the extremes of the subintervals of $\mathbb{S}_1$). The same argument is valid for the integral on $\mathbb{S}_2$. Given that the argument is valid for any $t\in[0,T]$, we have that (3.124) is $\mathbb{O}(\epsilon_1)$.

Then, Eq. (3.123) is written as

$$
\begin{aligned}
&\int_{\mathbb{T}} |u_0(x,y)-K|\,\varphi(x,y,0)dxdy+\int_0^T\int_{\mathbb{T}} |u(x,y,t,\epsilon)-K|\,\varphi_t(x,y,t)dxdydt \\
&+\int_0^T\int_{\mathbb{T}}\Big\{\frac{1}{4}\Big(P(K)\left[u_{\epsilon_1;\epsilon_2}(2f(u_{\epsilon_1;\epsilon_2})+f(u_{\epsilon_1+1;\epsilon_2})+f(u_{\epsilon_1-1;\epsilon_2})-4Kf(K)\right]\Big)\varphi_x\Big)dxdydt \geqslant \\
&\geqslant -I(\epsilon_1)+\mathbb{O}(\epsilon_1).
\end{aligned}
\tag{3.128}
$$

Using (3.115) and performing similar calculations, we obtain

$$\int_{\mathbb{T}} |u_0(x,y) - K|\,\varphi(x,y,0)dxdy + \int_0^T \int_{\mathbb{T}} |u(x,y,t,\epsilon) - K|\,\varphi_t(x,y,t)dxdydt +$$
$$\int_0^T \int_{\mathbb{T}} \Big\{ \frac{1}{4}\Big(16P(K)\left[u_{\epsilon_1;\epsilon_2}(2f(u_{\epsilon_1;\epsilon_2}) + f(u_{\epsilon_1+1;\epsilon_2}) + f(u_{\epsilon_1-1;\epsilon_2}) - 4Kf(K)\right]\Big)\varphi_x \Big) dxdydt +$$
$$\int_0^T \int_{\mathbb{T}} \Big\{ \frac{1}{4}\Big(16P(K)\left[u_{\epsilon_1;\epsilon_2}(2g(u_{\epsilon_1;\epsilon_2}) + g(u_{\epsilon_1;\epsilon_2+1}) + g(u_{\epsilon_1;\epsilon_2-1}) - 4Kg(K)\right]\Big)\varphi_y \Big) dxdydt \geqslant$$
$$\geqslant -I(\epsilon) + \mathbb{O}(\epsilon). \tag{3.129}$$

Here, $u_{\epsilon_1;\epsilon_2} = u(x,y,t,\epsilon)$ and $I(\epsilon) = I(\epsilon_1) + I(\epsilon_2)$. In 3.2.4, we show that family $u(x,y,t,\epsilon)$ for $\epsilon_1 > 0$ and $\epsilon_2 > 0$ and $\epsilon = (\epsilon_1, \epsilon_2)$ is a pre-compact sequence in $L^1(\mathbb{T}\times[0,T])$. Let $u(x,y,t)$ be an accumulation point of family $u(x,y,t,\epsilon)$. Thus, for a sub-sequence ϵ_r, we have that $u(x,y,t,\epsilon_r) \longrightarrow u(x,y,t)$ when $r \longrightarrow \infty$ in $L^1(\mathbb{T}\times[0,T])$. In other words, $u(x,y,t,\epsilon_r+1) \longrightarrow u(x,y,t)$ and $u(x,y,t,\epsilon_r-1) \longrightarrow u(x,y,t)$ when point-wise up to a set of null measure. Taking the limit as $\epsilon = \epsilon_r \longrightarrow 0$ in (3.128), we obtain the entropy relation, remembering that $I(\epsilon) + \mathbb{O}(\epsilon) \longrightarrow 0$ and noticing that $f(u_{\epsilon_1;\epsilon_2}) \longrightarrow f(u)$, $f(u_{\epsilon_1\pm1;\epsilon_2}) \longrightarrow f(u)$, $g(u_{\epsilon_1;\epsilon_2}) \longrightarrow g(u)$, and $g(u_{\epsilon_1;\epsilon_2\pm1}) \longrightarrow g(u)$. Thus, $u(x,y,t)$ satisfies Eq. (3.101).

In Eq. (3.101), $K \in [-\mu,\mu]$. However, for $|K| \geqslant \mu$, note that the inequality that is Eq. (3.101) reduces to the equality (weak solution),

$$\int_0^T \int_{\mathbb{T}} \Big(u(x,y,t)\varphi_t(x,y,t) + u(x,y,t)f(u)\varphi_x(x,y,t) + u(x,y,t)g(u)\varphi_y(x,y,t)\Big) dxdydt$$
$$+ \int_{\mathbb{T}} u_0(x,y)g(x,y,0)dx = 0.$$

From these results, we obtain that (3.101) holds for all $K \in \mathbb{R}$. Since $T > 0$ and $\varphi = \varphi(x,y,t) \in C_0^\infty(\mathbb{T}\times[0,T))$ are arbitrary functions, inequality (3.101) leads to solution $u(x,y,t)$, which is the (unique) entropy solution to (3.1). From the above, it is easy to see from (3.13) that an accumulation point $u(x,y,t)$ of $u(x,y,t,\epsilon)$ is unique. This implies that $u(x,y,t,\epsilon)$ converges to $u(x,y,t)$ as $\epsilon \to 0$ in $L^1_{loc}(\mathbb{T}\times[0,\infty))$ because T is arbitrary, which completes the proof. ▫.

Therefore, we prove that the SDLE method (3.3)-(3.7) obtained from (3.13)-(3.14) converges to the entropy solution of (3.1).

3.2.4 The pre-compactness of sequence $u(x,t,\epsilon)$

Here, for Lemma 1 and Corollary 3.2 below, we use the same notation employed in [2], i.e., $x = (x,y)$ for the 2D case.

To prove that sequence $u(x,t,\epsilon)$ is pre-compact, we used some of the results reported in [2]. The first result we need is Lemma 1 in [2].

Lemma 1. *Suppose that* $u(x) \in L^1(\mathbb{T}^n)$, $h > 0$. *Then*

$$\int_{\mathbb{T}^n} |u(x)(signu)^h(x) - |u(x)||dx \leqslant 2\omega^x(h),$$

where

$$\omega^x(h) = \sup_{|\Delta x| \leqslant h} \int_{\mathbb{T}^n} |u(x + \Delta x) - u(x)|dx$$

is the continuity modulus of $u(x)$ in $L^1(\mathbb{T}^n)$.

Here, $\mathbb{T}^n$ is the n-dimensional torus. In this study, we are interested in a one-dimensional problem. For $n = 1$, $\mathbb{T}^n$ reduces to $\mathbb{T}$. Since the proof of the previous Lemma does not depend on the scheme, we refer to [2].

Notice that $\omega^x(h)$ is a measure of $TVNI_\epsilon$, as described in Eq. (3.52). Thus, under the same hypothesis of Proposition 3.2, we can prove the following Corollary:

Corollary 3.2. *Let us assume that* $u(x, t, \epsilon)$ *is given by scheme* (3.13) *and satisfies the hypothesis of Proposition* 3.2. *Then, for all* $t > 0$, $\Delta x \in \mathbb{R}$, *we have that*

$$\int_{\mathbb{T}} |u(x + \Delta x, t, \epsilon) - u(x, t, \epsilon)|dx \leqslant \int_{\mathbb{T}} |u_0(x + \Delta x, t, \epsilon) - u_0(x, t, \epsilon)|dx \leqslant \omega^x(|\Delta x|), \quad (3.130)$$

where

$$\omega^x(|\Delta x|) \leqslant \sup_{|\Delta x| \leqslant h} \int_{\mathbb{T}} |u_0(x + \Delta x, t, \epsilon) - u_0(x, t, \epsilon)|dx$$

is the continuity modulus of initial data $u_0(x)$ *in* $\mathbb{T}$.

The proof of Corollary 3.2 follows from Proposition 3.2 and the supremum properties of a function. Now, we prove the result to obtain the pre-compactness of sequence $u(x, y, t, \epsilon)$. The first useful result, similar to that obtained in [2], is

Lemma 3.1. *Let us assume that* $\phi(x, y) \in C^1(\mathbb{T})$. *Then* $\forall \Delta t > 0$,

$$\int_{\mathbb{T}} (u(x, t + \Delta t, \epsilon) - u(x, t, \epsilon)\phi(x)dx \leqslant N||\nabla\phi||_\infty \zeta(\mathbb{T})\Delta t. \quad (3.131)$$

Here, $\zeta(\mathbb{T})$ is the measure of $\mathbb{T}$ and

$$N = \left(\frac{\hat{M}_1}{2} + M_1\right)\left(\mu + \frac{\epsilon_1}{8}\upsilon_1\right) + \left(\frac{\hat{M}_2}{2} + M_2\right)\left(\mu + \frac{\epsilon_2}{8}\upsilon_2\right) \quad \text{and} \quad \mu = ||u_0||_\infty.$$

Proof. Let us denote $I(t) = \int_{\mathbb{T}} u(x,t,\epsilon)\phi(x)dx$. Differentiating $I(t)$ from t and using (3.13), we have that

$$
\begin{aligned}
I'(t) = \int_{\mathbb{T}} \Bigg\{ & -\frac{1}{4\epsilon_1}\Bigg[\left(b^x_{\epsilon_1+1/2;\epsilon_2}\left(u_{\epsilon_1;\epsilon_2}+\frac{\epsilon_1}{4}(u_x)_{\epsilon_1;\epsilon_2}-\left(u_{\epsilon_1+1;\epsilon_2}-\frac{\epsilon_1}{4}(u_x)_{\epsilon_1;\epsilon_2}\right)\right)\right)+ \\
& +\left((f(u_{\epsilon_1;\epsilon_2})+f(u_{\epsilon_1+1;\epsilon_2}))\left(u_{\epsilon_1;\epsilon_2}+\frac{\epsilon_1}{4}(u_x)_{\epsilon_1;\epsilon_2}+\left(u_{\epsilon_1+1;\epsilon_2}-\frac{\epsilon_1}{4}(u_x)_{\epsilon_1+1;\epsilon_2}\right)\right)\right) \\
& -\left(b^x_{\epsilon_1-1/2;\epsilon_2}\left(u_{\epsilon_1-1;\epsilon_2}+\frac{\epsilon_1}{4}(u_x)_{\epsilon_1-1;\epsilon_2}-\left(u_{\epsilon_1;\epsilon_2}-\frac{\epsilon_1}{4}(u_x)_{\epsilon_1;\epsilon_2}\right)\right)\right)+ \\
& -\left((f(u_{\epsilon_1-1;\epsilon_2})+f(u_{\epsilon_1;\epsilon_2}))\left(u_{\epsilon_1-1;\epsilon_2}+\frac{\epsilon_1}{4}(u_x)_{\epsilon_1-1;\epsilon_2}+\left(u_{\epsilon_1;\epsilon_2}-\frac{\epsilon_1}{4}(u_x)_{\epsilon_1;\epsilon_2}\right)\right)\right)\Bigg] \\
& -\frac{1}{4\epsilon_2}\Bigg[\left(b^y_{\epsilon_1;\epsilon_2+1/2}\left(u_{\epsilon_1;\epsilon_2}+\frac{\epsilon_2}{4}(u_y)_{\epsilon_1;\epsilon_2}-\left(u_{\epsilon_1;\epsilon_2+1}-\frac{\epsilon_2}{4}(u_y)_{\epsilon_1;\epsilon_2}\right)\right)\right)+ \\
& +\left((g(u_{\epsilon_1;\epsilon_2})+g(u_{\epsilon_1;\epsilon_2+1}))\left(u_{\epsilon_1;\epsilon_2}+\frac{\epsilon_2}{4}(u_y)_{\epsilon_1;\epsilon_2}+\left(u_{\epsilon_1;\epsilon_2+1}-\frac{\epsilon_2}{4}(u_y)_{\epsilon_1;\epsilon_2+1}\right)\right)\right) \\
& -\left(b^y_{\epsilon_1;\epsilon_2-1/2}\left(u_{\epsilon_1;\epsilon_2-1}+\frac{\epsilon_2}{4}(u_y)_{\epsilon_1;\epsilon_2-1}-\left(u_{\epsilon_1;\epsilon_2}-\frac{\epsilon_2}{4}(u_y)_{\epsilon_1;\epsilon_2}\right)\right)\right)+ \\
& -\left((g(u_{\epsilon_1;\epsilon_2-1})+g(u_{\epsilon_1;\epsilon_2}))\left(u_{\epsilon_1;\epsilon_2-1}+\frac{\epsilon_2}{4}(u_y)_{\epsilon_1;\epsilon_2-1}+\left(u_{\epsilon_1;\epsilon_2}-\frac{\epsilon_2}{4}(u_y)_{\epsilon_1;\epsilon_2}\right)\right)\right)\Bigg]\Bigg\}\phi dxdy.
\end{aligned}
$$

Changing the order in the integration variable, we obtain

$$
\begin{aligned}
I'(t) = \int_{\mathbb{T}} \Bigg\{ & \frac{1}{4}\Bigg[\left(b^x_{\epsilon_1+1/2;\epsilon_2}\left(u_{\epsilon_1;\epsilon_2}+\frac{\epsilon_1}{4}(u_x)_{\epsilon_1;\epsilon_2}-\left(u_{\epsilon_1+1;\epsilon_2}-\frac{\epsilon_1}{4}(u_x)_{\epsilon_1+1;\epsilon_2}\right)\right)\right)+ \\
& +\left((f(u_{\epsilon_1;\epsilon_2})+f(u_{\epsilon_1+1;\epsilon_2}))\left(u_{\epsilon_1;\epsilon_2}+\frac{\epsilon_1}{4}(u_x)_{\epsilon_1;\epsilon_2}+\left(u_{\epsilon_1+1;\epsilon_2}-\frac{\epsilon_1}{4}(u_x)_{\epsilon_1+1;\epsilon_2}\right)\right)\right)\Bigg] \\
& \left(\frac{\phi(x+\epsilon_1,y)-\phi(x,y)}{\epsilon_1}\right) \\
& +\frac{1}{4}\Bigg[\left(b^y_{\epsilon_1;\epsilon_2+1/2}\left(u_{\epsilon_1;\epsilon_2}+\frac{\epsilon_2}{4}(u_y)_{\epsilon_1;\epsilon_2}-\left(u_{\epsilon_1;\epsilon_2+1}-\frac{\epsilon_2}{4}(u_y)_{\epsilon_1;\epsilon_2+1}\right)\right)\right)+ \\
& +\left((g(u_{\epsilon_1;\epsilon_2})+g(u_{\epsilon_1;\epsilon_2+1}))\left(u_{\epsilon_1;\epsilon_2}+\frac{\epsilon_2}{4}(u_y)_{\epsilon_1;\epsilon_2}+\left(u_{\epsilon_1;\epsilon_2+1}-\frac{\epsilon_2}{4}(u_y)_{\epsilon_1;\epsilon_2+1}\right)\right)\right)\Bigg] \\
& \left(\frac{\phi(x,y+\epsilon_2)-\phi(x,y)}{\epsilon_2}\right)\Bigg\}dxdy. \qquad (3.132)
\end{aligned}
$$

Since $I'(t) = G(t)$ implies that $|I(t+\Delta t)-I(t)| \leqslant \max G(t)\Delta t$, we can estimate the right hand side inside of the integral of Eq. (3.132) as

$$
\begin{aligned}
|RHS| \leqslant \Bigg\{ & \frac{1}{4}\Bigg[\left(\left|b^x_{\epsilon_1+1/2;\epsilon_2}\right|\left(\left|u_{\epsilon_1;\epsilon_2}\right|+\frac{\epsilon_1}{4}\left|(u_x)_{\epsilon_1;\epsilon_2}\right|-\left(u_{\epsilon_1+1;\epsilon_2}-\frac{\epsilon_1}{4}(u_x)_{\epsilon_1+1;\epsilon_2}\right)\right)\right)+ \\
& +\left((f(u_{\epsilon_1;\epsilon_2})+f(u_{\epsilon_1+1;\epsilon_2}))\left(\left|u_{\epsilon_1;\epsilon_2}\right|+\frac{\epsilon_1}{4}\left|(u_x)_{\epsilon_1;\epsilon_2}\right|+\left(\left|u_{\epsilon_1+1;\epsilon_2}\right|+\frac{\epsilon_1}{4}\left|(u_x)_{\epsilon_1+1;\epsilon_2}\right|\right)\right)\right)\Bigg] \\
& \left(\left|\frac{\phi(x+\epsilon_1,y)-\phi(x,y)}{\epsilon_1}\right|\right) \\
& +\frac{1}{4}\Bigg[\left(\left|b^y_{\epsilon_1;\epsilon_2+1/2}\right|\left(\left|u_{\epsilon_1;\epsilon_2}\right|+\frac{\epsilon_2}{4}\left|(u_y)_{\epsilon_1;\epsilon_2}\right|+\left(\left|u_{\epsilon_1;\epsilon_2+1}\right|+\frac{\epsilon_2}{4}\left|(u_y)_{\epsilon_1;\epsilon_2+1}\right|\right)\right)\right)+ \\
& +\left((\left|g(u_{\epsilon_1;\epsilon_2})\right|+\left|g(u_{\epsilon_1;\epsilon_2+1})\right|)\left(\left|u_{\epsilon_1;\epsilon_2}\right|+\frac{\epsilon_2}{4}\left|(u_y)_{\epsilon_1;\epsilon_2}\right|+\left(\left|u_{\epsilon_1;\epsilon_2+1}\right|+\frac{\epsilon_2}{4}\left|(u_y)_{\epsilon_1;\epsilon_2+1}\right|\right)\right)\right)\Bigg] \\
& \left(\left|\frac{\phi(x,y+\epsilon_2)-\phi(x,y)}{\epsilon_2}\right|\right).
\end{aligned}
$$

Using that

$$\left|\frac{\phi(x\pm\epsilon,y)-\phi(x)}{\epsilon_1}\right|\leqslant||\nabla\phi||_\infty \quad \text{and} \quad \left|\frac{\phi(x,y\pm\epsilon)-\phi(x)}{\epsilon_2}\right|\leqslant||\nabla\phi||_\infty,$$

$b^x_{\epsilon_1+1/2;\epsilon_2}=\hat{M}_1$, $b^y_{\epsilon_1;\epsilon_2+1/2}=\hat{M}_2$, $||(u_x)||_\infty\leqslant\upsilon_1$, $||(u_y)||_\infty\leqslant\upsilon_2$, $||u(x,t,\epsilon)||_\infty=\mu$, and M_1 and M_2 are given by (3.21), condition (3.131) is satisfied. □

Since we obtained similar estimates in [2], we used Lemma 3 in [2].

Lemma 3. *For every $t\geqslant 0$, $\Delta t>0$*

$$\int_{\mathbb{T}}|u(x,t+\Delta t,\epsilon)-u(x,t,\epsilon)|dx\leqslant\omega^t(\Delta t),$$

where $\omega^t(\Delta t)=\inf_{h>0}(4\omega^x(h)+cN\Delta t/h)$, and c is a universal constant.

Note that in $\omega^t(\Delta t)$, since this parameter is the infimun, $\omega^t(\Delta t)$, for fixed Δt, reduces to $\inf_{h>0}(4\omega^x(h))$.

Moreover, since $\omega^x(h)\longrightarrow 0$ as $h\longrightarrow 0$ and does not depend on ϵ (based on previous results), family $u(x,t,\epsilon)$ is uniformly bounded and equicontinuous in $L^1(\mathbb{T}\times[0,T])$ for every $T>0$. Thus, $u(x,t,\epsilon)$ is a pre-compact sequence in $L^1(\mathbb{T}\times[0,T])$, which implies that we can extract a sequence $\epsilon_k\longrightarrow 0$ such that $u_k(x,y,t)=u(x,y,t,\epsilon_k)\longrightarrow u(x,y,t)$ as $k\longrightarrow\infty$ in $L^1_{loc}(\mathbb{T}\times[0,\infty])$.

3.2.5 Weak solution of auxiliary problem

Here, we give the proof considering the classical weak solution defined in $\mathbb{R}^2\times\mathbb{R}^+$. The proof is similar for the domain $\mathbb{T}\times\mathbb{R}^+$. First, we consider the weak solution to (3.100) to be

$$\int_{\mathbb{R}^+}\int_{\mathbb{R}\times\mathbb{R}}\left(u\varphi_t+H(u-N)\varphi_x+G(u-N)\varphi_y\right)dxdydt+\int_{\mathbb{R}\times\mathbb{R}}(u_0(x,y)+N)\varphi_0dxdy=0, \tag{3.133}$$

where $\varphi_0=\varphi(x,y,0)$, and $\varphi=\varphi(x,y,t)$ is a test function with support in $\mathbb{R}^2\times\mathbb{R}^+$. If we consider the domain $\mathbb{T}\times\mathbb{R}^+$, the support of φ lies in domain $\mathbb{T}\times\mathbb{R}^+$.

By substituting $u-N=U$ in (3.133), we obtain

$$\begin{aligned}&\int_{\mathbb{R}^+}\int_{\mathbb{R}\times\mathbb{R}}\left((U+N)\varphi_t+H(U)\varphi_x+G(U)\varphi_y\right)dxdydt+\int_{\mathbb{R}\times\mathbb{R}}(u_0(x,y)+N)\varphi(x,y,0)dxdy=\\&\int_{\mathbb{R}^+}\int_{\mathbb{R}\times\mathbb{R}}\left(U\varphi_t+H(U)\varphi_x+G(U)\varphi_y\right)dxdydt+\int_{\mathbb{R}\times\mathbb{R}}(u_0(x,y)+N)\varphi(x,y,0)dxdy\\&+\int_{\mathbb{R}^+}\int_{\mathbb{R}\times\mathbb{R}}N\varphi_tdxdydt=0.\end{aligned} \tag{3.134}$$

Using Fubini's theorem for the integral and using that $\varphi(x,y,t)$ has compact support, then

$$\int_{\mathbb{R}^+}\int_{\mathbb{R}\times\mathbb{R}} N\varphi_t dxdydt = -\int_{\mathbb{R}\times\mathbb{R}} N\varphi(x,y,0)dxdy. \tag{3.135}$$

By substituting (3.135) in (3.134), we get

$$\int_{\mathbb{R}^+}\int_{\mathbb{R}\times\mathbb{R}} \left(U\varphi_t + H(U)\varphi_x + G(U)\varphi_y\right) dxdt + \int_{\mathbb{R}\times\mathbb{R}} u_0(x,y)\varphi(x,y,0)dx = 0, \tag{3.136}$$

which is the solution to (3.1). The previous calculations are reversible, i.e., (3.136) in (3.133). Thus, if $u(x,y,t)$ is the solution to (3.1), then $u(x,y,t) - N$ is the solution to (3.100), and the reciprocal is true.

A similar calculation can be performed to prove that the entropic solutions are the same.

3.3 Numerical experiments for scalar hyperbolic conservation laws in 2D

We provide robust numerical examples for verifying the theory and illustrating the capabilities of the semi-discrete approach. We present and discuss the application of the proposed semi-discrete scheme to nontrivial two-dimensional nonlinear scalar problems whose solutions lead to intricate wave interactions (e.g., 2D Inviscid Burgers' equation: Oblique Riemann problem, Buckley-Leverett equation with gravity and non-linear equation with non-convex fluxes). We will use hereafter "s" as the usual abbreviations to Seconds to report the elapsed time for each numerical experiment presented. The 2D SDLE scheme (3.3)-(3.7) only employs the available easy information of quantities u and fluxes $H(u)$ and $G(u)$, along with the *no-flow* CFL-type constraint (3.8) supported by the analysis summarized in the Eqs. (3.20), (3.21) and (3.50). In Section 4.3.4, numerical analysis are conducted with an Experimental Order of Convergence (EOC) in the L^1 norm of the relative error by the aid of our 2D semi-discrete method (3.3)-(3.7) to show numerical robustness of the no-flow curves, which are natural mathematical objects from the differential models under consideration.

Example 3.2. ***Numerical diffusion test*** *[64]*

In order to investigate the numerical behavior of our two-dimensional semi-discrete method when several time steps are used, we consider the two-dimensional linear hyperbolic problem,

$$\begin{cases} \dfrac{\partial u}{\partial t} + \dfrac{\partial u}{\partial x} + \dfrac{\partial u}{\partial y} = 0, \quad (x,y,t) \in [0,1]^2 \times [0,1], \\ u(x,y,0) = u_0(x,y), \end{cases} \tag{3.137}$$

where periodic initial datum and exact solution are given by

$$u_0(x,y) = \text{sen}^2(\pi x)\text{sen}^2(\pi y) \quad \text{and} \quad u(x,y,t) = \text{sen}^2(\pi(x-t))\text{sen}^2(\pi(y-t)), \tag{3.138}$$

respectively. The numerical solutions displayed on the right column of Figure 5 (from top to bottom) present a computational analysis linked to the novel SDLE scheme when several time steps are used in order to respond to a concrete situation that allows us to test if the numerical solution computed by the semi-discrete scheme is affected by excessive numerical diffusion. The new SDLE framework is capable to avoid excessive *numerical diffusion* in computational studies (e.g., see such effect in the experiments produced with the two-dimensional classical Lax-Friedrichs scheme in the left column in Figure 5). The resulting numerical solutions are convincing in verifying the theory and illustrating the capabilities of the semi-discrete Lagrangian-Eulerian scheme because of their excellent resemblance with the exact solution (*black contour*).

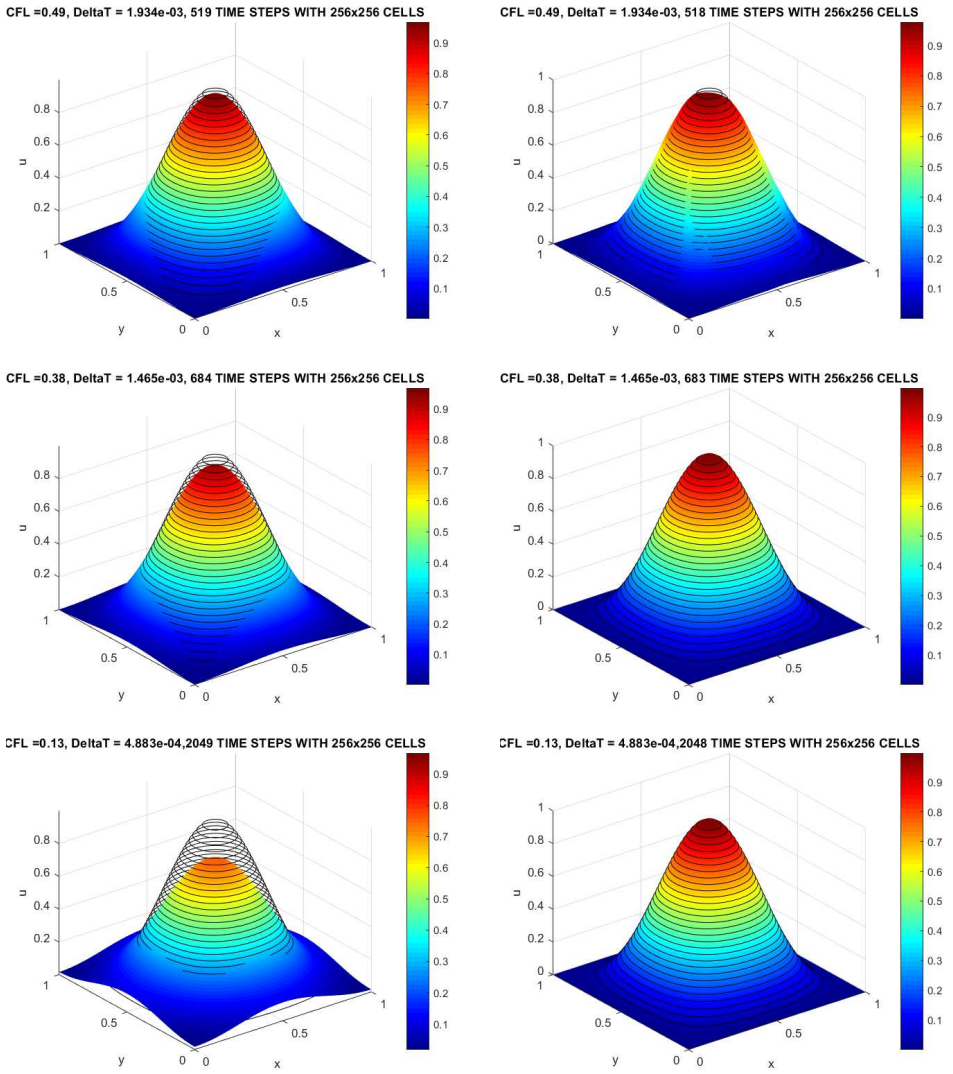

Figure 5 – A numerical diffusion study by the two-dimensional Lax-Friedrichs scheme (left column) and the two-dimensional semi-discrete Lagrangian-Eulerian scheme (3.3)-(3.4) (right column, $\alpha = 2$, $\zeta = 1$ and $\theta = 1.5$) with several time steps. *Black contour represents the simulation of the exact solution.*

Example 3.3. ***Two-dimensional inviscid Burgers' equation*** *[32]*

In this example, we focus on numerically studying the scalar 2D fundamental inviscid Burgers' equation with an oblique shock on the unit square as follows:

$$\frac{\partial u}{\partial t} + \frac{\partial}{\partial x}\left(\frac{u^2}{2}\right) + \frac{\partial}{\partial y}\left(\frac{u^2}{2}\right) = 0, \quad (x, y, t) \in [0, 1]^2 \times (0, 0.5], \tag{3.139}$$

along with the following Riemann initial condition:

$$u(x, y, 0) = \begin{cases} 2, & x < 0.25, \quad y < 0.25, \\ 3, & x > 0.25, \quad y > 0.25, \\ 1, & \text{otherwise}, \end{cases} \tag{3.140}$$

in conjunction with an exact boundary condition on the inflow portions of $\partial\Omega$. In fact, it is well known the solution for (3.139)-(3.140) is composed of two shock waves and two rarefactions that meet at the middle of the domain to form a cusp. As observed in Figure 6, we performed a mesh refinement study by the aid of our SDLE scheme (3.3)-(3.4) for several different grid cells at time $T = 1/12$ and with the following computational times: 0.46 s (64×64 grid cells), 3.24 s (128×128 grid cells) and 31.90 s (256×256 grid cells). The SDLE scheme, in its simplest form, proved to be computationally efficient and exhibited no spurious oscillations in sharp-front regions, no grid orientation difficulty with very good resolution.

Example 3.4. ***Two-dimensional inviscid Burgers' equation: oblique Riemann problem*** *[32]*

Let us consider the two-dimensional scalar hyperbolic equation given by (3.139) in domain $(x, y, t) \in [0, 1]^2 \times (0, 0.5]$ subject to the following "oblique" Riemann initial condition:

$$u(x, y, 0) = \begin{cases} -1.0, & x > 0.5, \quad y > 0.5, \\ -0.2, & x < 0.5, \quad y > 0.5, \\ +0.5, & x < 0.5, \quad y < 0.5, \\ +0.8, & x > 0.5, \quad y < 0.5, \end{cases} \tag{3.141}$$

in conjunction with an exact boundary condition on the inflow portions of $\partial\Omega$. As in the previous, the SDLE scheme captured the moving fronts and no spurious oscillations have been observed with very good resolution as we can see in Figure 7 at time $T = 0.5$ and with efficient computations 0.22 s (64×64 grid cells), 1.58 s (128×128 grid cells) and 14.39 s (256×256 grid cells).

Example 3.5. ***The Buckley-Leverett equation with gravity*** *[32]*

Let us consider the non-convex Buckley-Leverett model, which is motivated by the classical immiscible incompressible two-phase (e.g., water and oil) flow system with gravity for the reservoir water-flooding problem in oil recovery

$$\frac{\partial S_w}{\partial t} + \frac{\partial (f(S_w))}{\partial x} + \frac{\partial (g(S_w))}{\partial y} = 0, \qquad (x, y, t) \in [-1.5, 1.5]^2 \times [0, 0.5], \tag{3.142}$$

where $g(S_w) = f(S_w)(1 - C_g(1 - S_w)^2)$ is non-convex Buckley-Leverett fractional flow function of water with

$$f(S_w) = \frac{s_w^2}{S_w^2 + \frac{\mu_w}{\mu_0}(1 - S_w)^2}, \tag{3.143}$$

where μ_w and μ_0 are the viscosities of the water and oil phases, respectively. For the sake of simplicity, in the simulations discussed here, we have chosen $\dfrac{\mu_w}{\mu_0} = 1$, $C_g = 5$ and initial

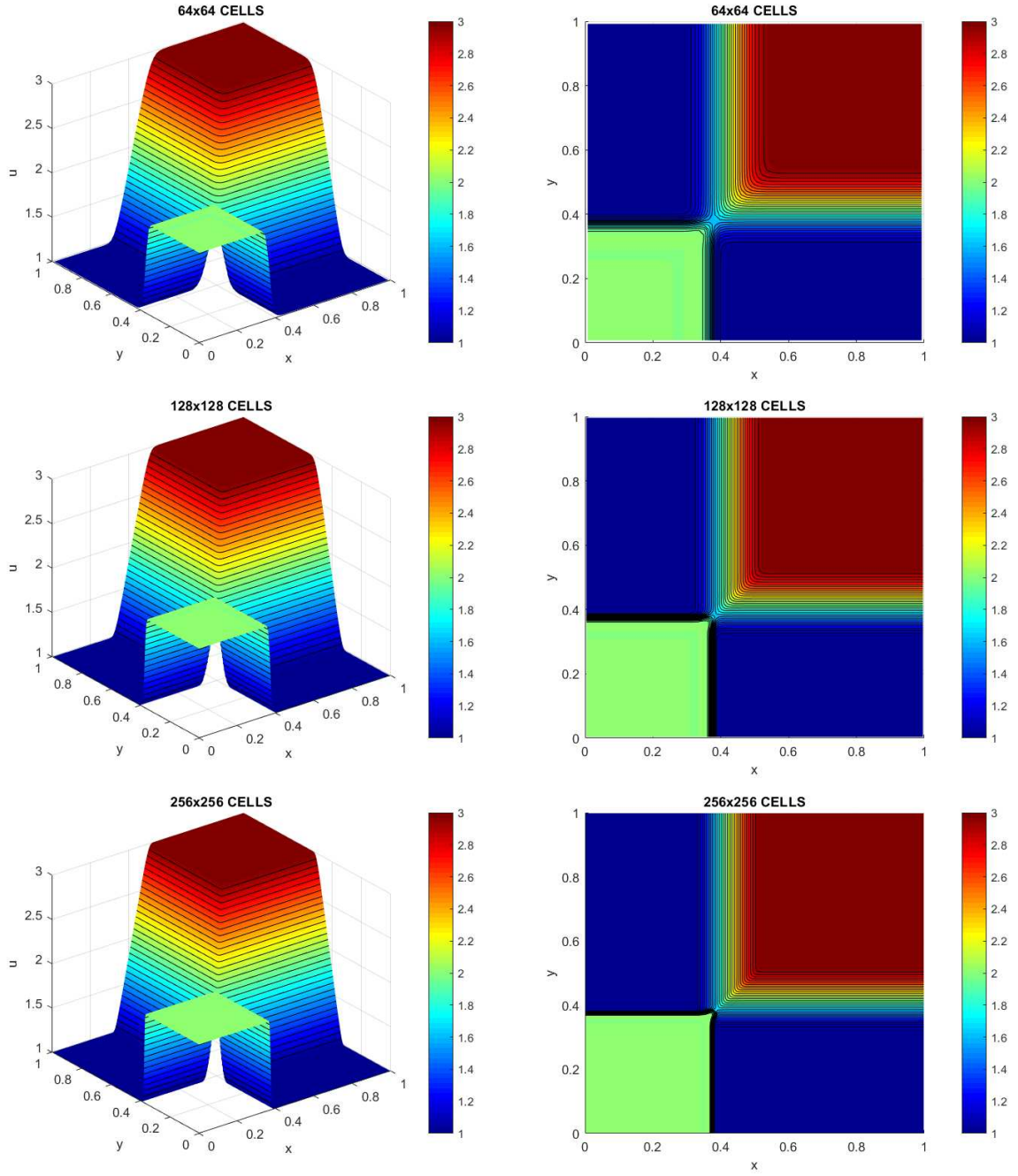

Figure 6 – 3D-plot's view angle (left column) and the corresponding 2D contour views (right column) of the numerical approximations for model (3.139)-(3.140) computed using the SDLE scheme with $\alpha = 2$, $\zeta = 2$, $\theta = 1.5$ and CFL $= 0.12$.

condition,

$$u(x, y, 0) = \begin{cases} 1, & x^2 + y^2 < 0.5, \\ 0, & \text{otherwise.} \end{cases} \tag{3.144}$$

Again, the corresponding numerical approximations for model (3.142)-(3.144) are displayed in Figure 8 with very good resolution with efficient computations: 0.17 s (64 $\times$ 64 grid cells), 1.34 s (128 $\times$ 128 grid cells) and 11.12 s (256 $\times$ 256 grid cells). As before,

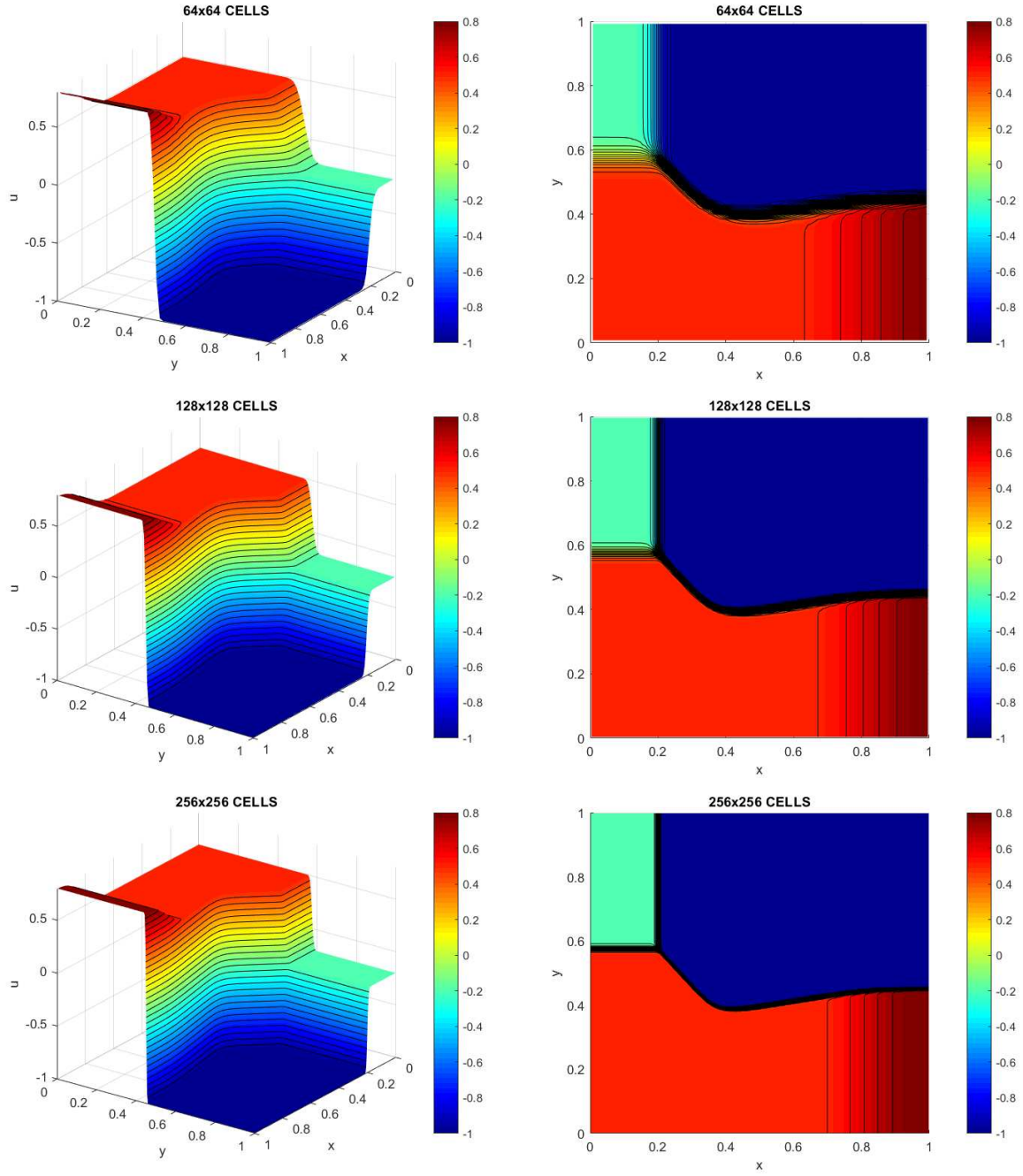

Figure 7 – The corresponding approximations for model (3.139)-(3.141) computed using the SDLE scheme with $\alpha = 1$, $\zeta = 3$, $\theta = 2$, and CFL $= 0.12$.

the SDLE scheme captured the sharp-front regions with no spurious oscillations.

Example 3.6. ***A nonlinear equation with non-convex fluxes*** *[32]*

Let us consider the following 2D initial value problem with non-convex fluxes $H(u)$ and $G(u)$ such that $H''(u)$ and $G''(u)$ change signs, given by:

$$\frac{\partial u}{\partial t} + \frac{\partial H(u)}{\partial x} + \frac{\partial G(u)}{\partial y} = 0, \qquad (x, y, t) \in [-2, 2] \times [-2.5, 1.5] \times [0, 1], \tag{3.145}$$

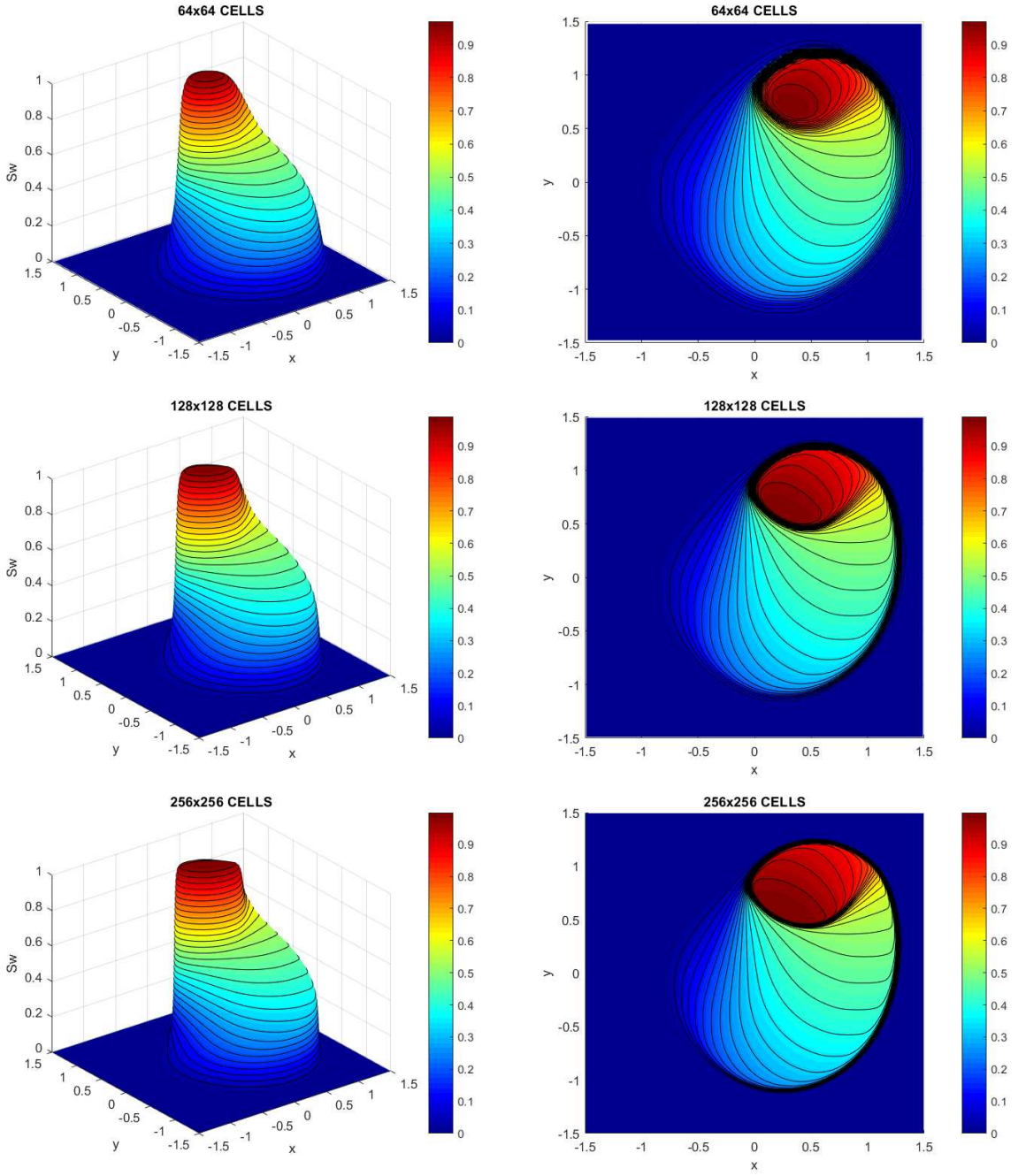

Figure 8 – A mesh refinement study of the numerical approximations for the two-dimensional hyperbolic problem (3.142)-(3.144) (3D-plot's view angle, left column and 2D contour, right column), which were computed using SDLE with $\alpha = 2$, $\zeta = 5$, $\theta = 1$, and CFL $= 0.07$ at time $T = 0.5$.

with $H(u) := \text{sen}(u)$ and $G(u) := \cos(u)$, subject to initial datum,

$$u(x, y, 0) = \begin{cases} 3.5\pi, & x^2 + y^2 < 1, \\ 0.25\pi, & \text{otherwise}, \end{cases} \tag{3.146}$$

in conjunction with an exact boundary condition on the inflow portions of $\partial\Omega$. In this model problem (3.145)-(3.146), the flux in the x-direction of (3.145) has three inflection

points, while that in the y-direction has four. Figure 9 shows the resulting solution to the Riemann problem, which is computed with the SDLE scheme ($\alpha = 1$, $\zeta = 2$, and $\theta = 2$) at time $T = 1$. Again, we can see the shock capturing scheme SDLE (3.3)-(3.4), along with (3.5)-(3.7), provides numerical approximations that are total variation non-increasing (Section 3.2.2) and good resolution of the discontinuous features with computational efficiency: 0.36 s (64×64 cells), 2.83 s (128×128 cells) and 22.87 s (256×256 cells).

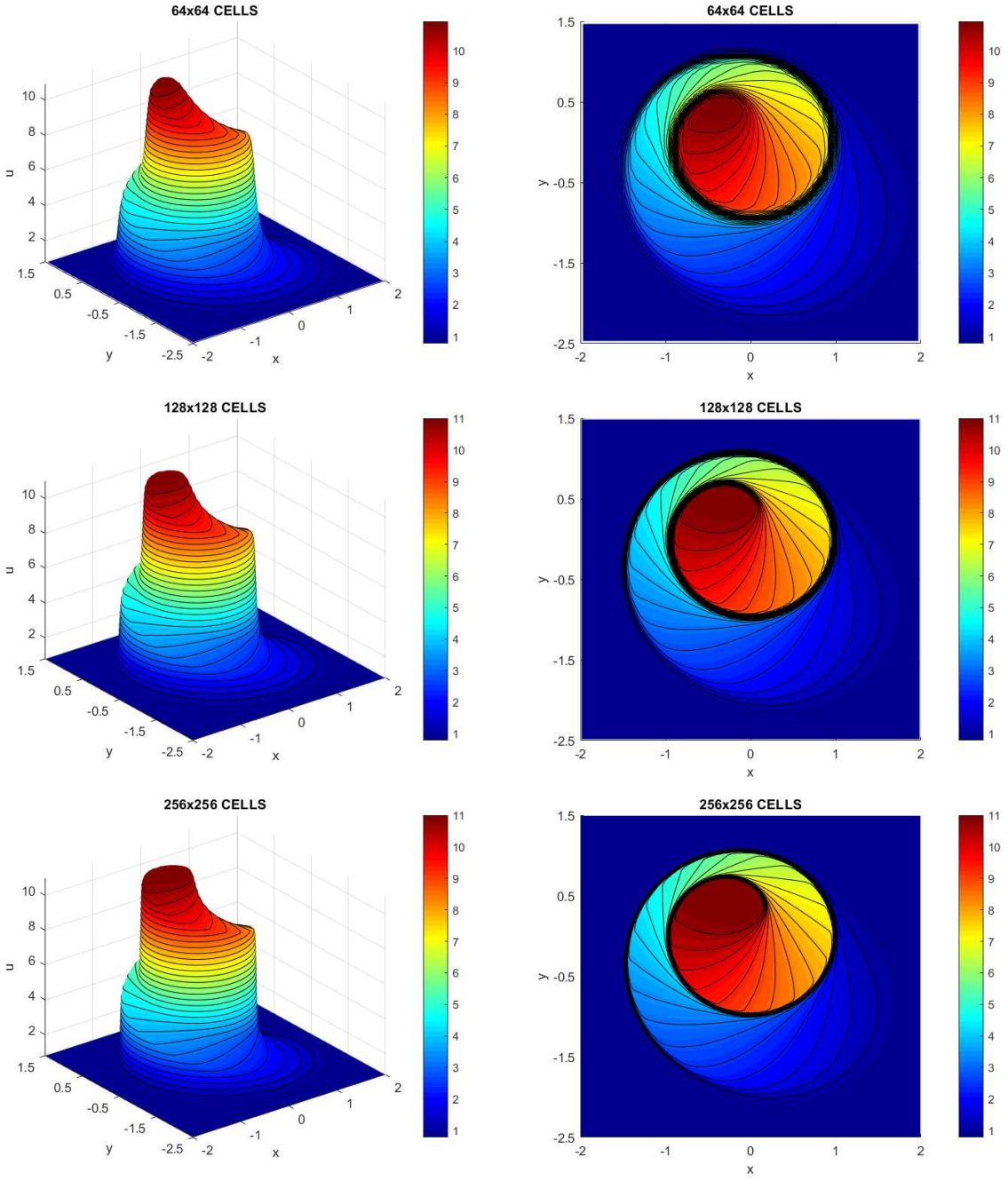

Figure 9 – 3D-plot's view angle (left column) and 2D contour view (right column) of the numerical approximations for the 2D model (3.145)-(3.146), which is computed using the SDLE scheme with $\alpha = 1$, $\zeta = 2$, $\theta = 2$, and CFL = 0.075.

4 The semi-discrete scheme for systems of hyperbolic conservation laws in one dimension and two space dimensions

The implementation of the semi-discrete scheme in the case of systems is a straightforward component-wise application of the multidimensional scalar case (1D, 2D) presented in the previous chapters, with no need of any dimensional splitting strategies, since no (local) Riemann problems are solved; hence, time-consuming field-by-field type decompositions are avoided. The component-wise extension of the Lagrangian–Eulerian framework systems is greatly facilitated via the no-flow curves as well.

4.1 1D semi-discrete Lagrangian-Eulerian scheme for systems of hyperbolic conservation laws

Here we deal with $N \times N$ system of hyperbolic problems, but for the sake of simplicity and with no loss of generality we will present the procedure of the semi-discrete scheme for a 2×2 system of hyperbolic conservation laws (applying it to 3 by 3 systems and 4 by 4 as well) given by

$$\frac{\partial u_1}{\partial t} + \frac{\partial H_1(u_1,u_2)}{\partial x} = 0, \quad \frac{\partial u_2}{\partial t} + \frac{\partial H_2(u_1,u_2)}{\partial x} = 0, \quad \text{where} \quad H_1, H_2 \in C^2. \tag{4.1}$$

The system (4.1) can be written in a simple compact form as follows,

$$\frac{\partial U}{\partial t} + \frac{\partial H(U)}{\partial x} = 0, \quad U = (u_1,u_2)^T, \quad H = (H_1,H_2)^T, \tag{4.2}$$

and for systems of N equations it could be defined as

$$\frac{\partial U}{\partial t} + \frac{\partial H(U)}{\partial x} = 0, \quad U = (u_1,u_2,\cdots,u_N)^T, \quad H = (H_1,H_2,\cdots,H_N)^T.$$

As before, we consider the space-time control finite volumes for each variable u_1 and u_2 as follows (see Figure 10);

$$D_{l,j}^{n,n+1} = \{(x,t) \;/\; \sigma_{u_l,j}^n(t) \leqslant x \leqslant \sigma_{u_l,j+1}^n(t), \quad t^n \leqslant t \leqslant t^{n+1}\}, \quad l = 1,2. \tag{4.3}$$

Here $\sigma_{u_l,j}^n(t)$ are parameterized curves and define the "lateral boundaries" of the *no-flow region* for each primitive variable u_1 and u_2. Formally, writing the Eq. (4.2) in its

divergent form for each variable as in scalar case and apply the divergence theorem over the space-time finite volumes $D_{l,j}^{n,n+1}$, we have

$$\oint_{\partial D_{l,j}^{n,n+1}} \begin{bmatrix} H_l(U) \\ u_l \end{bmatrix} \cdot \vec{n} dS = 0, \qquad S = \partial D_{l,j}^{n,n+1}, \quad l = 1, 2. \tag{4.4}$$

Applying the same procedure used in the scalar case, Section 2.1, we obtain the *no-flow curves* expression as a system of ordinary differential equation given by

$$\begin{cases} \dfrac{d\sigma_{u_l,p}^n(t)}{dt} = \dfrac{H_l(u_1(\sigma_{u_1,p}^n(t),t)), u_2(\sigma_{u_2,p}^n(t),t))}{u_l(\sigma_{u_l,p}^n(t),t)}, \qquad t^n \leqslant t \leqslant t^{n+1}, \quad p = j, j+1, \\ \sigma_{u_l,p}^n(t^n) = x_p^n, \end{cases} \tag{4.5}$$

where $\sigma_{u_l,p}^n(t^0) = x_p^0$ along with $u_l(\sigma_{u_l,p}^n(t^0), t^0) = u_{l,0}(x)$ for all the indexes p in the mesh grid, which is simply the initial data at the initial time. Using the fact that the integrals over the curves $\sigma_{u_l,p}^n$ vanish in the line integral over the boundary of the region $D_{l,j}^{n,n+1}$ we have the local conservation relation in different meshes,

$$\int_{\bar{x}_{u_l,j}^{n+1}}^{\bar{x}_{u_l,j+1}^{n+1}} u_l(x, t^{n+1}) dx = \int_{x_j^n}^{x_{j+1}^n} u_l(x, t^n) dx, \quad l = 1, 2.$$

As the framework of finding the scalar semi-discrete scheme (see Section 2.1) is naturally

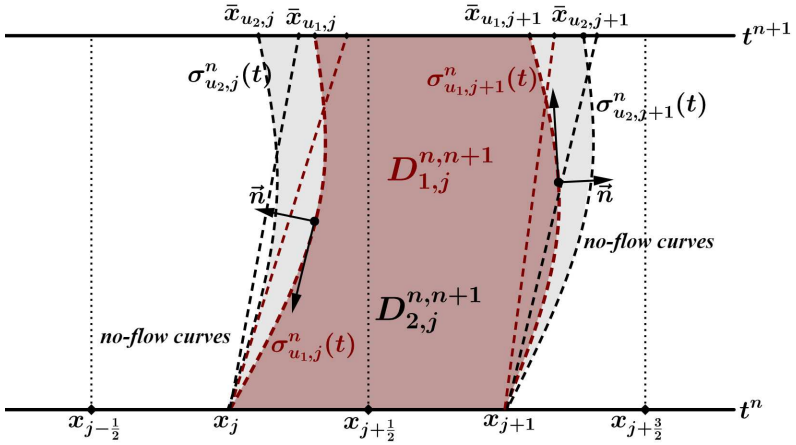

Figure 10 – Geometric representation of the Lagrangian-Eulerian space-time control volumes $D_{l,j}^{n,n+1}$ (*and no-flow curves* $\sigma_{u_l,j}^n(t)$ *and* $\sigma_{u_l,j+1}^n(t)$, $l = 1, 2$) and its first-order approximation (straight lines) from time level t^n to time level t^{n+1}.

similar for systems, then our *semi-discrete Lagrangian-Eulerian* formulation for systems of hyperbolic conservation laws is given by the equation

$$\frac{d}{dt} u_{l,j}(t) = -\frac{1}{\Delta x} \left[\mathcal{F}_{u_l}(u_{l,j}, u_{l,j+1}) - \mathcal{F}_{u_l}(u_{l,j-1}, u_{l,j}) \right], \quad l = 1, 2, \tag{4.6}$$

which shall be extended in the next section to multi-dimensional systems of hyperbolic problem. Here the numerical flux function for each variable is given by

$$\mathcal{F}_{u_l}(u_{l,j}, u_{l,j+1}) = \frac{1}{4} \left[b_{l,j+\frac{1}{2}} \left(u_{l,j+\frac{1}{2}}^- - u_{l,j+\frac{1}{2}}^+ \right) + (f_{u_l,j} + f_{u_l,j+1}) \left(u_{l,j+\frac{1}{2}}^- + u_{l,j+\frac{1}{2}}^+ \right) \right] \tag{4.7}$$

with $u^{+}_{l,j+\frac{1}{2}} = u_{l,j+1} - \dfrac{\Delta x}{4}\left((u_l)_x\right)_{j+1}$, $u^{-}_{l,j+\frac{1}{2}} = u_{l,j} + \dfrac{\Delta x}{4}\left((u_l)_x\right)_j$ and $\left((u_l)_x\right)_j$ denotes the numerical derivatives for each variable, i.e., $l = 1, 2$, and can be expressed as in (2.8).

Based on the *no-flow* estimates for numerically stable computations given in Proposition 2.1, we use in a similar fashion of the well-known stability condition by Courant–Friedrichs–Lewy the no-flow estimates $b_{l,j+\frac{1}{2}} = \zeta \max_j \{|f_{u_l,j} + f_{u_l,j+1}|\}$, with ζ $(1 \leqslant \zeta \leqslant 3)$ a parameter that depends on the problem to be treated along the CFL condition $\max_j\{|f_{u_1,j}|, |f_{u_2,j}|\}\dfrac{\Delta t}{\Delta x} < \dfrac{1}{2}$ without the need to use the eigenvalues (exact and approximate values) of the pertinent Jacobian of the numerical flux functions (see Eq. 2.54). Here the no-flow curve approximation is given by $f_{u_l,j} \equiv \dfrac{H_l(U_j)}{u_{l,j}} \approx \dfrac{H_l(U)}{u_l}$ for each variable.

4.2 2D semi-discrete Lagrangian-Eulerian scheme for systems of hyperbolic conservation laws

In the sequel, we turn our attention to the construction of the semi-discrete Lagrangian-Eulerian scheme for systems of hyperbolic conservation laws in 2D of the form,

$$\frac{\partial u_1}{\partial t} + \frac{\partial H_1(u_1,u_2)}{\partial x} + \frac{\partial G_1(u_1,u_2)}{\partial y} = 0, \qquad \frac{\partial u_2}{\partial t} + \frac{\partial H_2(u_1,u_2)}{\partial x} + \frac{\partial G_2(u_1,u_2)}{\partial y} = 0, \quad (4.8)$$

where H_l, $G_l \in C^2$, $l = 1, 2$. The semi-discrete scheme can be formally extended to the case of $N \times N$ systems of conservation laws in a multidimensional component-wise fashion, as presented in Section 3.1. It is well-known that the theory for such general situation and related fundamental questions for entropy solutions to multidimensional conservation laws remains an open problem and is still in active progress (see, e.g., [24, 72, 78] and references cited therein). Therefore, we will present the scheme for the case of the 2×2 system (4.8) and apply it to 3×3 and 4×4 systems as well, for which results can be found in the literature. System (4.8) can be written in a compact form as follows:

$$\frac{\partial U}{\partial t} + \frac{\partial H(U)}{\partial x} + \frac{\partial G(U)}{\partial y} = 0, \qquad U = (u_1,u_2)^T, \quad H = (H_1,H_2)^T,\ G = (G_1,G_2)^T. \quad (4.9)$$

As the framework for finding the semi-discrete scheme in 2D is naturally a straightforward component-wise application of the two-dimensional scalar case (although coupled and genuinely multidimensional), we simultaneously apply the procedure to each variable (i.e., u_1, u_2). The 2D SDLE scheme for systems of conservation laws is given by

$$\frac{d}{dt}u_{l,j,k}(t) = -\frac{\mathcal{F}^l_{j+1/2,k} - \mathcal{F}^l_{j-1/2,k}}{\Delta x} - \frac{\mathcal{G}^l_{j,k+1/2} - \mathcal{G}^l_{j,k-1/2}}{\Delta y}, \quad l = 1, 2, \qquad (4.10)$$

with the corresponding multidimensional numerical fluxes in the $x-$ and $y-$directions, which are, respectively, given by

$$\begin{aligned}\mathcal{F}^{l}_{j+\frac{1}{2},k} =& \frac{1}{4}\left[b^{x}_{l,j+\frac{1}{2},k}\left(u^{-}_{l,j+\frac{1}{2},k}-u^{+}_{l,j+\frac{1}{2},k}\right)+\left(f_{u_l,j,k}+f_{u_l,j+1,k}\right)\left(u^{-}_{l,j+\frac{1}{2},k}+u^{+}_{l,j+\frac{1}{2},k}\right)\right] \quad \text{and}\\ \mathcal{G}^{l}_{j,k+\frac{1}{2}} =& \frac{1}{4}\left[b^{y}_{l,j,k+\frac{1}{2}}\left(u^{-}_{l,j,k+\frac{1}{2}}-u^{+}_{l,j,k+\frac{1}{2}}\right)+\left(g_{u_l,j,k}+g_{u_l,j,k+1}\right)\left(u^{-}_{l,j,k+\frac{1}{2}}+u^{+}_{l,j,k+\frac{1}{2}}\right)\right], \quad (4.11)\end{aligned}$$

along with the discretized multidimensional (2D) no-flow curves,

$$f_{u_l,j,k}\equiv\frac{H_l(U_{j,k})}{u_{l,j,k}} \quad \text{and} \quad g_{u_l,j,k}\equiv\frac{G_l(U_{j,k})}{u_{l,j,k}}, \quad l=1,2. \tag{4.12}$$

As before, the intermediate values and the numerical derivatives are given by Eqs. (3.6) and (3.7), respectively, for each variable (u_1,u_2), again in a straightforward component-wise application of the two-dimensional scalar case.

4.2.1 Positivity principle of the semi-discrete scheme for multi-dimensional systems

It is well known that system of hyperbolic equations, generically, do not exhibit $TVNI$ solutions. These $TVNI$ schemes exist only for scalar conservation laws, and for linear hyperbolic systems in one space variable [65, 66].

On the other hand, Liu and Lax introduced in [65, 66], the notion of *Positivity* that can be applied for nonlinear systems of hyperbolic equations of multi-dimensional type. Systems that exhibits these property present evidence of stability and have bounded increasing for the time steps.

Here, we consider the system of following form:

$$U_t+\sum_{s=1}^{d}\frac{\partial H_s(U)}{\partial x_s}=0, \tag{4.13}$$

where $U=(u_1,u_2,\cdots,u_N)^T\in\mathbb{R}^N$ is the vector of conserved quantities and $x=(x_1,x_2,\cdots,x_d)\in\mathbb{R}^d$ is the spatial multi-D vector. The flux function is $H=(H_1,\cdots,H_N)^T$, notice that we have d vectors H. We also define:

$$F_i=\frac{H_i}{u_i}, \text{ where } i=1,\cdots,N \quad \text{for all} \quad s=\{1,\cdots,d\} \quad \text{and} \quad F=(F_1,\cdots,F_N)^T. \tag{4.14}$$

We say that a numerical scheme used to solve (4.13) is *positive* if it can be written in the following form:

$$U^{n}_{j}=\sum_{K}C_{J,K}U_{J+K}, \tag{4.15}$$

with the coefficient matrices $C_{J,K}$ satisfying the following properties:

$$\begin{aligned} &(i) \quad C_{J,K} \text{ is symmetric and semi-positive definite,} \\ &(ii) \quad \sum_K C_{J,K} = I, \text{ where } I \text{ is the identity matrix,} \\ &(iii) \quad C_{J,K} = 0 \text{ except for a finite set of } K. \end{aligned} \tag{4.16}$$

If in addition to conditions (i)-(iii) of (4.16), the numerical scheme satisfies

$$(iv) \quad C_{J,K} \text{ depends Lipschitz continuously on } x \tag{4.17}$$

the scheme (4.15) satisfies for the discrete l^2 norm, see [65, 66]:

$$||U^{n+1}||_2 \leqslant (1 + const\Delta)||U^n||_2, \quad \text{where} \quad ||U||_2 = \sqrt{\sum_J (U_J, U_J)}, \tag{4.18}$$

here (U_J, U_J) is the canonical inner product of R^n and Δ is the variation on the variables x.

The first two properties in (4.16), for the scalar case, imply that the solution in U^{n+1} is a convex combination of the solution U^n, which leads to a local maximum - minimum principle be satisfied. The third property echos the fact that the propagation speed of waves is finite for hyperbolic systems. The positivity principle presented above is used to obtain the stability of numerical solutions of general multi-dimensional hyperbolic systems.

Here, we prove that our numerical scheme satisfies the properties of positivity (4.16)-(4.17). The extension of the numerical scheme (3.13) for systems of form (4.13) is written as:

$$\partial_t(U_\epsilon) = -\sum_{s=1}^{d} \frac{1}{\epsilon_s} \left[\mathcal{F}_s(U_\epsilon; U_{\epsilon+\epsilon_s}) - \mathcal{F}_s(U_{\epsilon-\epsilon_s}; U_\epsilon)\right], \tag{4.19}$$

where

$$U_{\epsilon+i\epsilon_s} = U(x_1, \cdots, x_{s-1}, x_s + i\epsilon_s, x_{s+1}, \cdots, x_d, t), \tag{4.20}$$

and the numerical flux functions $\mathcal{F} = (\mathcal{F}_1, \cdots, \mathcal{F}_N)$ for each $s = 1, \cdots, d$.

$$\mathcal{F}_s(U_\epsilon; U_{\epsilon+\epsilon_s}) = \frac{1}{4}\left[B^s_{\epsilon+\frac{\epsilon_s}{2}}\left(U^-_{\epsilon+\frac{\epsilon_s}{2}} - U^+{}_{\epsilon+\frac{\epsilon_s}{2}}\right) + (F_s(U_\epsilon)) + F_s(U_{\epsilon+\epsilon_s}))\left(U^-_{\epsilon+\frac{\epsilon_s}{2}} + U^+{}_{\epsilon+\frac{\epsilon_s}{2}}\right)\right] \tag{4.21}$$

where F is given by (4.14) for each $s = \{1, 2, \cdots, d\}$ and the product between F and U is taken term by term, i.e., $FU = (F_1u_1, F_2u_2, \cdots, F_Nu_N)^T$, $B^s_{\epsilon+\frac{\epsilon_s}{2}}$ is the diagonal matrix

$$B^s_{\epsilon+\frac{\epsilon_s}{2}} = \begin{pmatrix} (b^s_1)_{\epsilon+\frac{\epsilon_s}{2}} & 0 & \cdots & 0 \\ 0 & (b^s_2)_{\epsilon+\frac{\epsilon_s}{2}} & \cdots & 0 \\ 0 & 0 & \ddots & 0 \\ 0 & 0 & \cdots & (b^s_N)_{\epsilon+\frac{\epsilon_s}{2}} \end{pmatrix}, \tag{4.22}$$

and $U^+_{\epsilon-\frac{\epsilon_s}{2}}$ and $U^-_{\epsilon+\frac{\epsilon_s}{2}}$ are the functions

$$U^+_{\epsilon-\frac{\epsilon_s}{2}} = U_\epsilon - \frac{1}{4}\Phi^+_{\epsilon-\frac{\epsilon_s}{2}}(U_{\epsilon+\epsilon_s} - U_\epsilon) \quad \text{and} \quad U^-_{\epsilon+\frac{\epsilon_s}{2}} = U_\epsilon + \frac{1}{4}\Phi^-_{\epsilon+\frac{\epsilon_s}{2}}(U_\epsilon - U_{\epsilon-\epsilon_s}) \tag{4.23}$$

$\Phi^+_{\epsilon-\frac{\epsilon_s}{2}}$ and $\Phi^-_{\epsilon+\frac{\epsilon_s}{2}}$ are diagonal matrices

$$\Phi^+_{\epsilon-\frac{\epsilon_s}{2}} = \begin{pmatrix} \phi^s\left(\left(\theta^+_1\right)_{\epsilon-\frac{\epsilon_s}{2}}\right) & 0 & \cdots & 0 \\ 0 & \phi^s\left(\left(\theta^+_2\right)_{\epsilon-\frac{\epsilon_s}{2}}\right) & \cdots & 0 \\ 0 & 0 & \ddots & 0 \\ 0 & 0 & \cdots & \phi^s\left(\left(\theta^+_N\right)_{\epsilon-\frac{\epsilon_s}{2}}\right) \end{pmatrix},$$

$$\Phi^-_{\epsilon+\frac{\epsilon_s}{2}} = \begin{pmatrix} \phi^s\left(\left(\theta^-_1\right)_{\epsilon+\frac{\epsilon_s}{2}}\right) & 0 & \cdots & 0 \\ 0 & \phi^s\left(\left(\theta^-_2\right)_{\epsilon+\frac{\epsilon_s}{2}}\right) & \cdots & 0 \\ 0 & 0 & \ddots & 0 \\ 0 & 0 & \cdots & \phi^s\left(\left(\theta^-_N\right)_{\epsilon+\frac{\epsilon_s}{2}}\right) \end{pmatrix}.$$

These matrices depend on $\left(\theta^+_i\right)_{\epsilon-\frac{\epsilon_s}{2}}$ and $\left(\theta^-_i\right)_{\epsilon+\frac{\epsilon_s}{2}}$ that are

$$\left(\theta^+_i\right)_{\epsilon-\frac{\epsilon_s}{2}} = \frac{(U_\epsilon - U_{\epsilon-\epsilon_s})_i}{(U_{\epsilon+\epsilon_s} - U_\epsilon)_i} \quad \text{and} \quad \left(\theta^-_i\right)_{\epsilon+\frac{\epsilon_s}{2}} = \frac{(U_{\epsilon+\epsilon_s} - U_\epsilon)_i}{(U_\epsilon - U_{\epsilon-\epsilon_s})_i}, \quad \text{for } i = 1, \cdots, N. \tag{4.24}$$

The original flux limiter functions ϕ^s, see [80], satisfy $0 \leqslant \phi^s(\theta_i) \leqslant 2$ for $1 \leqslant i \leqslant N$ and $1 \leqslant i \leqslant d$ and $\phi^s(1) = 1$. However, for our modelling, and for stability, we require that

$$0 \leqslant \phi^s(\theta) \leqslant 4 \quad \text{that implies that} \quad 0 \leqslant \Phi^+_{\epsilon-\frac{\epsilon_s}{2}} \leqslant 4I \quad \text{and} \quad 0 \leqslant \Phi^-_{\epsilon+\frac{\epsilon_s}{2}} \leqslant 4I. \tag{4.25}$$

In smooth regions (except at extrema), for each s and i, we have that $\left(\theta^+_i\right)_{\epsilon-\frac{\epsilon}{2}} = 1 + O(\Delta\epsilon_s)$, from (4.25) and (4.23)

$$U^+_{\epsilon-\frac{\epsilon_s}{2}} = U_\epsilon - \frac{1}{4}\frac{U_{\epsilon+\epsilon_s} - U_\epsilon}{\epsilon_s}\epsilon_s + O(\Delta\epsilon_s) = U_\epsilon - \frac{1}{4}(U_{x_s})_\epsilon\epsilon_s + O(\Delta\epsilon_s), \tag{4.26}$$

here (U_{x_s}) is the approximation for the partial derivative of U with respect to x_s. Notice that (4.26) recovery the original form proposed for $U^+_{\epsilon-\frac{\epsilon_s}{2}}$. The same is valid for $U^-_{\epsilon+\frac{\epsilon_s}{2}}$ for all s.

Remark 4.1. *Because of the form of approximation of the derivatives, we can obtain* $U^+_{\epsilon-\frac{\epsilon_s}{2}}$ *and* $U^-_{\epsilon+\frac{\epsilon_s}{2}}$ *as*

$$U^+_{\epsilon-\frac{\epsilon_s}{2}} = U_\epsilon - \frac{1}{4}\hat{\Phi}^+_{\epsilon-\frac{\epsilon_s}{2}}(U_\epsilon - U_{\epsilon-\epsilon_s}) \quad \textit{and} \quad U^-_{\epsilon+\frac{\epsilon_s}{2}} = U_\epsilon + \frac{1}{4}\hat{\Phi}^-_{\epsilon+\frac{\epsilon_s}{2}}(U_{\epsilon+\epsilon_s} - U_\epsilon) \tag{4.27}$$

with $\hat{\Phi}^+_{\epsilon-\frac{\epsilon_s}{2}}$ *and* $\hat{\Phi}^-_{\epsilon+\frac{\epsilon_s}{2}}$ *defined (and with the same properties) as* $\Phi^+_{\epsilon-\frac{\epsilon_s}{2}}$ *and* $\Phi^-_{\epsilon+\frac{\epsilon_s}{2}}$.

Now, we are able to prove that our numerical method (4.19) satisfies the positivity principle. First, we notice that to obtain the solution of (4.19) we need to solve a ODE in the variable t for the parameter ϵ. To achieve second order accuracy in time we use the following second order accurate Runge-Kutta method and we prove also that in this case the numerical method (4.19) is bounded if the method satisfies the positivity. This $2nd$ order is written as:

$$U_{\epsilon}^{*} = U_{\epsilon} - \sum_{s=1}^{d} \frac{\Delta t}{\epsilon_s} \left[\mathcal{F}_s(U_{\epsilon}; U_{\epsilon+\epsilon_s}) - \mathcal{F}_s(U_{\epsilon-\epsilon_s}; U_{\epsilon})\right], \tag{4.28}$$

$$U_{\epsilon}^{**} = U_{\epsilon}^{*} - \sum_{s=1}^{d} \frac{\Delta t}{\epsilon_s} \left[\mathcal{F}_s(U_{\epsilon}^{*}; U_{\epsilon+\epsilon_s}^{*}) - \mathcal{F}_s(U_{\epsilon-\epsilon_s}^{*}; U_{\epsilon}^{*})\right], \tag{4.29}$$

$$U_{\epsilon}^{n+1} = \frac{1}{2}\left(U_{\epsilon}^{*} + U_{\epsilon}^{**}\right). \tag{4.30}$$

Thus, we obtain conditions to prove that (4.28) and (4.29) satisfy the positivity conditions. In the next theorem, we define the diagonal matrices P_s and Q_s :

$$P_s = \begin{pmatrix} p_s & 0 & \cdots & 0 \\ 0 & p_s & \cdots & 0 \\ 0 & 0 & \ddots & 0 \\ 0 & 0 & \cdots & p_s \end{pmatrix} \quad \text{and} \quad Q_s = \begin{pmatrix} q_s & 0 & \cdots & 0 \\ 0 & q_s & \cdots & 0 \\ 0 & 0 & \ddots & 0 \\ 0 & 0 & \cdots & q_s \end{pmatrix}, \tag{4.31}$$

with $P_s + Q_s = 2I \quad q_s \geqslant 0, p_s \geqslant 0$. In the proof of the next theorem, F_s represent the matrix $F_s I$, for I being the identity matrix.

We also use that the matrix A_s is the Jacobian of F_s and with eigenvalues denote as $(\gamma_j)_s$ and the maximum eigenvalue of matrix A_s, we denote as γ_s.

We state our result as:

Theorem 4.1. *The numerical scheme* (4.19)*, solved by 2nd order Runge-Kutta method* (4.28)-(4.30) *is positive if the following conditions are satisfied for all* $i = \{1, \cdots, N\}$ *and* $s = \{1, \cdots, d\}$

$$\lambda_s \left((b_i^s)_{\epsilon+\frac{\epsilon_s}{2}} + (F_i)_s(U_{\epsilon}) + (F_i)_s(U_{\epsilon+\epsilon_s}) + max\left\{\left|\gamma_s\left(\widehat{U}_{\epsilon}\right)\right|, \left|\gamma_s\left(\widehat{U}_{\epsilon-1}\right)\right|\right\}\left(U^{-}_{\epsilon-\frac{\epsilon_s}{2}} + U^{+}_{\epsilon-\frac{\epsilon_s}{2}}\right)\right) \leqslant \frac{p_s}{d}, \tag{4.32}$$

$$(F_i)_s(U_{\epsilon}) + (F_i)_s(U_{\epsilon+\epsilon_s}) + max\left\{\left|\gamma_s\left(\widehat{U}_{\epsilon}\right)\right|, \left|\gamma_s\left(\widehat{U}_{\epsilon-1}\right)\right|\right\}\left(U^{-}_{\epsilon-\frac{\epsilon_s}{2}} + U^{+}_{\epsilon-\frac{\epsilon_s}{2}}\right) \leqslant (b_i^s)_{\epsilon+\frac{\epsilon_s}{2}}, \tag{4.33}$$

$$max\left\{\left|\gamma_s\left(\widehat{U}_{\epsilon}\right)\right|, \left|\gamma_s\left(\widehat{U}_{\epsilon-1}\right)\right|\right\}\left(U^{-}_{\epsilon-\frac{\epsilon_s}{2}} + U^{+}_{\epsilon-\frac{\epsilon_s}{2}}\right) \leqslant \frac{p_s}{d} \tag{4.34}$$

$$\lambda_s max\left\{\left|\gamma_s\left(\widehat{U}_{\epsilon}\right)\right|, \left|\gamma_s\left(\widehat{U}_{\epsilon-1}\right)\right|\right\}\left(U^{-}_{\epsilon-\frac{\epsilon_s}{2}} + U^{+}_{\epsilon-\frac{\epsilon_s}{2}}\right) + p_s\left(\phi^s\left(\left(\theta_i^{+}\right)_{\epsilon-\frac{\epsilon_s}{2}}\right) + \phi^s\left(\left(\theta_i^{-}\right)_{\epsilon+\frac{\epsilon_s}{2}}\right)\right) \leqslant 8q_s. \tag{4.35}$$

Proof: We consider the numerical method (4.19) using the approximation (4.28). For the numerical scheme using the approximation (4.28) and the flux (4.21), we obtain:

$$\begin{aligned} U_\epsilon^* =& U_\epsilon - \frac{1}{4}\sum_{s=1}^{d}\lambda_s\left[B^s_{\epsilon+\frac{\epsilon_s}{2}}\left(U^-_{\epsilon+\frac{\epsilon_s}{2}} - U^+{}_{\epsilon+\frac{\epsilon_s}{2}}\right) + (F_s(U_\epsilon)) + F_s(U_{\epsilon+\epsilon_s})\right)\left(U^-_{\epsilon+\frac{\epsilon_s}{2}} + U^+{}_{\epsilon+\frac{\epsilon_s}{2}}\right)\Big] \\ &+ \frac{1}{4}\sum_{s=1}^{d}\lambda_s\left[B^s_{\epsilon-\frac{\epsilon_s}{2}}\left(U^-_{\epsilon-\frac{\epsilon_s}{2}} - U^+{}_{\epsilon-\frac{\epsilon_s}{2}}\right) + (F_s(U_{\epsilon-\epsilon_s})) + F_s(U_\epsilon)\right)\left(U^-_{\epsilon-\frac{\epsilon_s}{2}} + U^+{}_{\epsilon-\frac{\epsilon_s}{2}}\right)\Big], \end{aligned} \tag{4.36}$$

where $\lambda_s = \Delta t/\epsilon_s$. Now, we decompose $U_\epsilon = \dfrac{(P_sU_\epsilon + Q_sU_\epsilon)}{2}$, with P_s and Q_s diagonal matrices given by (4.31) and we write (4.36) as:

$$\begin{aligned} U_\epsilon^* =& \frac{1}{4}\sum_{s=1}^{d}\Big[(P_sU_\epsilon + Q_sU_\epsilon) - \lambda_s\Big\{B^s_{\epsilon+\frac{\epsilon_s}{2}}\left(U^-_{\epsilon+\frac{\epsilon_s}{2}} - U^+{}_{\epsilon+\frac{\epsilon_s}{2}}\right) \\ &+ (F_s(U_\epsilon)) + F_s(U_{\epsilon+\epsilon_s})\left(U^-_{\epsilon+\frac{\epsilon_s}{2}} + U^+{}_{\epsilon+\frac{\epsilon_s}{2}}\right)\Big\}\Big] \\ &+ \frac{1}{4}\sum_{s=1}^{d}\Big[P_sU_\epsilon + Q_sU_\epsilon) + \lambda_s\Big\{B^s_{\epsilon-\frac{\epsilon_s}{2}}\left(U^-_{\epsilon-\frac{\epsilon_s}{2}} - U^+{}_{\epsilon-\frac{\epsilon_s}{2}}\right) \\ &+ (F_s(U_{\epsilon-\epsilon_s})) + F_s(U_\epsilon)\left(U^-_{\epsilon-\frac{\epsilon_s}{2}} + U^+{}_{\epsilon-\frac{\epsilon_s}{2}}\right)\Big\}\Big]. \end{aligned} \tag{4.37}$$

Using (4.23), we can write, for each $s = \{1, \cdots, N\}$, U_ϵ as adequate combination of $U^+_{\epsilon-\frac{\epsilon_s}{2}}$ or $U^-_{\epsilon+\frac{\epsilon_s}{2}}$:

$$U_\epsilon = \frac{1}{d}\sum_{s=1}^{d}\left(U^+_{\epsilon-\frac{\epsilon_s}{2}} + \frac{1}{4}\Phi^+_{\epsilon-\frac{\epsilon_s}{2}}(U_{\epsilon+\epsilon_s} - U_\epsilon)\right) \text{ or } U_\epsilon = \frac{1}{d}\sum_{s=1}^{d}\left(U^-_{\epsilon+\frac{\epsilon_s}{2}} - \frac{1}{4}\Phi^-_{\epsilon+\frac{\epsilon_s}{2}}(U_\epsilon - U_{\epsilon-\epsilon_s})\right). \tag{4.38}$$

Substituting U_ϵ by (4.38) in (4.37), we obtain:

$$\begin{aligned} U_\epsilon^* =& \frac{1}{4}\sum_{s=1}^{d}\Big[\frac{P_s}{d}\left(U^-_{\epsilon+\frac{\epsilon_s}{2}} - \frac{1}{4}\Phi^-_{\epsilon+\frac{\epsilon_s}{2}}(U_\epsilon - U_{\epsilon-\epsilon_s})\right) + Q_sU_\epsilon \\ &-\lambda_s\Big\{B^s_{\epsilon+\frac{\epsilon_s}{2}}\left(U^-_{\epsilon+\frac{\epsilon_s}{2}} - U^+{}_{\epsilon+\frac{\epsilon_s}{2}}\right) + (F_s(U_\epsilon)) + F_s(U_{\epsilon+\epsilon_s})\left(U^-_{\epsilon+\frac{\epsilon_s}{2}} + U^+{}_{\epsilon+\frac{\epsilon_s}{2}}\right)\Big\}\Big] \\ &+ \frac{1}{4}\sum_{s=1}^{d}\Big[\frac{P_s}{d}\left(U^+_{\epsilon-\frac{\epsilon_s}{2}} + \frac{1}{4}\Phi^+_{\epsilon-\frac{\epsilon_s}{2}}(U_{\epsilon+\epsilon_s} - U_\epsilon)\right) + Q_sU_\epsilon \\ &+\lambda_s\Big\{B^s_{\epsilon-\frac{\epsilon_s}{2}}\left(U^-_{\epsilon-\frac{\epsilon_s}{2}} - U^+{}_{\epsilon-\frac{\epsilon_s}{2}}\right) + (F_s(U_{\epsilon-\epsilon_s})) + F_s(U_\epsilon)\left(U^-_{\epsilon-\frac{\epsilon_s}{2}} + U^+{}_{\epsilon-\frac{\epsilon_s}{2}}\right)\Big\}\Big]. \end{aligned} \tag{4.39}$$

Rearranging the terms and using that $Q_s U_\epsilon = sQ_s U_\epsilon/s$, Eq. (4.39) becomes

$$\begin{aligned}
U_\epsilon^* = \frac{1}{4}\sum_{s=1}^{d}\Bigg[&\left(\frac{P_s}{d} - \lambda_s\left\{B^s_{\epsilon+\frac{\epsilon_s}{2}} + \left(F_s(U_\epsilon) + F_s\left(U_{\epsilon+\epsilon_s}\right)\right\}\right)U^-_{\epsilon+\frac{\epsilon_s}{2}}\\
&+\lambda_s\left(B^s_{\epsilon+\frac{\epsilon_s}{2}} - \left(F_s(U_\epsilon) + F_s\left(U_{\epsilon+\epsilon_s}\right)\right)U^+_{\epsilon+\frac{\epsilon_s}{2}}\right.\\
&\frac{1}{d}\left(2Q_s - \frac{P_s}{4}\Phi^-_{\epsilon+\frac{\epsilon_s}{2}} - \frac{P_s}{4}\Phi^+_{\epsilon-\frac{\epsilon_s}{2}}\right)U_\epsilon + \left(\frac{P_s}{d} - \lambda_s\left\{B^s_{\epsilon-\frac{\epsilon_s}{2}} - \left(F_s(U_{\epsilon-\epsilon_s}) + F_s\left(U_\epsilon\right)\right\}\right)U^+_{\epsilon-\frac{\epsilon_s}{2}}\\
&+\lambda_s\left(B^s_{\epsilon-\frac{\epsilon_s}{2}} + \left(F_s(U_{\epsilon-\epsilon_s}) + F_s\left(U_\epsilon\right)\right)U^-_{\epsilon-\frac{\epsilon_s}{2}} + \frac{P_s}{4d}\Phi^-_{\epsilon+\frac{\epsilon_s}{2}}U_{\epsilon-\epsilon_s} + \frac{P_s}{4d}\Phi^+_{\epsilon-\frac{\epsilon_s}{2}}U_{\epsilon+\epsilon_s}.
\end{aligned} \tag{4.40}$$

Notice that each matrix multiplying $U^-_{\epsilon-\frac{\epsilon_s}{2}}$, $U^-_{\epsilon+\frac{\epsilon_s}{2}}$, $U^+_{\epsilon-\frac{\epsilon_s}{2}}$, $U^+_{\epsilon+\frac{\epsilon_s}{2}}$ and U_ϵ is diagonal, thus symmetric. However, to prove that (ii) of (4.16) is satisfied is necessary to manipulate the expression in order to linearize each nonlinear F_s. To do so, in Eq. (4.39), after some calculations, we can write:

$$\begin{aligned}
&\left(F_s(U_\epsilon)) + F_s(U_{\epsilon+\epsilon_s})\right)\left(U^-_{\epsilon+\frac{\epsilon_s}{2}} + {U^+}_{\epsilon+\frac{\epsilon_s}{2}}\right) - \left(\left(F_s(U_{\epsilon-\epsilon_s})) + F_s(U_\epsilon)\right)\left(U^-_{\epsilon-\frac{\epsilon_s}{2}} + {U^+}_{\epsilon-\frac{\epsilon_s}{2}}\right)\right)\\
&= \left(F_s(U_\epsilon) + F_s(U_{\epsilon+1)})\right)\left(U^-_{\epsilon+\frac{\epsilon_s}{2}} - {U^-}_{\epsilon-\frac{\epsilon_s}{2}} + U^+_{\epsilon+\frac{\epsilon_s}{2}} - {U^+}_{\epsilon-\frac{\epsilon_s}{2}}\right) +\\
&\qquad + \left(F_s(U_{\epsilon+\epsilon_s})) - F_s(U_\epsilon) + F_s(U_\epsilon)) - F_s(U_{\epsilon-\epsilon_s})\right)\left(U^-_{\epsilon-\frac{\epsilon_s}{2}} + U^+_{\epsilon-\frac{\epsilon_s}{2}}\right).
\end{aligned} \tag{4.41}$$

Here, in the last term of (4.41), we utilize the Roe's matrix expansion, where we write:

$$F_s(U_{\epsilon+\epsilon_s})) - F_s(U_\epsilon) = A_s\left(\widehat{U}_\epsilon\right)\left(U_{\epsilon+\epsilon_s} - U_\epsilon\right), \tag{4.42}$$

where A_s is the Jacobian matrix of F_s and $\widehat{U}_\epsilon$ is a value that belongs to a curve connecting U_ϵ and $U_{\epsilon+\epsilon_s}$. By substituting (4.42) in (4.41), we obtain:

$$\begin{aligned}
&\left(F_s(U_\epsilon)) + F_s(U_{\epsilon+\epsilon_s})\right)\left(U^-_{\epsilon+\frac{\epsilon_s}{2}} + {U^+}_{\epsilon+\frac{\epsilon_s}{2}}\right) - \left(\left(F_s(U_{\epsilon-\epsilon_s})) + F_s(U_\epsilon)\right)\left(U^-_{\epsilon-\frac{\epsilon_s}{2}} + {U^+}_{\epsilon-\frac{\epsilon_s}{2}}\right)\right)\\
&= \left(F_s(U_\epsilon) + F_s(U_{\epsilon+\epsilon_s}\right)\left(U^-_{\epsilon+\frac{\epsilon_s}{2}} - {U^-}_{\epsilon-\frac{\epsilon_s}{2}} + U^+_{\epsilon+\frac{\epsilon_s}{2}} - {U^+}_{\epsilon-\frac{\epsilon_s}{2}}\right) +\\
&\qquad + \left(A_s\left(\widehat{U}_\epsilon\right)\left(U_{\epsilon+\epsilon_s} - U_\epsilon\right) + A_s\left(\widehat{U}_{\epsilon-\epsilon_s}\right)\left(U_\epsilon - U_{\epsilon-\epsilon_s}\right)\right)\left(U^-_{\epsilon-\frac{\epsilon_s}{2}} + U^+_{\epsilon-\frac{\epsilon_s}{2}}\right).
\end{aligned} \tag{4.43}$$

Now, we can write,

$$\begin{aligned}
&\left(A_s\left(\widehat{U}_\epsilon\right)\left(U_{\epsilon+\epsilon_s} - U_\epsilon\right) + A_s\left(\widehat{U}_{\epsilon-\epsilon_s}\right)\left(U_\epsilon - U_{\epsilon-\epsilon_s}\right)\right)\left(U^-_{\epsilon-\frac{\epsilon_s}{2}} + U^+_{\epsilon-\frac{\epsilon_s}{2}}\right) =\\
&A_s\left(\widehat{U}_\epsilon\right)\left(U^-_{\epsilon-\frac{\epsilon_s}{2}} + U^+_{\epsilon-\frac{\epsilon_s}{2}}\right)\left(U_{\epsilon+\epsilon_s} - U_\epsilon\right) + A_s\left(\widehat{U}_{\epsilon-\epsilon_s}\right)\left(U^-_{\epsilon-\frac{\epsilon_s}{2}} + U^+_{\epsilon-\frac{\epsilon_s}{2}}\right)\left(U_\epsilon - U_{\epsilon-\epsilon_s}\right),
\end{aligned} \tag{4.44}$$

where the product of the matrix $A_s\left(\widehat{U}_\epsilon\right)$ with the column vector $\left(U^-_{\epsilon-\frac{\epsilon_s}{2}} + U^+_{\epsilon-\frac{\epsilon_s}{2}}\right)$ is taken multiplying the i-th row of matrix with the i-th element of column vector.

Now, in (4.44), using (4.23) and (4.27), we write:

$$U_{\epsilon+\epsilon_s} - U_\epsilon = U^+_{\epsilon+\frac{\epsilon_s}{2}} - U^+_{\epsilon-\frac{\epsilon_s}{2}} + \frac{1}{4}\left(\widehat{\Phi}^+_{\epsilon+\frac{\epsilon_s}{2}} - \Phi^+_{\epsilon-\frac{\epsilon_s}{2}}\right)\left(U_{\epsilon+\epsilon_s} - U_\epsilon\right) \tag{4.45}$$

$$U_\epsilon - U_{\epsilon-\epsilon_s} = U^-_{\epsilon+\frac{\epsilon_s}{2}} - U^-_{\epsilon-\frac{\epsilon_s}{2}} - \frac{1}{4}\left(\Phi^-_{\epsilon+\frac{\epsilon_s}{2}} + \widehat{\Phi}^-_{\epsilon-\frac{\epsilon_s}{2}}\right)\left(U_\epsilon - U_{\epsilon-\epsilon_s}\right). \tag{4.46}$$

Substituting (4.45) and (4.46) in (4.44) and then in (4.43), we obtain:

$$
\begin{aligned}
&(F_s(U_\epsilon)) + F_s(U_{\epsilon+\epsilon_s}))\left(U^-_{\epsilon+\frac{\epsilon_s}{2}} + U^+{}_{\epsilon+\frac{\epsilon_s}{2}}\right) - \left((F_s(U_{\epsilon-\epsilon_s})) + F_s(U_\epsilon)\right)\left(U^-_{\epsilon-\frac{\epsilon_s}{2}} + U^+{}_{\epsilon-\frac{\epsilon_s}{2}}\right)\Big) \\
&= \left(F_s(U_\epsilon) + F_s(U_{\epsilon+\epsilon_s}) + A_s\left(\widehat{U}_\epsilon\right)\left(U^-_{\epsilon-\frac{\epsilon_s}{2}} + U^+_{\epsilon-\frac{\epsilon_s}{2}}\right)\right)\left(U^+_{\epsilon+\frac{\epsilon_s}{2}} - U^+{}_{\epsilon-\frac{\epsilon_s}{2}}\right) + \\
&+ \left(F_s(U_\epsilon) + F_s(U_{\epsilon+\epsilon_s}) + A_s\left(\widehat{U}_{\epsilon-\epsilon_s}\right)\left(U^-_{\epsilon-\frac{\epsilon_s}{2}} + U^+_{\epsilon-\frac{\epsilon_s}{2}}\right)\right)\left(U^-_{\epsilon+\frac{\epsilon_s}{2}} - U^-{}_{\epsilon-\frac{\epsilon_s}{2}}\right) + \\
&+ \frac{A_s\left(\widehat{U}_\epsilon\right)}{4}\left(U^-_{\epsilon-\frac{\epsilon_s}{2}} + U^+_{\epsilon-\frac{\epsilon_s}{2}}\right)\left(\widehat{\Phi}^+_{\epsilon+\frac{\epsilon_s}{2}} - \Phi^+_{\epsilon-\frac{\epsilon_s}{2}}\right)(U_{\epsilon+\epsilon_s} - U_\epsilon) \\
&- \frac{A_s\left(\widehat{U}_{\epsilon-\epsilon_s}\right)}{4}\left(U^-_{\epsilon-\frac{\epsilon_s}{2}} + U^+_{\epsilon-\frac{\epsilon_s}{2}}\right)\left(\Phi^-_{\epsilon+\frac{\epsilon_s}{2}} + \widehat{\Phi}^-_{\epsilon-\frac{\epsilon_s}{2}}\right)(U_\epsilon - U_{\epsilon-\epsilon_s})\,. \qquad (4.47)
\end{aligned}
$$

By substituting (4.47) in (4.40), we obtain:

$$
\begin{aligned}
&U^*_\epsilon = \\
&\frac{1}{4}\sum_{s=1}^{d}\Bigg[\left(\frac{P_s}{d} - \lambda_s\left\{B^s_{\epsilon+\frac{\epsilon_s}{2}} + \left(F_s(U_\epsilon) + F_s(U_{\epsilon+\epsilon_s}) + A_s\left(\widehat{U}_{\epsilon-\epsilon_s}\right)\left(U^-_{\epsilon-\frac{\epsilon_s}{2}} + U^+_{\epsilon-\frac{\epsilon_s}{2}}\right)\right)\right\}\right)U^-_{\epsilon+\frac{\epsilon_s}{2}} \\
&+ \lambda_s\left(B^s_{\epsilon+\frac{\epsilon_s}{2}} - \left(F_s(U_\epsilon) + F_s(U_{\epsilon+\epsilon_s}) + A_s\left(\widehat{U}_\epsilon\right)\left(U^-_{\epsilon-\frac{\epsilon_s}{2}} + U^+_{\epsilon-\frac{\epsilon_s}{2}}\right)\right)\right)U^+_{\epsilon+\frac{\epsilon_s}{2}} \\
&+ \left(\frac{P_s}{d} - \lambda_s\left\{B^s_{\epsilon-\frac{\epsilon_s}{2}} - \left(F_s(U_\epsilon) + F_s(U_{\epsilon+\epsilon_s}) + A_s\left(\widehat{U}_\epsilon\right)\left(U^-_{\epsilon-\frac{\epsilon_s}{2}} + U^+_{\epsilon-\frac{\epsilon_s}{2}}\right)\right)\right\}\right)U^+_{\epsilon-\frac{\epsilon_s}{2}} \\
&+ \lambda_s\left(B^s_{\epsilon-\frac{\epsilon_s}{2}} + \left(F_s(U_\epsilon) + F_s(U_{\epsilon+\epsilon_s}) + A_s\left(\widehat{U}_{\epsilon-\epsilon_s}\right)\left(U^-_{\epsilon-\frac{\epsilon_s}{2}} + U^+_{\epsilon-\frac{\epsilon_s}{2}}\right)\right)\right)U^-_{\epsilon-\frac{\epsilon_s}{2}} \\
&\frac{1}{d}\Bigg\{2Q_s - \frac{P_s}{4}\Phi^-_{\epsilon+\frac{\epsilon_s}{2}} - \frac{P_s}{4}\Phi^+_{\epsilon-\frac{\epsilon_s}{2}} + \lambda_s\Bigg(\Bigg[A_s\left(\widehat{U}_\epsilon\right)\left(\widehat{\Phi}^+_{\epsilon+\frac{\epsilon_s}{2}} - \Phi^+_{\epsilon-\frac{\epsilon_s}{2}}\right) \\
&+A_s\left(\widehat{U}_{\epsilon-\epsilon_s}\right)\left(\Phi^-_{\epsilon+\frac{\epsilon_s}{2}} + \widehat{\Phi}^-_{\epsilon-\frac{\epsilon_s}{2}}\right)\Bigg]\left(U^-_{\epsilon-\frac{\epsilon_s}{2}} + U^-_{\epsilon-\frac{\epsilon_s}{2}}\right)\Bigg)\Bigg\}U_\epsilon \\
&+ \left(\frac{P_s}{4d}\Phi^-_{\epsilon+\frac{\epsilon_s}{2}} - \lambda_s\frac{A_s\left(\widehat{U}_\epsilon\right)}{4}\left(U^-_{\epsilon-\frac{\epsilon_s}{2}} + U^+_{\epsilon-\frac{\epsilon_s}{2}}\right)\left(\widehat{\Phi}^+_{\epsilon+\frac{\epsilon_s}{2}} - \Phi^+_{\epsilon-\frac{\epsilon_s}{2}}\right)\right)U_{\epsilon-\epsilon_s} \\
&+ \left(\frac{P_s}{4d}\Phi^+_{\epsilon-\frac{\epsilon_s}{2}} - \lambda_s\frac{A_s\left(\widehat{U}_{\epsilon-\epsilon_s}\right)}{4}\left(U^-_{\epsilon-\frac{\epsilon_s}{2}} + U^+_{\epsilon-\frac{\epsilon_s}{2}}\right)\left(\Phi^-_{\epsilon+\frac{\epsilon_s}{2}} + \widehat{\Phi}^-_{\epsilon-\frac{\epsilon_s}{2}}\right)\right)U_{\epsilon+\epsilon_s}. \qquad (4.48)
\end{aligned}
$$

Moreover, if the conditions (4.32)-(4.35) are satisfied each matrix is semi-positive definite. All conditions guarantee that (i)-(iii) of (4.16) are satisfied, and the numerical scheme (4.19) is positive. ▫

Remark 4.2. *The conditions* (4.32)-(4.35) *are very restrictive. In general, it is not necessary to obtain the eigenvalues to guarantee the stability of the method. Notice that if*

the conditions

$$\lambda_s\left(\left(b_i^s\right)_{\epsilon+\frac{\epsilon_s}{2}}+\left((F_i)_s(U_\epsilon)+(F_i)_s(U_{\epsilon+\epsilon_s})\right)\leqslant\frac{p_s}{d}\ \text{for all } i=\{1,\cdots,N\}\ \text{and } s=\{1,\cdots,d\},\tag{4.49}$$

$$(F_i)_s(U_\epsilon)+(F_i)_s(U_{\epsilon+\epsilon_s})\leqslant\left(b_i^s\right)_{\epsilon+\frac{\epsilon_s}{2}}\quad\text{for all}\quad i=\{1,\cdots,N\}\ \text{and } s=\{1,\cdots,d\}\quad\text{and}\tag{4.50}$$

$$\phi^s\left(\left(\theta_i^+\right)_{\epsilon-\frac{\epsilon_s}{2}}\right)+\phi^s\left(\left(\theta_i^-\right)_{\epsilon+\frac{\epsilon_s}{2}}\right)\leqslant\frac{8q_s}{p_s}\quad\text{for all}\quad i=\{1,\cdots,N\}\ \text{and } s=\{1,\cdots,d\}.\tag{4.51}$$

are satisfied $U_i>0$, and ϵ_s are small enough such that $(U_i)^+\geqslant 0$ and $(U_i)^-\geqslant 0$ for all i, thus the conditions (i) and (iii) are satisfied in (4.16), since each matrix in (4.40) are symmetric and definite positive, but, to obtain the condition (ii) is necessary to linearize the flux of function as we perform in the previous proof. However, in the most part of numerical simulations the conditions (4.49)-(4.51) are enough to guarantee the stability of the method, thus we say that the method satisfy the ***positivity in the weak sense*** *if (i) and (iii) of (4.16) are satisfied. Moreover, we can prove that if (4.49)-(4.51) are satisfied, thus each coordinate satisfies the L^1 norm.*

Proof: *In the proof of Theorem 4.1, we show that the numerical method satisfies (4.40). Notice that from the construction of the numerical method and the no-flow curve, we can decouple the equations in the system, thus from (4.40), we can write for each U_i, for $i=1,\cdots,N$, of $U=(U_1,\cdots,U_N)$:*

$$\begin{aligned}(U_i)_\epsilon^*=&\frac{1}{4}\sum_{s=1}^{d}\Bigg[\left(\frac{p_s}{d}-\lambda_s\left\{\left(b_i^s\right)_{\epsilon+\frac{\epsilon_s}{2}}+\left((F_i)_s(U_\epsilon)+(F_i)_s\left(U_{\epsilon+\epsilon_s}\right)\right\}\right)(U_i)^-_{\epsilon+\frac{\epsilon_s}{2}}\\&+\lambda_s\left(\left(b_i^s\right)_{\epsilon+\frac{\epsilon_s}{2}}-\left((F_i)_s(U_\epsilon)+(F_i)_s\left(U_{\epsilon+\epsilon_s}\right)\right)\right)(U_i)^+_{\epsilon+\frac{\epsilon_s}{2}}\\&+\frac{1}{d}\left(2q_s-\frac{p_s}{4}\phi^s\left(\left(\theta_i^-\right)_{\epsilon+\frac{\epsilon_s}{2}}\right)-\frac{p_s}{4}\phi^s\left(\left(\theta_i^+\right)_{\epsilon-\frac{\epsilon_s}{2}}\right)\right)(U_i)_\epsilon\\&+\left(\frac{p_s}{d}-\lambda_s\left\{\left(b_i^s\right)_{\epsilon-\frac{\epsilon_s}{2}}-\left((F_i)_s(U_{\epsilon-\epsilon_s})+(F_i)_s\left(U_\epsilon\right)\right\}\right)(U_i)^+_{\epsilon-\frac{\epsilon_s}{2}}\\&+\lambda_s\left(\left(b_i^s\right)_{\epsilon-\frac{\epsilon_s}{2}}+\left((F_i)_s(U_{\epsilon-\epsilon_s})+(F_i)_s\left(U_\epsilon\right)\right)\right)(U_i)^-_{\epsilon-\frac{\epsilon_s}{2}}\\&+\frac{p_s}{4d}\phi^s\left(\left(\theta_i^-\right)_{\epsilon+\frac{\epsilon_s}{2}}\right)(U_i)_{\epsilon-\epsilon_s}+\frac{P_s}{4d}\phi^s\left(\left(\theta_i^+\right)_{\epsilon-\frac{\epsilon_s}{2}}\right)(U_i)_{\epsilon+\epsilon_s}.\end{aligned}\tag{4.52}$$

By considering that the numerical scheme satisfies (4.49)-(4.51) and $U_i>0$, i.e., $|U_i|=U_i$, and ϵ_s are small enough such that $(U_i)^+\geqslant 0$ and $(U_i)^-\geqslant 0$ for all i and integrating (for

each spatial dimension), we obtain:

$$\begin{aligned}\int_{\mathbb{T}}(U_i)_\epsilon^* dx = \int_{\mathbb{T}}\Bigg\{ & \frac{1}{4}\sum_{s=1}^{d}\Bigg[\left(\frac{p_s}{d}-\lambda_s\left\{(b_i^s)_{\epsilon+\frac{\epsilon_s}{2}}+((F_i)_s(U_\epsilon)+(F_i)_s\left(U_{\epsilon+\epsilon_s}\right)\right\}\right)(U_i)^-_{\epsilon+\frac{\epsilon_s}{2}} \\ & +\lambda_s\left((b_i^s)_{\epsilon+\frac{\epsilon_s}{2}}-((F_i)_s(U_\epsilon)+(F_i)_s\left(U_{\epsilon+\epsilon_s}\right))\right)(U_i)^+_{\epsilon+\frac{\epsilon_s}{2}} \\ & +\frac{1}{d}\left(2q_s-\frac{p_s}{4}\phi^s\left(\left(\theta_i^-\right)_{\epsilon+\frac{\epsilon_s}{2}}\right)-\frac{p_s}{4}\phi^s\left(\left(\theta_i^+\right)_{\epsilon-\frac{\epsilon_s}{2}}\right)\right)(U_i)_\epsilon \\ & +\left(\frac{p_s}{d}-\lambda_s\left\{(b_i^s)_{\epsilon-\frac{\epsilon_s}{2}}-((F_i)_s(U_{\epsilon-\epsilon_s})+(F_i)_s\left(U_\epsilon\right)\right\}\right)(U_i)^+_{\epsilon-\frac{\epsilon_s}{2}} \\ & +\lambda_s\left((b_i^s)_{\epsilon-\frac{\epsilon_s}{2}}+((F_i)_s(U_{\epsilon-\epsilon_s})+(F_i)_s\left(U_\epsilon\right))\right)(U_i)^-_{\epsilon-\frac{\epsilon_s}{2}} \\ & +\frac{p_s}{4d}\phi^s\left(\left(\theta_i^-\right)_{\epsilon+\frac{\epsilon_s}{2}}\right)(U_i)_{\epsilon-\epsilon_s}+\frac{P_s}{4d}\phi^s\left(\left(\theta_i^+\right)_{\epsilon-\frac{\epsilon_s}{2}}\right)(U_i)_{\epsilon+\epsilon_s}\Bigg]\Bigg\}dx. \end{aligned} \tag{4.53}$$

Due to mutual cancellations and using that

$$\begin{aligned}\int_{\mathbb{T}}\left(\phi^s\left(\left(\theta_i^-\right)_{\epsilon+\frac{\epsilon_s}{2}}\right)+\phi^s\left(\left(\theta_i^+\right)_{\epsilon-\frac{\epsilon_s}{2}}\right)\right)(U_i)_\epsilon dx = & \int_{\mathbb{T}}\phi^s\left(\left(\theta_i^-\right)_{\epsilon+\frac{\epsilon_s}{2}}\right)(U_i)_{\epsilon-\epsilon_s}dx \\ & +\int_{\mathbb{T}}\phi^s\left(\left(\theta_i^+\right)_{\epsilon-\frac{\epsilon_s}{2}}\right)(U_i)_{\epsilon+\epsilon_s}dx,\end{aligned} \tag{4.54}$$

we obtain that

$$\int_{\mathbb{T}}(U_i)_\epsilon^* dx=\frac{1}{4}\left(p_s\left(\int_{\mathbb{T}}(U_i)_\epsilon^+dx+\int_{\mathbb{T}}(U_i)_\epsilon^-dx\right)\right)+2q_s\int_{\mathbb{T}}(U_i)_\epsilon dx=\int_{\mathbb{T}}(U_i)_\epsilon dx. \tag{4.55}$$

In the last equality of (4.55)*, we use that* $\int_{\mathbb{T}}(U_i)_\epsilon^+dx+\int_{\mathbb{T}}(U_i)_\epsilon^-dx=2\int_{\mathbb{T}}(U_i)_\epsilon dx$ *and* (4.31)*. In addition, the equality* (4.54) *is true, from the definition of* $(U_i)_\epsilon^-$ *and* $(U_i)_\epsilon^+$*.*

Since we assume that each F_s is a Lipschitz continuous function and $B_{\epsilon+\frac{\epsilon_s}{2}}$ can be chosen such that is also Lipschitz continuous. In this case the numerical method satisfies (4.18).

As observed in [65, 66], the same conditions are valid also for (4.29), thus we obtain, using (4.18), that

$$||U_\epsilon^{**}||_2\leqslant(1+const\Delta)||U^*||_2\leqslant(1+const\Delta)||U^n||_2. \tag{4.56}$$

Applying to (4.18) and (4.56) in (4.30), we obtain:

$$||U_\epsilon^{n+1}||_2\leqslant\frac{1}{2}\left(||U_\epsilon^*||_2+||U_\epsilon^{**}||_2\right)\leqslant(1+const\Delta)||U^n||_2. \tag{4.57}$$

In the proof of Theorem 4.1, we use the matrices P_s and Q_s, because this theorem is general for multi-D system of (4.13) and for numerical methods with our without reconstruction, and we can choose the parameters depending of our problem.

Example 4.1. *As example of the weak positivity criterion to be satisfied, we consider the* $2-D$ *system of hyperbolic equations. In this case* $d=2$*. Applying this to the conditions* (4.32)-(4.35)*, we obtain:*

$$\frac{\Delta t}{\epsilon_1}\left(\left(b_i^1\right)_{\epsilon+\frac{\epsilon_1}{2}}+((F_i)_1(U_\epsilon)+(F_i)_1(U_{\epsilon+\epsilon_1})\right)\leqslant\frac{p_1}{2},$$
$$\frac{\Delta t}{\epsilon_2}\left(\left(b_i^2\right)_{\epsilon+\frac{\epsilon_2}{2}}+((F_i)_2(U_\epsilon)+(F_i)_2(U_{\epsilon+\epsilon_2})\right)\leqslant\frac{p_2}{2}, \tag{4.58}$$
$$(F_i)_1(U_\epsilon)+(F_i)_1(U_{\epsilon+\epsilon_1})\leqslant\left(b_i^1\right)_{\epsilon+\frac{\epsilon_1}{2}},\quad (F_i)_2(U_\epsilon)+(F_i)_2(U_{\epsilon+\epsilon_s})\leqslant\left(b_i^2\right)_{\epsilon+\frac{\epsilon_s}{2}}, \tag{4.59}$$
$$\phi^1\left(\left(\theta_i^+\right)_{\epsilon-\frac{\epsilon_1}{2}}\right)+\phi^1\left(\left(\theta_i^-\right)_{\epsilon+\frac{\epsilon_1}{2}}\right)\leqslant\frac{8q_1}{p_1},\quad \phi^2\left(\left(\theta_i^+\right)_{\epsilon-\frac{\epsilon_2}{2}}\right)+\phi^2\left(\left(\theta_i^-\right)_{\epsilon+\frac{\epsilon_2}{2}}\right)\leqslant\frac{8q_2}{p_2}. \tag{4.60}$$

If we assume that (4.25) *is true, we obtain from* (4.60) *that* $p_1=q_1=1$ *and* $p_2=q_2=1$*, since* $p_i+q_i=2$*, for all* i*.*

If we consider for $i=\{1,\cdots,N\}$ *and* $j=\{1,2\}$

$$\left(b_i^j\right)_{\epsilon+\frac{\epsilon_i}{2}}=2max_U|(F_i)_j(U)|=M_i^j, \tag{4.61}$$

then the condition (4.59) *is satisfied and if we get*

$$\frac{\Delta t}{\epsilon_1}M_i^1\leqslant\frac{1}{8}\quad and\quad \frac{\Delta t}{\epsilon_1}M_i^1\leqslant\frac{1}{8}, \tag{4.62}$$

then the condition (4.58) *is also satisfied and the numerical scheme* (4.19) *is positive.*

If on the other hand, we disregard the reconstruction such that $\Phi^+=\Phi^-=0$*, we take* $q_i=0$*, and thus* $p_i=2$ *for all* $i=\{1,\cdots,d\}$*. For the* $2-D$ *scheme, the scheme is positive if we substitute* (4.62) *by:*

$$\frac{\Delta t}{\epsilon_1}M_i^1\leqslant\frac{1}{4}\quad and\quad \frac{\Delta t}{\epsilon_1}M_i^1\leqslant\frac{1}{4}. \tag{4.63}$$

4.3 Numerical Experiments

In order to illustrate the performance of our semi-discrete scheme, we present a set of numerical experiments for hyperbolic system of conservation laws starting with a shallow-water flow system linked to a *flux separation strategy*, then we numerically analyze the entropy glitch effect on our scheme by treating the Burgers' equation and the Euler equations of gas dynamics. Finally, we verify the theory and illustrate the capabilities of the semi-discrete approach in three cases (1) a 4×4 system of compressible Euler flows (Double Mach reflection and Wind tunnel problems), (2) a 3×3 shallow-water system of equations with and without bottom discontinuous topography, and (3) 2×2 non-strictly hyperbolic three-phase flows with a resonance point. For instance, the numerical tests show that the discretizations resulting from the flux separation strategy seem to be of good quality when applied to two-by-two shallow-water and two-dimensional compressible

Euler equations. In computing practice (Section 3.3), we have observed stable solutions when only using the control volume over the no-flow equations (3.5), which is consistent with the results of our rigorous analysis (Sections 3.2, 3.2.2, and 3.2.3). In fact, this is also the case of the systems addressed in Section 4.2.1 because the SDLE scheme also satisfies the positivity principle. This is a substantial advantage for multidimensional systems as presented in Section 4.3.3.

4.3.1 One dimensional systems of hyperbolic conservation laws

Example 4.2. ***Shallow-water equations and the flux separation strategy***

We consider the following model (see, e.g., [10, 13]):

$$\begin{cases} h_t + (hv)_x = 0, \\ (hv)_t + (v^2 h + \dfrac{1}{2}h^2)_x = 0, \end{cases} \quad \text{or} \quad \begin{cases} v_t + \left(\dfrac{v^2}{2} + \varphi\right)_x = 0, \\ \varphi_t + (v\varphi)_x = 0, \end{cases} \tag{4.64}$$

where $\varphi = h$; the horizontal velocity, $v = v(x,t)$, is roughly constant across any cross-section of the channel; and $h = h(x,t)$ denotes the height. The quantity hv is often referred to as the discharge in shallow water theory because it measures the flow rate of water past a point, where h is the height of the free surface; and v, the averaged horizontal velocity. This system models the flow of water downing in a channel with a rectangular cross-section. In model (4.64.*b*), one observes that the nonlinear *no-flow curve* $\lim\limits_{v\to 0} \dfrac{H_1(v,\varphi)}{v}$, where $H_1(v,\varphi) = \dfrac{v^2}{2} + \varphi$, is not well defined. To overcome this situation, we will employ a suitable *flux separation strategy* along with the SDLE scheme. Such strategy was also successfully implemented in [10, 13] for fully-discrete Lagrangian-Eulerian formulations. This approach consists in transforming hyperbolic equation $v_t + H_1(v,\varphi)_x = 0$ into a suitable form that resembles a *balance law model* given by $v_t + (H_1^a)_x = -(H_1^b)_x$, where formally $H_1 = H_1^a + H_1^b$. It should be noted that such flux separation strategy is admissible and retains all the properties of the original hyperbolic model.

Considering the proposed SDLE scheme (2.17)-(2.19) discussed in Section 2.1, the average of variable s in the similar balance law model $(s_t + H_1^a(s)_x = -H_1^b(s)_x)$ as mentioned above over interval $[\overline{x}_j^{n+1}, \overline{x}_{j+1}^{n+1}]$ is given by

$$s_{j+\frac{1}{2}}^{n+1} = \frac{1}{\bar{\Delta}x_j}\int_{\bar{x}_j}^{\bar{x}_{j+1}} s(\xi, t^{n+1})d\xi + \frac{1}{\bar{\Delta}x_j}\iint\limits_{D_j^{n,n+1}} (-H_1^b(s)_x)dx\,dt.$$

Thus, we obtain the approximate cell average in time t^{n+1} as follows:

$$s_{j+\frac{1}{2}}^{n+1} = \frac{1}{\bar{\Delta}x_j}\left[\left[\frac{\Delta x}{2}\left(s_j^n + s_{j+1}^n\right) + \frac{\Delta x^2}{8}\left((s_x)_j^n - (s_x)_{j+1}^n\right)\right] - \iint\limits_{D_j^{n,n+1}} (H_1^b(s)_x)dxdt\right]. \tag{4.65}$$

In addition, if we denote $\mathcal{G}(s(x,t)) = -H_1^b(s(x,t))$, apply the fundamental theorem of calculus to the integral over the control volume, we have

$$\iint\limits_{D_j^{n,n+1}} \mathcal{G}(s(x,t))_x dx\, dt = \int_{t^n}^{t^{n+1}} \left[\mathcal{G}(s(\sigma_{j+1}^n(t),t)) - \mathcal{G}(s(\sigma_j^n(t),t))\right] dt \tag{4.66}$$

$$\approx \Delta t \left[\mathcal{G}(s(\sigma_{j+1}^n(t^n),t^n)) - \mathcal{G}(s(\sigma_j^n(t^n),t^n))\right]. \tag{4.67}$$

Therefore, Eq. (4.65) can be written as

$$s_{j+\frac{1}{2}}^{n+1} = \frac{1}{\bar{\Delta}x_j}\left[\frac{\Delta x}{2}\left(s_j^n + s_{j+1}^n\right) + \frac{\Delta x^2}{8}\left((s_x)_j^n - (s_x)_{j+1}^n\right)\right] + \frac{1}{\bar{\Delta}x_j}\mathcal{A}_j,$$

where $\mathcal{A}_j$ is the approximation of the RHS of Eq. (4.67) and is given by

$$\mathcal{A}_j = \Delta t \left[\mathcal{G}(s_{j+1}^n) - \mathcal{G}(s_j^n)\right].$$

Through a projection over the original grid, the local approximation, s_j^{n+1}, for all $j \in \mathbb{Z}$ is given by

$$s_j^{n+1} = \frac{1}{\Delta x}\left[m_{1j} s_{j-\frac{1}{2}}^{n+1} + m_{2j} s_{j+\frac{1}{2}}^{n+1}\right],$$

where projection coefficients m_{1j} and m_{2j} are given by (2.13) for variable s. Using the same procedure presented in Subsection 2.1.1, our SDLE scheme can be written in a conservative form as

$$\frac{d}{dt}s_j(t) = -\frac{1}{\Delta x}\left[\mathcal{P}\left(s_j, s_{j+1}\right) - \mathcal{P}\left(s_{j-1}, s_j\right)\right], \tag{4.68}$$

where

$$\mathcal{P}\left(s_j, s_{j+1}\right) = \mathcal{F}\left(s_j, s_{j+1}\right) - 0.5(\mathcal{G}(s_j) + \mathcal{G}(s_{j+1})), \tag{4.69}$$

$\mathcal{F}\left(s_j, s_{j+1}\right)$ is the Lagrangian numerical flux function (2.18) for variable s, and $f_{s,j} \approx \dfrac{H_1^a(s_j)}{s_j}$ the new no-flow curve approximation.

By means of the *flux separation strategy*, system (4.64.*b*) can be written as

$$\begin{cases} v_t + \left(\dfrac{v^2}{2}\right)_x = -\varphi_x, \\ \varphi_t + (v\varphi)_x = 0, \end{cases} \tag{4.70}$$

with initial velocity $v_0 = 1.699$, while the initial height of the free surface consists in a triangular perturbation of the uniform flow level, $h_0(x) = x + 1.5$, $-0.5 \leqslant x \leqslant 0$, $h_0(x) = -x + 1.5$, $0 \leqslant x \leqslant 0.5$, and 1 elsewhere. The quantities shown in this numerical experiment include the height (h) and the velocity (v), with $\mathcal{G}(v_j) = -\varphi_j$ and $\mathcal{G}(\varphi_j) = 0$, $j \in \mathbb{Z}$. Figure 11 compares a reference numerical solution with 2560 grid cells with the numerical solutions obtained with our semi-discrete method on a grid having 640 grid cells at a given output time and with CFL number $C_{CFL} = 0.23$. As expected from the analysis in [61], we have two waves moving in opposite directions. Therefore, the proposed scheme is also able to accurately capture the correct qualitative behavior for hyperbolic shallow-water problem (4.64).

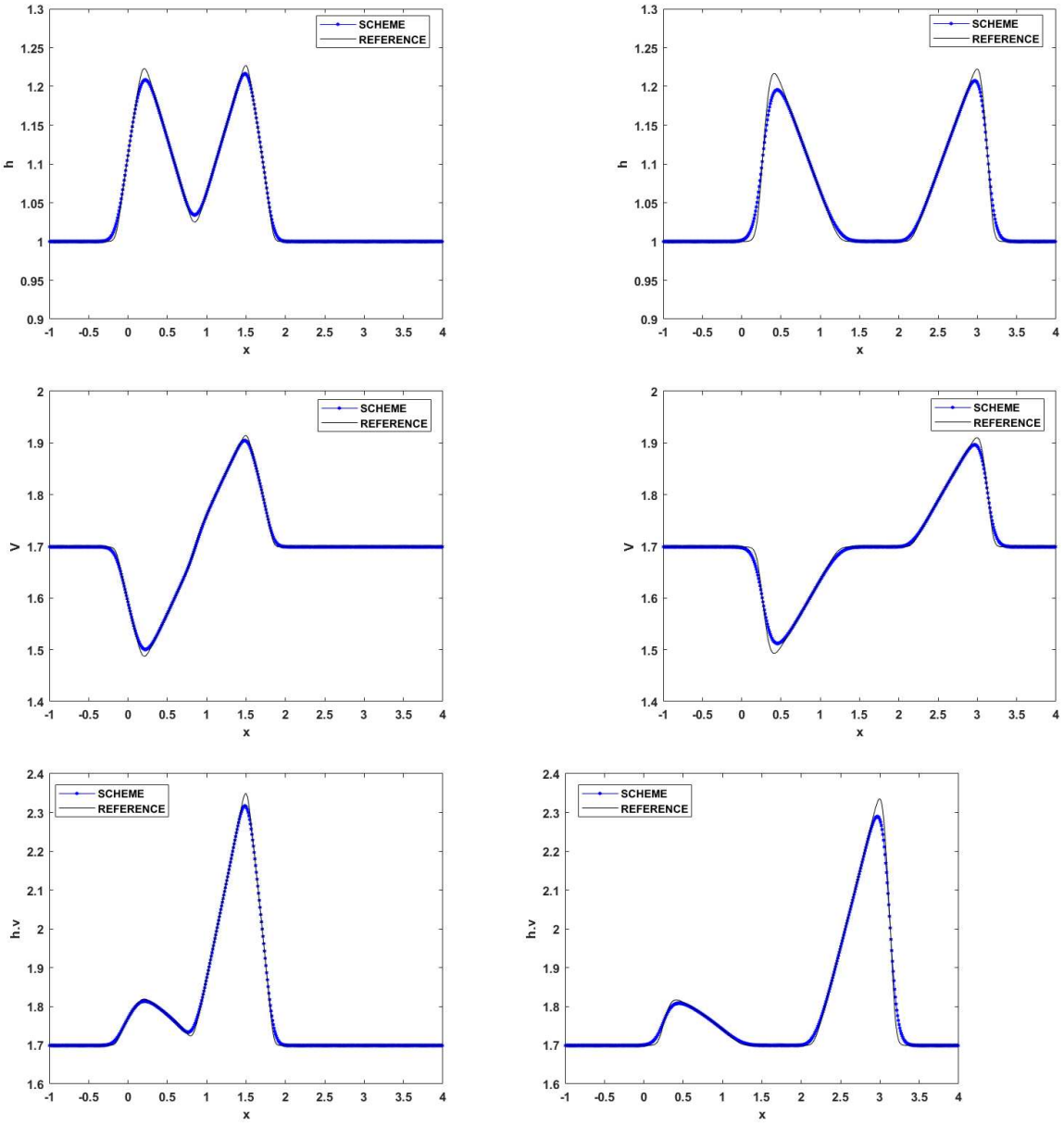

Figure 11 – Numerical approximation of the shallow-water equation with 640 grid cells at times $T = 0.5$ (left) and $T = 1$ (right), and with $\alpha = 1$, $\zeta = 2$ and $\theta = 2$.

4.3.2 The sonic point glitch effect

Recently, many efforts have been made to design numerical schemes to capture shock waves and contact discontinuities, included the resolution of rarefaction wave, which can be resulted in a non-physical phenomenon around the sonic point (A point where a sign change in the wave speeds is observed). Such phenomenon arises in the presence of sonic rarefaction waves due to the change in signal of the wave speeds and it is called the "*sonic glitch or entropy glitch*" [81] (e.g., see such un-physical effect in the experiments produced by the classical Godunov scheme in the left column in Figure 12). Here we will analyze numerically the glitch effect in our semi-discrete scheme considering the inviscid

Burgers' equation and the Euler equations of gas dynamics.

Example 4.3. ***Inviscid Burgers' equation with discontinuous initial data.***

Here we shall investigate numerical evolution of the sonic rarefaction wave by considering Eq. (2.1) with Burgers' flux function given by $H(u) = \dfrac{u^2}{2}$ along with initial data $u(x,0) = -1, x < 0$ and $u(x,0) = 1, x > 0$. In Figure 12 are shown snapshot graphs at time $T = 1$ of simulation for a moving rarefaction wave, where the rarefaction wave is spreading out correctly and matching with the exact solution using our semi-discrete scheme (2.17)-(2.19) with $\alpha = 2$, $\zeta = 1$ and $\theta = 2$ in a mesh grid refinement study composed with 80 cells, 160 cells and 320 cells. We notice that our semi-discrete scheme handles correctly the well-known spurious entropy glitch effect in the sonic rarefaction fan and with no need of any numerical technique to eliminate the glitch effect (Figure 12, right column).

Example 4.4. ***Euler equations of gas dynamics*** [79].

Let us consider the one-dimensional Euler System in the form

$$\begin{cases} \rho_t + (\rho v)_x = 0, & \text{(conservation of mass)}, \\ (\rho v)_t + (\rho v^2 + p)_x = 0, & \text{(conservation of momentum)}, \\ E_t + (v(E+p))_x = 0, & \text{(conservation of energy)}. \end{cases} \tag{4.71}$$

Here ρ is the mass density, v is the velocity while $E = (p/\rho)(\gamma - 1)^{-1} + (v^2/2)$ is the total specific energy, $\gamma > 1$. The system is closed by a constitutive relation of the form $p = p(\rho, e)$, giving the pressure as a function of the density and the internal energy e. The particular form of p depends on the gas under consideration [70, 79, 82]. Let's denote the conserved quantities as $q = (\rho, m, E)^T$ and the flux vector function is $H(q) = (m, \rho v^2 + p, v(E+p))$ where $m = \rho v$. We solve this system subject to the Riemann initial data

$$q(x,0) = \begin{cases} q_L, & \text{if} \quad x \leqslant 0.5, \\ q_R, & \text{if} \quad x > 0.5 \end{cases}$$

where $q_L = (1, 0, 2.5)$ and $q_R = (0.125, 0, 0.25)$ presented in Figure 13. Thus, using the *flux separation approach* in Eq. (4.71) componentwisely we obtain

$$\begin{cases} \rho_t + m_x = 0, & \text{(conservation of mass)}, \\ (\rho v)_t + (\rho v^2)_x = -p_x, & \text{(conservation of momentum)}, \\ E_t + (vE)_x = -(vp)_x, & \text{(conservation of energy)}. \end{cases} \tag{4.72}$$

In our current numerical approximation for this one dimensional Euler system, we use our semi-discrete Lagrangian-Eulerian scheme (4.68)-(4.69) with $s = \rho, m, E$ and

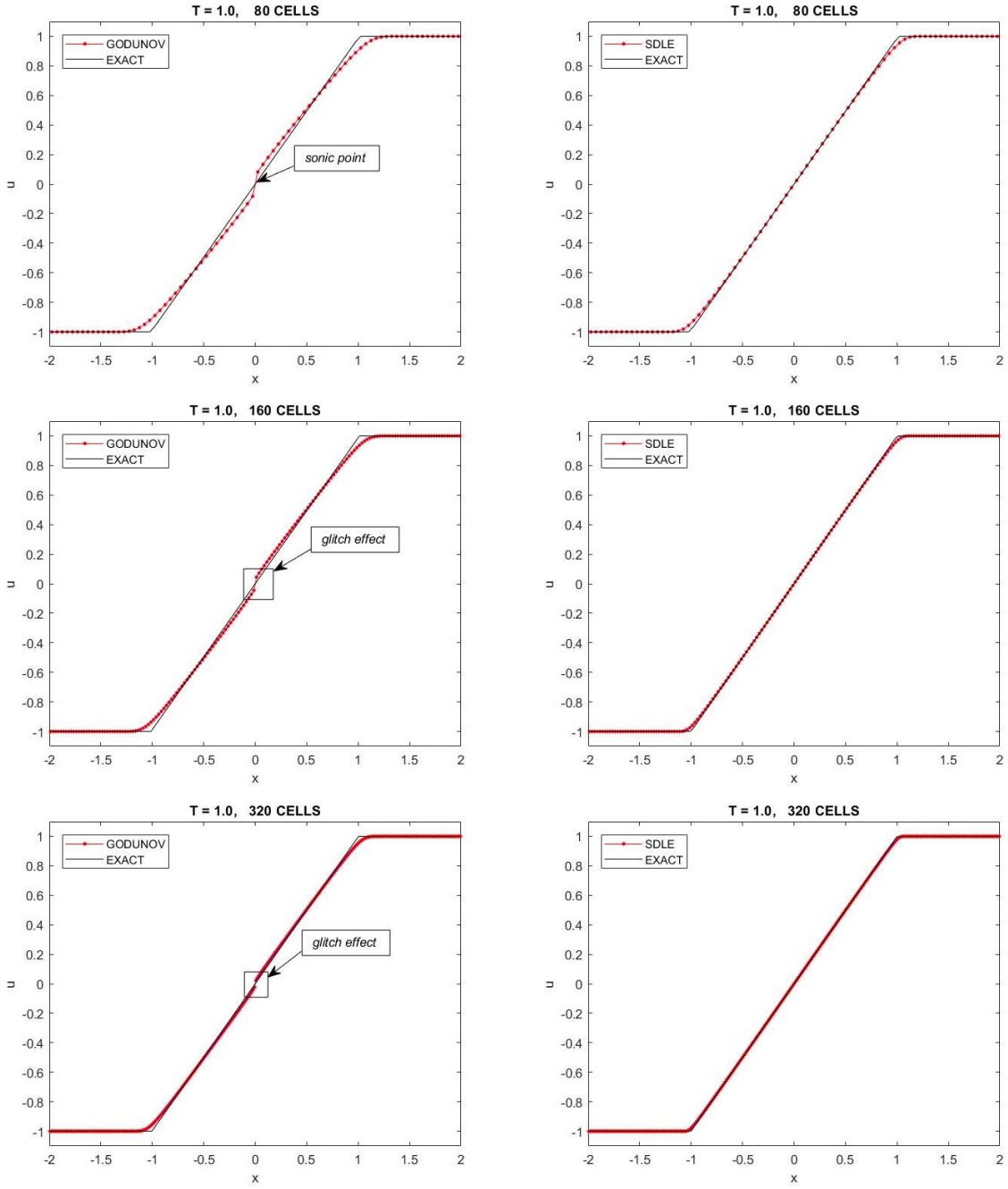

Figure 12 – Approximated solutions computed by the semi-discrete Lagrangian-Eulerian scheme (2.17)-(2.19) ($\alpha = 2$, $\zeta = 1$, $\theta = 2$ and CFL=0.13) at time $T = 1$ (right column) and approximated solutions computed by the Godunov scheme affected by the entropy glitch in the vicinity of the sonic point (left column) at time $T = 1$.

$\mathcal{G}(\rho_j) = 0$, $\mathcal{G}(m_j) = -p_j$, $\mathcal{G}(E_j) = -(vp)_j$. The quantities shown in this experiment are the mass density $\rho = \rho(x,t)$, the velocity $v = v(x,t)$ and the pressure $p = p(x,t)$. The solution of this Riemann problem consists of a right shock wave, a right traveling contact wave and a left sonic rarefaction wave (Figure 13); this example is very useful in assessing the entropy satisfaction property of numerical methods.

Figure 13 shows comparison between exact solution and numerical solution at a given output time obtained by our semi-discrete method with 320 and 1280 grid cells. One positive feature of our numerical approximation of the discontinuities is that our no-flow estimate $b_{j+\frac{1}{2}}$ gives the correct speed of propagation. The rarefaction wave is a smooth flow feature and is reasonably well approximated by our method and with no spurious entropy glitch effect in the sonic rarefaction [81]. It appears that the numerical solution given by the aid of our method converge to the exact entropy solution as the grid is refined.

4.3.3 Multidimensional systems of hyperbolic conservation laws

We turn our attention to discuss the application of the semi-discrete schemes given in general form by (4.10)-(4.11) for multidimensional systems of hyperbolic conservation laws. Firstly, recall our scheme satisfy the positivity principle in the sense of the papers of Lax and Liu [65, 66]. We provide robust numerical examples to verify the theory and illustrate the capabilities of the semi-discrete approach in three cases (1) a 4×4 system of compressible Euler flows (the cases with Double Mach reflection as well as Wind tunnel), (2) a 3×3 shallow-water system of equations (with and without bottom discontinuous topography), and (3) a 2×2 non-strictly hyperbolic three-phase flow (with a resonance point).

The multidimensional (2D) no-flow curves in (4.12) allow us to construct a positive SDLE scheme (Section 4.2.1) which does not use field-by-field decompositions, i.e., our scheme does not make use of the Jacobian and the matrix of eigenvectors.

Thanks to the no-flow curves in (4.12), we also devise a CFL-type constraint (3.8), which does not require the need to employ the eigenvalues (exact and approximate values) of the relevant Jacobian of the numerical flux functions. Another interesting feature of the no-flow Lagrangian-Eulerian construction is that the matrices are symmetric for free (actually, they are diagonal), which is independent for a general class of hyperbolic flux for scalar problems and systems as well. The component-wise extension of the Lagrangian-Eulerian framework is facilitated with the no-flow curves and the same positive SDLE scheme (3.3)-(3.4) is applied as a straightforward manner and with the same simplicity for the above mentioned model of multidimensional systems of hyperbolic conservation laws.

The positive semi-discrete Lagrangian-Eulerian scheme handles quite easily the issue of boundary conditions (as in the case with Double Mach reflection as well as Wind tunnel for compressible Euler flows as well as in the injection problem for a non-strictly hyperbolic three-phase flow with a resonance point. As we will see in what follow, the SDLE scheme is able to capture steep gradients as well as regions with shocks with very good resolution with efficiency. For all numerical experiments there is no spurious oscillations nor any numerical noise and much less stringent computing limitations, since the CFL

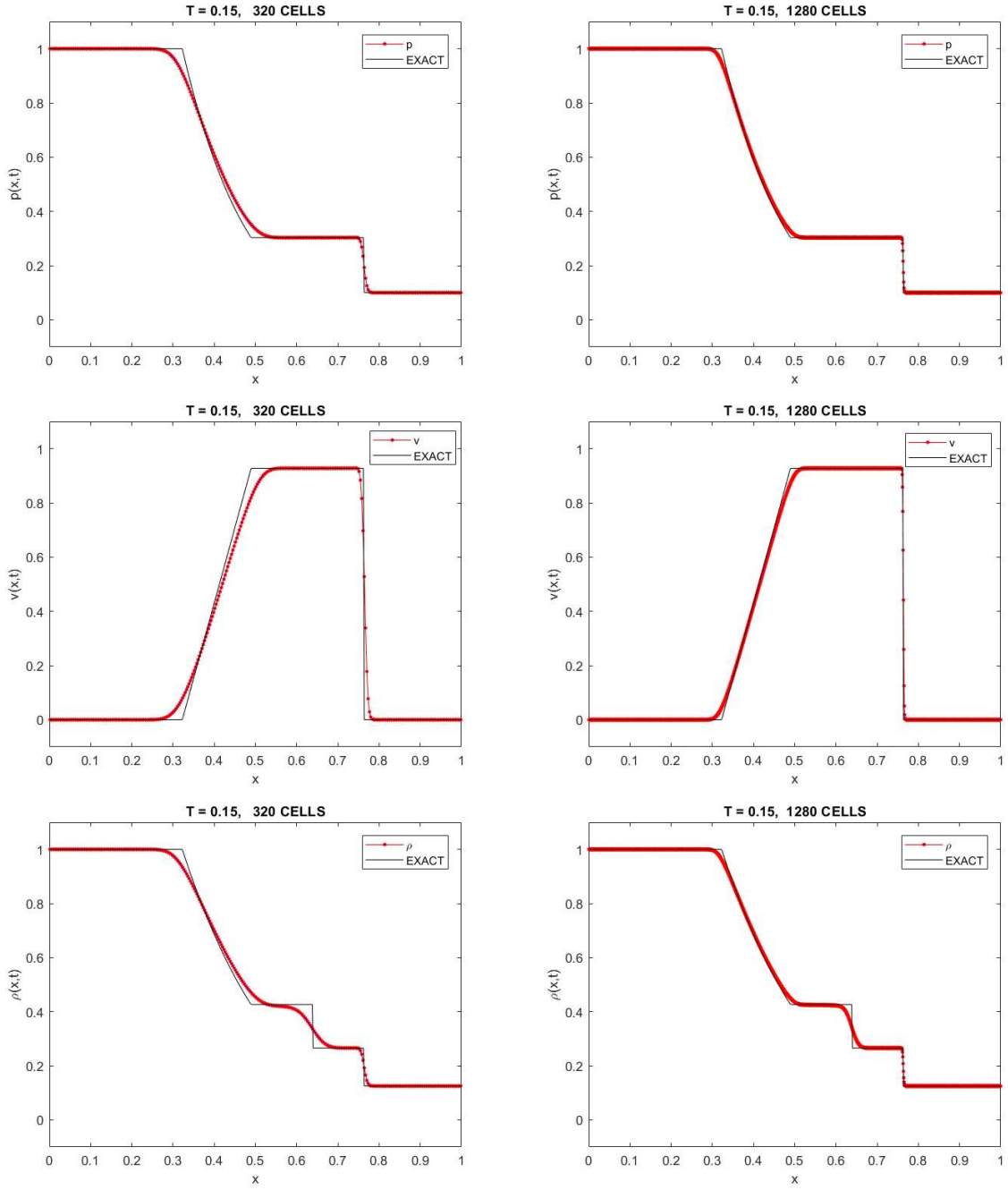

Figure 13 – Numerical approximations of the Euler of gas Dynamics problem computed with the semi-discrete Lagrangian-Eulerian scheme at time $T = 0.15$ with $\alpha = 1$, $\zeta = 3$, $\theta = 2$ and CFL=0.13.

condition and the SDLE scheme do not need the eigenvalues (exact and approximate values). From the numerical test, we observed the non-classical solution in the three-phase flow model, the weak oblique shock is resolved in the Wind tunnel model as well as the curved reflected shock and the reflecting wall in the Double Mach reflection and the case of bottom discontinuous topography in shallow-water system of equations are well resolved with all the physics of the problems at hand preserved in the simulations.

Example 4.5. ***A non-strictly hyperbolic three-phase flow model in porous media*** *[1, 69]*

The nonlinear wave structure in a non-strictly hyperbolic three-phase flow model in porous media is very rich and intricate (for more details see [26, 69] and references cited therein). Various studies into fluid flow in porous media have been reported in the literature in a wide range of application fields, including oil production and groundwater treatment and remediation (see, e.g., [1, 4, 26] and references cited therein). Let us consider a horizontal flow in a homogeneous (2D) porous medium caused by the simultaneous injection of two immiscible fluids (water and gas) to displace the in-situ oil. The porous medium and the fluids are assumed to be incompressible; and the permeability of the medium, isotropic. We assume that there are no internal sources or sinks. Mass transfer between the phases, as well as the thermal and gravitational effects, are neglected. This three-phase flow model is given by

$$\begin{aligned} \frac{\partial s_w}{\partial t} + \frac{\partial}{\partial x}(f_w(s_w, s_g)) + \frac{\partial}{\partial y}(f_w(s_w, s_g)) = 0, \\ \frac{\partial s_g}{\partial t} + \frac{\partial}{\partial x}(f_g(s_w, s_g)) + \frac{\partial}{\partial y}(f_g(s_w, s_g)) = 0, \end{aligned} \tag{4.73}$$

and $s_o = 1 - s_w - s_g$, and is subject to two Riemann problems ($RP1$ and $RP2$), which are, respectively, given by

$$RP1 = \begin{cases} s_w^L = 0.613 \text{ and } s_w^R = 0.05, \\ s_g^L = 0.387 \text{ and } s_g^R = 0.15, \end{cases} \quad \text{and} \quad RP2 = \begin{cases} s_w^L = 0.721 \text{ and } s_w^R = 0.05, \\ s_g^L = 0.279 \text{ and } s_g^R = 0.15, \end{cases} \tag{4.74}$$

where the phases are referred to as gas, oil, and water and are denoted by subscripts g, o, and w, respectively. Fractional flow functions $f_w(s_w, s_g)$ and $f_g(s_w, s_g)$ are defined in terms of relative permeability functions k_w, k_g, and k_o and fluid viscosities μ_w, μ_g, and μ_o and are, respectively, given by

$$f_w = \frac{k_w/\mu_w}{k_w/\mu_w + k_g/\mu_g + k_o/\mu_o} \quad \text{and} \quad f_g = \frac{k_g/\mu_g}{k_w/\mu_w + k_g/\mu_g + k_o/\mu_o},$$

for each variable. Following [1, 4, 26, 69], we use the quadratic model developed by Corey-Pope, which has been extensively employed for phase relative permeabilities $k_w = s_w^2$, $k_o = s_o^2$, and $k_g = s_g^2$. In addition, we consider the following viscosity values: $\mu_o = 1.0$, $\mu_w = 0.5$, and $\mu_g = 0.3$. The injection at $x = 0$ is specified at time zero as the initial state (s_w^L, s_g^L) from Riemann data (4.74) such that $f_w(s_w^L, s_g^L)$ and $f_g(s_w^L, s_g^L)$ on the spatial interval, where the reservoir initial state is given by saturation values (s_w^R, s_g^R) from Riemann data (4.74).

In immiscible three-phase flow model (4.73) with the Corey-Pope and the Riemann Problem (4.74.*b*), the leading oil moving front can split into two, a Buckley-Leverett shock wave followed by a new type of shock wave and composite wave comprising

a shock wave and adjoining rarefaction. The same three-phase flow model (4.73) along with the Riemann Problem (4.74.*a*) leads to a Buckley-Leverett shock wave followed by composite wave comprising a shock wave and adjoining rarefaction, that is, there is no occurrence of the *non-classical transitional shock* in the case (4.74.*a*).

The simulations are numerically calculated in a bounded 2D reservoir, $\Omega = [0, X] \times [0, Y]$, with aspect ratio X/Y=1, by discretizing in a uniform mesh with 512×512 grid cells. As mentioned, the injection imposed by $f_w(s_w^L, s_g^L)$ and $f_g(s_w^L, s_g^L)$ on the at $x = 0$ and $y \in [0, Y]$ is specified at time zero as the initial state (s_w^L, s_g^L) from Riemann data (4.74). No-flow is allowed across the boundaries with $y = 0$, $y = Y$, and $x \in [0, X]$ and production of the three-phase mixture take place at $x = L$ and $y \in [0, Y]$.

Figures 14, 15 and 16 describe the Riemann solution for the injection of a mixture of water and gas into a reservoir with high initial oil content for Riemann Problems (4.74.*a*) and (4.74.*b*). From [1, 69], one can recognize the expected correct structure of the solutions in the non-classical three-phase model under consideration. A transitional shock wave is present in the solution to $RP2$ but not in that to $RP1$. Moreover, in Figures 14, 15 and 16 are shown a grid refinement study conducted using $RP1$ (left column) and $RP2$ (right column). We obtain evidence of the numerical convergence with SDLE scheme with computational times 6 s (128×128 grid cells), 61.1 s (256×256 grid cells) for $RP1$ as well as 3.3 s (128×128 grid cells), 36.7 s (256×256 grid cells) for $RP2$, along with numerical parameters $\alpha = 1$, $\zeta = 2$, and $\theta = 1.5$. On the third row (to the bottom) is shown the corresponding numerical solutions in a very fine computational mesh, which the solution structures are good agreement with those reported in the available literature [1, 69].

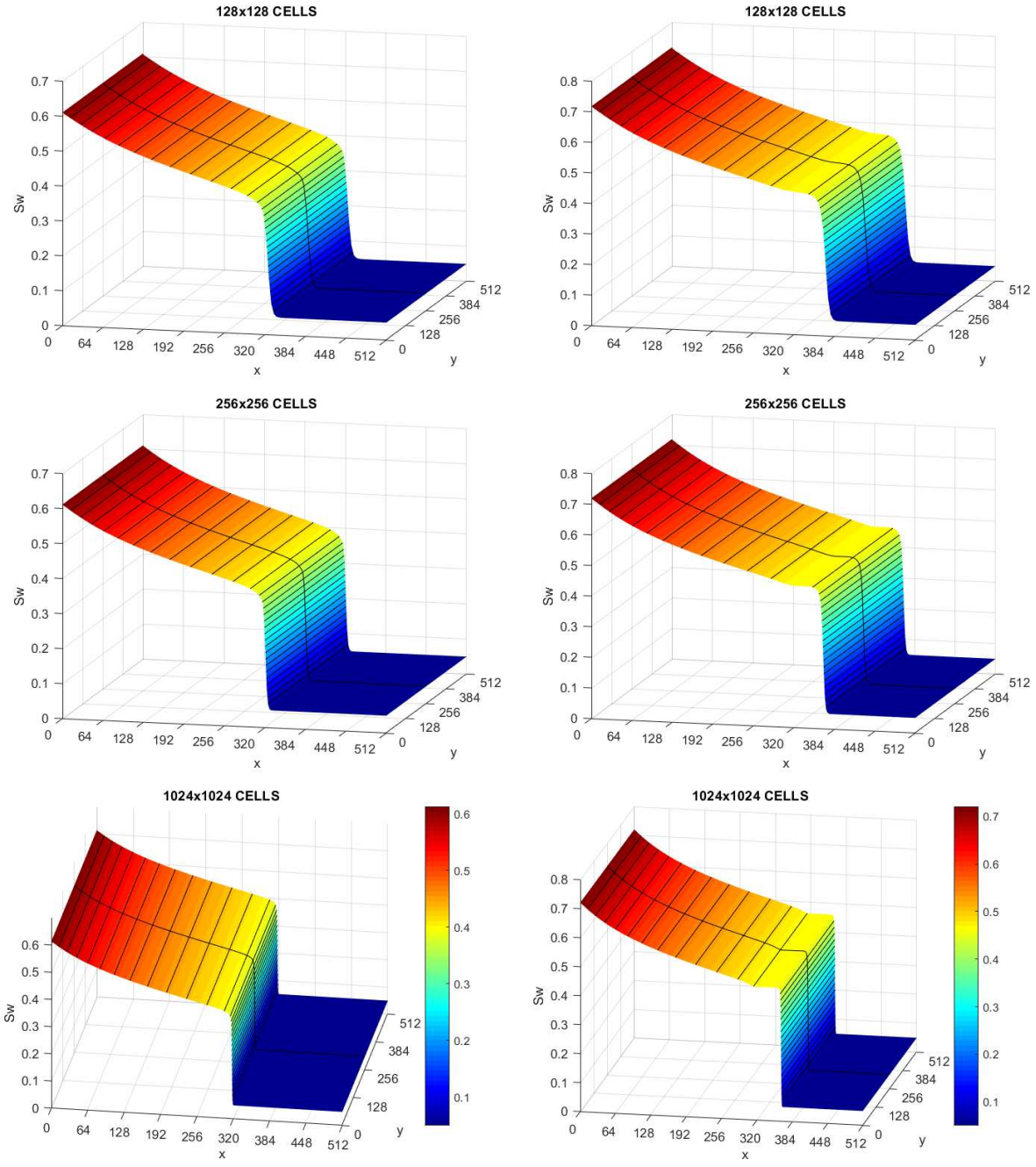

Figure 14 – A numerical convergence study for three-phase model (4.73) linked to (4.74) with a superimposed approximation corresponding to the 1D Euler System: $\frac{\partial s_w}{\partial t} + \frac{\partial}{\partial x} f_w(s_w, s_g) = 0$, $\frac{\partial s_g}{\partial t} + \frac{\partial}{\partial x} f_g(s_w, s_g) = 0$ (solid line).

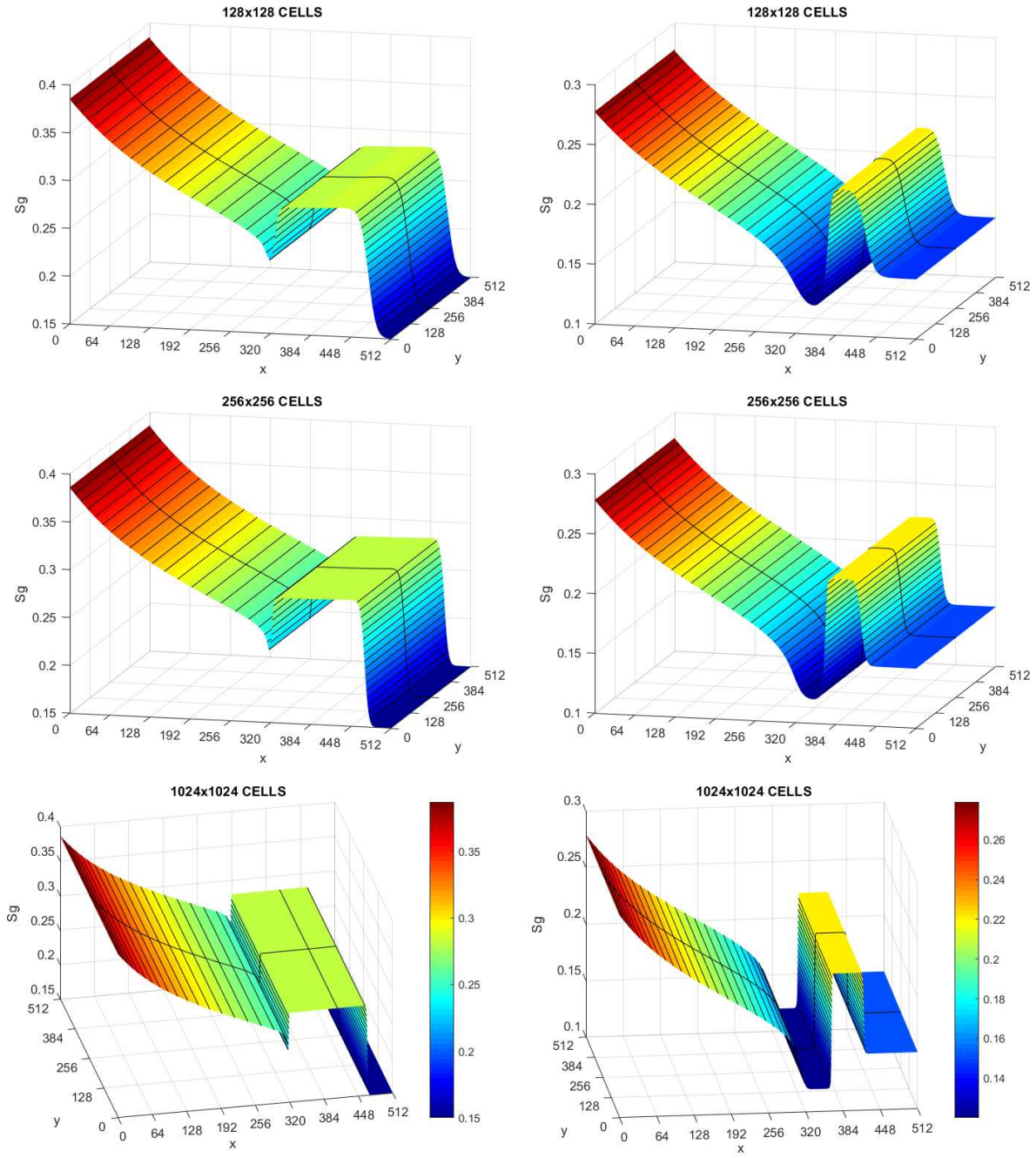

Figure 15 – A numerical convergence study for three-phase model (4.73) linked to (4.74) with a superimposed approximation corresponding to the 1D Euler System: $\frac{\partial s_w}{\partial t} + \frac{\partial}{\partial x} f_w(s_w, s_g) = 0$, $\frac{\partial s_g}{\partial t} + \frac{\partial}{\partial x} f_g(s_w, s_g) = 0$ (solid line).

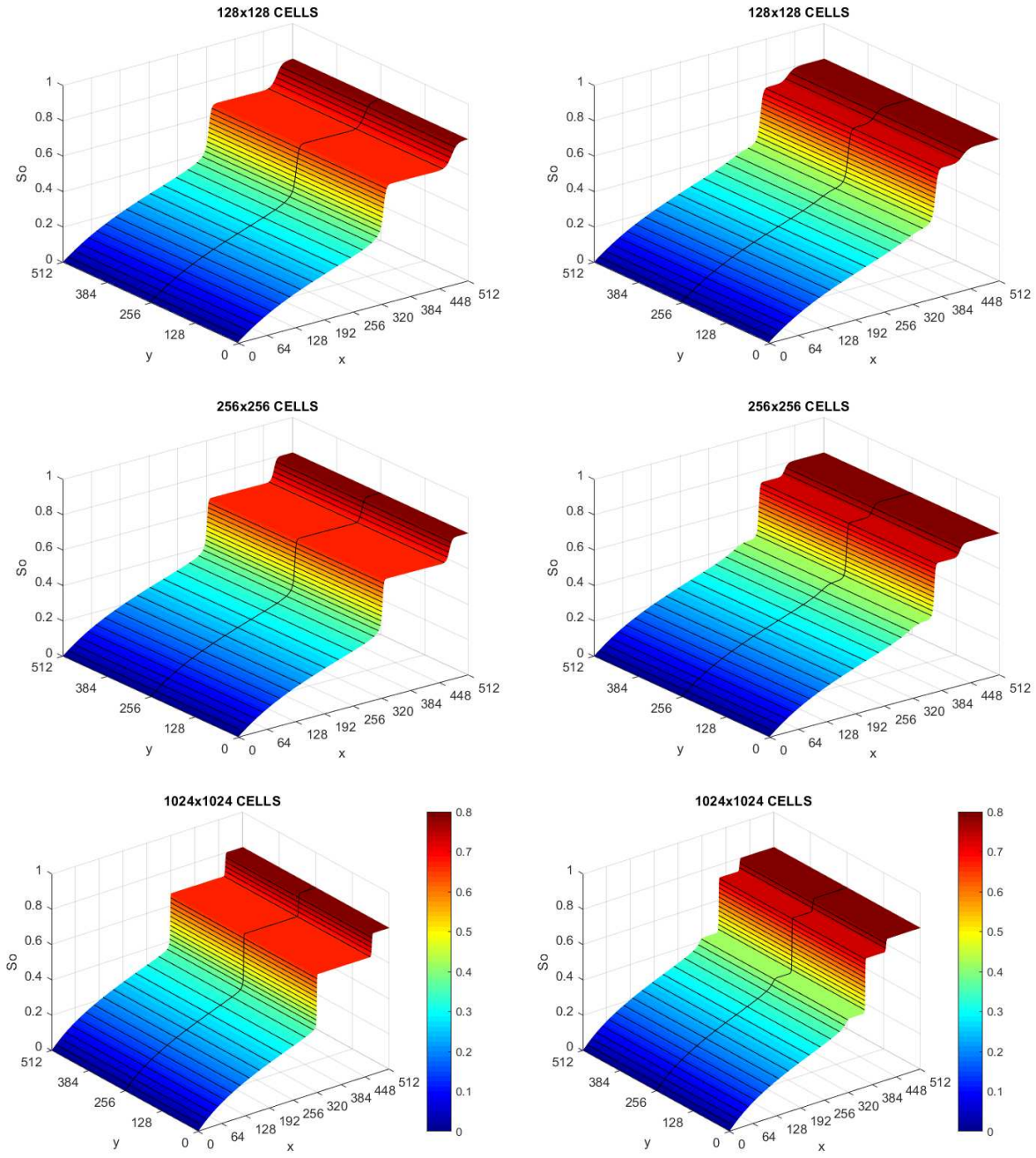

Figure 16 – A numerical convergence study for three-phase model (4.73) linked to (4.74) with a superimposed approximation corresponding to the 1D Euler System: $\frac{\partial s_w}{\partial t} + \frac{\partial}{\partial x} f_w(s_w, s_g) = 0$, $\frac{\partial s_g}{\partial t} + \frac{\partial}{\partial x} f_g(s_w, s_g) = 0$ (solid line).

Example 4.6. ***Two-dimensional compressible Euler equations: cases involving slip line initial data***

We will apply the SDLE scheme (4.10)-(4.11) with $l = 1, 2, 3, 4$, to numerically solve a 2D Euler system for cases involving slip line initial data given by

$$\begin{cases} \rho_t + (\rho u)_x + (\rho v)_y = 0, \\ (\rho u)_t + (\rho u^2 + p)_x + (\rho uv)_y = 0, \\ (\rho v)_t + (\rho uv)_x + (\rho v^2 + p)_y = 0, \\ E_t + (u(E+p))_x + (v(E+p))_y = 0, \end{cases} \tag{4.75}$$

where ρ is the mass density; $u = u(x, y, t)$ and $v = v(x, y, t)$, the x- and y-components of the velocity, respectively; and $E = pe + \frac{1}{2}\rho(u^2 + v^2)$ the total energy per unit volume. For a perfect gas, $p = \rho e(\gamma - 1)$, where constant γ denotes the ratio of specific heats; and e, the internal energy of the gas. In all tests, we consider $\gamma = 1.4$.

We solve the Euler system (4.75) subject to the slip line initial data for the two Riemann data in Table 1 as follows:

$$(\rho, u, v, p)^T (x, y, 0) = \begin{cases} (\rho_1, u_1, v_1, p_1)^T, & x > 0.5, \quad y > 0.5, \\ (\rho_2, u_2, v_2, p_2)^T, & x < 0.5, \quad y > 0.5, \\ (\rho_3, u_3, v_3, p_3)^T, & x < 0.5, \quad y < 0.5, \\ (\rho_4, u_4, v_4, p_4)^T, & x > 0.5, \quad y < 0.5, \end{cases}$$

where

Riemann Problem I	Riemann Problem II
$(\rho_1, u_1, v_1, p_1)^T = (+1, -0.75, -0.5, +1)^T$	$(\rho_1, u_1, v_1, p_1)^T = (+0.5313, +0.1, +0.1, +0.4)^T$
$(\rho_2, u_2, v_2, p_2)^T = (+2, -0.75, +0.5, +1)^T$	$(\rho_2, u_2, v_2, p_2)^T = (+1.0222, -0.6179, +0.1, +1)^T$
$(\rho_3, u_3, v_3, p_3)^T = (+1, +0.75, +0.5, +1)^T$	$(\rho_3, u_3, v_3, p_3)^T = (+0.8, +0.1, +0.1, +1)^T$
$(\rho_4, u_4, v_4, p_4)^T = (+3, +0.75, -0.5, +1)^T$	$(\rho_4, u_4, v_4, p_4)^T = (+1, +0.1, +0.8276, +1)^T$

Table 1 – Riemann Initial conditions for the Euler equations of gas dynamics.

For Riemann Problem I, we have slip lines that entering in a subsonic area and end in a spiral (in the center) as shown in Figure 17 (left column), while for Riemann Problem II, we have four slip lines in subsonic area that bend and end in two spirals as shown in Figure 17 (right column); see [76, 77] and references cited therein for more details on the complex structure of solutions to the Riemann problem to two-dimensional gas dynamics.

To apply our SDLE scheme, we use the *flux separation approach* (see [13]) componentwisely in the 2D Euler system given by (4.75) to obtain

$$\begin{cases} \rho_t + (\rho u)_x + (\rho v u)_y = 0, \\ (\rho u)_t + (\rho u^2)_x + (\rho u v)_y = -(p)_x, \\ (\rho v)_t + (\rho u v)_x + (\rho v^2)_y = -(p)_y, \\ E_t + (uE)_x + (vE)_y = -(up)_x - (vp)_y. \end{cases} \tag{4.76}$$

Roughly speaking, the flux separation strategy is as follows. Consider a *model problem* as $u_t + H(u)_x = G(u)$. A flux separation strategy transforms the later equation in the equivalent form $u_t + H_1(u)_x = G(u) - H_2(u)_x$, with $H = H_1 + H_2$. This simple trick allows construction numerically stable Lagrangian-Eulerian no-flow curves. This strategy is very robust and efficient for both two-dimensional systems discussed in this work, namely, the compressible Euler flows and the shallow-water equations.

From the numerical solutions presented in Figure 17 (Riemann Problem I, left column and Riemann Problem II, right column) for model problem (4.76), the SDLE scheme has proven to be stable and accurate these problems in capturing true physical behavior, which is containing strong shock waves with very good resolution.

The quantity shown in these experiments is the mass density (ρ) presented in Figure 17, for the two Riemann problems, as the contour curves. In both 2D Riemann problems for gas dynamics, we considered initial data to be constant in each quadrant in a (x, y)-plane domain $[0, 1] \times [0, 1]$ with a center located at position $(x, y) = (1/2, 1/2)$, as observed for each of the two configurations. For each configuration, the numerical solution is analyzed and illustrated by means of a "2D-plot's view angle (displayed in Figure 17). We show a numerical refinement study conducted with 200×200 grid cells, 400×400 grid cells, 800×800 grid cells, and 1600×1600 grid cells with the help of our semi-discrete scheme at times $T = 0.23$ (Figure 17, left column) and $T = 0.2$ (Figure 17, right column).

The component-wise application of the SDLE scheme is effective in capturing all the main characteristics of the wave patterns appearing in the corresponding problems as seem from the available literature (see, e.g., [62, 65, 66]). In addition, we did not use any dimensional splitting strategy, and no (local) Riemann solvers had to be applied and hence, time-consuming field-by-field type decompositions are avoided in the case of systems.

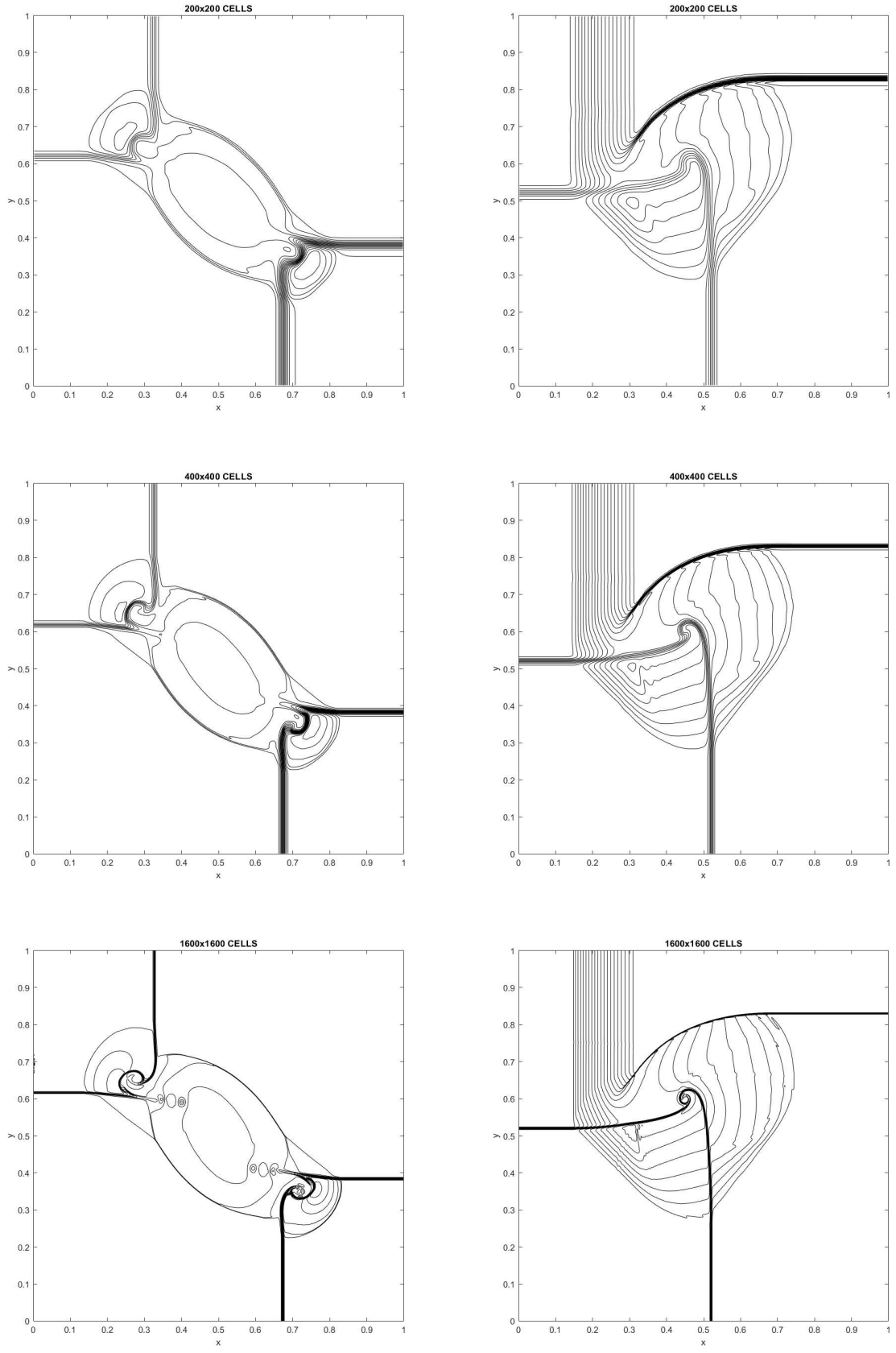

Figure 17 – Numerical refinement study with SDLE scheme ($\alpha = 2$, $\zeta = 2$, $\theta = 1.25$, and CFL = 0.03); for Riemann problem I at time $T = 0.23$: 5.66 s (200×200 grid cells) and 49.04 s (400×400 grid cells) and for Riemann problem II at time $T = 0.2$: 4.89 s (200×200 grid cells) and 43.27 s (400×400 grid cells) are consistent with the reference solution (1600×1600 grid cells).

Example 4.7. ***Two-dimensional compressible Euler equations: Double Mach reflection*** *[65, 66, 84]*

This test problem, originally proposed by Woodward and Colella [84] is initiated with a right-moving Mach 10 shock in air ($\gamma = 1.4$) positioned at $(x, y) = (1/6,\ 0)$ and makes a 60° angle with the $x-$axis. We display numerical approximations for the two-dimensional Euler equations (4.76) on a rectangular 2D domain of size $[0,\ 4] \times [0,\ 1]$ by the aid of our positive semi-discrete Lagrangian-Eulerian scheme along with the pre-and-post shock initial condition

$$(\rho, p, u, v)^T (x, y, 0) = \begin{cases} (1.4, 1, 0, 0)^T, & x > x_s(0), \\ (8, 116.5, 4.125\sqrt{3}, -4.125)^T, & \text{otherwise}, \end{cases} \tag{4.77}$$

where $x_s(t) = 10t/\text{sen}(\pi/3) + 1/6 + y/\text{tg}(\pi/3)$ is the shock position.

The bottom boundary condition on $0 \leqslant x \leqslant 1/6$ at $y = 0$ (the post-shock state) is fixed in time with the initial values so that the reflected shock is attached to the bottom surface. Typical reflecting boundary condition is specified on the rest of the bottom surface. On the upper boundary $y = 1$, we make that the pre-shock and the post-shock state move exactly as a function of time ($x_s(t) = 10t/\text{sen}(\pi/3) + 1/6 + 1/\text{tg}(\pi/3)$) such that the numerical simulation of the dynamics follows the oblique shock propagation without any planar distortion, capturing the tronts without introducing too much artificial dissipation, nor spurious oscillations as presented in Figure 18. At $x = 0$, we impose an inflow boundary condition, and the outflow/Neumann boundary condition at $x = 4$. In Figure 18, numerical simulations are performed with the new semi-discrete Lagrangian-Eulerian scheme ($\alpha = 2$, $\zeta = 3$, $\theta = 1.6$, CFL=0.033) using a standard second order Runge-Kutta method through a mesh grid refinement 480×120 grid cells, 720×180 grid cells, 1080×270 grid cells and 1620×405 grid cells at time $T = 0.2$. In each plot 30 equally spaced contours are shown. Our method has proved to be robust and easy to implement. In addition, our semi-discrete method captures well shocks propagation in all directions and the main aspects of the simulation, such as the formation of the jet and the incident shock.

Example 4.8. ***A Mach 3 wind tunnel with a step*** *[65, 66, 84]*

In another test problem for our semi-discrete Lagrangian-Eulerian scheme, we solve numerically the two-dimensional Euler system (4.75) written as (4.76) linked to the two dimensional Cartesian shock reflection problem on the computational domain consisting of a box $[0,\ 3] \times [0,\ 1]$ along with a forward step at $x = 0.6$, of a height of 0.2. The step, the upper and lower walls of the channel are reflecting boundaries. For the right-hand x-boundary, we use an outflow/Neumann boundary condition, while on the left-hand side we use an inflow boundary condition. The initial condition throughout the

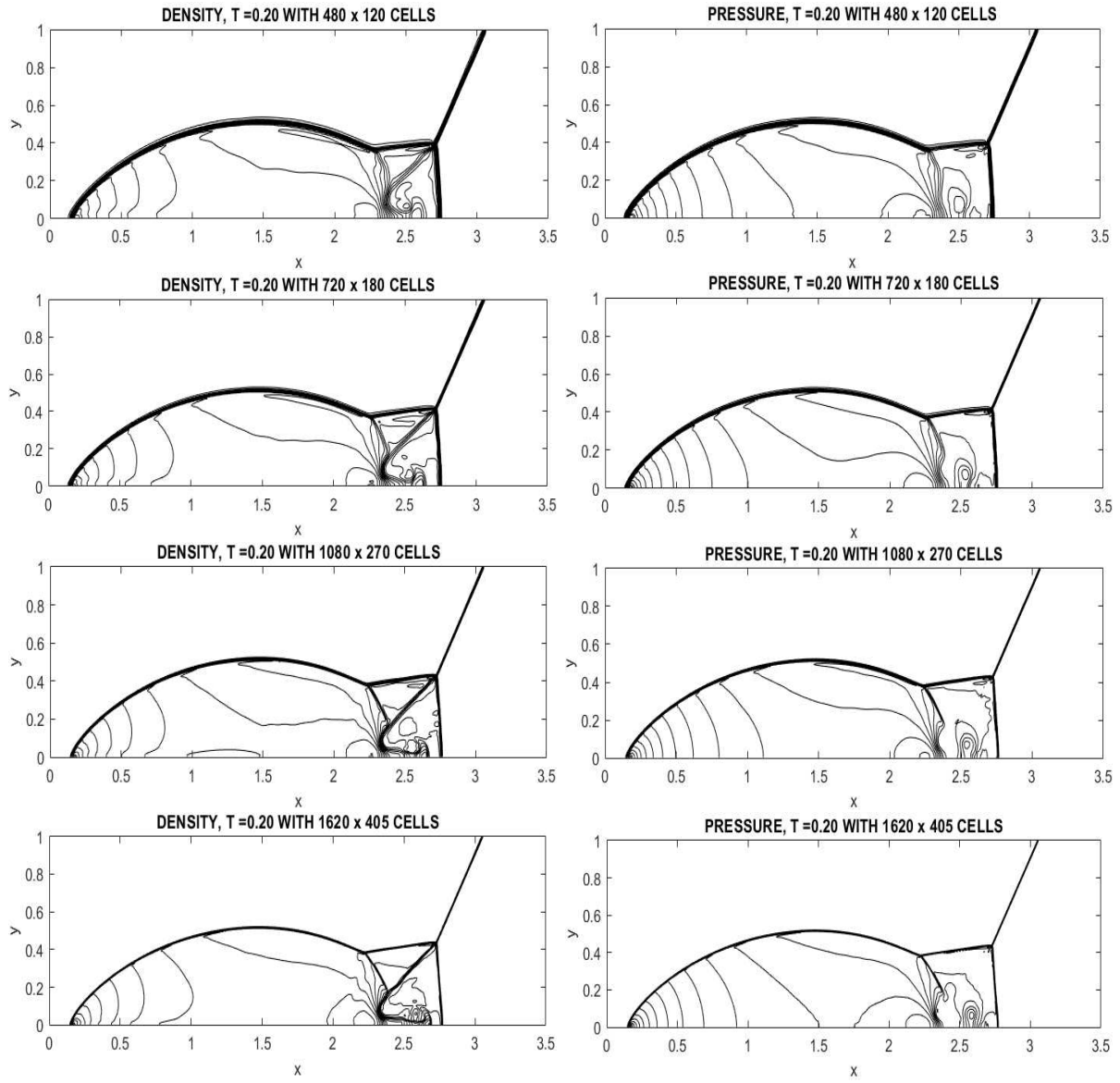

Figure 18 – Numerical approximation of the density (left column) and the pressure (right column) contours for the double Mach reflection test with 480 × 120 grid cells (229 s) and 720 × 180 grid cells (761 s). In this case, stable, consistent computational experiments with finer mesh grids show good evidence of numerical convergence for 1080 × 270 grid cells and 1620 × 405 grid cells as observed in [65, 66, 84].

channel is:

$$(\rho, p, u, v)^T (x, y, 0) = \begin{cases} (1.4, 1, 3, 0)^T, & x \leqslant 0.6 \quad \text{and} \quad y \quad \geqslant 0, \\ (0, 0, 0, 0)^T, & x > 0.6, \quad y > 0 \quad \text{and} \quad y \leqslant 0.2, \\ (1.4, 1, 3, 0)^T, & x > 0.6 \quad \text{and} \quad y > 0.2, \end{cases} \tag{4.78}$$

where ρ is the mass density, $u = u(x, y, t)$ and $v = v(x, y, t)$ are $x-$and $y-$components of the velocity, respectively. For a perfect gas the pressure $p = \rho e(\gamma - 1)$ where the constant γ is the ratio of specific heats and e is the internal energy of the gas. In Figure 19, a mesh

grid refinement study is presented with 240 × 80 grid cells, 360 × 120 grid cells, 540 × 180 grid cells and 810 × 270 grid cells for density (left) and pressure (right) distributions at time $T = 4$ by the aid of our 2D semi-discrete Lagrangian-Eulerian scheme ($\alpha = 2$, $\zeta = 2$, $\theta = 1.65$, CFL=0.022) using second order Runge-Kutta method. All the main features of the wave patterns appearing in the corresponding simulations presented in [65, 66, 84] are reproduced by our semi-discrete scheme with good resolution of the solution and with no particular treatment at the singular point. The contact discontinuities are well resolved by our semi-discrete scheme and they are in the correct position. The time evolution, up to time $T = 4$, of the density distribution (left column) and the pressure distribution (right column) in the wind tunnel are displayed in Figure 20. At the bottom surface the reflected shock is well captured and has reflected from the top of the step moving leftward to the singular point over time.

Example 4.9. ***The SDLE scheme for 2D shallow water systems with non-flat bottom and discontinuous topography***

Let us consider the following balance law form of the 2D system of shallow-water equations ([83, 85]):

$$\begin{cases} h_t + (hu)_x + (hv)_y = 0, \\ (hu)_t + (hu^2 + gh^2/2)_x + (huv)_y = -ghZ_x, \\ (hv)_t + (huv)_x + (hv^2 + gh^2/2)_y = -ghZ_y, \end{cases} \tag{4.79}$$

or

$$\begin{cases} H_t + (Hu)_x + (Hv)_y = (Zu)_x + (Zv)_y, \\ (hu)_t + (hu^2 + gh^2/2)_x + (huv)_y = -ghZ_x, \\ (hv)_t + (huv)_x + (hv^2 + gh^2/2)_y = -ghZ_y, \end{cases} \tag{4.80}$$

where $h = H - Z$ and which includes the continuity and momentum equations. We follow [83] to write (4.79) in the form (4.80). Quantity $h = h(x, y, t)$ denotes the water height measured from the bottom topography, $Z = Z(x, y)$, with the total height given by $H = h + Z$. Additionally, constant g is the gravitational acceleration. The fluid velocities are given by $u = u(x, y, t)$ in the x-direction and $v = v(x, y, t)$ in the y-direction. We shall study the 2D system (4.80) subject to the initial condition

$$h(x, y, 0) = \begin{cases} 3.5 - Z(x, y), & x < 5, \\ 2.5 - Z(x, y), & x > 5, \end{cases} \tag{4.81}$$

along with fluid velocities $u(x, y, 0) = v(x, y, 0) = 0$ on the square domain $\Omega = [0, 10] \times [0, 10]$. The gravitational constant is set to $g = 1$. We perform a study of the SDLE scheme (4.10)-(4.11) for numerical approximation of the shallow water system (4.80)-(4.81)

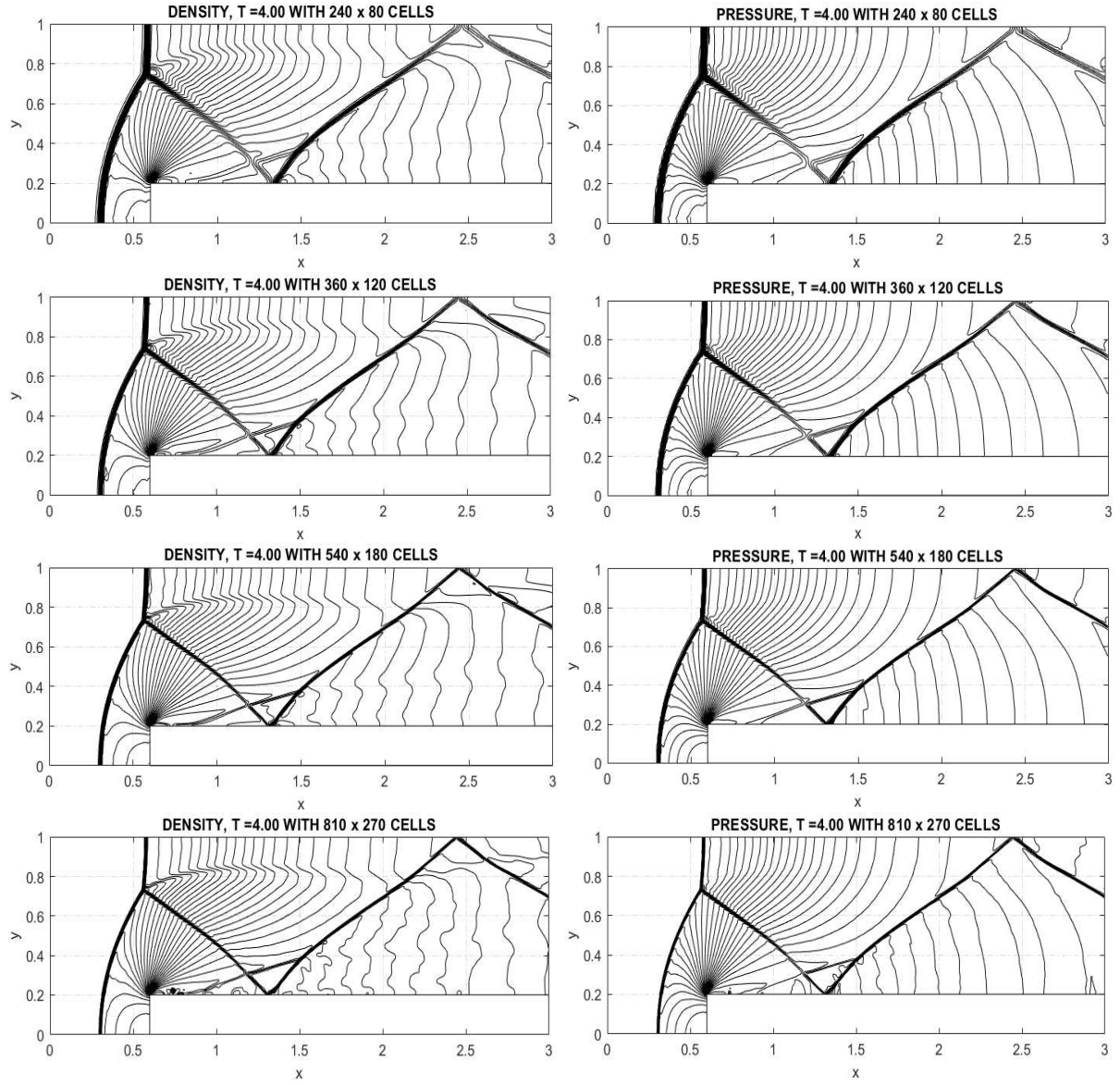

Figure 19 – "2D-plot's view angle" of the density (left column) and the pressure (right column) contours with 240 × 180 grid cells (139.25 s or 2 minutes), 360 × 120 grid cells (428.03 s or 7 minutes), 540 × 180 grid cells (1411.25 s or 24 minutes) and 810 × 270 grid cells (21062.19 s or 5 hours) at time $T = 4$.

considering several non-flat bottom and discontinuous topographies $Z(x, y)$ motivated by applications (see, e.g., [11, 13, 25, 83, 85]). This is a prototype dam-break flood system. We have two waves traveling in opposite directions: (i) a shock wave moving to the right in the x-direction, and (ii) a rarefaction wave moving to the left in the x-direction. In Figure 21, we see the SDLE scheme is able to resolve the expected behavior in the solutions of the dam-break flood with several topographies $Z(x, y)$ with no spurious noises or some undesired numerical artifacts.

In Figures 21, 22 we provide numerical approximations with good resolution for solving the shallow water system (4.80)-(4.81) performed on relatively coarse grids (first

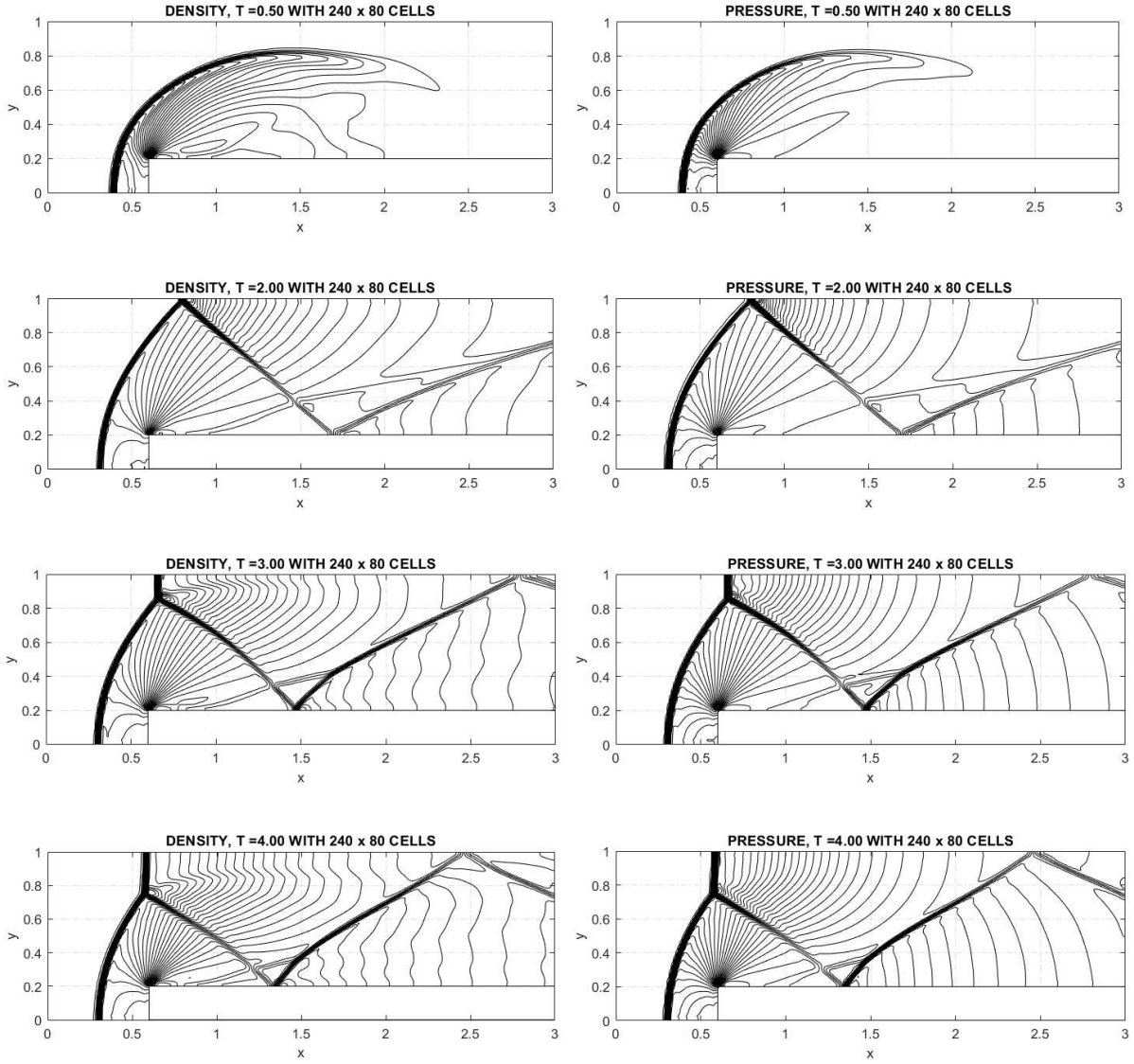

Figure 20 – Time evolution of the Mach 3 wind tunnel with our semi-discrete scheme using a uniform grid $\Delta x = \Delta y = 1/80$. The contours of density (left) and of pressure (right) are shown at several times (from top to bottom) T=0.5, 2, 3 and 4. This is in agreement with [65, 66, 84].

and second row of plots) allowing verify the capabilities of the SDLE scheme (4.10)-(4.11) and to show numerical robustness of the flux separation strategy for the correct treatment of non-flat bottom and discontinuous topography of distinct types. In the last (third row) in Figures 21, 22 we provide the corresponding solutions for each model considered in each column, but in a very fine mesh computed with the SDLE scheme aiming a twofold purpose 1) to show numerical evidence of convergence and 2) to display that we are computing the main features of the expected solutions.

The computational times and parameters are presented in the caption of Figures 21, 22. In the first column of Figure 21, we consider purely hyperbolic shallow-water

equation (4.80)-(4.81) (no bottom topography),

$$Z(x,y) \equiv Z_0 = 0. \tag{4.82}$$

In the second column of Figure 21, we consider the shallow water system (4.80)-(4.81) subject to the initial condition with bottom topography

$$Z(x,y) \equiv Z_1 = \begin{cases} 2-(x-5)^2-(y-5)^2, & \text{if} \quad |x-5|<1 \quad \text{and} \quad |y-5|<1, \\ 0, \qquad \text{otherwise.} \end{cases} \tag{4.83}$$

In the first column of Figure 22, we consider (4.80)-(4.81) with bottom topography

$$Z(x,y) \equiv Z_2 = \begin{cases} 2-(x-6)^2-(y-4)^2, & \text{if} \quad |x-6|<0.5 \quad \text{and} \quad |y-4|<0.5, \\ 2-(x-6)^2-(y-8)^2, & \text{if} \quad |x-6|<0.5 \quad \text{and} \quad |y-8|<0.5, \\ 0, \qquad \text{otherwise,} \end{cases} \tag{4.84}$$

and finally in the second column of Figure 22, we consider the same model (4.80)-(4.81) with topography

$$Z(x,y) \equiv Z_3 = \begin{cases} 2-(x-3)^2-(y-6)^2, & \text{if} \quad |x-3|<0.5 \quad \text{and} \quad |y-6|<0.5, \\ 2-(x-6)^2-(y-6)^2, & \text{if} \quad |x-6|<0.5 \quad \text{and} \quad |y-6|<0.5, \\ 2-(x-9)^2-(y-6)^2, & \text{if} \quad |x-9|<0.5 \quad \text{and} \quad |y-6|<0.5, \\ 0, \qquad \text{otherwise.} \end{cases} \tag{4.85}$$

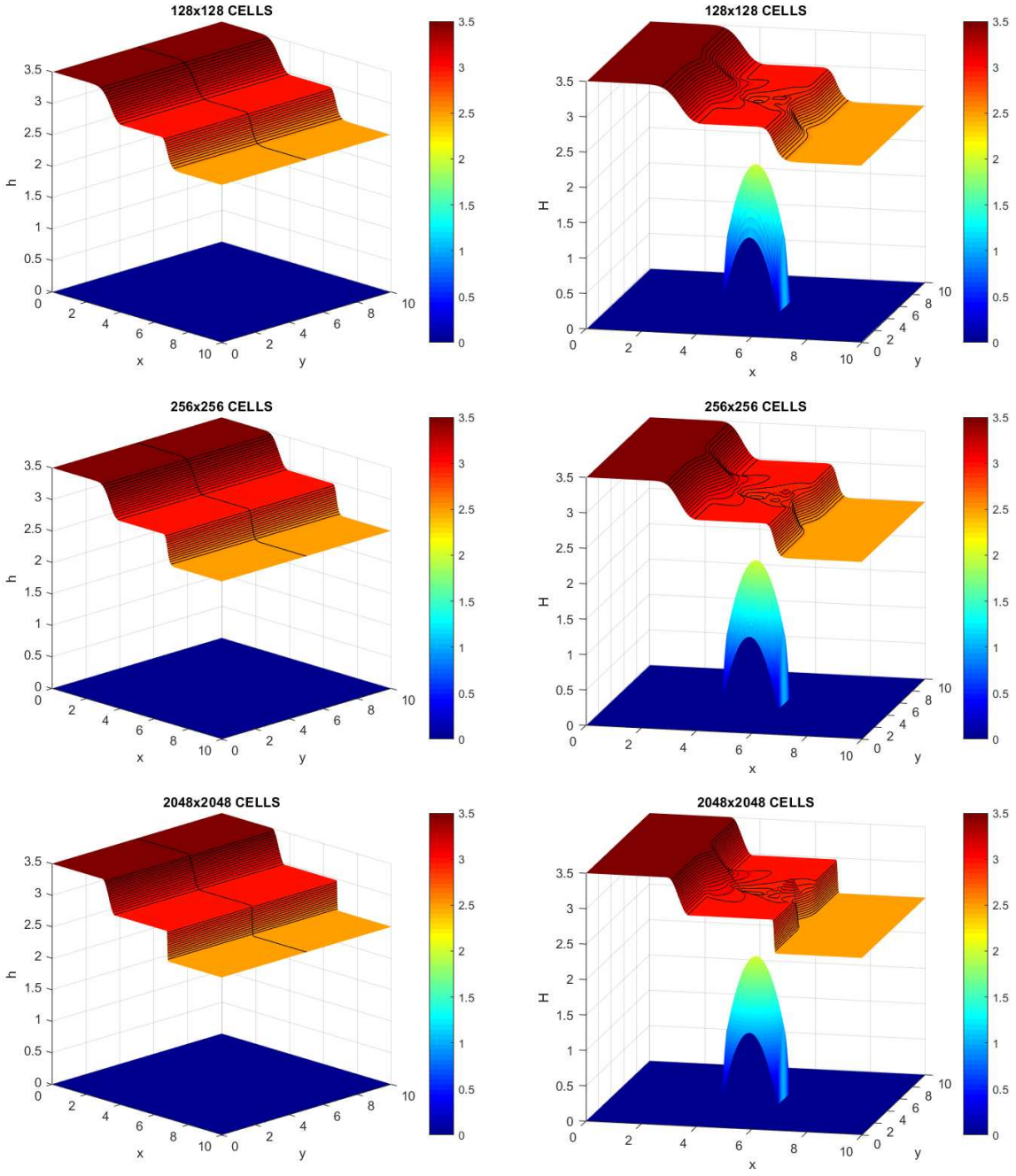

Figure 21 – The summary of numerical parameters in the SDLE scheme (4.10)-(4.11) for numerical approximation of the shallow water system (4.80)-(4.81) is: In the first column, *time* $T = 1$ *with 4.17 s (128* $\times$ *128 grid cells) and 36.48 s (256* $\times$ *256 grid cells) and* ($\alpha = 1$, $\zeta = 4$, $\theta = 1$, *CFL=0.05).* In the second column, *time* $T = 1$ *with 5.64 s (128* $\times$ *128 grid cells) and 49.08 s (256* $\times$ *256 grid cells) and* ($\alpha = 1$, $\zeta = 4$, $\theta = 1$, *CFL=0.05).*

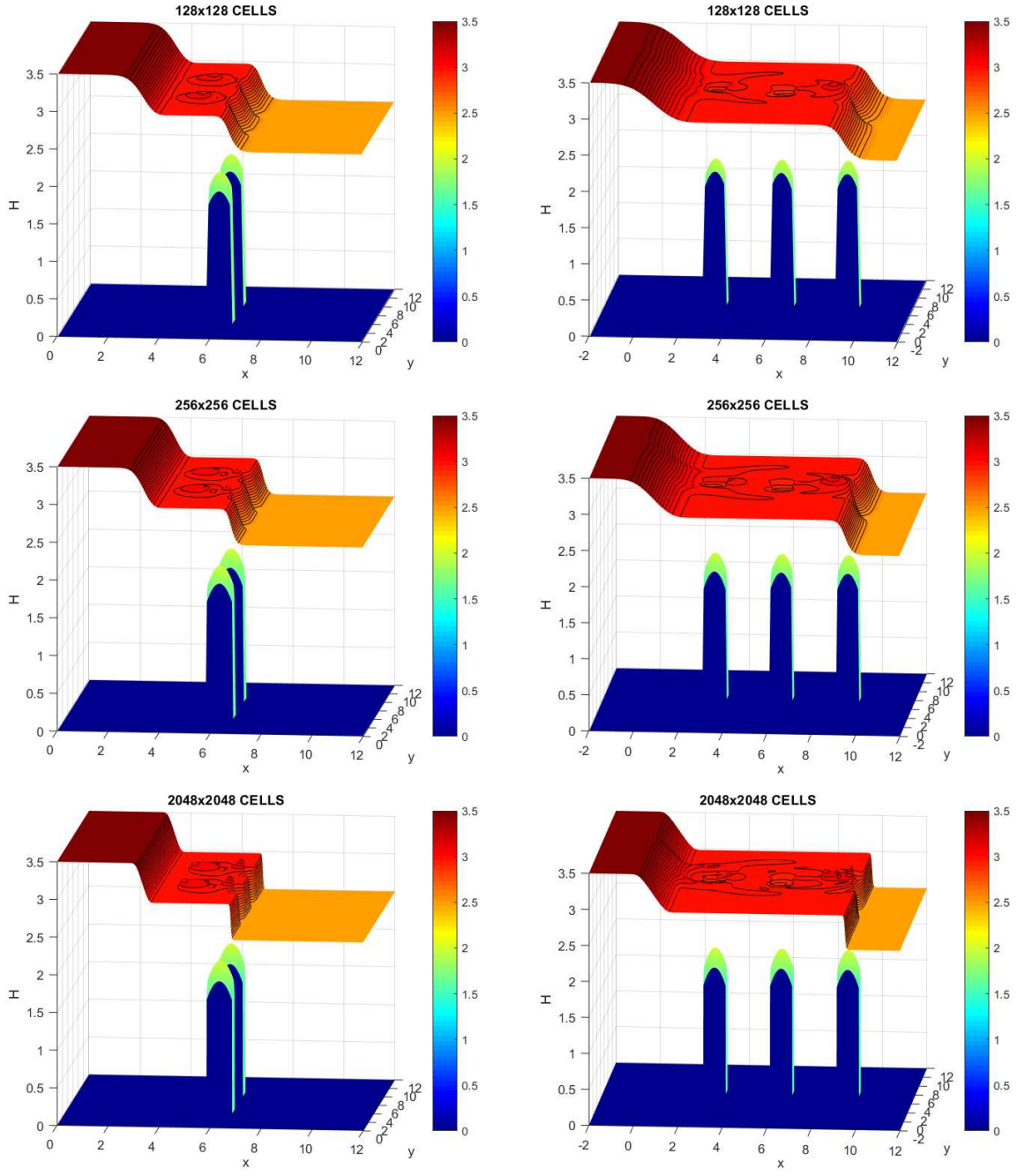

Figure 22 – The summary of numerical parameters in the SDLE scheme (4.10)-(4.11) for numerical approximation of the shallow water system (4.80)-(4.81) is: In the first column, *time* $T = 1$ *with 3.3 s (128* $\times$ *128 grid cells) and 26.2 secs (256* $\times$ *256 grid cells) and* ($\alpha = 1$, $\zeta = 4$, $\theta = 1$, *CFL=0.06).* Finally, in the second column, *time* $T = 2.5$ *with 8.4 s (128* $\times$ *128 grid cells) and 70 s (256* $\times$ *256 grid cells) and* ($\alpha = 1$, $\zeta = 4$, $\theta = 1$, *CFL=0.06).*

4.3.4 On the robustness on the no-flow curves on the models: experimental convergence order and error history

The objective of this section is to present a representative set of numerical studies for several hyperbolic systems and balance law models under consideration in this work (Example 3.2, Example 3.3, Example 3.4, Example 3.5, Example 3.6, Example 4.6, Example 4.9), aiming to show the numerical robustness of the multidimensional no-flow curves (3.5). First, it is worth remembering the CFL stability estimate as established in this work is based on the coefficients $b^x_{j+\frac{1}{2},k}$ and $b^y_{j,k+\frac{1}{2}}$, which are constructed from the no-flow curves. In short, no special choice of numerical parameters at the multidimensional numerical fluxes $\mathcal{F}_{j+\frac{1}{2},k}$ and $\mathcal{G}_{j,k+\frac{1}{2}}$ in (3.4) is necessary. Additionally, as shown in Tables 2-10, we verified that for any simple choice of parameters into the stability estimate coefficients $b^x_{j+\frac{1}{2},k}$ and $b^y_{j,k+\frac{1}{2}}$ we obtain very good results along with accurate resolution, and therefore confirming and verifying the developed theory in this work as well as yielding the robustness of the proposed semi-discrete approach. In addition, Tables 2-10 show the error history via a representative set of numerical study of convergence, in which the Experimental Order of Convergence (EOC) remains robust and consistent as the mesh grid is refined, that is, the numerical results obtained are shown to be very satisfactory even with relatively coarse mesh discretizations. From Tables 2-10, we can also find the desired residual error is monotonically decreasing as it would be expected under mesh grid refinement, which is another way to confirm evidence of the robustness of the approximations obtained through our semi-discrete scheme. For concreteness, the quantities $b^x_{j+\frac{1}{2},k}$ and $b^y_{j,k+\frac{1}{2}}$ appearing in multidimensional numerical fluxes $\mathcal{F}_{j+\frac{1}{2},k}$ and $\mathcal{G}_{j,k+\frac{1}{2}}$ in (3.4) are written in terms of the corresponding 2D no-flow curves (3.5), for which, in this study, we used the following simple formulas:

$$b^x_{j+\frac{1}{2},k} = \zeta \max_{j,k} \left(|f_{j,k} + f_{j+1,k}| \right) \quad \text{and} \quad b^y_{j,k+\frac{1}{2}} = \zeta \max_{j,k} \left(|g_{j,k} + g_{j,k+1}| \right), \quad 1 \leqslant \zeta \leqslant 5. \tag{4.86}$$

Notice that the above *no-flow* CFL-type constraint (3.8) does not require the need to employ the eigenvalues as the eigenvectors as well (exact and approximate values) of the relevant Jacobian of the numerical flux functions. This advantage is very relevant in practical problems. The 2D SDLE scheme (3.3)-(3.7) only employs in a direct way the available easy information of quantities u and fluxes $H(u)$ and $G(u)$, along with the *no-flow* CFL-type constraint (3.8) supported by the analysis summarized in the equations (3.20), (3.21) and (3.50). It should be recalled that the implementation of the scheme in the case of systems is a straightforward component-wise application of the multidimensional scalar case, but, importantly, the semi-discrete approach does not require dimensional splitting strategies nor time-consuming field-by-field decompositions. The SDLE scheme seems to fit well for treatment of with boundary conditions, based on the evidences in the numerical solutions of the specific models: the cases with Double Mach reflection as well

as Wind tunnel for the system of compressible Euler flows and the porous media injection problem for a non-strictly hyperbolic three-phase flow with a resonance point.

To complement some good evidences that we are computing the correct qualitative structure of the solutions (as presented in Section 4.3.1 and in Section 4.3.3, we also have numerically evaluated the accuracy of the SDLE scheme (3.3) and (3.4), along with (3.5)-(3.7), by computing the decay at which the residual-based discrepancies approaches zero when the step sizes (time and space) approaches zero. In what follows, we present this numerical study for some multidimensional problems presented and discussed in Section 3.3 and in Section 4.3. In this regards, we present a numerical study conducted with an Experimental Order of Convergence (EOC) in the L^1- norm of the relative error. To analyze the numerical convergence rate using our semi-discrete scheme (3.3)-(3.4) or (4.10)-(4.11) for systems, we use the relative norm of the errors. In what follows, we have an Experimental Order of Convergence (EOC) in the L^1- norm of the relative error,

$$(e_i)_1 = \|E\|_{L^1} / \|U\|_{L^1} \text{ where } \quad \|E\|_{L^1} = \Delta x \times \Delta y \sum_j \sum_k |E_{jk}| .$$

Here, E is the difference between the analytic solution U (whenever available) and the approximate solution. When the analytic solution is not known, we employ the relative norm of the errors as follows:

$$(e_i)_1 = \|u_{i+1} - u_i\|_{L^1} / \|u_{i+1}\|_{L^1} , \quad \text{with} \quad i,\, i+1 \ \text{ as the consecutive refinement numbers.}$$

The EOC is given by the following relation: $EOC = \dfrac{\log((e_i)_1/(e_{i+1})_1)}{\log(\Delta_{i+1}/\Delta_i)}$, where Δ_i is the number of elements and i defines the refinement number.

In the captions of each table are displayed informations about the model problem and the numerical parameters. We would like to mention that we are using the same classical second-order Runge–Kutta method for all simulation without any type of additional stability constrain.

Table 2 – L^1-norms of the relative errors $(e_i)_1$ between the numerical approximations and the exact solution by SDLE (3.3)-(3.4) with $\alpha = 2$, $\zeta = 1$ and $\theta = 1.5$ for the problem (3.137).

i	Δ_i	$\Delta x \times \Delta y$	$(e_i)_1$	EOC
1	32x32	9.7656e-04	4.57188e-02	-
2	64x64	2.4414e-04	1.27859e-02	0.91912
3	128x128	6.1035e-05	3.33203e-03	0.97004
4	256x256	1.5259e-05	8.44300e-04	0.99029
5	512x512	3.8147e-06	2.12240e-04	0.99603
6	1024x1024	9.5367e-07	5.30599e-05	1.00000
7	2048x2048	2.3842e-07	1.32754e-05	0.99943

Table 3 – L^1-norm of the relative error $(e_i)_1$ between the numerical successive approximations obtained with SDLE (3.3)-(3.4) ($\alpha = 2$, $\zeta = 2$, and $\theta = 1.5$) using the classical second-order Runge–Kutta method for solving the scalar 2D inviscid Burgers' model (3.139)-(3.140) as displayed in Figure 6.

i	Δ_i	$\Delta x \times \Delta y$	$(e_i)_1$	EOC
1	64x64	2.4414e-04	1.60488e-02	-
2	128x128	6.1035e-05	8.50289e-03	0.45822
3	256x256	1.5259e-05	4.30923e-03	0.49026
4	512x512	3.8147e-06	2.17945e-03	0.49173
5	1024x1024	9.5367e-07	1.09448e-03	0.49686
6	2048x2048	2.3842e-07	5.48519e-04	0.49832

Table 4 – L^1-norm of the relative error $(e_i)_1$ between the numerical approximations, U, and the analytic solution, u, obtained with SDLE scheme (3.3)-(3.4) ($\alpha = 1$, $\zeta = 3$, and $\theta = 2$) using the classical second-order Runge-Kutta method for solving the scalar inviscid Burgers' equation with the oblique Riemann problem (3.139) and (3.141) as displayed in Figure 7.

i	Δ_i	$\Delta x \times \Delta y$	$(e_i)_1$	EOC
1	32x32	9.7656e-04	7.99226e-02	-
2	64x64	2.4414e-04	4.58331e-02	0.40111
3	128x128	6.1035e-05	2.58630e-02	0.41275
4	256x256	1.5259e-05	1.40135e-02	0.44204
5	512x512	3.8147e-06	7.71611e-03	0.43043
6	1024x1024	9.5367e-07	4.16194e-03	0.44531
7	2048x2048	2.3842e-07	2.26866e-03	0.43771

Table 5 – L^1-norm of the relative error $(e_i)_1$ between the numerical successive approximations obtained with SDLE (3.3)-(3.4) scheme ($\alpha = 2$, $\zeta = 5$, and $\theta = 1$), along with the classical second-order Runge-Kutta method with scheme, for solving non-convex Buckley-Leverett with gravity (3.142), (3.143) and (3.144) as displayed in Figure 8.

i	Δ_i	$\Delta x \times \Delta y$	$(e_i)_1$	EOC
1	64x64	2.1973e-03	1.44642e-01	-
2	128x128	5.4932e-04	7.69098e-02	0.45562
3	256x256	1.3733e-04	4.40846e-02	0.40145
4	512x512	3.4332e-05	2.45543e-02	0.42215
5	1024x1024	8.5831e-06	1.38692e-02	0.41205
6	2048x2048	2.1458e-06	7.49800e-03	0.44365

Table 6 – L^1-norm of the relative error $(e_i)_1$ between the numerical successive approximations obtained with SDLE (3.3)-(3.4) ($\alpha = 1$, $\zeta = 2$, and $\theta = 2$) using the classical second-order Runge–Kutta method for solving the nonlinear equation (3.145) and (3.146) with non-convex fluxes as displayed in Figure 9.

i	Δ_i	$\Delta x \times \Delta y$	$(e_i)_1$	EOC
1	64x64	3.9063e-03	7.56655e-02	-
2	128x128	9.7656e-04	4.61182e-02	0.35715
3	256x256	2.4414e-04	2.73861e-02	0.37594
4	512x512	6.1035e-05	1.62218e-02	0.37776
5	1024x1024	1.5259e-05	9.60208e-03	0.37826
6	2048x2048	3.8147e-06	5.84318e-03	0.35830

Table 7 – L^1-norm of the relative error $(e_i)_1$ between the numerical successive approximations obtained with SDLE scheme (4.10)-(4.11) ($\alpha = 2$, $\zeta = 2$, and $\theta = 1.25$) at time $T = 0.23$ using the classical second-order Runge–Kutta method for solving 2D compressible Euler equations (4.76) (with Riemann problem I at time $T = 0.23$) and (with Riemann problem II at time $T = 0.2$) as displayed in Figure 17.

i	Δ_i	$\Delta x \times \Delta y$	$(e_i)_1$	EOC_I	$(e_i)_1$	EOC_{II}
1	100x100	1.0000e-04	2.20290e-02	-	9.02320e-03	-
2	200x200	2.5000e-05	1.65190e-02	0.20764	5.45930e-03	0.36246
3	400x400	6.2500e-06	1.21600e-02	0.22099	3.07470e-03	0.41414
4	800x800	1.5625e-06	9.00920e-03	0.21634	1.69800e-03	0.42830
5	1600x1600	3.9063e-07	7.15900e-03	0.16582	9.62720e-04	0.40932

Table 8 – L^1-norm of the relative error $(e_i)_1$ between the numerical successive approximations obtained with with SDLE (4.10)-(4.11) ($\alpha = 1$, $\zeta = 4$, $\theta = 1$, at time $T = 0.5$ (left) and at time $T = 1$ (right)) using the classical second-order Runge–Kutta method for solving the shallow-water equations: dam break over a flat bottom - the hyperbolic case (4.80)-(4.81) and topography (4.82) as displayed at the top in Figure 21, left column.

i	Δ_i	$\Delta x \times \Delta y$	$(e_i)_1$	EOC
1	64x64	2.4414e-02	3.56222e-03	-
2	128x128	6.1035e-03	2.51747e-03	0.25040
3	256x256	1.5259e-03	1.57188e-03	0.33974
4	512x512	3.8147e-04	1.02885e-03	0.30573
5	1024x1024	9.5367e-05	6.67311e-04	0.31230
6	2048x2048	2.3842e-05	4.18327e-04	0.33686

i	Δ_i	$\Delta x \times \Delta y$	$(e_i)_1$	EOC
1	64x64	2.4414e-02	5.03379e-03	-
2	128x128	6.1035e-03	3.14375e-03	0.33958
3	256x256	1.5259e-03	2.05770e-03	0.30573
4	512x512	3.8147e-04	1.33462e-03	0.31230
5	1024x1024	9.5367e-05	8.36654e-04	0.33686
6	2048x2048	2.3842e-05	5.07923e-04	0.36001

Table 9 – L^1-norm of the relative error $(e_i)_1$ between the numerical successive approximations obtained with SDLE (4.10)-(4.11) ($\alpha = 1$, $\zeta = 4$, and $\theta = 1$) at time $T = 0.5$ (left) and at time $T = 1$ (right) using the classical second-order Runge–Kutta method for solving shallow-water equations: dam break over a discontinuous bump (4.80)-(4.81) and topography (4.83) as displayed in Figure 21, right column.

i	Δ_i	$\Delta x \times \Delta y$	$(e_i)_1$	EOC
1	64x64	2.4414e-02	3.02769e-03	-
2	128x128	6.1035e-03	2.13303e-03	0.25266
3	256x256	1.5259e-03	1.54533e-03	0.23249
4	512x512	3.8147e-04	1.12766e-03	0.22729
5	1024x1024	9.5367e-05	7.76564e-04	0.26908
6	2048x2048	2.3842e-05	5.10131e-04	0.30312

i	Δ_i	$\Delta x \times \Delta y$	$(e_i)_1$	EOC
1	64x64	2.4414e-02	4.18225e-03	-
2	128x128	6.1035e-03	3.07023e-03	0.22297
3	256x256	1.5259e-03	2.25068e-03	0.22399
4	512x512	3.8147e-04	1.57979e-03	0.25531
5	1024x1024	9.5367e-05	1.03887e-03	0.30236
6	2048x2048	2.3842e-05	6.48133e-04	0.34033

Table 10 – L^1-norms of the relative error $(e_i)_1$ between the numerical successive approximations with the SDLE ($\alpha = 1$, $\zeta = 4$, $\theta = 1$) for the dam break flood model (4.80)-(4.81) with topography (4.84) at time $T = 1$ (left column) as well as the same model with topography (4.85) at time $T = 2.5$ (right column) as displayed in Figure 22 using the SDLE along with a classical second-order Runge-Kutta method.

i	Δ_i	$\Delta x \times \Delta y$	$(e_i)_1$	EOC
1	64x64	4.7852e-02	6.06308e-03	-
2	128x128	1.1963e-02	4.90050e-03	0.15356
3	256x256	2.9907e-03	3.42405e-03	0.25861
4	512x512	7.4768e-04	2.45496e-03	0.24000
5	1024x1024	1.8692e-04	1.54043e-03	0.33618
6	2048x2048	4.6730e-05	9.71881e-04	0.33224

i	Δ_i	$\Delta x \times \Delta y$	$(e_i)_1$	EOC
1	64x64	4.7852e-02	5.94887e-03	-
2	128x128	1.1963e-02	4.77183e-03	0.15904
3	256x256	2.9907e-03	3.32779e-03	0.25999
4	512x512	7.4768e-04	2.35739e-03	0.24869
5	1024x1024	1.8692e-04	1.44833e-03	0.35140
6	2048x2048	4.6730e-05	9.18119e-04	0.32882

5 Concluding remarks and perspectives for the future

5.1 Concluding remarks

In the course of this thesis, we designed and analyzed a new class of positive semi-discrete Lagrangian-Eulerian schemes for solving multidimensional scalar and systems of initial value problems for models of conservation laws. The scheme is based on a dynamic space-time parametric no-flow equations, which allowed:

- To circumvent the *nature of the blow-up singularity* in the numerical flux functions, thus yielding a new class of explicit semi-discrete Lagrangian-Eulerian schemes. The no-flow curves are used as a new desingularization analysis tool for construction of computationally stable numerical flux in conservative form (Subsection 2.1.1).
- The one-dimensional scalar semi-discrete Lagrangian-Eulerian scheme is extended in a natural, but non-trivial way to two-dimensional semi-discrete scheme (Chapter 3). This extension brings technical challenges when it comes up to prove convergence of approximate solutions generated by the scheme to the unique entropy solution (Section 3.2).
- The extension to systems is made by a straightforward componentwise application of the multidimensional scalar case (1D and 2D) with no need to use any dimensional splitting strategies, as well as to solve (local) Riemann problems and, hence, time-consuming field-by-field decompositions are avoided (Sections 4.1, 4.2).
- The weak asymptotic analysis is applied to the semi-discrete scheme to prove that our scheme satisfies the maximum principle along with relevant estimates, including robust TVNI conditions (scalar case), which also imply the uniqueness of the weak solution satisfying Kruzhkov entropy condition (Sections 2.2, 3.2). We found from the weak asymptotic analysis that the numerical stability condition (CFL) becomes more restraint in more than one-dimensional space (Eq. (3.8)) and the proof for Total Variation Non-Increasing (TVNI) is based on a completely different approach from that used in one-dimensional space (Subsection 3.2.2).

As a new tool in the formulation of the semi-discrete method, the *no-flow* estimates permit:

- The new semi-discrete Lagrangian-Eulerian scheme, in the more general context of multidimensional hyperbolic systems of conservation laws, also satisfies the positivity principle (Subsection 4.2.1).

- To find a CFL-type stability condition of multidimensional systems, for robust simulations, but without the need to employ the eigenvalues (exact and/or approximate values) of the relevant Jacobian of the numerical flux functions to guarantee the stability of our numerical scheme (Eq. (4.63)).

- The conditions for the weak positivity and the fact that each equation can be decoupled (using the no-flow construction) with $U_i > 0$, $(U_i)^+ \geqslant 0$ and $(U_i)^- \geqslant 0$ for all i ensure that the integral L^1 is conserved. In particular, this result does not need any calculation of eigenvalues (exact and/or approximate values) of the relevant Jacobian matrix associated to the hyperbolic flux functions (Remark 4.2, Example 4.1).

- The positivity condition does not guarantee convergence, but it is a quantity idealized by Liu and Lax [65, 66], so it may be stronger than necessary. however, the positivity condition is more restrictive than the weak positivity, which does not need to calculate eigenvalues to guarantee the stability of numerical solutions of general multi-dimensional hyperbolic systems (see Theorem 4.1 and Remark 4.2). Our SDLE scheme satisfies the positivity properties under more restrictive assumptions, but effectively, numerical experiments are done under hypothesis of novel conditions of the weak positivity (Section 4.3).

- The no-flow curves permit to use the scheme in its simplest form, providing convincing numerical computations for multidimensional systems and scalar equations whose solutions exhibited non-trivial fronts and rarefaction–shock interactions. Neither difficulties regarding the treatment of the (numerical) boundaries and the initial data nor spurious oscillations were observed (Sections 2.3, 3.3, 4.3).

- In addition, the multidimensional semi-discrete Lagrangian-Eulerian scheme retains simplicity with a very good resolution and efficiency. These features are significant and ensure the feasibility of this class of positive semi-discrete schemes in a wide range of applications.

5.2 Perspectives for future work

Previous results obtained from the first class of semi-discrete scheme writing in a Lagrangian-Eulerian framework for hyperbolic problems allow us to consider several paths for further development of this work. Here we will mention the most important at

the moment, considering the evolution of the state of the art, to be able to mention for example;

- **Model with discontinuous flux function in space:**

  Consider an immiscible and incompressible displacement two-phase flow model of water and oil (denoted by w and o, respectively) in heterogeneous porous media with Ω a domain in $\mathbb{R}^2$. The governing equations are of great importance in petroleum engineering [1, 6, 12], and they are giving by

$$\nabla \cdot \mathbf{v} = 0, \quad \mathbf{v} = -\lambda(u)\mathbf{K}(\mathbf{x})\nabla \cdot p, \quad \mathbf{x} \in \Omega, \quad t > 0, \tag{5.1}$$

$$\partial_t u + \nabla \cdot (H(u)\mathbf{v}) = 0, \quad \mathbf{x} \in \Omega, \quad t > 0, \tag{5.2}$$

  with the effects of capillarity and gravity neglected. Here $\mathbf{v}$ is the total seepage velocity, u is the water saturation, $\mathbf{K}(\mathbf{x})$ is the absolute permeability, $H(u)$ is water fractional flow function and p is the pressure. The total mobility, $\lambda(u)$ is defined in terms of the relative permeabilities $k_{ri}(u)$ and phase viscosities μ_i by
  $\lambda(u) = \dfrac{k_{rw}(u)}{\mu_w} + \dfrac{k_{ro}(u)}{\mu_o}$.
  In this work, our multidimensional semi-discrete scheme (1D and 2D) was used to deal numerically with a set of problems in porous media, such as the Buckley-Leverett-type model (Section 3.3, Example 3.5) and a 2×2 non-strictly hyperbolic three-phase flow model (Subsection 4.3.3, Example 4.5), which is the first approach for the multidimensional case without considering the forced convection dictated by a velocity-pressure problem. In this context, new perspectives are now opened to revisit other models in porous media with applications, such as the elliptic-pressure-velocity model 5.1. We intend to treat the hyperbolic-transport model 5.2 more efficiently, in that instead of the hyperbolic flux being treated with a fully-discrete scheme [6], it will be treated with our semi-discrete Lagrangian-Eulerian scheme. Here we will consider the generic flux function in the model 5.2 to be discontinuous, i.e., $H = H(\mathbf{x}, u)$. Recently, a large number of conservation law problems with discontinuous flux functions in the context of the model 5.2 have received a lot of attention in the literature, such problems arise in *oil trapping phenomenon* [18], a *Whitham model of car traffic flow on a highway* [22, 56], just to name a few.

- **Models with Non-local flux function:**

  The model of conservation laws with non-local flux aims to describe the behavior of drivers that adapt their speed to what happens in front of them. Such models have been very important in the recent past years in many fields of application as sedimentation [23], conveyor belts [49], granular flows and crowd dynamics [30, 34]. The general form of non-local conservation laws can be represented by

$$\partial_t \rho + \nabla \cdot H = 0, \quad H = H(\mathbf{x}, t, \rho, \omega \star \rho) \quad t > 0, \quad \mathbf{x} \in \mathbb{R}^d, \tag{5.3}$$

where $\rho(\mathbf{x},t) \in \mathbb{R}^N$ and $\omega(\mathbf{x},t) \in \mathbb{R}^N$. The term "non-local" refers to the dependence of the flux function H on the convolution term $\omega \star \rho$, where ω is a properly chosen matrix of kernel functions and ρ is the vector of conserved quantities. Consider the following scalar conservation law with non-local flux function;

$$\partial_t \rho + \partial_x (H(\rho) v(\omega_\eta \star \rho)) = 0, \quad x \in \mathbb{R}, \quad t > 0, \tag{5.4}$$

where

$$\omega_\eta \star \rho(x,t) := \int_x^{x+\eta} \omega_\eta(y-x)\rho(y,t)dy, \quad \eta > 0, \tag{5.5}$$

with the following hypothesis:

$$\begin{aligned} &H \in \mathbf{C}^1(I, \mathbb{R}^+), \quad I = [a,b] \subseteq \mathbb{R}^+, \\ &v \in \mathbf{C}^2(I, \mathbb{R}^+)\, s.t. \quad v' \leqslant 0, \\ &\omega_\eta \in \mathbf{C}^1([0,\eta], \mathbb{R}^+)\, s.t. \quad \omega_\eta' \leqslant 0, \\ &\int_0^\eta \omega_\eta(x)dx = J_0, \quad \forall \eta > 0, \quad \lim_{\eta \longrightarrow 0} \omega_\eta(0) = 0. \end{aligned} \tag{5.6}$$

The integral J_0 is the interaction strength. The physical meaning of ρ in Eq. (5.4) is density, so it makes sense that it is positive.

Many schemes in the literature have been used to approximate problem of conservation laws with non-local flux, such as Lax-Friedrichs-type numerical scheme [16, 17], Godunov-type numerical scheme [47], Lagrangian-Anti-diffusive Remap schemes [31], discontinuous Galerkin [29], finite volume WENO schemes [46]. Recently in the literature, the fully-discrete Lagrangian-Eulerian scheme has been applied to this model, see [5]. Now on, as a continuation of this work we intend to use and analyze our semi-discrete scheme to approximate the non-local conservation laws linked to Eqs. (5.4)-(5.6).

- **Relaxation model:**

  An example of hyperbolic balance laws is the shallow water systems with non-flat bottom and discontinuous topography (Example 4.9), which has been well approximated by our semi-discrete scheme. We intend to go further and clarify our knowledge on the theory in the study of the partial differential-algebraic equation (PDAEs) with diffusive, dispersive, and source terms of the form:

$$\partial_t G(u) + \partial_x F(u) = \partial_x \left[B(u)\partial_x u\right] + R(u) \tag{5.7}$$

$$H(u) = 0, \quad \text{with initial conditions} \quad u(x,0) = u_0(x), \tag{5.8}$$

  where the variables $u = (u_1, u_2, \cdots, u_n) : \mathbb{Q} \subset \mathbb{R} \times \mathbb{R}^+ \longrightarrow \Psi \subset \mathbb{R}^n$. The space Ψ is the *phase space*; the accumulation and the flux functions are $G = (G_1(u), \cdots, G_k(u))^T : \Psi \subset \mathbb{R}^n \longrightarrow \mathbb{R}^k$, $F = (F_1(u), \cdots, F_k(u))^T : \Psi \subset \mathbb{R}^n \longrightarrow \mathbb{R}^k$.

Here $R = (R_1(u), \cdots, R_k(u))^T : \Psi \subset \mathbb{R}^n \longrightarrow \mathbb{R}^k$ is the source terms. The algebraic relationships are represented by the vector function $H = (H_1(u), H_2(u), \cdots, H_p(u))^T : \Psi \subset \mathbb{R}^n \longrightarrow \mathbb{R}^p$, where $n = p + k$. In [60], the authors substitute the system of algebraic equations with uncertainties (5.8) by the relaxed system:

$$\partial_t H(u) = -\frac{1}{\tau} H(u),\ \tau > 0 \quad \text{with initial conditions} \quad u(x,0) = u_0(x) \tag{5.9}$$

to obtain the system of equations (5.7)-(5.9) with relaxation terms. We assume that the functions G, F, H are sufficiently smooth. Here $B(u)$ is an operator. The matrix $B(u)$ is a not positive definite matrix, but in [60] it has been handled in such a way to find a positive definite sub-matrix that depends only on u (and none of them derivatives), the above system is a convective-diffusive system. The Eq. (5.8) is proposed in such a way that the manifold defined by $H(u) = 0$ (for which the conditions defined by H are satisfied) is an attractor. This condition allows that the solution "relaxes" on the phase space Ψ for a region for which the algebraic condition is not satisfied. We intend to use our novel semi-discrete scheme to solve numerically the system (5.7)-(5.8) and (5.7)-(5.9) in the same spirit as in [60].

Bibliography

[1] E. Abreu, *Numerical modelling of three-phase immiscible flow in heterogeneous porous media with gravitational effects*, Mathematics and Computers in Simulation **97** (2014), no. 2, 234–259.

[2] E. Abreu, M. Colombeau, and E. Panov, *Weak asymptotic methods for scalar equations and systems*, Journal of mathematical analysis and applications **444** (2016), no. 2, 1203–1232.

[3] E. Abreu, M. Colombeau, and E. Y. Panov, *Approximation of entropy solutions to degenerate nonlinear parabolic equations*, Zeitschrift für angewandte Mathematik und Physik **68** (2017), no. 6, 133.

[4] E. Abreu and D. Conceição, *Numerical modeling of degenerate equations in porous media flow*, Journal of Scientific Computing **55** (2013), no. 3, 688–717.

[5] E. Abreu, J. C. De la Cruz, R. Juajibioy, and W. Lambert, *Lagrangian-Eulerian approach for nonlocal conservation laws*, (2019).

[6] E. Abreu, C. Diaz, J. Galvis, and J. Pérez, *On the conservation properties in multiple scale coupling and simulation for Darcy flow with hyperbolic-transport in complex flows*, Multiscale Modeling & Simulation **18** (2020), no. 4, 1375–1408.

[7] E. Abreu, J. François, W. Lambert, and J. Pérez, *A class of positive semi-discrete Lagrangian-Eulerian schemes for multidimensional systems of hyperbolic conservation laws*, submitted.

[8] E. Abreu, W. Lambert, J. Pérez, and A. Santo, *Convergence of a Lagrangian-Eulerian scheme via the weak asymptotic method*, submitted.

[9] ———, *A Lagrangian-Eulerian algorithm for solving hyperbolic conservation laws with applications, proceedings of the 6th international conference on approximation methods and numerical modelling in environment and natural resources*, (2015), no. 6, 599–617.

[10] ———, *A new finite volume approach for transport models and related applications with balancing source terms*, Mathematics and Computers in Simulation **137** (2017), 2–28.

[11] E. Abreu, V. Matos, J. Pérez, and P. Rodriguez-Bermudez, *A class of Lagrangian–Eulerian shock-capturing schemes for first-order hyperbolic problems with forcing terms*, Journal of Scientific Computing **86** (2021), no. 1, 1–47.

[12] E. Abreu, F. Pereira, and S. Ribeiro, *Central schemes for porous media flows*, Computational & Applied Mathematics **28** (2009), no. 1, 87–110.

[13] E. Abreu and J. Pérez, *A fast, robust, and simple Lagrangian–Eulerian solver for balance laws and applications*, Computers & Mathematics with Applications **77** (2019), no. 9, 2310–2336.

[14] E. Abreu, J. Pérez, and A. Santo, *A conservative Lagrangian-Eulerian finite volume approximation method for balance law problems*, Proceeding Series of the Brazilian Society of Computational and Applied Mathematics **6** (2018), no. 1.

[15] ———, *Lagrangian-Eulerian approximation methods for balance laws and hyperbolic conservation laws*, Revista UIS Ingenierías **17** (2018), no. 1, 191–200.

[16] A. Aggarwal, R. M. Colombo, and P. Goatin, *Nonlocal systems of conservation laws in several space dimensions*, SIAM Journal on Numerical Analysis **53** (2015), no. 2, 963–983.

[17] P. Amorim, R. M. Colombo, and A. Teixeira, *On the numerical integration of scalar nonlocal conservation laws*, ESAIM: Mathematical Modelling and Numerical Analysis **49** (2015), no. 1, 19–37.

[18] B. Andreianov and C. Cancès, *Vanishing capillarity solutions of Buckley–Leverett equation with gravity in two-rocks' medium*, Computational Geosciences **17** (2013), no. 3, 551–572.

[19] B. Andreianov and M. Maliki, *A note on uniqueness of entropy solutions to degenerate parabolic equations in r^n*, Nonlinear Differential Equations and Applications NoDEA **17** (2010), no. 1, 109–118.

[20] J. Aquino, A. S. Francisco, F. Pereira, T. J. Pereira, and H. P. A. Souto, *A Lagrangian strategy for the numerical simulation of radionuclide transport problems*, Progress in Nuclear Energy **52** (2010), no. 3, 282–291.

[21] J. Aquino, A. S. Francisco, F. Pereira, and H. P. A. Souto, *An overview of Eulerian–Lagrangian schemes applied to radionuclide transport in unsaturated porous media*, Progress in Nuclear Energy **50** (2008), no. 7, 774–787.

[22] S. Berres, R. Bürger, and K. H. Karlsen, *Central schemes and systems of conservation laws with discontinuous coefficients modeling gravity separation of polydisperse suspensions*, Journal of Computational and Applied Mathematics **164** (2004), 53–80.

[23] F. Betancourt, R. Bürger, K. H. Karlsen, and E. M. Tory, *On nonlocal conservation laws modelling sedimentation*, Nonlinearity **24** (2011), no. 3, 855.

[24] A. Bressan, M. T. Chiri, and W. Shen, *A posteriori error estimates for numerical solutions to hyperbolic conservation laws*, arXiv preprint arXiv:2010.00428 (2020).

[25] J. A. Carrillo, S. Kalliadasis, S. P. Pérez, and C. Shu, *Well-balanced finite-volume schemes for hydrodynamic equations with general free energy*, Multiscale Modeling & Simulation **18** (2020), no. 1, 502–541.

[26] P. Castañeda, E. Abreu, F. Furtado, and D. Marchesin, *On a universal structure for immiscible three-phase flow in virgin reservoirs*, Computational Geosciences **20** (2016), no. 1, 171–185.

[27] M. A. Celia, *Eulerian-Lagrangian localized adjoint methods for contaminant transport simulations*, International conference on computational methods in water resources, 1994, pp. 207–216.

[28] M. A. Celia, T. F. Russell, I. Herrera, and R. E. Ewing, *An Eulerian-Lagrangian localized adjoint method for the advection-diffusion equation*, Advances in Water Resources **13** (1990), no. 4, 187–206.

[29] C. Chalons, P. Goatin, and L. M. Villada, *High-order numerical schemes for one-dimensional nonlocal conservation laws*, SIAM Journal on Scientific Computing **40** (2018), no. 1, A288–A305.

[30] F. A. Chiarello, *Non-local conservation laws for traffic flow modeling*, Ph.D. thesis, COMUE Université Côte d'Azur (2015-2019), 2019.

[31] F. A. Chiarello, P. Goatin, and L. M. Villada, *Lagrangian-Antidiffusive remap schemes for non-local multi-class traffic flow models*, Computational and Applied Mathematics **39** (2020), no. 2, 1–22.

[32] I. Christov and B. Popov, *New non-oscillatory central schemes on unstructured triangulations for hyperbolic systems of conservation laws*, Journal of Computational Physics **227** (2008), no. 11, 5736–5757.

[33] B. Cockburn and C. W. Shu, *TVB Runge-Kutta local projection discontinuous galerkin finite element method for conservation laws. ii. general framework*, Mathematics of computation **52** (1989), no. 186, 411–435.

[34] R. M. Colombo and M. Lécureux-Mercier, *Nonlocal crowd dynamics models for several populations*, Acta Mathematica Scientia **32** (2012), no. 1, 177–196.

[35] F. Coquel, J. M. Hérard, K. Saleh, and N. Seguin, *A robust entropy-satisfying finite volume scheme for the isentropic Baer- Nunziato model*, ESAIM: Mathematical Modelling and Numerical Analysis **48** (2014), no. 1, 165–206.

[36] H. K. Dahle, M. S. Espedal, R. E. Ewing, and O. Sævereid, *Characteristic adaptive subdomain methods for reservoir flow problems*, Numerical Methods for Partial Differential Equations **6** (1990), no. 4, 279–309.

[37] V. Danilov, *On the relation between the Maslov-Whitham method and the weak asymptotics method*, Banach Center Publications **1** (2010), no. 88, 55–65.

[38] V. Danilov and V. Shelkovich, *Delta-shock wave type solution of hyperbolic systems of conservation laws*, Quarterly of Applied Mathematics **63** (2005), no. 3, 401–427.

[39] V. G. Danilov and D. Mitrovic, *Delta shock wave formation in the case of triangular hyperbolic system of conservation laws*, Journal of Differential Equations **245** (2008), no. 12, 3704–3734.

[40] V. G. Danilov, G. A. Omel'Yanov, and V. M. Shelkovich, *Weak asymptotics method and interaction of nonlinear waves*, Translations of the American Mathematical Society-Series 2 **208** (2003), 33–164.

[41] V. G. Danilov and V. M. Shelkovich, *Dynamics of propagation and interaction of δ-shock waves in conservation law systems*, Journal of Differential Equations **211** (2005), no. 2, 333–381.

[42] J. Douglas, F. Furtado, and F. Pereira, *On the numerical simulation of waterflooding of heterogeneous petroleum reservoirs*, Oceanographic Literature Review **3** (1998), no. 45, 594.

[43] J. Douglas, F. Pereira, and L. Yeh, *A locally conservative Eulerian–Lagrangian numerical method and its application to nonlinear transport in porous media*, Computational Geosciences **4** (2000), no. 1, 1–40.

[44] J. Douglas, Jr and T. F. Russell, *Numerical methods for convection-dominated diffusion problems based on combining the method of characteristics with finite element or finite difference procedures*, SIAM Journal on Numerical Analysis **19** (1982), no. 5, 871–885.

[45] U. S. Fjordholm and S. Solem, *Second-order convergence of monotone schemes for conservation laws*, SIAM Journal on Numerical Analysis **54** (2016), no. 3, 1920–1945.

[46] J. Friedrich and O. Kolb, *Maximum principle satisfying CWENO schemes for nonlocal conservation laws*, SIAM Journal on Scientific Computing **41** (2019), no. 2, A973–A988.

[47] J. Friedrich, O. Kolb, and S. Göttlich, *A godunov type scheme for a class of LWR traffic flow models with non-local flux*, arXiv preprint arXiv:1802.07484 (2018).

[48] L. Gosse and G. Toscani, *Asymptotic-preserving & well-balanced schemes for radiative transfer and the Rosseland approximation*, Numerische Mathematik **98** (2004), no. 2, 223–250.

[49] S. Göttlich, S. Hoher, P. Schindler, V. Schleper, and A. Verl, *Modeling, simulation and validation of material flow on conveyor belts*, Applied mathematical modelling **38** (2014), no. 13, 3295–3313.

[50] D. Gottlieb and J. S. Hesthaven, *Spectral methods for hyperbolic problems*, Journal of Computational and Applied Mathematics **128** (2001), no. 1-2, 83–131.

[51] J. M. Greenberg and A. Y. LeRoux, *A well-balanced scheme for the numerical processing of source terms in hyperbolic equations*, SIAM Journal on Numerical Analysis **33** (1996), no. 1, 1–16.

[52] J. M. Greenberg, A. Y. Leroux, R. Baraille, and A. Noussair, *Analysis and approximation of conservation laws with source terms*, SIAM Journal on Numerical Analysis **34** (1997), no. 5, 1980–2007.

[53] A. Harten, *High resolution schemes for hyperbolic conservation laws*, Journal of computational physics **3** (1983), no. 49, 357–393.

[54] A. Harten and S. Osher, *Uniformly high-order accurate nonoscillatory schemes. i*, SIAM Journal on Numerical Analysis **24** (1987), no. 2, 279–309.

[55] C. S. Huang and T. Arbogast, *An eulerian-lagrangian weighted essentially nonoscillatory scheme for nonlinear conservation laws: Eulerian-lagrangian weno scheme*, Numerical Methods for Partial Differential Equations **33** (2016), no. 3.

[56] K. H. Karlsen and J. D. Towers, *Convergence of the Lax-Friedrichs scheme and stability for conservation laws with a discontinuous space-time dependent flux*, Chinese Annals of Mathematics **25** (2004), no. 03, 287–318.

[57] A. Kurganov and D. Levy, *A third-order semi-discrete central scheme for conservation laws and convection-diffusion equations*, SIAM Journal on Scientific Computing **22** (2000), no. 4, 1461–1488.

[58] A. Kurganov, S. Noelle, and G. Petrova, *Semi-discrete central-upwind schemes for hyperbolic conservation laws and Hamilton–Jacobi equations*, SIAM Journal on Scientific Computing **23** (2001), no. 3, 707–740.

[59] A. Kurganov and E. Tadmor, *New high-resolution central schemes for nonlinear conservation laws and convection–diffusion equations*, Journal of Computational Physics **160** (2000), no. 1, 241–282.

[60] W. Lambert, A. Alvarez, I. Ledoino, D. Tadeu, D. Marchesin, and J. Bruining, *Mathematics and numerics for balance partial differential-algebraic equations (pdaes)*, Journal of Scientific Computing **84** (2020), no. 2, 1–56.

[61] J. O. Langseth, A. Tveito, and R. Winther, *On the convergence of operator splitting applied to conservation laws with source terms*, SIAM journal on numerical analysis **33** (1996), no. 3, 843–863.

[62] P. D. Lax and X. D. Liu, *Solution of two-dimensional Riemann problems of gas dynamics by positive schemes*, SIAM Journal on Scientific Computing **19** (1998), no. 2, 319–340.

[63] R. J. LeVeque, *Finite volume methods for hyperbolic problems*, vol. 31, Cambridge university press, 2002.

[64] D. Levy, G. Puppo, and G. Russo, *A fourth-order central WENO scheme for multidimensional hyperbolic systems of conservation laws*, SIAM Journal on scientific computing **24** (2002), no. 2, 480–506.

[65] X. D. Liu and P. D. Lax, *Positive schemes for solving multi-dimensional hyperbolic systems of conservation laws ii*, Journal of Computational Physics **187** (2003), no. 2, 428–440.

[66] ———, *Positive schemes for solving multi-dimensional hyperbolic systems of conservation laws*, Selected Papers Volume I (2005), 337–360.

[67] R. Loubère, P. H. Maire, M. Shashkov, J. Breil, and S. Galera, *ReALE: a reconnection-based arbitrary-Lagrangian–Eulerian method*, Journal of Computational Physics **229** (2010), no. 12, 4724–4761.

[68] M. Maliki and H. Touré, *Uniqueness of entropy solutions for nonlinear degenerate parabolic problems*, Journal of Evolution Equations **3** (2003), no. 4, 603–622.

[69] D. Marchesin, B. J. Plohr, et al., *Wave structure in WAG recovery*, SPE Annual Technical Conference and Exhibition, Society of Petroleum Engineers, 2001.

[70] S. Mishra, *Numerical methods for conservation laws and related equations*, Lecture Notes, ETH Zurich (2010), 74.

[71] H. Natarajan and G. B. Jacobs, *An explicit semi-Lagrangian, spectral method for solution of Lagrangian transport equations in Eulerian-Lagrangian formulations*, Computers & Fluids (2020), 104526.

[72] E. Y. Panov, *On decay of entropy solutions to multidimensional conservation laws*, SIAM Journal on Mathematical Analysis **52** (2020), no. 2, 1310–1317.

[73] L. Pareschi, *Central differencing based numerical schemes for hyperbolic conservation laws with relaxation terms*, SIAM journal on numerical analysis **39** (2001), no. 4, 1395–1417.

[74] J. Pérez, *Lagrangian-Eulerian approximation methods for balance laws and hyperbolic conservation laws university of campinas*, Ph.D. thesis, University of Campinas, 2015.

[75] A. Santo, *Conservative numerical formulations for approximating hyperbolic models with source terms and related transport models*, Ph.D. thesis, University of Campinas, 2017.

[76] C. W. Schulz-Rinne, *Classification of the Riemann problem for two-dimensional gas dynamics*, SIAM journal on mathematical analysis **24** (1993), no. 1, 76–88.

[77] C. W. Schulz-Rinne, J. P. Collins, and H. M. Glaz, *Numerical solution of the Riemann problem for two-dimensional gas dynamics*, SIAM Journal on Scientific Computing **14** (1993), no. 6, 1394–1414.

[78] D. Serre and L. Silvestre, *Multi-dimensional Burgers equation with unbounded initial data: well-posedness and dispersive estimates*, Archive for Rational Mechanics and Analysis **234** (2019), no. 3, 1391–1411.

[79] G. A. Sod, *A survey of several finite difference methods for systems of nonlinear hyperbolic conservation laws*, Journal of computational physics **27** (1978), no. 1, 1–31.

[80] P. K. Sweby, *High resolution schemes using flux limiters for hyperbolic conservation laws*, SIAM journal on numerical analysis **21** (1984), no. 5, 995–1011.

[81] H. Tang, *On the sonic point glitch*, Journal of Computational Physics **202** (2005), no. 2, 507–532.

[82] J. W. Thomas, *Numerical partial differential equations: conservation laws and elliptic equations*, vol. 33, Springer Science & Business Media, 2013.

[83] N. Wintermeyer, A. R. Winters, G. J. Gassner, and D. A. Kopriva, *An entropy stable nodal discontinuous Galerkin method for the two dimensional shallow water equations on unstructured curvilinear meshes with discontinuous bathymetry*, Journal of Computational Physics **340** (2017), 200–242.

[84] P. Woodward and P. Colella, *The numerical simulation of two-dimensional fluid flow with strong shocks*, Journal of computational physics **54** (1984), no. 1, 115–173.

[85] Y. Xing and C. W. Shu, *A survey of high order schemes for the shallow water equations*, J. Math. Study **47** (2014), no. 3, 221–249.